

Non-Perturbative Renormalization Flow in Quantum Field Theory and Statistical Physics

Jürgen Berges*

*Center for Theoretical Physics, Massachusetts Institute of Technology
Cambridge, Massachusetts 02139, U.S.A.*

Nikolaos Tetradis[†]

*Scuola Normale Superiore, 56126 Pisa, Italy and
Nuclear and Particle Physics Section, University of Athens
15771 Athens, Greece*

Christof Wetterich[‡]

*Institut für Theoretische Physik, Universität Heidelberg
69120 Heidelberg, Germany*

Abstract

We review the use of an exact renormalization group equation in quantum field theory and statistical physics. It describes the dependence of the free energy on an infrared cutoff for the quantum or thermal fluctuations. Non-perturbative solutions follow from approximations to the general form of the coarse-grained free energy or effective average action. They interpolate between the microphysical laws and the complex macroscopic phenomena. Our approach yields a simple unified description for $O(N)$ -symmetric scalar models in two, three or four dimensions, covering in particular the critical phenomena for the second-order phase transitions, including the Kosterlitz-Thouless transition and the critical behavior of polymer chains. We compute the aspects of the critical equation of state which are universal for a large variety of physical systems and establish a direct connection between microphysical and critical quantities for a liquid-gas transition. Universal features of first-order phase transitions are studied in the context of scalar matrix models. We show that the quantitative treatment of coarse graining is essential for a detailed estimate of the nucleation rate. We discuss quantum statistics in thermal equilibrium or thermal quantum field theory with fermions and bosons and we describe the high temperature symmetry restoration in quantum field theories with spontaneous symmetry breaking. In particular we explore chiral symmetry breaking and the high temperature or high density chiral phase transition in quantum chromodynamics using models with effective four-fermion interactions.

This work is dedicated to the 60th birthday of Franz Wegner.

*Email: Berges@ctp.mit.edu

†Email: Tetradis@cibs.sns.it

‡Email: C.Wetterich@thphys.uni-heidelberg.de

Contents

1	Introduction	3
1.1	From simplicity to complexity	3
1.2	Fluctuations and the infrared problem	9
2	Non-Perturbative flow equation	14
2.1	Average action	14
2.2	Exact flow equation	20
2.3	Truncations	24
2.4	Flow equation for the average potential	26
2.5	A simple example: the quartic potential	28
3	Solving the flow equation	32
3.1	Scaling form of the exact flow equation for the potential	32
3.2	Threshold functions	34
3.3	Large- N expansion	37
3.4	Graphical representation and resummed perturbation theory	40
3.5	Exact flow of the propagator	43
3.6	Approach to the convex potential for spontaneous symmetry breaking	46
4	$O(N)$-symmetric scalar models	50
4.1	Introduction	50
4.2	The running average potential	52
4.3	Universal critical equation of state	59
4.4	Gas-liquid transition and the Ising universality class	62
4.5	Universal and non-universal critical properties	69
4.6	Equation of state for first order transitions	74
4.7	Critical behavior of polymer chains	79
4.8	Two dimensional models and the Kosterlitz-Thouless transition	81
5	Scalar matrix models	87
5.1	Introduction	87
5.2	Scalar matrix model with $U(2) \times U(2)$ symmetry	88
5.3	Scale dependence of the effective average potential	90
5.4	Renormalization group flow of couplings	96
5.5	Phase structure of the $U(2) \times U(2)$ model	100
5.6	Universal equation of state for weak first order phase transitions	105
5.7	Summary	109
6	Spontaneous nucleation and coarse graining	111
6.1	Introduction	111
6.2	Calculation of the nucleation rate	115
6.3	Region of validity of homogeneous nucleation theory	120
6.4	Radiatively induced first-order phase transitions	125

6.5	Testing the approach through numerical simulations	129
7	Quantum statistics for fermions and bosons	131
7.1	Quantum universality	131
7.2	Exact flow equation for fermions	134
7.3	Thermal equilibrium and dimensional reduction	137
7.4	The high-temperature phase transition for the ϕ^4 quantum field theory	139
8	Fermionic models	145
8.1	Introduction	145
8.2	Linear quark meson model	146
8.3	Flow equations and infrared stability	149
8.4	High temperature chiral phase transition	153
8.5	Renormalization flow at nonzero chemical potential	157
8.6	High density chiral phase transition	160
Appendix A	Threshold functions	162
Appendix B	Anomalous dimension in the sharp cutoff limit	164

1 Introduction

1.1 From simplicity to complexity

A few fundamental microscopic interactions govern the complexity of the world around us. The standard model of electroweak and strong interactions combined with gravity is a triumph for the way of unification and abstraction. Even though some insufficiencies become apparent in astrophysical and cosmological observations – the oscillations of neutrinos, the missing dark matter and the need for cosmological inflation and baryogenesis – there is little doubt that no further basic interactions are needed for an understanding of “everyday physics”. For most phenomena the relevant basic interactions are even reduced to electromagnetism and gravity. Still, for many common observations there is a long way to go before quantitative computations and predictions from the microscopic laws become feasible. How to go back from the simplicity of microphysics to the complexity of macrophysics?

We will deal here only with very simple systems of many particles, like pure water or vapor, where the interactions between molecules are reasonably well understood. We also concentrate on the most simple situations like thermal equilibrium. Concerning dynamics we only touch on properties that can be calculated in equilibrium, whereas we omit the complicated questions of the time evolution of statistical systems. Nevertheless, it remains a hard task to compute quantitatively such simple things as the phase transition from water to vapor, starting from the well-known microscopic interactions. How can we calculate the pressure dependence of the transition temperature from atomic physics or the van der Waals interactions between molecules? How do the optical properties change as we approach the endpoint of the critical line? What would be the rate of formation of vapor bubbles if we heat extremely pure water in space at a given temperature T slightly above the critical temperature T_c ? Similar questions may be asked about the temperature dependence of the density of superfluid He^4 or the magnetization in ferromagnets. One often takes a higher level of abstraction and asks for the properties of simplified theoretical models, like the two-dimensional Hubbard model, which is widely believed to describe high T_c -superconductivity, or the Heisenberg model for the description of ferromagnetism or antiferromagnetism. Despite the considerable simplifications of these models as compared to real physics they remain very difficult to solve.

Common to all these questions is the role of fluctuations in statistical many-body systems. Statistical physics and thermodynamics offer a powerful framework for the macroscopic behavior of systems with a very large number of degrees of freedom. The statistical treatment makes the predictions about the behavior of stationary many-body systems independent of many irrelevant details of the microscopic dynamics. Nevertheless, one needs to bridge the gap between the known microscopic interactions and the thermodynamic potentials and similar quantities which embody the effective macroscopic laws. This is the way to complexity.

For a thermodynamic equilibrium system of many identical microscopic degrees of freedom the origin of the problems on the way to complexity is threefold. First, there is often no small parameter which can be used for a systematic perturbative expansion. Second, the correlation length can be substantially larger than the characteristic distance between the microscopic objects. Collective effects become important. Finally, the relevant degrees of freedom which

permit a simple formulation of the macroscopic laws may be different from the microscopic ones. A universal theoretical method for the transition from micro- to macrophysics should be able to cope with these generic features. We propose here a version of non-perturbative flow equations based on an exact renormalization group equation. This theoretical tool acts like a microscope with variable resolution. The way from a high-resolution picture of an effectively small piece of surface or volume (microphysics) to a rough resolution for large volumes (macrophysics) is done stepwise, where every new step in the resolution only uses information from the previous step [1]–[7]. We use here a formulation in terms of the effective average action [8, 9], which permits non-perturbative approximations for practical computations. Our method may be considered as an analytical counterpart of the often successful numerical simulation techniques.

Modern particle physics is confronted with precisely the same problems on the way from the beautiful simplicity of fundamental interactions to a “macroscopic” description. Basically, only the relevant length scales are different. Whereas statistical physics may have to translate from Angströms to micrometers, particle physics must build a bridge from the Fermi scale ($\sim (100 \text{ GeV})^{-1}$) to a fermi ($1 \text{ fm} = 10^{-15} \text{ m} = (197.33 \text{ MeV})^{-1}$). For interactions with small couplings, particle physics has mastered this transition as far as the vacuum properties are concerned – this includes the dynamics of the excitations, e.g. the particles. The perturbative renormalization group [10] interpolates between the Fermi scale and the electron mass¹ or even between a grand unification scale $\sim 10^{16} \text{ GeV}$ and the Fermi scale. The dynamics of electrons, positrons and photons in vacuum can be predicted with extremely high accuracy. This extends to weak interactions between leptons.

The situation is very different for strong interactions. The running gauge coupling grows large at a scale below 1 GeV and the generic problems of statistical physics reappear. Whereas quantum electrodynamics may be compared with a dilute gas of weakly interacting molecules, strong interactions are analogous to dense systems with a large correlation length. At microscopic distances, e.g. the Fermi scale, quantum chromodynamics (QCD) can give precise predictions in terms of only one gauge coupling and the particle masses. At the “macroscopic scale” of around 1 fm numerical simulations approach only slowly the computation of the masses and interactions of the relevant degrees of freedom, namely baryons and mesons, and no analytical method has achieved this goal yet.

The smallness of microscopic couplings is no guarantee for a simple transition to “macrophysics”. The vacuum fluctuations may enhance considerably the relevant effective coupling at longer distances, as in the case of QCD. In the presence of thermal fluctuations a similar phenomenon happens even for the electroweak interactions. In fact, at high temperature the electroweak interactions have a large effective gauge coupling and show all properties of a strongly interacting model, very similar to QCD [11, 12]. The evidence for this behavior is striking if one looks at the recently computed spectrum of quasiparticles for the standard model at high temperature [13]. In the language of statistical physics the hot plasma in thermal equilibrium is dense at sufficiently high temperature, with a correlation

¹We employ the word scale for distance as well as momentum or mass scales. In our units $\hbar = c = k_B = 1$ they are simply the inverse of each other.

length (typically given by the inverse magnetic mass of the gauge bosons) substantially larger than the inverse temperature.

The high-temperature behaviour of strong or electroweak interactions has attracted much interest recently. It is relevant for the hot plasma in the very early universe. Possible phase transitions may even have left observable “relics” behind that could serve as observational tests of cosmology before nucleosynthesis. From a statistical physics viewpoint the particle physics systems are extremely pure – no dirt, dotation with other atoms, impurities, seeds of nucleation, gravitational effects etc. need to be considered. In principle, tests of particle physics in thermodynamic equilibrium would be ideal experiments for statistical physics². Unfortunately, these “ideal experiments” are difficult to perform – it is not easy to prepare a high-temperature plasma of particles in equilibrium in a laboratory. Nevertheless, an impressive experimental program is already under way, aiming at a test of high temperature and high density QCD and possible phase transitions [14]. This highlights the need of a theoretical understanding of the QCD phase diagram at high temperature and density, including such interesting issues as color superconductivity and the possibility of (multi-) critical points with observable effects from long-range correlations [15, 16, 17]. Renormalization group methods should be an important tool in this attempt.

From a theoretical point of view there is actually no difference between thermal quantum field theory and quantum-statistical systems. In a modern language, both are formulated as Euclidean functional integrals with “Euclidean time” wrapped around a torus with circumference T^{-1} . (For dynamical questions beyond the equilibrium properties the time coordinate has to be analytically continued to real Minkowski time.) The only special features of the particle physics systems are the very precisely known microscopic interactions with their high degree of symmetry in the limit of vanishing temperature. This concerns, in particular, the Lorentz symmetry or its Euclidean counterpart of four-dimensional rotations and Osterwalder-Schrader positivity [18]. In this line of thought the recent high precision numerical simulations of the high temperature electroweak interactions [19, 20] can be considered as a fine example of a quantitative (theoretical) transition from microphysics to macrophysics, despite the presence of strong effective interactions and a large correlation length. They have confirmed that the high temperature first-order phase transition which would be present in the standard model with modified masses turns into a crossover for realistic masses, as has been suggested earlier by analytical methods [11, 12, 21, 22].

Beyond the identical conceptual setting of particle and statistical physics there is also quantitative agreement for certain questions. The critical exponents at the endpoint of the critical line of the electroweak phase transition (the onset of crossover) are believed to be precisely the same as for the liquid-gas transition near the critical pressure or for magnetic transitions in the Ising universality class³. This reveals universality as a powerful feature for the transition to complexity. Indeed, the transition to macrophysics does not involve only complications. For certain questions it can also bring enormous simplifications. Due to partial

²The microwave background radiation provides so far the most precise test of the spectrum of black-body radiation.

³Numerical simulations [23] are consistent with this picture.

fixed points in the renormalization flow of effective couplings between short and long distances much of the microscopic details can be lost. If the fluctuation effects are strong enough, the long-distance behavior loses memory of the microscopic details of the model. This is the reason why certain features of high temperature QCD may be testable in magnets or similar statistical systems. For example, it is possible that the temperature and density dependence of the chiral condensate in QCD can be approximated in a certain range by the critical equation of state of the $O(4)$ Heisenberg model [24]-[28] or by the Ising model at a nonzero density critical endpoint [29, 30].

Exact renormalization group equations describe the scale dependence of some type of “effective action”. In this context an effective action is a functional of fields from which the physical properties at a given length or momentum scale can be computed. The exact equations can be derived as formal identities from the functional integral which defines the theory. They are cast in the form of functional differential equations. Different versions of exact renormalization group equations have already a long history [1]–[7]. The investigation of the generic features of their solutions has led to a deep insight into the nature of renormalizability. In particle physics, the discussion of perturbative solutions has led to a new proof of perturbative renormalizability of the ϕ^4 -theory [6]. Nevertheless, the application of exact renormalization group methods to non-perturbative situations has been hindered for a long time by the complexity of functional differential equations. First considerable progress for the description of critical phenomena has been achieved using the scaling-field method [31]. In this approach the exact renormalization group equation is transformed into an infinite hierarchy of nonlinear ordinary differential equations for scaling fields [32]. Estimates for non-trivial critical exponents and scaling functions, e.g. for three-dimensional scalar $O(N)$ -models, are obtained from a truncated expansion around the trivial (Gaussian) fixed point and certain balance assumptions constraining what operators to include in the approximation [31]. Another very fruitful approach is based on evaluating the effective action functional for constant fields and neglecting all non-trivial momentum dependencies. This so-called local potential approximation, originally considered in [33], was first employed in [34, 7] to compute critical exponents for three-dimensional scalar $O(N)$ -models. Unfortunately, the formulation used in that work could not be used for a systematic inclusion of the neglected momentum dependencies. Some type of expansion is needed, however, if one wants to exploit the exactness of the functional differential equation in practice – otherwise any reasonable guess of a realistic renormalization group equation does as well.

Since exact solutions to functional differential equations seem only possible for some limiting cases⁴, it is crucial to find a formulation which permits non-perturbative approximations. Those proceed by a truncation of the most general form of the effective action and therefore need a qualitative understanding of its properties. The formulation of an exact renormalization group equation based on the effective average action [8, 9] has been proven successful in this respect. It is the basis of the non-perturbative flow equations which we discuss in this review. The effective average action is the generating functional of

⁴An example is the $O(N)$ -model for $N \rightarrow \infty$ discussed in subsection 3.3.

one-particle irreducible correlation functions in presence of an infrared cutoff scale k . Only fluctuations with momenta larger than k are included in its computation. For $k \rightarrow 0$ all fluctuations are included and one therefore obtains the usual effective action from which appropriate masses and vertices can be read off directly. The k dependence is described by an exact renormalization group equation that closely resembles a renormalization group improved one-loop equation [9]. In fact, the transition from classical propagators and vertices to effective propagators and vertices transforms the one-loop expression into an exact result. This close connection to perturbation theory for which we have intuitive understanding is an important key for devising non-perturbative approximations. Furthermore, the one-loop expression is manifestly infrared and ultraviolet finite and can be used directly in arbitrary number of dimensions, even in the presence of massless modes.

The aim of this report is to show that this version of flow equations can be used in practice for the transition from microphysics to macrophysics, even in the presence of strong couplings and a large correlation length. We derive the exact renormalization group equation and various non-perturbative truncations in section 2. In particular, we demonstrate in section 2.5 that already an extremely simple truncation gives a unified picture of the phase transitions in $O(N)$ -symmetric scalar theories in arbitrary dimensions d , including the critical exponents for $d = 3$ and the Kosterlitz-Thouless phase transition for $d = 2$, $N = 2$. In section 3 we discuss the solutions to the flow equation in more detail. We present an exact solution for the limit $N \rightarrow \infty$. We also propose a renormalization group-improved perturbation theory as an iterative solution. We show how the effective potential becomes convex in the limit $k \rightarrow 0$ in case of spontaneous symmetry-breaking where the perturbative potential is nonconvex. Section 4 discusses the universality class of $O(N)$ -symmetric scalar models in more detail. We derive the universal critical equation of state. For the special example of carbon dioxide we explicitly connect the microphysics with the macrophysics. In addition to the universal part this also yields the non-universal critical amplitudes in the vicinity of the second-order phase transition at the endpoint of the critical line. After a short discussion of the critical behavior of polymer chains we turn to the Kosterlitz-Thouless phase transition for two-dimensional models with a continuous abelian symmetry.

First-order phase transitions are discussed in section 4.6 and section 5. The matrix model investigated in section 5 gives an example of a radiatively induced first-order transition as it is also characteristic for the abelian Higgs model relevant for low T_c superconductivity. We discuss under which conditions first-order transitions are characterized by universal behavior. In particular, we present a universal critical equation of state for first order transitions which involves two scaling variables and we discuss its range of applicability. In section 6 we turn to the old problem of spontaneous nucleation in first-order transitions. We show that a detailed understanding of coarse graining is crucial for a quantitative computation of the nucleation rate. We also discuss the limits of validity of spontaneous nucleation theory, in particular for radiatively induced first order transitions. Our results agree well with recent numerical simulations.

Section 7 is devoted to quantum statistics and quantum field theory in thermal equilibrium. The flow equation generalizes easily to the Matsubara formalism and one sees that dimensional

reduction arises as a natural consequence. Whereas for momenta larger than the temperature the (four-dimensional) quantum statistics are relevant, the momenta below T are governed by classical (three-dimensional) statistics. Correspondingly, the flow changes from a four-dimensional to a three-dimensional flow as k crosses the temperature. This section also contains the flow equation for fermions. We show how the renormalization flow leads to a consistent picture of a second order phase transition for the high temperature ϕ^4 -quantum field theory and introduce the notion of quantum universality. Finally, section 8 deals with the chiral phase transition in QCD. We discuss both the high temperature and the high density chiral phase transition within effective fermionic models with multi-quark interactions. In particular, we relate the universal critical behavior at the high temperature phase transition or crossover to particle masses and decay constants in the vacuum for QCD with two light quarks. After reading section 2 all sections are essentially self-contained, with the exception of section 8 relying on results from section 7. Section 3 contains some more advanced topics that are not mandatory for a first understanding of the concrete models in sections 4-8. In the second part of the introduction we briefly review the basics of the fluctuation problem in statistical physics and quantum field theory. This section may be skipped by the experienced reader.

Several results in statistical physics and particle physics have been obtained first with the method presented here. This includes the universal critical equation of state for spontaneous breaking of a continuous symmetry in Heisenberg models [36], the universal critical equation of state for first-order phase transitions in matrix models [37], the non-universal critical amplitudes with an explicit connection of the critical behavior to microphysics (CO_2) [38], a quantitatively reliable estimate of the rate of spontaneous nucleation [39, 40], a classification of all possible fixed points for (one component) scalar theories in two and three dimensions in case of a weak momentum dependence of the interactions [41], the second-order phase transition in the high temperature φ^4 quantum field theory [42], the phase diagram for the abelian Higgs model for N charged scalar fields [43, 44], the prediction that the electroweak interactions become strong at high temperature, with the suggestion that the standard model may show a crossover instead of a phase transition [11, 12]; in strong interaction physics the interpolation between the low temperature chiral perturbation theory results and the high temperature critical behavior for two light quarks in an effective model [28]. All these results are in the non-perturbative domain. In addition, the approach has been tested successfully through a comparison with known high precision results on critical exponents and universal critical amplitude ratios and effective couplings.

Our main conclusion can already be drawn at this place: the method works in practice. If needed and with sufficient effort high precision results can be obtained in many non-perturbative situations. New phenomena become accessible to a reliable analytical treatment.

We do not attempt to give an overview over all relevant results. Rather we concentrate on a systematic development which should enable the reader to employ the method by himself. For an extensive review on work for scalar field theories and a comprehensive reference list we refer the reader to C. Bagnuls and C. Bervillier [45]. For a review including the basis and origins of renormalization group ideas in statistical physics and condensed matter theory we

refer to M. E. Fisher [46]. We have omitted two important issues: the formulation of the flow equations for gauge theories [47, 11], [48]–[76] and for composite operators [78]. The latter is important in order to achieve a change of effective degrees of freedom during the flow.

1.2 Fluctuations and the infrared problem

(This introductory subsection may be skipped by experienced readers.)

The basic object in statistical physics is the (canonical) partition function

$$Z = \text{Tr } e^{-\beta H} \tag{1.1}$$

with H the Hamiltonian and $\beta = T^{-1}$. The trace involves an integration over all microscopic degrees of freedom. For classical statistics it typically stands for a (generalized) phase space integral and the classical Hamiltonian is simply a function of the integration variables. In most circumstances it can be decomposed as $H = H_1 + H_2$ with H_2 quadratic in some momentum-type variable on which H_1 does not depend. The Gaussian integration over the momentum-type variable is then trivial and usually omitted. We will be concerned with many-body systems where the remaining degrees of freedom $\chi_a(\vec{x})$ can be associated with points \vec{x} in space. For simplicity we discuss in this introduction only a single real variable $\chi(x)$. The partition function can then be written in the form of a “functional integral”

$$Z = \int D\chi e^{-S[\chi]}, \tag{1.2}$$

where $S = \beta H_1$. If the space points \vec{x} are on some discrete lattice with finite volume, the functional measure is simply the product of integrations at every point

$$\int D\chi \equiv \prod_{\vec{x}} \int d\chi(\vec{x}) \tag{1.3}$$

This can be generalized to the limits of continuous space (when the lattice distance goes to zero) and of infinite volume. In this review we concentrate on continuous space with the appropriate translation and rotation symmetries. (Our formalism is, however, not restricted to this case.) As a typical example one may associate $\chi(x)$ with a density field $n(x)$ by $\chi(x) = a + b n(x)$ and consider a Hamiltonian containing local and gradient interactions⁵

$$S = \int d^3x \left\{ \frac{1}{2} \vec{\nabla} \chi(x) \vec{\nabla} \chi(x) + \frac{m^2}{2} \chi^2(x) + \frac{\lambda}{8} \chi^4(x) \right\}. \tag{1.4}$$

The mean values or expectation values can be computed as weighted integrals, e.g.

$$\langle \chi(x) \chi(y) \rangle = Z^{-1} \int D\chi \chi(x) \chi(y) e^{-S[\chi]}. \tag{1.5}$$

⁵The constants a, b can be chosen such that there is no cubic term $\sim \chi^3(x)$ and the gradient term has standard normalization. A linear term will be included below as a “source” term.

A few generalizations are straightforward: In presence of a chemical potential μ for some conserved quantity N we will consider the grand canonical partition function

$$Z = \text{Tr} e^{-\beta(H-\mu N)} \quad (1.6)$$

The μ -dependent part can either be included in the definition of $S = \beta(H_1 - \mu N)$ or, if linear in χ , be treated as a source (see below and subsection 2.1). For quantum statistics H is an operator acting on the microphysical states. Nevertheless, the partition function can again be written as a functional integral, now in four dimensions. We will discuss this case in section 7. Furthermore, the relevant physics may only involve degrees of freedom on a surface, a line or a single point. Classical statistics is then given by a D -dimensional functional integral and quantum statistics by a $D + 1$ dimensional functional integral, with $D = 2, 1, 0$, respectively. Particle physics can be derived from a four-dimensional functional integral, the Feynman path integral in Euclidean space. Except for the dimensionality, we therefore can treat particle physics and classical statistical physics on the same footing. There is no difference⁶ between the formulation of particle physics – i.e. quantum field theory – and the theory of many-body quantum statistical systems, besides the symmetries particular to particle physics.

The thermodynamic potential

$$W[J] = \ln Z[J] \quad (1.7)$$

is related to an extension of the partition function in the presence of arbitrary inhomogeneous “sources” or “external fields” $J(x)$ that multiply a term linear in χ :

$$Z[J] = \int D\chi \exp \left\{ -S[\chi] + \int d^d x \chi(x) J(x) \right\}. \quad (1.8)$$

W and Z are functionals of $J(x)$. The (functional) derivatives of W with respect to $J(x)$ generate the connected correlation functions, e.g. the average density or the density-density correlation

$$\frac{\delta W}{\delta J(x)} = \langle \chi(x) \rangle \equiv \varphi(x) \quad (1.9)$$

$$\frac{\delta^2 W}{\delta J(x) \delta J(y)} = \langle \chi(x) \chi(y) \rangle - \langle \chi(x) \rangle \langle \chi(y) \rangle. \quad (1.10)$$

Here the mean values depend on the sources, e.g. $\varphi \equiv \varphi[J]$. The effective action $\Gamma[\varphi]$ is another thermodynamic potential, related to $W[J]$ by a Legendre transform

$$\Gamma[\varphi] = -W[J] + \int d^d x \varphi(x) J(x), \quad (1.11)$$

with $J[\varphi]$ obtained by the inversion of $\varphi[J]$ from eq. (1.9). $\Gamma[\varphi]$ is easier to compute than $W[J]$ and the physical observables can be extracted very simply from it (see section 2.1).

⁶In the modern view, quantum field theory is not considered to be valid up to arbitrarily short distances. Similarly to statistical physics, a given model should be considered as an effective description for momenta below some ultraviolet cutoff Λ . This cutoff typically appears in all momentum integrals. For the standard model it indicates the onset of new physics like grand unification or unification with gravity.

The effective action can be written as an implicit functional integral in the presence of a “background field” φ

$$\exp\{-\Gamma[\varphi]\} = \int D\chi' \exp \left\{ -S[\varphi + \chi'] + \int d^d x \frac{\delta\Gamma}{\delta\varphi}(x) \chi'(x) \right\}. \quad (1.12)$$

A perturbative expansion treats the fluctuations χ' around the background φ in a saddle point approximation. In lowest order (tree approximation) one has $\Gamma^{(0)}[\varphi] = S[\varphi]$. For the one-loop order we expand

$$\begin{aligned} S[\varphi + \chi'] &= S[\varphi] + \int d^d x \frac{\delta S}{\delta\varphi}(x) \chi'(x) + \\ &\frac{1}{2} \int d^d x d^d y \chi'(x) S^{(2)}(x, y) \chi'(y) + \dots \end{aligned} \quad (1.13)$$

with

$$S^{(2)}(x, y) = \frac{\delta^2 S}{\delta\varphi(x) \delta\varphi(y)}. \quad (1.14)$$

The linear terms cancel in this order and one finds from the Gaussian integral

$$\Gamma[\varphi] = S[\varphi] + \frac{1}{2} \text{Tr} \ln S^{(2)}[\varphi] + \dots \quad (1.15)$$

For constant φ this yields the one-loop effective potential $U_0 = \Gamma/V_d$

$$\begin{aligned} U_0(\varphi) &= \frac{1}{2} m^2 \varphi^2 + \frac{1}{8} \lambda \varphi^4 + U_0^{(1)}(\varphi) + \dots \\ U_0^{(1)}(\varphi) &= \frac{1}{2} \int \frac{d^d q}{(2\pi)^d} \ln \left(q^2 + m^2 + \frac{3}{2} \lambda \varphi^2 \right), \end{aligned} \quad (1.16)$$

with $V_d = \int d^d x$. A typical Landau theory results from the assumption that the fluctuation effects induce a change of the “couplings” m^2 and λ (“renormalization”) without a modification of the quartic form of the potential.

Let us consider classical statistics ($d = 3$) and perform the momentum integration with some ultraviolet cutoff⁷ $q^2 \leq \Lambda^2$

$$U_0^{(1)}(\rho) = \frac{3\lambda\Lambda}{4\pi^2} \rho - \frac{1}{12\pi} (m^2 + 3\lambda\rho)^{3/2}, \quad \rho = \frac{1}{2} \varphi^2. \quad (1.17)$$

Here we have neglected corrections which are suppressed by powers of $(m^2 + 3\lambda\rho)/\Lambda^2$. Defining renormalized couplings⁸

$$m_R^2 = \frac{\partial U_0}{\partial \rho}(0), \quad \lambda_R = \frac{\partial^2 U_0}{\partial \rho^2}(0) \quad (1.18)$$

one obtains ($m^2 \geq 0$)

$$\begin{aligned} m_R^2 &= m^2 + \frac{3\lambda\Lambda}{4\pi^2} - \frac{3\lambda}{8\pi} m \\ \lambda_R &= \lambda - \frac{9\lambda^2}{16\pi m}. \end{aligned} \quad (1.19)$$

⁷On a cubic lattice, Λ would be related to the lattice distance a by $\Lambda = \pi/a$ and one has to replace for the inverse propagator $q^2 \rightarrow (2/a^2) \sum_{\mu} (1 - \cos a q_{\mu})$.

⁸We omit here for simplicity the wave function renormalization.

As expected, the corrections are large for large couplings λ . In addition, the correction to λ diverges as $m \rightarrow 0$. Since the correlation length ξ is given by m_R^{-1} , we see here the basic reasons why the transition from microphysics to macrophysics becomes difficult for large couplings and large correlation length.

Due to the linear “ultraviolet divergence” in the mass renormalization⁹ $\sim 3\lambda\Lambda/4\pi^2$, a large correlation length m_R^{-1} actually requires a negative value of m^2 . On the other hand, we note that the saddle point expansion is valid only for $m^2 + 3\lambda\rho > 0$ and breaks down at $\rho = 0$ if m^2 becomes negative. The situation can be improved by using in the one-loop expression (1.17) the renormalized parameters m_R and λ_R instead of m and λ . For the second term in eq. (1.17) the justification¹⁰ for the “renormalization group improvement” arises from the observation that the momentum integral is dominated by momenta $q^2 \approx m^2$. Through an iterative procedure corresponding to the inclusion of higher loops, the physical infrared cutoff should be replaced by m_R . We will see later in more detail how this renormalization improvement arises through the formulation of flow equations.

Writing U_0 in terms of renormalized parameters

$$U_0 = \left(m_R^2 + \frac{3\lambda_R m_R}{8\pi}\right)\rho + \frac{1}{2}\left(\lambda_R + \frac{9\lambda_R^2}{16\pi m_R}\right)\rho^2 - \frac{1}{12\pi}(m_R^2 + 3\lambda_R\rho)^{3/2} \quad (1.20)$$

we can compute the deviations from the Landau theory, i.e.

$$\frac{\partial^3 U_0}{\partial \rho^3}(0) = \frac{27\lambda_R^3}{32\pi m_R^3}. \quad (1.21)$$

We can also formulate a criterion for the validity of the renormalization group-improved saddle-point approximation, namely that the one-loop contributions to m_R and λ_R should not dominate these couplings. This yields

$$\frac{\lambda_R}{m_R} < \frac{16\pi}{9}. \quad (1.22)$$

The renormalized coupling λ_R is not independent of m_R . If we take the renormalization group improvement literally, we could solve the relation (cf. eq. (1.19))

$$\lambda = \lambda_R + \frac{9\lambda_R^2}{16\pi m_R} \quad (1.23)$$

for fixed λ and find

$$\frac{\lambda_R}{m_R} = \frac{8\pi}{9} \left(\sqrt{1 + \frac{9\lambda}{4\pi m_R}} - 1 \right). \quad (1.24)$$

We see that for an arbitrary positive λ the condition (1.22) breaks down in the limit of infinite correlation length $m_R \rightarrow 0$. For a second-order phase transition this is exactly what happens near the critical temperature, and we encounter here the infrared problem for critical phenomena.

⁹For finite Λ there is of course no divergence. We employ here the language of particle physics which refers to the limit $\Lambda \rightarrow \infty$.

¹⁰For the correction to $m^2 \sim \lambda\Lambda$ this replacement is not justified.

One concludes that fluctuation effects beyond the Landau theory become important for

$$m_R \lesssim \frac{3\lambda}{4\pi}. \quad (1.25)$$

If one is close (but not too close) to the phase transition, a linear approximation $m_R = A(T - T_c)$ remains a good guide. This provides a typical temperature interval around the critical temperature for which the Landau theory fails, namely

$$\frac{|T - T_c|}{T_c} \lesssim \frac{3\lambda}{4\pi AT_c}. \quad (1.26)$$

The width of the interval depends on the dimensionless quantities A and λ/T_c . Inside the interval (1.26) the physics is governed by the universal critical behavior. In fact, we should not trust the relation (1.23) for values of m_R for which (1.22) is violated. The correct behavior of $\lambda_R(m_R)$ will be given by the renormalization group and leads to a fixed point for the ratio $\lim_{m_R \rightarrow 0} (\lambda_R/m_R) \rightarrow \text{const.}$ As an example of universal behavior we observe that the φ^6 -coupling (1.21) is completely determined by the ratio λ_R/m_R , independently of the value of the microphysical coupling λ . This is generalized to a large class of microscopic potentials. We see how universality is equivalent to the “loss of memory” of details of the microphysics. Similar features in four dimensions are the basis for the impressive predictive power of particle physics.

In this report we present a version of the renormalization group equation where an infrared cutoff k is introduced for the momentum integral (1.16). In a rough version we use a sharp cutoff $k^2 < q^2 < \Lambda^2$ in order to define the scale-dependent potential U_k [8, 9]. The dependence of the “average potential” U_k on k is simply computed ($d = 3$) as

$$\partial_k U_k(\rho) = -\frac{k^2}{4\pi^2} \ln \left(\frac{k^2 + V' + 2\rho V''}{k^2} \right), \quad (1.27)$$

where we have introduced the classical potential

$$V = m^2 \rho + \frac{1}{2} \lambda \rho^2 \quad (1.28)$$

and subtracted an irrelevant ρ -independent constant. (Primes denote derivatives with respect to ρ .) The renormalization group improvement¹¹ replaces $V(\rho)$ by $U_k(\rho)$ and therefore leads to the nonlinear partial differential equation

$$\partial_k U_k(\rho) = -\frac{k^2}{4\pi^2} \ln \left\{ 1 + \frac{U'_k(\rho)}{k^2} + \frac{2\rho U''_k(\rho)}{k^2} \right\}. \quad (1.29)$$

This simple equation already describes correctly the qualitative behavior of $U_0 = \lim_{k \rightarrow 0} U_k$. We will encounter it later (cf. eq. (3.30)) as an approximation to the exact renormalization group equation. The present report motivates this equation and provides a formalism for

¹¹For a detailed justification see refs. [8, 9].

computing corrections to it¹². We also generalize this equation to other forms of the infrared cutoff. In section 2.5 we show how this type of equation, even in the simple quartic approximation for the potential, gives a unified picture of the phase transitions for $O(N)$ -symmetric scalar theories in arbitrary¹³ dimensions.

2 Non-Perturbative flow equation

2.1 Average action

We will concentrate on a flow equation which describes the scale dependence of the effective average action Γ_k [9]. The latter is based on the quantum field theoretical concept of the effective action Γ , i.e. the generating functional of the Euclidean one-particle irreducible (1PI) correlation functions or proper vertices (cf. eq. (1.11)). This functional is obtained after “integrating out” the quantum fluctuations. The scattering amplitudes and cross sections follow directly from an analytic continuation of the 1PI correlation functions in a standard way. Furthermore, the field equations derived from the *effective action* are exact as all quantum effects are included. In thermal and chemical equilibrium Γ includes in addition the thermal fluctuations and depends on the temperature T and chemical potential μ . In statistical physics Γ is related to the free energy as a functional of some space-dependent order parameter $\varphi(x)$. For vanishing external fields the equilibrium state is given by the minimum of Γ . More generally, in the presence of (spatially varying) external fields or sources the equilibrium state obeys

$$\frac{\delta\Gamma}{\delta\varphi(x)} = J(x), \quad (2.1)$$

and the precise relation to the thermodynamic potentials like the free energy F reads

$$F = T\Gamma_{eq} + \mu N - T \int dx \varphi_{eq}(x) J(x). \quad (2.2)$$

Here $\varphi_{eq}(x)$ solves (2.1), $\Gamma_{eq} = \Gamma[\varphi_{eq}]$, and N is the conserved quantity to which the chemical potential is associated. For homogeneous $J = j/T$ the equilibrium value of the order parameter φ is often also homogeneous. In this case the energy density ϵ , entropy density s , “particle density” n and pressure p can be simply expressed in terms of the effective potential $U(\varphi) = T\Gamma/V$, namely

$$\begin{aligned} \epsilon &= U - T \frac{\partial U}{\partial T} - \mu \frac{\partial U}{\partial \mu}, \quad s = -\frac{\partial U}{\partial T} + \frac{j\varphi}{T}, \\ n &= -\frac{\partial U}{\partial \mu}, \quad p = -U = -T\Gamma/V \end{aligned} \quad (2.3)$$

¹²Eq. (1.29) can also be obtained as the sharp cutoff limit of the Polchinski equation [6] and was discussed in ref. [7]. However, in this approach it is difficult to include the wave function renormalization and to use eq. (1.29) as a starting point of a systematic procedure.

¹³For the Kosterlitz-Thouless phase transition for $d = 2, N = 2$ the wave function renormalization must be included.

Here U has to be evaluated for the solution of $\partial U/\partial\varphi = j$, $n = N/V$ and V is the total volume of (three-dimensional) space. Evaluating U for arbitrary φ yields the equation of state in presence of homogeneous magnetic fields or other appropriate sources¹⁴.

More formally, the effective action Γ follows from a Legendre transform of the logarithm of the partition function in presence of external sources or fields (see below). Knowledge of Γ is in a sense equivalent to the “solution” of a theory. Therefore Γ is the macroscopic quantity on which we will concentrate. In particular, the effective potential U contains already a large part of the macroscopic information relevant for homogeneous states. We emphasize that the concept of the effective potential is valid universally for classical statistics and quantum statistics, or quantum field theory in thermal equilibrium, or the vacuum¹⁵.

The average action Γ_k is a simple generalization of the effective action, with the distinction that only fluctuations with momenta $q^2 \gtrsim k^2$ are included. This is achieved by implementing an infrared (IR) cutoff $\sim k$ in the functional integral that defines the effective action Γ . In the language of statistical physics, Γ_k is a type of coarse-grained free energy with a coarse graining length scale $\sim k^{-1}$. As long as k remains large enough, the possible complicated effects of coherent long-distance fluctuations play no role and Γ_k is close to the microscopic action. Lowering k results in a successive inclusion of fluctuations with momenta $q^2 \gtrsim k^2$ and therefore permits to explore the theory on larger and larger length scales. The average action Γ_k can be viewed as the effective action for averages of fields over a volume with size k^{-d} [8] and is similar in spirit to the action for block-spins on the sites of a coarse lattice.

By definition, the average action equals the standard effective action for $k = 0$, i.e. $\Gamma_0 = \Gamma$, as the IR cutoff is absent in this limit and all fluctuations are included. On the other hand, in a model with a physical ultraviolet (UV) cutoff Λ we can associate Γ_Λ with the microscopic or classical action S . No fluctuations with momenta below Λ are effectively included if the IR cutoff equals the UV cutoff. Thus the average action Γ_k has the important property that it interpolates between the classical action S and the effective action Γ as k is lowered from the ultraviolet cutoff Λ to zero:

$$\Gamma_\Lambda \approx S, \quad \lim_{k \rightarrow 0} \Gamma_k = \Gamma. \quad (2.4)$$

The ability to follow the evolution to $k \rightarrow 0$ is equivalent to the ability to solve the theory. Most importantly, the dependence of the average action on the scale k is described by an exact non-perturbative flow equation which is presented in the next subsection.

Let us consider the construction of Γ_k for a simple model with real scalar fields χ_a , $a = 1 \dots N$, in d Euclidean dimensions with classical action S . We start with the path

¹⁴For the special case where $\varphi(x)$ corresponds to the density of a conserved quantity and $j = \mu$ one has $F = T\Gamma_{eq}$. The thermodynamic relations appropriate for this case are specified in sect. 4.4. Our notation is adapted to classical statistics where $\int dx \equiv \int d^3x$. For quantum statistics or quantum field theory one has to use $\int dx \equiv \int d^4x$ where the “Euclidean time” is a torus with circumference $1/T$. The relations (2.3) remain valid for a homogeneous source $J = j$.

¹⁵The only difference concerns the evaluation of the partition function Z or $W = \ln Z = -(F - \mu N)/T$. For classical statistics it involves a D -dimensional functional integral, whereas for quantum statistics the dimension in the Matsubara formalism is $D + 1$. The vacuum in quantum field theory corresponds to $T \rightarrow 0$, with V/T the volume of Euclidean “spacetime”.

integral representation of the generating functional for the connected correlation functions in the presence of an IR cutoff. It is given by the logarithm of the (grand) canonical partition function in the presence of inhomogeneous external fields or sources J_a

$$W_k[J] = \ln Z[J] = \ln \int D\chi \exp \left(-S[\chi] - \Delta S_k[\chi] + \int d^d x J_a(x) \chi^a(x) \right). \quad (2.5)$$

In classical statistical physics S is related to the Hamiltonian H by $S = H/T$, so that e^{-S} is the usual Boltzmann factor. The functional integration $\int D\chi$ stands for the sum over all microscopic states. In turn, the field $\chi_a(x)$ can represent a large variety of physical objects like a (mass-) density field ($N = 1$), a local magnetisation ($N = 3$) or a charged order parameter ($N = 2$). The only modification as compared to the construction of the standard effective action is the addition of an IR cutoff term $\Delta S_k[\chi]$ which is quadratic in the fields and reads in momentum space ($\chi_a(-q) \equiv \chi_a^*(q)$)

$$\Delta S_k[\chi] = \frac{1}{2} \int \frac{d^d q}{(2\pi)^d} R_k(q) \chi_a(-q) \chi^a(q). \quad (2.6)$$

Here the IR cutoff function R_k is required to vanish for $k \rightarrow 0$ and to diverge for $k \rightarrow \infty$ (or $k \rightarrow \Lambda$) and fixed q^2 . This can be achieved, for example, by the exponential form

$$R_k(q) \sim \frac{q^2}{e^{q^2/k^2} - 1}. \quad (2.7)$$

For fluctuations with small momenta $q^2 \ll k^2$ this cutoff behaves as $R_k(q) \sim k^2$ and allows for a simple interpretation: Since $\Delta S_k[\chi]$ is quadratic in the fields, all Fourier modes of χ with momenta smaller than k acquire an effective mass $\sim k$. This additional mass term acts as an effective IR cutoff for the low momentum modes. In contrast, for $q^2 \gg k^2$ the function $R_k(q)$ vanishes so that the functional integration of the high momentum modes is not disturbed. The term $\Delta S_k[\chi]$ added to the classical action is the main ingredient for the construction of an effective action that includes all fluctuations with momenta $q^2 \gtrsim k^2$, whereas fluctuations with $q^2 \lesssim k^2$ are suppressed.

The expectation value of χ , i.e. the macroscopic field ϕ , in the presence of $\Delta S_k[\chi]$ and J reads

$$\phi^a(x) \equiv \langle \chi^a(x) \rangle = \frac{\delta W_k[J]}{\delta J_a(x)}. \quad (2.8)$$

We note that the relation between ϕ and J is k -dependent, $\phi = \phi_k[J]$ and therefore $J = J_k[\phi]$. In terms of W_k the average action is defined via a modified Legendre transform

$$\Gamma_k[\phi] = -W_k[J] + \int d^d x J_a(x) \phi^a(x) - \Delta S_k[\phi], \quad (2.9)$$

where we have subtracted the term $\Delta S_k[\phi]$ in the rhs. This subtraction of the IR cutoff term as a function of the macroscopic field ϕ is crucial for the definition of a reasonable coarse-grained free energy with the property $\Gamma_\Lambda \approx S$. It guarantees that the only difference between Γ_k and Γ is the effective infrared cutoff in the fluctuations. Furthermore, it has the consequence

that Γ_k does not need to be convex, whereas a pure Legendre transform is always convex by definition. The coarse-grained free energy has to become convex [79, 80] only for $k \rightarrow 0$. These considerations are important for an understanding of spontaneous symmetry breaking and, in particular, for a discussion of nucleation in a first-order phase transition.

In order to establish the property $\Gamma_\Lambda \approx S$ we consider an integral equation for Γ_k that is equivalent to (2.9). In an obvious matrix notation, where $J\chi \equiv \int d^d x J_a(x)\chi^a(x) = \int \frac{d^d p}{(2\pi)^d} J_a(-p)\chi_a(p)$ and $R_{k,ab}(q, q') = R_k(q)\delta_{ab}(2\pi)^d\delta(q - q')$, we represent (2.5) as

$$\exp\left(W_k[J]\right) = \int D\chi \exp\left(-S[\chi] + J\chi - \frac{1}{2}\chi R_k \chi\right). \quad (2.10)$$

As usual, we can invert the Legendre transform (2.9) to express

$$J = \frac{\delta\Gamma_k}{\delta\phi} + \phi R_k. \quad (2.11)$$

It is now straightforward to insert the definition (2.9) into (2.10). After a variable substitution $\chi' = \chi - \phi$ one obtains the functional integral representation of Γ_k

$$\exp(-\Gamma_k[\phi]) = \int D\chi' \exp\left(-S[\phi + \chi'] + \frac{\delta\Gamma_k}{\delta\phi}\chi' - \frac{1}{2}\chi' R_k \chi'\right). \quad (2.12)$$

This expression resembles closely the background field formalism for the effective action which is modified only by the term $\sim R_k$. For $k \rightarrow \infty$ the cutoff function R_k diverges and the term $\exp(-\chi' R_k \chi'/2)$ behaves as a delta functional $\sim \delta[\chi']$, thus leading to the property $\Gamma_k \rightarrow S$ in this limit. For a model with a sharp UV cutoff Λ it is easy to enforce the identity $\Gamma_\Lambda = S$ by choosing a cutoff function R_k which diverges for $k \rightarrow \Lambda$, like $R_k \sim q^2(e^{q^2/k^2} - e^{q^2/\Lambda^2})^{-1}$. We note, however, that the property $\Gamma_\Lambda = S$ is not essential, as the short distance laws may be parameterized by Γ_Λ as well as by S . For momentum scales much smaller than Λ universality implies that the precise form of Γ_Λ is irrelevant, up to the values of a few relevant renormalized couplings. Furthermore, the microscopic action may be formulated on a lattice instead of continuous space and can involve even variables different from $\chi_a(x)$. In this case one can still compute Γ_Λ in a first step by evaluating the functional integral (2.12) approximately. Often a saddle point expansion will do, since no long-range fluctuations are involved in the transition from S to Γ_Λ . In this report we will assume that the first step of the computation of Γ_Λ is done and consider Γ_Λ as the appropriate parametrization of the microscopic physical laws. Our aim is the computation of the effective action Γ from Γ_Λ – this step may be called “transition to complexity” and involves fluctuations on all scales. We emphasize that for large Λ the average action Γ_Λ can serve as a formulation of the microscopic laws also for situations where no physical cutoff is present, or where a momentum UV cutoff may even be in conflict with the symmetries, like the important case of gauge symmetries.

A few properties of the effective average action are worth mentioning:

1. All symmetries of the model which are respected by the IR cutoff ΔS_k are automatically symmetries of Γ_k . In particular this concerns translation and rotation invariance, and

the approach is not plagued by many of the problems encountered by a formulation of the block-spin action on a lattice. Nevertheless, our method is not restricted to continuous space. For a cubic lattice with lattice distance a the propagator only obeys the restricted lattice translation and rotation symmetries, e.g. a next neighbor interaction leads in momentum space to

$$S = \frac{2}{a^2} \int \frac{d^d q}{(2\pi)^d} \sum_{\mu} (1 - \cos a q_{\mu}) \chi^*(q) \chi(q) + \dots \quad (2.13)$$

The momentum cutoff $|q_{\mu}| \leq \Lambda$, $\Lambda = \pi/a$ also reflects the lattice symmetry. A rotation and translation symmetric cutoff R_k which only depends on q^2 obeys automatically all possible lattice symmetries. The only change as compared to continuous space will be the reduced symmetry of Γ_k .

2. In consequence, Γ_k can be expanded in terms of invariants with respect to these symmetries with couplings depending on k . For the example of a scalar $O(N)$ -model in continuous space one may use a derivative expansion ($\rho = \Phi^a \Phi_a / 2$)

$$\Gamma_k = \int d^d x \left\{ U_k(\rho) + \frac{1}{2} Z_{\Phi,k}(\rho) \partial^{\mu} \Phi_a \partial_{\mu} \Phi^a + \dots \right\} \quad (2.14)$$

and expand further in powers of ρ

$$\begin{aligned} U_k(\rho) &= \frac{1}{2} \bar{\lambda}_k (\rho - \rho_0(k))^2 + \frac{1}{6} \bar{\gamma}_k (\rho - \rho_0(k))^3 + \dots \\ Z_{\Phi,k}(\rho) &= Z_{\Phi,k}(\rho_0) + Z'_{\Phi,k}(\rho_0) (\rho - \rho_0) + \dots \end{aligned} \quad (2.15)$$

Here ρ_0 denotes the (k -dependent) minimum of the effective average potential $U_k(\rho)$. We see that Γ_k describes infinitely many running couplings.

3. Up to an overall scale factor the limit $k \rightarrow 0$ of U_k corresponds to the effective potential $U = T\Gamma/V$, from which the thermodynamic quantities can be derived for homogeneous situations according to eq. (2.3). The overall scale factor is fixed by dimensional considerations. Whereas the dimension of U_k is $(\text{mass})^d$ the dimension of U in eq. (2.3) is $(\text{mass})^4$ (for $\hbar = c = k_B = 1$). For classical statistics in $d = 3$ dimensions one has $U_k = \Gamma_k/V$ and $U = T \lim_{k \rightarrow 0} U_k$. For two dimensional systems an additional factor $\sim \text{mass}$ appears since $U_k = \Gamma_k/V_2 = L\Gamma_k/V$ implies $U = TL^{-1} \lim_{k \rightarrow 0} U_k$. Here L is the typical thickness of the two dimensional layers in a physical system. In the following we will often omit these scale factors.
4. The functional $\tilde{\Gamma}_k[\Phi] = \Gamma_k[\Phi] + \Delta S_k[\Phi]$ is the Legendre transform of W_k and therefore convex. This implies that all eigenvalues of the matrix of second functional derivatives $\Gamma^{(2)} + R_k$ are positive semi-definite. In particular, one finds for a homogeneous field Φ_a and $q^2 = 0$ the simple exact bounds for all k and ρ

$$\begin{aligned} U'_k(\rho) &\geq -R_k(0) \\ U'_k(\rho) + 2\rho U''_k(\rho) &\geq -R_k(0), \end{aligned} \quad (2.16)$$

where primes denote derivatives with respect to ρ . Even though the potential $U(\phi)$ becomes convex for $k \rightarrow 0$ it may exhibit a minimum at $\rho_0(k) > 0$ for all $k > 0$. Spontaneous breaking of the $O(N)$ -symmetry is characterized by $\lim_{k \rightarrow 0} \rho_0(k) > 0$.

5. For a formulation which respects the reparametrization invariance of physical quantities under a rescaling of the variables $\chi_a(x) \rightarrow \alpha \chi_a(x)$ the infrared cutoff should contain a wave function renormalization, e.g.

$$R_k(q) = \frac{Z_k q^2}{e^{q^2/k^2} - 1}. \quad (2.17)$$

One may choose $Z_k = Z_{\phi,k}(\rho_0)$. This choice guarantees that no intrinsic scale is introduced in the inverse average propagator

$$Z_k q^2 + R_k = Z_k P(q) = Z_k q^2 p\left(\frac{q^2}{k^2}\right). \quad (2.18)$$

This is important in order to obtain scale-invariant flow equations for critical phenomena.

6. There is no problem incorporating chiral fermions, since a chirally invariant cutoff R_k can be formulated [81, 82] (cf. section 7.2).
7. Gauge theories can be formulated along similar lines¹⁶ [47, 11], [48]–[76] even though ΔS_k may not be gauge invariant¹⁷. In this case the usual Ward identities receive corrections for which one can derive closed expressions [50]. These corrections vanish for $k \rightarrow 0$. On the other hand they appear as “counterterms” in Γ_Λ and are crucial for preserving the gauge invariance of physical quantities.
8. For the choice (2.18) the high momentum modes are very effectively integrated out because of the exponential decay of R_k for $q^2 \gg k^2$. Nevertheless, it is sometimes technically easier to use a cutoff without this fast decay property, e.g. $R_k \sim k^2$ or $R_k \sim k^4/q^2$. In the latter cases one has to be careful with possible remnants of an incomplete integration of the short distance modes. An important technical simplification can also be achieved by a sharp momentum cutoff [3]. This guarantees complete integration of the short distance modes, but poses certain problems with analyticity [8, 83, 84, 85, 86]. In contrast, a smooth cutoff like (2.18) does not introduce any non-analytical behavior. The results for physical quantities are independent of the choice of the cutoff scheme R_k . On the other hand, both Γ_Λ and the flow with k are scheme-dependent. The scheme dependence of the final results is a good check for approximations [8, 87, 88, 89, 90].
9. Despite a similar spirit and many analogies, there is a conceptual difference to the Wilsonian effective action S_Λ^W . The Wilsonian effective action describes a set of different actions (parameterized by Λ) for one and the same model — the n -point functions are

¹⁶See also [77] for applications to gravity.

¹⁷For a manifestly gauge invariant formulation in terms of Wilson loops see ref. [69].

independent of Λ and have to be computed from S_Λ^W by further functional integration. In contrast, Γ_k can be viewed as the effective action for a set of different “models” — for any value of k the effective average action is related to the generating functional of $1PI - n$ -point functions for a model with a different action $S_k = S + \Delta S_k$. The n -point functions depend on k . The Wilsonian effective action does not generate the $1PI$ Green functions [91].

10. Because of the incorporation of an infrared cutoff, Γ_k is closely related to an effective action for averages of fields [8] where the average is taken over a volume $\sim k^{-d}$.

2.2 Exact flow equation

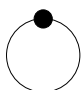
The dependence of the average action Γ_k on the coarse graining scale k is described by an exact non-perturbative flow equation [9, 92, 93, 94]

$$\frac{\partial}{\partial k} \Gamma_k[\phi] = \frac{1}{2} \text{Tr} \left\{ \left[\Gamma_k^{(2)}[\phi] + R_k \right]^{-1} \frac{\partial}{\partial k} R_k \right\}. \quad (2.19)$$

The trace involves an integration over momenta or coordinates as well as a summation over internal indices. In momentum space it reads $\text{Tr} = \sum_a \int d^d q / (2\pi)^d$, as appropriate for the unit matrix $\mathbf{1} = (2\pi)^d \delta(q - q') \delta_{ab}$. The exact flow equation describes the scale dependence of Γ_k in terms of the inverse average propagator $\Gamma_k^{(2)}$, given by the second functional derivative of Γ_k with respect to the field components

$$\left(\Gamma_k^{(2)} \right)_{ab}(q, q') = \frac{\delta^2 \Gamma_k}{\delta \phi^a(-q) \delta \phi^b(q')}. \quad (2.20)$$

It has a simple graphical expression as a one-loop equation

$$\frac{\partial \Gamma_k}{\partial k} = \frac{1}{2} \text{Tr} \left(\text{Propagator} \right)$$


with the full k -dependent propagator associated to the propagator line and the dot denoting the insertion $\partial_k R_k$.

Due to the appearance of the exact propagator $(\Gamma_k^{(2)} + R_k)^{-1}$, eq. (2.19) is a functional differential equation. It is remarkable that the transition from the classical propagator in presence of the infrared cutoff, $(S^{(2)} + R_k)^{-1}$, to the full propagator turns the one-loop expression into an exact identity which incorporates effects of arbitrarily high loop order as well as genuinely non-perturbative effects¹⁸ like instantons in QCD.

The exact flow equation (2.19) can be derived in a straightforward way [9]. Let us write

$$\Gamma_k[\phi] = \tilde{\Gamma}_k[\phi] - \Delta S_k[\phi], \quad (2.21)$$

¹⁸We note that anomalies which arise from topological obstructions in the functional measure manifest themselves already in the microscopic action Γ_Λ . The long-distance non-perturbative effects (“large-size instantons”) are, however, completely described by the flow equation (2.19).

where, according to (2.9),

$$\tilde{\Gamma}_k[\phi] = -W_k[J] + \int d^d x J(x)\phi(x) \quad (2.22)$$

and $J = J_k(\phi)$. We consider for simplicity a one-component field and derive first the scale dependence of $\tilde{\Gamma}$:

$$\frac{\partial}{\partial k} \tilde{\Gamma}_k[\phi] = - \left(\frac{\partial W_k}{\partial k} \right) [J] - \int d^d x \frac{\delta W_k}{\delta J(x)} \frac{\partial J(x)}{\partial k} + \int d^d x \phi(x) \frac{\partial J(x)}{\partial k}. \quad (2.23)$$

With $\phi(x) = \delta W_k / \delta J(x)$ the last two terms in (2.23) cancel. The k -derivative of W_k is obtained from its defining functional integral (2.5). Since only R_k depends on k this yields

$$\frac{\partial}{\partial k} \tilde{\Gamma}_k[\phi] = \langle \frac{\partial}{\partial k} \Delta S_k[\chi] \rangle = \langle \frac{1}{2} \int d^d x d^d y \chi(x) \frac{\partial}{\partial k} R_k(x, y) \chi(y) \rangle. \quad (2.24)$$

where $R_k(x, y) \equiv R_k(i\partial_x)\delta(x - y)$ and

$$\langle A[\chi] \rangle = Z^{-1} \int D\chi A[\chi] \exp(-S[\chi] - \Delta_k S[\chi] + \int d^d x J(x)\chi(x)). \quad (2.25)$$

Let $G(x, y) = \delta^2 W_k / \delta J(x) \delta J(y)$ denote the connected 2-point function and decompose

$$\langle \chi(x)\chi(y) \rangle = G(x, y) + \langle \chi(x) \rangle \langle \chi(y) \rangle \equiv G(x, y) + \phi(x)\phi(y). \quad (2.26)$$

Plugging this decomposition into (2.24) the scale dependence of $\tilde{\Gamma}_k$ can be expressed as

$$\begin{aligned} \frac{\partial}{\partial k} \tilde{\Gamma}_k[\phi] &= \frac{1}{2} \int d^d x d^d y \left\{ \frac{\partial}{\partial k} R_k(x, y) G(y, x) + \phi(x) \frac{\partial}{\partial k} R_k(x, y) \phi(y) \right\} \\ &\equiv \frac{1}{2} \text{Tr} \left\{ G \frac{\partial}{\partial k} R_k \right\} + \frac{\partial}{\partial k} \Delta S_k[\phi]. \end{aligned} \quad (2.27)$$

The exact flow equation for the average action Γ_k follows now through (2.21)

$$\frac{\partial}{\partial k} \Gamma_k[\phi] = \frac{1}{2} \text{Tr} \left\{ G \frac{\partial}{\partial k} R_k \right\} = \frac{1}{2} \text{Tr} \left\{ \left[\Gamma_k^{(2)}[\phi] + R_k \right]^{-1} \frac{\partial}{\partial k} R_k \right\} \quad (2.28)$$

For the last equation we have used that $\tilde{\Gamma}_k^{(2)}(x, y) \equiv \delta^2 \tilde{\Gamma}_k / \delta \phi(x) \delta \phi(y) = \delta J(x) / \delta \phi(y)$ is the inverse of $G(x, y) \equiv \delta^2 W_k / \delta J(x) \delta J(y) = \delta \phi(x) / \delta J(y)$:

$$\int d^d y G(x, y) (\Gamma_k^{(2)} + R_k)(y, z) = \delta(x - z) \quad (2.29)$$

It is straightforward to write the above identities in momentum space and to generalize them to N components by using the matrix notation introduced above.

Let us point out a few properties of the exact flow equation:

1. For a scaling form of the evolution equation and a formulation closer to the usual β -functions one may replace the partial k -derivative in (2.19) by a partial derivative with respect to the logarithmic variable $t = \ln(k/\Lambda)$.

2. Exact flow equations for n -point functions can be easily obtained from (2.19) by differentiation. The flow equation for the two-point function $\Gamma_k^{(2)}$ involves the three and four-point functions, $\Gamma_k^{(3)}$ and $\Gamma_k^{(4)}$, respectively. One may write schematically

$$\begin{aligned}
\frac{\partial}{\partial t} \Gamma_k^{(2)} &= \frac{\partial}{\partial t} \frac{\partial^2 \Gamma_k}{\partial \phi \partial \phi} \\
&= -\frac{1}{2} \text{Tr} \left\{ \frac{\partial R_k}{\partial t} \frac{\partial}{\partial \phi} \left(\left[\Gamma_k^{(2)} + R_k \right]^{-1} \Gamma_k^{(3)} \left[\Gamma_k^{(2)} + R_k \right]^{-1} \right) \right\} \\
&= \text{Tr} \left\{ \frac{\partial R_k}{\partial t} \left[\Gamma_k^{(2)} + R_k \right]^{-1} \Gamma_k^{(3)} \left[\Gamma_k^{(2)} + R_k \right]^{-1} \Gamma_k^{(3)} \left[\Gamma_k^{(2)} + R_k \right]^{-1} \right\} \\
&\quad - \frac{1}{2} \text{Tr} \left\{ \frac{\partial R_k}{\partial t} \left[\Gamma_k^{(2)} + R_k \right]^{-1} \Gamma_k^{(4)} \left[\Gamma_k^{(2)} + R_k \right]^{-1} \right\} .
\end{aligned} \tag{2.30}$$

Evaluating this equation for $\phi = 0$ one sees immediately the contributions to the flow of the two-point function from diagrams with three- and four-point vertices. Below we will see in more detail that the diagrammatics is closely linked to the perturbative graphs. In general, the flow equation for $\Gamma_k^{(n)}$ involves $\Gamma_k^{(n+1)}$ and $\Gamma_k^{(n+2)}$.

3. As already mentioned, the flow equation (2.19) closely resembles a one-loop equation. Replacing $\Gamma_k^{(2)}$ by the second functional derivative of the classical action, $S^{(2)}$, one obtains the corresponding one-loop result. Indeed, the one-loop formula for Γ_k reads

$$\Gamma_k[\phi] = S[\phi] + \frac{1}{2} \text{Tr} \ln (S^{(2)}[\phi] + R_k) \tag{2.31}$$

and taking a k -derivative of (2.31) gives a one-loop flow equation very similar to (2.19). The “full renormalization group improvement” $S^{(2)} \rightarrow \Gamma_k^{(2)}$ turns the one-loop flow equation into an exact non-perturbative flow equation. Replacing the propagator and vertices appearing in $\Gamma_k^{(2)}$ by the ones derived from the classical action, but with running k -dependent couplings, and expanding the result to lowest non-trivial order in the coupling constants, one recovers standard renormalization group improved one-loop perturbation theory.

4. The additional cutoff function R_k with a form like the one given in eq. (2.17) renders the momentum integration implied in the trace of (2.19) both infrared and ultraviolet finite. In particular, for $q^2 \ll k^2$ one has an additional mass-like term $R_k \sim k^2$ in the inverse average propagator. This makes the formulation suitable for dealing with theories which are plagued by infrared problems in perturbation theory. For example, the flow equation can be used in three dimensions in the phase with spontaneous symmetry breaking despite the existence of massless Goldstone bosons for $N > 1$. We recall that all eigenvalues of the matrix $\Gamma^{(2)} + R_k$ must be positive semi-definite (cf. eq. (2.16)). We note that the derivation of the exact flow equation does not depend on the particular choice of the cutoff function. Ultraviolet finiteness, however, is related to a fast decay of $\partial_t R_k$ for $q^2 \gg k^2$. If for some other choice of R_k the rhs of the flow equation would not remain ultraviolet finite this would indicate that the high momentum modes have not

yet been integrated out completely in the computation of Γ_k . Unless stated otherwise we will always assume a sufficiently fast decaying choice of R_k in the following.

5. Since no infinities appear in the flow equation, one may “forget” its origin from a functional integral. Indeed, for a given choice of the cutoff function R_k all microscopic physics is encoded in the microscopic effective action Γ_Λ . The model is completely specified by the flow equation (2.19) and the “initial value” Γ_Λ . In a quantum field theoretical sense the flow equation defines a regularization scheme. The “ERGE”-scheme is specified by the flow equation, the choice of R_k and the “initial condition” Γ_Λ . This is particularly important for gauge theories where other regularizations in four dimensions and in the presence of chiral fermions are difficult to construct. For gauge theories Γ_Λ has to obey appropriately modified Ward identities. In the context of perturbation theory a first proposal for how to regularize gauge theories by use of flow equations can be found in [48]. We note that in contrast to previous versions of exact renormalization group equations there is no need in the present formulation to construct an ultraviolet momentum cutoff – a task known to be very difficult in non-Abelian gauge theories.

As for all regularizations the physical quantities should be independent of the particular regularization scheme. In our case different choices of R_k correspond to different trajectories in the space of effective actions along which the unique infrared limit Γ_0 is reached. Nevertheless, once approximations are applied not only the trajectory but also its end point may depend on the precise definition of the function R_k . As mentioned above, this dependence may be used to study the robustness of the approximation.

6. Extensions of the flow equations to gauge fields [47, 11], [48]–[76] and fermions [81, 82] are available.
7. We emphasize that the flow equation (2.19) is formally equivalent to the Wilsonian exact renormalization group equation [2, 3, 4, 5, 6, 7]. The latter describes how the Wilsonian effective action S_Λ^W changes with an ultraviolet cutoff Λ . Polchinski’s continuum version of the Wilsonian flow equation [6]¹⁹ can be transformed into eq. (2.19) by means of a Legendre transform, a suitable field redefinition and the association $\Lambda = k$ [92, 96, 97]. Although the formal relation is simple, the practical calculation of S_k^W from Γ_k (and vice versa) can be quite involved²⁰. In the presence of massless particles the Legendre transform of Γ_k does not remain local and S_k^W is a comparatively complicated object. We will argue below that the crucial step for a practical use of the flow equation in a non-perturbative context is the ability to devise a reasonable approximation scheme or truncation. It is in this context that the close resemblance of eq. (2.19) to a perturbative expression is of great value.
8. In contrast to the Wilsonian effective action no information about the short-distance physics is effectively lost as k is lowered. Indeed, the effective average action for fields

¹⁹For a detailed presentation see e.g. [95].

²⁰If this problem could be solved, one would be able to construct an UV momentum cutoff which preserves gauge invariance by starting from the Ward identities for Γ_k .

with high momenta $q^2 \gg k^2$ is already very close to the effective action. Therefore Γ_k generates quite accurately the vertices with high external momenta. More precisely, this is the case whenever the external momenta act effectively as an independent “physical” IR cutoff in the flow equation for the vertex. There is then only a minor difference between $\Gamma_k^{(n)}$ and the exact vertex $\Gamma^{(n)}$.

9. An exact equation of the type (2.19) can be derived whenever R_k multiplies a term quadratic in the fields, cf. (2.6). The feature that R_k acts as a good infrared cutoff is not essential for this. In particular, one can easily write down an exact equation for the dependence of the effective action on the chemical potential [98]. Another interesting exact equation describes the effect of a variation of the microscopic mass term for a field, as, for example, the current quark mass in QCD. In some cases an additional UV-regularization may be necessary since the UV-finiteness of the momentum integral in (2.19) may not be given.

2.3 Truncations

Even though intuitively simple, the replacement of the (RG-improved) classical propagator by the full propagator turns the solution of the flow equation (2.19) into a difficult mathematical problem: The evolution equation is a functional differential equation. Once Γ_k is expanded in terms of invariants (e.g. Eqs.(2.14), (2.15)) this is equivalent to a coupled system of non-linear partial differential equations for infinitely many couplings. General methods for the solution of functional differential equations are not developed very far. They are mainly restricted to iterative procedures that can be applied once some small expansion parameter is identified. This covers usual perturbation theory in the case of a small coupling, the $1/N$ -expansion or expansions in the dimensionality $4 - d$ or $d - 2$. It may also be extended to less familiar expansions like a derivative expansion which is related in critical three dimensional scalar theories to a small anomalous dimension [99]. In the absence of a clearly identified small parameter one nevertheless needs to truncate the most general form of Γ_k in order to reduce the infinite system of coupled differential equations to a (numerically) manageable size. This truncation is crucial. It is at this level that approximations have to be made and, as for all non-perturbative analytical methods, they are often not easy to control.

The challenge for non-perturbative systems like critical phenomena in statistical physics or low momentum QCD is to find flow equations which (a) incorporate all the relevant dynamics so that neglected effects make only small changes, and (b) remain of manageable size. The difficulty with the first task is a reliable estimate of the error. For the second task the main limitation is a practical restriction for numerical solutions of differential equations to functions depending only on a small number of variables. The existence of an exact functional differential flow equation is a very useful starting point and guide for this task. At this point the precise form of the exact flow equation is quite important. Furthermore, it can be used for systematic expansions through enlargement of the truncation and for an error estimate in this way. Nevertheless, this is not all. Usually, physical insight into a model is necessary to device a useful non-perturbative truncation!

Several approaches to non-perturbative truncations have been explored so far ($\rho \equiv \frac{1}{2}\Phi_a\Phi^a$):

(i) *Derivative expansion.* We can classify invariants by the number of derivatives

$$\Gamma_k[\Phi] = \int d^d x \left\{ U_k(\rho) + \frac{1}{2}Z_k(\rho)\partial_\mu\Phi^a\partial^\mu\Phi_a + \frac{1}{4}Y_k(\rho)\partial_\mu\rho\partial^\mu\rho + \mathcal{O}(\partial^4) \right\}. \quad (2.32)$$

The lowest level only includes the scalar potential and a standard kinetic term. The first correction includes the ρ -dependent wave function renormalizations $Z_k(\rho)$ and $Y_k(\rho)$. The next level involves then invariants with four derivatives etc.

One may wonder if a derivative expansion has any chance to account for the relevant physics of critical phenomena, in a situation where we know that the critical propagator is non-analytic in the momentum²¹. The reason why it can work is that the nonanalyticity builds up only gradually as $k \rightarrow 0$. For the critical temperature a typical qualitative form of the inverse average propagator is

$$\Gamma_k^{(2)} \sim q^2(q^2 + ck^2)^{-\eta/2} \quad (2.33)$$

with η the anomalous dimension. Thus the behavior for $q^2 \rightarrow 0$ is completely regular. In addition, the contribution of fluctuations with small momenta $q^2 \ll k^2$ to the flow equation is suppressed by the IR cutoff R_k . For $q^2 \gg k^2$ the “nonanalyticity” of the propagator is already manifest. The contribution of this region to the momentum integral in (2.19) is, however, strongly suppressed by the derivative $\partial_k R_k$. For cutoff functions of the type (2.17) only a small momentum range centered around $q^2 \approx k^2$ contributes substantially to the momentum integral in the flow equation. This suggests the use of a hybrid derivative expansion where the momentum dependence of $\Gamma_k - \int d^d x U_k$ is expanded around $q^2 = k^2$. Nevertheless, due to the qualitative behavior (2.33), also an expansion around $q^2 = 0$ should yield valid results. We will see in section 4 that the first order in the derivative expansion (2.32) gives a quite accurate description of critical phenomena in three dimensional $O(N)$ models, except for an (expected) error in the anomalous dimension.

(ii) *Expansion in powers of the fields.* As an alternative ordering principle one may expand Γ_k in n -point functions $\Gamma_k^{(n)}$

$$\Gamma_k[\Phi] = \sum_{n=0}^{\infty} \frac{1}{n!} \int \left(\prod_{j=0}^n d^d x_j [\Phi(x_j) - \Phi_0] \right) \Gamma_k^{(n)}(x_1, \dots, x_n). \quad (2.34)$$

If one chooses $[8]^{22} \Phi_0$ as the k -dependent expectation value of Φ , the series (2.34) starts effectively at $n = 2$. The flow equations for the $1PI$ Green functions $\Gamma_k^{(n)}$ are obtained by functional differentiation of (2.19). Similar equations have been discussed first in [5] from a somewhat different viewpoint. They can also be interpreted as a differential form of Schwinger–Dyson equations [108].

²¹See [100, 101] for early applications of the derivative expansion to critical phenomena. For a recent study on convergence properties of the derivative expansion see [102].

²²See also [103, 104] for the importance of expanding around $\Phi = \Phi_0$ instead of $\Phi = 0$ and refs. [105, 106, 107].

(iii) *Expansion in the canonical dimension.* We can classify the couplings according to their canonical dimension. For this purpose we expand Γ_k around some constant field ρ_0

$$\begin{aligned} \Gamma_k[\Phi] = & \int d^d x \left\{ U_k(\rho_0) + U'_k(\rho_0)(\rho - \rho_0) + \frac{1}{2}U''_k(\rho_0)(\rho - \rho_0)^2 + \dots \right. \\ & - \frac{1}{2} \left(Z_k(\rho_0) + Z'_k(\rho_0)(\rho - \rho_0) + \frac{1}{2}Z''_k(\rho_0)(\rho - \rho_0)^2 + \dots \right) \Phi^a \partial_\mu \partial^\mu \Phi_a \\ & + \frac{1}{2} \left(\dot{Z}_k(\rho_0) + \dot{Z}'_k(\rho_0)(\rho - \rho_0) + \dots \right) \Phi^a (\partial_\mu \partial^\mu)^2 \Phi_a \\ & \left. - \frac{1}{4} Y_k(\rho_0) \rho \partial_\mu \partial^\mu \rho + \dots \right\}. \end{aligned} \quad (2.35)$$

The field ρ_0 may depend on k . In particular, for a potential U_k with minimum at $\rho_0(k) > 0$ the location of the minimum can be used as one of the couplings. In this case $\rho_0(k)$ replaces the coupling $U'_k(\rho_0)$ since $U'_k(\rho_0(k)) = 0$. In three dimensions one may start by considering an approximation that takes into account only couplings with positive canonical mass dimension, i.e. $U'_k(0)$ with mass dimension M^2 and $U''_k(0)$ with dimension M^1 in the symmetric regime (potential minimum at $\rho = 0$). Equivalently, in the spontaneously broken regime (potential minimum for $\rho \neq 0$) we may take $\rho_0(k)$ and $U''_k(\rho_0)$. The first correction includes then the dimensionless parameters $U'''_k(\rho_0)$ and $Z_k(\rho_0)$. The second correction includes $U_k^{(4)}(\rho_0)$, $Z'_k(\rho_0)$ and $Y_k(\rho_0)$ with mass dimension M^{-1} and so on. Already the inclusion of the dimensionless couplings gives a very satisfactory description of critical phenomena in three dimensional scalar theories (see section 4.2).

2.4 Flow equation for the average potential

For a discussion of the ground state, its preserved or spontaneously broken symmetries and the mass spectrum of excitations the most important quantity is the average potential $U_k(\rho)$. In the absence of external sources the minimum ρ_0 of $U_{k \rightarrow 0}$ determines the expectation value of the order parameter. The symmetric phase with unbroken $O(N)$ symmetry is realized if $\rho_0(k \rightarrow 0) = 0$ whereas spontaneous symmetry breaking occurs for $\rho_0(k \rightarrow 0) > 0$. Except for the wave function renormalization to be discussed later the squared particle masses M^2 are given by $M^2 \sim U'(\rho_0 = 0)$ for the symmetric phase. Here primes denote derivatives with respect to ρ . For $\rho_0 \neq 0$ one finds a radial mode with $M^2 \sim U'(\rho_0) + 2\rho_0 U''(\rho_0)$ and $N - 1$ Goldstone modes with $M^2 \sim U'(\rho_0)$. For vanishing external sources the Goldstone modes are massless.

We therefore want to concentrate on the flow of $U_k(\rho)$. The exact flow equation is obtained by evaluating eq. (2.19) for a constant value of φ_a , say $\varphi_a(x) = \varphi \delta_{a1}$, $\rho = \frac{1}{2}\varphi^2$. One finds the exact equation

$$\partial_t U_k(\rho) = \frac{1}{2} \int \frac{d^d q}{(2\pi)^d} \frac{\partial R_k}{\partial t} \left(\frac{N-1}{M_0} + \frac{1}{M_1} \right) \quad (2.36)$$

with

$$\begin{aligned} M_0(\rho, q^2) &= Z_k(\rho, q^2) q^2 + R_k(q) + U'_k(\rho) \\ M_1(\rho, q^2) &= \tilde{Z}_k(\rho, q^2) q^2 + R_k(q) + U'_k(\rho) + 2\rho U''_k(\rho) \end{aligned} \quad (2.37)$$

parametrizing the (a, a) and $(1,1)$ element of $\Gamma_k^{(2)} + R_k$ ($a \neq 1$).

As expected, this equation is not closed since we need information about the ρ and q^2 -dependent wave function renormalizations Z_k and \tilde{Z}_k for the Goldstone and radial modes, respectively. The lowest order in the derivative expansion would take $\tilde{Z}_k = Z_k = Z_k(\rho_0, k^2)$ independent of ρ and q^2 , so that only the anomalous dimension

$$\eta = -\frac{\partial}{\partial t} \ln Z_k \quad (2.38)$$

is needed in addition to the partial differential equation (2.36). For a first discussion let us also neglect the contribution $\sim \partial_t Z_k$ in $\partial_t R_k$ and write

$$\frac{\partial}{\partial t} U_k(\rho) = 2v_d k^d \left[(N-1)l_0^d \left(\frac{U'_k(\rho)}{Z_k k^2} \right) + l_0^d \left(\frac{U'_k(\rho) + 2\rho U''_k(\rho)}{Z_k k^2} \right) \right] \quad (2.39)$$

with

$$v_d^{-1} = 2^{d+1} \pi^{d/2} \Gamma\left(\frac{d}{2}\right), \quad v_2 = \frac{1}{8\pi}, \quad v_3 = \frac{1}{8\pi^2}, \quad v_4 = \frac{1}{32\pi^2} \quad (2.40)$$

Here we have introduced the dimensionless threshold function

$$l_0^d(w) = \frac{1}{4} v_d^{-1} k^{-d} \int \frac{d^d q}{(2\pi)^d} \frac{\partial_t (R_k(q)/Z_k)}{q^2 + Z_k^{-1} R_k(q) + k^2 w} \quad (2.41)$$

It depends on the renormalized particle mass $w = M^2/(Z_k k^2)$ and has the important property that it decays rapidly for $w \gg 1$. This describes the decoupling of modes with renormalized squared mass M^2/Z_k larger than k^2 . In consequence, only modes with mass smaller than k contribute to the flow. The flow equations ensure automatically the emergence of effective theories for the low mass modes! The explicit form of the threshold functions (2.41) depends on the choice of R_k . We will discuss several choices in section 3.2. For a given explicit form of the threshold functions eq. (2.39) turns into a nonlinear partial differential equation for a function U depending on the two variables k and ρ . This can be solved numerically by appropriate algorithms [109] as is shown in later sections.

Eq. (2.39) was first derived [8] as a renormalization group improved perturbative expression and its intuitive form close to perturbation theory makes it very suitable for practical investigations. Here it is important to note that the use of the average action allows for the inclusion of propagator corrections (wave function renormalization effects) in a direct and systematic way. Extensions to more complicated scalar models or models with fermions [81] are straightforward. In the limit of a sharp cutoff (see section 3.2) and for vanishing anomalous dimension eq. (2.39) coincides with the Wegner-Houghton equation [3] for the potential, first discussed in [33] (see also [35, 34, 7, 110]).

Eq. (2.39) can be used as a practical starting point for various systematic expansions. For example, it is the lowest order in the derivative expansion. The next order includes q^2 -independent wave function renormalizations $Z(\rho)$, $\tilde{Z}(\rho)$ in eq. (2.37). For $N = 1$ the first order in the derivative expansion leads therefore to coupled partial nonlinear differential equations for two functions $U_k(\rho)$ and $Z_k(\rho)$ depending on two variables k and ρ . We have solved these

differential equations numerically and the result is plotted in fig. 1. The initial values of the integration correspond to the phase with spontaneous symmetry breaking. More details can be found in sect. 4.

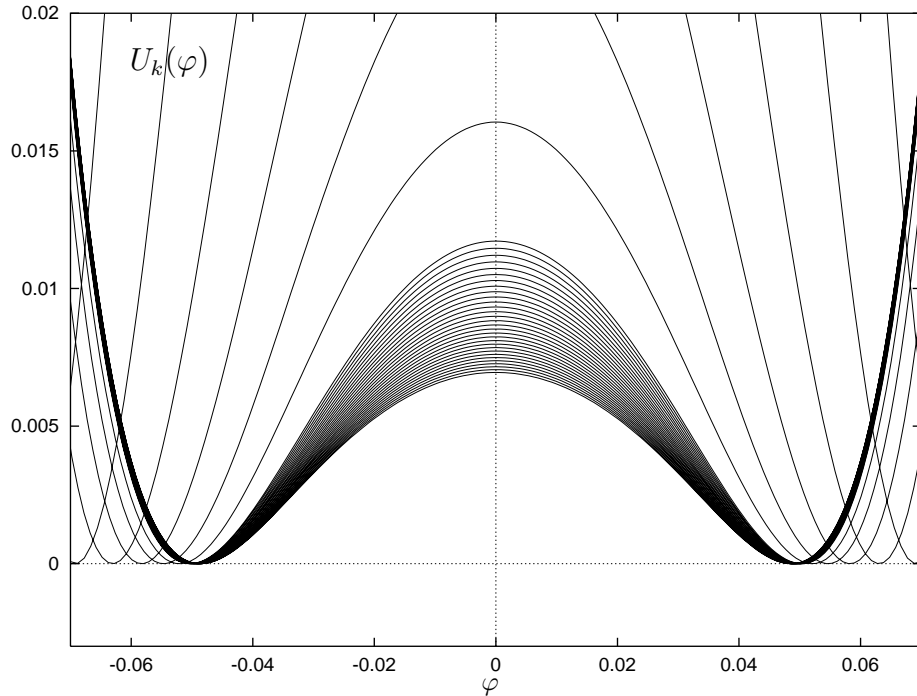


Figure 1: Average potential $U_k(\varphi)$ for different scales $k = e^t$. The shape of U_k is stored in smaller intervals $\Delta t = -0.02$ after the minimum has settled. This demonstrates the approach to convexity in the “inner region”, while the “outer region” becomes k -independent for $k \rightarrow 0$.

2.5 A simple example: the quartic potential

Before we describe the solutions of more sophisticated truncations of the flow equation (2.36) we consider here a very simple polynomial approximation to U_k , namely

$$U_k(\rho) = \frac{1}{2} \bar{\lambda}_k (\rho - \rho_0(k))^2 . \quad (2.42)$$

The two parameters $\rho_0(k)$ and $\bar{\lambda}_k$ correspond to the renormalizable couplings in four dimensions. It is not surprising that the flow of $\bar{\lambda}_k$ will reproduce for $d = 4$ the usual one-loop β -function. As compared to standard perturbation theory, one gets in addition a flow equation for the k -dependent potential minimum $\rho_0(k)$ which reflects the quadratic renormalization of the mass term. It is striking, however, that with the inclusion of the anomalous dimension η the simple ansatz (2.42) also describes [8] the physics for lower dimensions $d = 3$ or $d = 2$! This includes the second-order phase transition for $d = 3$ with nontrivial critical exponents and even the Kosterlitz-Thouless transition for $d = 2$, $N = 2$! In consequence, we obtain a simple unified picture for the ϕ^4 -model in all dimensions. This is an excellent starting point for more elaborate approximations.

All characteristic features of the flow can already be discussed with the approximation (2.42). We use this ansatz to rewrite eq. (2.39) as a coupled set of ordinary differential equations for the minimum of the potential $\rho_0(k)$ and the quartic coupling $\bar{\lambda}_k$. This system is closed for a given anomalous dimension η (2.38). The flow of the potential minimum can be inferred from the identity

$$0 = \frac{d}{dt} U'_k(\rho_0(k)) = \partial_t U'_k(\rho_0(k)) + U''_k(\rho_0(k)) \partial_t \rho_0(k). \quad (2.43)$$

Here $\partial_t U'_k(\rho)$ is the partial t -derivative with ρ held fixed which is computed by differentiating eq. (2.39) with respect to ρ . Defining the “higher” threshold functions by

$$\begin{aligned} l_1^d(w) &= -\frac{\partial}{\partial w} l_0^d(w) \\ l_{n+1}^d(w) &= -\frac{1}{n} \frac{\partial}{\partial w} l_n^d(w), \quad n \geq 1 \end{aligned} \quad (2.44)$$

and constants $l_n^d = l_n^d(0)$ one obtains

$$\partial_t \rho_0 = 2v_d k^{d-2} Z_k^{-1} \left\{ 3l_1^d \left(\frac{2\rho_0 \bar{\lambda}}{Z_k k^2} \right) + (N-1)l_1^d \right\}. \quad (2.45)$$

We conclude that $\rho_0(k)$ always decreases as the infrared cutoff k is lowered. For $d = 2$ and $N \geq 2$ only a Z -factor increasing without bounds can prevent $\rho_0(k)$ from reaching zero at some value $k > 0$. We will see that this unbounded Z -factor occurs for $N = 2$ in the low temperature phase. If $\rho_0(k)$ reaches zero for $k_s > 0$ the flow for $k < k_s$ can be continued with a truncation $U_k(\rho) = m_k^2 \rho + \frac{1}{2} \bar{\lambda}_k \rho^2$ with $m_k^2 > 0$. This situation corresponds to the symmetric or disordered phase with N massive excitations. On the other hand, the phase with spontaneous symmetry breaking or the ordered phase is realized for $\lim_{k \rightarrow 0} \rho_0(k) > 0$.

It is convenient to introduce renormalized dimensionless couplings as

$$\kappa = Z_k k^{2-d} \rho_0, \quad \lambda = Z_k^{-2} k^{d-4} \bar{\lambda}. \quad (2.46)$$

For our simple truncation one has

$$u = \frac{1}{2} \lambda (\tilde{\rho} - \kappa)^2 \quad (2.47)$$

and the flow equations for κ and λ read

$$\partial_t \kappa = \beta_\kappa = (2-d-\eta)\kappa + 2v_d \left\{ 3l_1^d(2\lambda\kappa) + (N-1)l_1^d \right\} \quad (2.48)$$

$$\partial_t \lambda = \beta_\lambda = (d-4+2\eta)\lambda + 2v_d \lambda^2 \left\{ 9l_2^d(2\lambda\kappa) + (N-1)l_2^d \right\}. \quad (2.49)$$

In this truncation the anomalous dimension η is given by [8]

$$\eta = \frac{16v_d}{d} \lambda^2 \kappa m_{2,2}^d(0, 2\lambda\kappa) \quad (2.50)$$

where $m_{2,2}^d$ is another threshold function defined in sect. 4.2. It has the property

$$\eta = \frac{1}{4\pi\kappa} \text{ for } d = 2, \quad \lambda\kappa \gg 1. \quad (2.51)$$

The universal critical behavior of many systems of statistical mechanics is described by the field theory for scalars with $O(N)$ symmetry. This covers the gas–liquid and many chemical transitions described by Ising models with a discrete symmetry $Z_2 \equiv O(1)$, superfluids with continuous abelian symmetry $O(2)$, Heisenberg models for magnets with $N = 3$, etc. In $2 < d \leq 4$ dimensions all these models have a continuous second order phase transition. In two dimensions one observes a second order transition for the Ising model, a Kosterlitz–Thouless phase transition [111] for $N = 2$ and no phase transition for non–abelian symmetries $N \geq 3$. It is known [112] that a continuous symmetry cannot be broken in two dimensions in the sense that the expectation value of the unrenormalized scalar field vanishes in the limit of vanishing sources, $\Phi_a = \langle \chi_a(x) \rangle = 0$. We want to demonstrate that the two differential equations (2.48), (2.49) describe all qualitative features of phase transitions in two or three dimensions correctly. A quantitative numerical analysis using more sophisticated truncations will be presented in section 4.

In four dimensions the anomalous dimension and the product $\lambda\kappa$ become rapidly small quantities as k decreases. We then recognize in eq. (2.49) the usual perturbative one-loop β -function for the quartic coupling

$$\partial_t \lambda = \frac{N+8}{16\pi^2} \lambda^2 \quad (2.52)$$

Eqs. (2.48), (2.49) also exhibit the well-known property of “triviality” which means that the quartic coupling vanishes for $k \rightarrow 0$ for the massless model.

For $d = 3$ the equations (2.48) and (2.49) exhibit a fixed point (κ_*, λ_*) where $\beta_\kappa = \beta_\lambda = 0$. This is a first example of a “scaling solution” for which all couplings evolve according to an effective dimension which is composed from their canonical dimension and anomalous dimension, i.e.

$$Z_k \sim k^{-\eta_*}, \quad \rho_0 \sim k^{d-2+\eta_*}, \quad \bar{\lambda} \sim k^{4-d-2\eta_*}. \quad (2.53)$$

From the generic form $\beta_\lambda = -\lambda + \lambda^2(c_1 + c_2(\lambda\kappa))$ one concludes that λ essentially corresponds to an infrared stable coupling which is attracted towards its fixed point value λ_* as k is lowered. On the other hand, $\beta_\kappa = -\kappa + c_3 + c_4(\lambda\kappa)$ shows that κ is essentially an infrared unstable or relevant coupling. Starting for given λ_Λ with $\kappa_\Lambda = \kappa_*(\lambda_\Lambda) + \delta\kappa_\Lambda$, $\delta\kappa_\Lambda = \kappa_T(T_c - T)$, $\kappa_T > 0$, one either ends in the symmetric phase for $\delta\kappa_\Lambda < 0$, or spontaneous symmetry breaking occurs for $\delta\kappa_\Lambda > 0$. The fixed point corresponds precisely to the critical temperature of a second order phase transition. Critical exponents can be computed from solutions in the vicinity of the scaling solution. The index ν characterizes the divergence of the correlation length for $T \rightarrow T_c$, i.e., $\xi \sim m_R^{-1} \sim |T - T_c|^{-\nu}$ with $m_R^2 = \lim_{k \rightarrow 0} 2\rho_0 \bar{\lambda} Z_k^{-1}$. It corresponds to the negative eigenvalue of the “stability matrix” $A_{ij} = (\partial\beta_i/\partial\lambda_j)(\kappa_*, \lambda_*)$ with $\lambda_i \equiv (\kappa, \lambda)$. (This can be generalized for more than two couplings.) The critical exponent η determines the long distance behavior of the two–point function for $T = T_c$. It is given by the anomalous

dimension at the fixed point, $\eta = \eta(\kappa_*, \lambda_*)$. It is remarkable that already in a very simple polynomial truncation the critical exponents come out with reasonable accuracy [8, 113]. In three dimensions the anomalous dimension comes out to be small and can be neglected for a rough treatment, further simplifying the flow equations (2.48), (2.49). As an example, for the critical exponent ν for $N = 3$ and $\eta = 0$ one finds $\nu = 0.74$, to be compared with the known value $\nu = 0.71$. (See also [87] for a discussion of the $N = 1$ case in three dimensions and section 4.)

In two dimensions the term linear in κ vanishes in β_κ . This changes the fixed point structure dramatically as can be seen from

$$\lim_{\kappa \rightarrow \infty} \beta_\kappa = \frac{N-2}{4\pi} \quad (2.54)$$

where $l_1^2 = 1$ was used. Since β_κ is always positive for $\kappa = 0$ a fixed point requires that β_κ becomes negative for large κ . This is the case for the Ising model [8, 69, 114] where $N = 1$. On the other hand, for a non-abelian symmetry with $N \geq 3$ no fixed point and therefore no phase transition occurs. The location of the minimum always reaches zero for some value $k_s > 0$. The only phase corresponds to a linear realization of $O(N)$ with N degenerate masses $m_R \sim k_s$. It is interesting to note that the limit $\kappa \rightarrow \infty$ describes the non-linear sigma model. The non-abelian coupling g of the non-linear model is related to κ by $g^2 = 1/(2\kappa)$ and eq. (2.54) reproduces the standard one-loop beta function for g

$$\frac{\partial g^2}{\partial t} = -\frac{N-2}{2\pi} g^4 \quad (2.55)$$

which is characterized by asymptotic freedom [115]. The ‘‘confinement scale’’ where the coupling g becomes strong can be associated with k_s . The strongly interacting physics of the non-linear model finds a simple description in terms of the symmetric phase of the linear $O(N)$ -model [8]! This may be regarded as an example of duality: the dual description of the non-linear σ -model for large coupling is simply the linear φ^4 -model.

Particularly interesting is the abelian continuous symmetry for $N = 2$. Here β_κ vanishes for $\kappa \rightarrow \infty$ and κ becomes a marginal coupling. As is shown in more detail in section 4.8 one actually finds [116] a behavior consistent with a second order phase transition with $\eta \simeq 0.25$ near the critical trajectory. The low temperature phase ($\kappa_\Lambda > \kappa_*$) is special since it has many characteristics of the phase with spontaneous symmetry breaking, despite the fact that $\rho_0(k \rightarrow 0)$ must vanish according to the Mermin–Wagner theorem [112]. There is a massless Goldstone-type boson (infinite correlation length) and one massive mode. Furthermore, the exponent η depends on κ_Λ or the temperature (cf. eq. (2.51)), since κ flows only marginally. These are the characteristic features of a Kosterlitz–Thouless phase transition [111]. The puzzle of the Goldstone boson in the low temperature phase despite the absence of spontaneous symmetry breaking is solved by the observation that the wave function renormalization never stops running with k :

$$Z_k = \bar{Z} \left(\frac{k}{\Lambda} \right)^{-\eta}. \quad (2.56)$$

Even though the renormalized field $\chi_R = Z_k^{1/2} \chi$ acquires a non-zero expectation value $\langle \chi_R \rangle = \sqrt{2\kappa}$, for $k \rightarrow 0$ the unrenormalized order parameter vanishes due to the divergence

of Z_k ,

$$\langle \chi(k) \rangle = \sqrt{\frac{2\kappa}{\bar{Z}}} \left(\frac{k}{\Lambda} \right)^{\frac{1}{4\pi\kappa}}. \quad (2.57)$$

Also the inverse Goldstone boson propagator behaves as $(q^2)^{1-1/(8\pi\kappa)}$ and circumvents Coleman's no-go theorem [117] for free massless scalar fields in two dimensions. It is remarkable that all these features arise from the solution of a simple one-loop type equation without ever invoking non-perturbative vortex configurations.

3 Solving the flow equation

3.1 Scaling form of the exact flow equation for the potential

In this section we discuss analytical approaches to the solution of the exact flow equation for the average potential and for the propagator. They prove to be a useful guidance for the numerical solutions of truncated partial differential equations. After writing the exact equation for the potential in a scale-invariant form and discussing explicitly the threshold functions, we present an exact solution of the flow equation in the limit $N \rightarrow \infty$. A renormalization group improved perturbation theory is developed as the iterative solution of the flow equations. This incorporates the usual gap equation and can be used as a systematic procedure with the gap equation as a starting point. We write down the exact flow equation for the propagator as a basis for a systematic computation of the anomalous dimension and related quantities. Finally, we show how the average potential approaches for $k \rightarrow 0$ a convex form for the nontrivial case of spontaneous symmetry breaking.

Let us first come back to the exact flow equation (2.36) and derive an explicitly scale-invariant form of it. This will be a useful starting point for the discussion of critical phenomena in later sections. It is convenient to use a dimensionless cutoff function

$$r_k \left(\frac{x}{k^2} \right) = \frac{R_k(x)}{Z_k x}, \quad x \equiv q^2, \quad Z_k = Z_k(\rho_0, k^2) \quad (3.1)$$

and write the flow equations as

$$\frac{\partial}{\partial t} U_k(\rho) = v_d \int_0^\infty dx x^{\frac{d}{2}} s_k \left(\frac{x}{k^2} \right) \left(\frac{N-1}{M_0/Z_k} + \frac{1}{M_1/Z_k} \right) \quad (3.2)$$

with

$$s_k \left(\frac{x}{k^2} \right) = \frac{\partial}{\partial t} r_k \left(\frac{x}{k^2} \right) - \eta r_k \left(\frac{x}{k^2} \right) = -2x \frac{\partial}{\partial x} r_k \left(\frac{x}{k^2} \right) - \eta r_k \left(\frac{x}{k^2} \right) \quad (3.3)$$

We parametrize the wave function renormalization by

$$\begin{aligned} z_k(\rho) &= \frac{Z_k(\rho, k^2)}{Z_k}, \quad z_k(\rho_0) \equiv 1, \quad \rho \tilde{y}_k(\rho) = \frac{\tilde{Z}_k(\rho, k^2) - Z_k(\rho, k^2)}{Z_k^2} k^{d-2}, \\ \Delta z_k(\rho, \frac{x}{k^2}) &= \frac{Z_k(\rho, x) - Z_k(\rho, k^2)}{Z_k}, \quad \Delta z_k(\rho, 1) = 0 \\ Z_k k^{2-d} \rho \Delta \tilde{y}_k(\rho, \frac{x}{k^2}) &= \frac{\tilde{Z}_k(\rho, x) - \tilde{Z}_k(\rho, k^2)}{Z_k} - \Delta z_k(\rho, \frac{x}{k^2}), \quad \Delta \tilde{y}_k(\rho, 1) = 0 \end{aligned} \quad (3.4)$$

so that

$$\frac{\partial}{\partial t} U_k = 2v_d k^d [(N-1)l_0^d \left(\frac{U'_k}{Z_k k^2}; \eta, z_k \right) + l_0^d \left(\frac{U'_k + 2\rho U''_k}{Z_k k^2}; \eta, z_k + Z_k \rho \tilde{y}_k k^{2-d} \right)] + \Delta\zeta_k k^d \quad (3.5)$$

where $l_0^d(w; \eta, z)$ is a generalized dimensionless threshold function ($y = x/k^2$)

$$l_0^d(w; \eta, z) = \frac{1}{2} \int_0^\infty dy y^{\frac{d}{2}} s_k(y) [(z + r_k(y))y + w]^{-1} \quad (3.6)$$

The correction $\Delta\zeta_k$ contributes only in second order in a derivative expansion. Finally, we may remove the explicit dependence on Z_k and k by using scaling variables

$$u_k = U_k k^{-d}, \quad \tilde{\rho} = Z_k k^{2-d} \rho \quad (3.7)$$

Evaluating the t -derivative at fixed $\tilde{\rho}$ and denoting by $u' = \partial u / \partial \tilde{\rho}$ etc. one obtains the scaling form of the exact evolution equation for the average potential

$$\begin{aligned} \partial_t u|_{\tilde{\rho}} &= -du + (d-2+\eta)\tilde{\rho}u' + \zeta_k \\ \zeta_k &= 2v_d \left\{ (N-1)l_0^d(u'; \eta, z) + l_0^d(u' + 2\tilde{\rho}u'', \eta, z + \tilde{\rho}\tilde{y}) \right\} + \Delta\zeta_k \end{aligned} \quad (3.8)$$

with

$$\begin{aligned} \Delta\zeta_k &= -v_d \int_0^\infty dy y^{\frac{d}{2}+1} s_k(y) \left\{ \frac{(N-1)\Delta z(y)}{[(z+r_k(y))y+u'][(z+\Delta z(y)+r_k(y))y+u']} \right. \\ &\quad \left. + \frac{\Delta z(y) + \tilde{\rho}\Delta\tilde{y}(y)}{[(z+\tilde{\rho}\tilde{y}+r_k(y))y+u'+2\tilde{\rho}u''][(z+\tilde{\rho}\tilde{y}+\Delta z(y)+\tilde{\rho}\Delta\tilde{y}(y)+r_k(y))y+u'+2\tilde{\rho}u'']} \right\} \end{aligned} \quad (3.9)$$

All explicit dependence on the scale k or the wave function renormalization Z_k has disappeared. Reparametrization invariance under field scaling is obvious in this form. For $\rho \rightarrow \alpha^2 \rho$ one also has $Z_k \rightarrow \alpha^{-2} Z_k$ so that $\tilde{\rho}$ is invariant. This property needs the factor Z_k in R_k . This version is therefore most appropriate for a discussion of critical behavior. The universal features of the critical behavior for second-order phase transitions are related to the existence of a scaling solution²³. This scaling solution solves the differential equation for k -independent functions $u(\tilde{\rho})$, $z(\tilde{\rho})$ etc., which results from (3.8) by setting $\partial_t u = 0$. For a constant wave function renormalization the scaling potential can be directly obtained by solving the second order differential equation $\partial_t u = 0$. Of all possible solutions it has been shown that the physical fixed point corresponds to the solution $u(\tilde{\rho})$ which is non-singular in the field [118, 119, 107, 120].

The scaling form of the evolution equation is the best starting point for attempts of an analytical solution. In fact, in the approximation where ζ_k can be expressed as a function of u' and η one may find the general form of the solution by the method of characteristics. For this purpose we consider the $\tilde{\rho}$ -derivative of eq. (3.8)

$$\partial_t u' = -(2-\eta)u' + (d-2+\eta)\tilde{\rho}u'' - \psi_k u'' , \quad \psi_k = -\frac{\partial \zeta_k}{\partial u'} \quad (3.10)$$

²³More precisely, $\partial_t u' = 0$ is a sufficient condition for the existence of a scaling solution. The universal aspects of first-order transitions are also connected to exact or approximate scaling solutions.

We further assume for a moment that the dependence of $\psi_k(u', \eta)$ on η has (approximately) the form

$$\psi_k(u', \eta) = (2 - \eta)|u'|^{\frac{d}{2-\eta}} \hat{\psi}_k(u') \quad (3.11)$$

For $u' > 0$ one finds the solution

$$\tilde{\rho}(u')^{1-\frac{d}{2-\eta}} + G(u') = F_+(u' \exp\{2t - \int_0^t dt' \eta(t')\}) \quad (3.12)$$

with $G(u')$ obeying the differential equation

$$\frac{\partial G}{\partial u'} = \frac{1}{2-\eta} (u')^{-\frac{d}{2-\eta}} \psi_k = \hat{\psi}_k(u') \quad (3.13)$$

and $F_+(w)$ an arbitrary function. Similarly, for $u' < 0$ one has

$$\tilde{\rho}(-u')^{1-\frac{d}{2-\eta}} + H(-u') = F_-(u' \exp\{2t - \int_0^t dt' \eta(t')\}) \quad (3.14)$$

with

$$\frac{\partial H}{\partial(-u')} = \frac{1}{2-\eta} (-u')^{-\frac{d}{2-\eta}} \psi_k = \hat{\psi}_k(u') \quad (3.15)$$

and $F_-(w)$ again arbitrary. For known $\hat{\psi}_k$ one can now solve the ordinary differential equations for G and H . The initial value of the microscopic potential u'_Λ fixes the free functions F_\pm by evaluating (3.12) and (3.14) for $t = 0$. We finally note that the solution for constant η can be obtained from the solution for $\eta = 0$ by the replacements $d \rightarrow d_\eta = 2d/(2-\eta)$, $t \rightarrow t_\eta = t(2-\eta)/2$, $G \rightarrow G_\eta = 2G/(2-\eta)$, $H \rightarrow H_\eta = 2H/(2-\eta)$.

We will see below that this solution becomes exact in the large N limit. For finite N it may still be used if the functions $\tilde{\rho}u''$, z , $\tilde{\rho}\tilde{y}$ appearing in eq. (3.8) can be expressed in terms of u' and η . The condition (3.11) may actually be abandoned in regions of k where η varies only slowly. If $\hat{\psi}_k$ depends on η , the corrections to the generic solution (3.12), (3.14) are $\sim (\partial\hat{\psi}_k/\partial\eta)(\partial_t\eta)$.

3.2 Threshold functions

In situations where the momentum dependence of the propagator can be approximated by a standard form of the kinetic term and is weak for the other 1PI-correlation functions, the “non-perturbative” effects beyond one loop arise to a large extent from the threshold functions. We will therefore discuss in this subsection their most important properties and introduce the notations

$$\begin{aligned} l_n^d(w; \eta, z) &= \frac{n + \delta_{n,0}}{4} v_d^{-1} k^{2n-d} \int \frac{d^d q}{(2\pi)^d} \partial_t R_k(q) (Z_k z q^2 + R_k(q) + w k^2)^{-(n+1)}, \\ l_{n+1}^d(w; \eta, z) &= -\frac{1}{n + \delta_{n,0}} \frac{\partial}{\partial w} l_n^d(w; \eta, z), \\ l_n^d(w; \eta) &= l_n^d(w; \eta, 1), \quad l_n^d(w) = l_n^d(w; 0, 1), \quad l_n^d = l_n^d(0) \end{aligned} \quad (3.16)$$

The precise form of the threshold functions depends on the choice of the cutoff function $R_k(q)$. There are, however, a few general features which are independent of the particular scheme:

1. For $n = d/2$ one has the universal property

$$l_n^{2n} = 1 \quad (3.17)$$

This is crucial to guarantee the universality of the perturbative β -functions for the quartic coupling in $d = 4$ or for the coupling in the nonlinear σ -model in $d = 2$.

2. If the momentum integrals are dominated by $q^2 \approx k^2$ and $R_k(q) \lesssim k^2$, the threshold functions obey for large w

$$l_n^d(w) \sim w^{-(n+1)} \quad (3.18)$$

We will see below that this property is not realized for sharp cutoffs where $l_n^d(w) \sim w^{-n}$.

3. The threshold functions diverge for some negative value of w . This is related to the fact that the average potential must become convex for $k \rightarrow 0$.

It is instructive to evaluate the threshold function explicitly for a simple cutoff function of the form

$$R_k = Z_k k^2 \Theta(k^2 - q^2) \quad (3.19)$$

where $(x = q^2)$

$$l_0^d(w) = k^{2-d} \int_0^{k^2} dx x^{\frac{d}{2}-1} [x + (w+1)k^2]^{-1} + k^{4-d} \int_0^\infty dx x^{\frac{d}{2}-1} \frac{\delta(x - k^2)}{x + k^2 \Theta(k^2 - x) + k^2 w} \quad (3.20)$$

The second term in the expression for l_0^d has to be defined and we consider eq. (3.19) as the limit $\gamma \rightarrow \infty$ of a family of cutoff functions

$$R_k = \frac{2\gamma}{1+\gamma} Z_k k^2 \left(\frac{q^2}{k^2}\right)^\gamma \left[\exp \left\{ \frac{2\gamma}{1+\gamma} \left(\frac{q^2}{k^2}\right)^\gamma \right\} - 1 \right]^{-1} \quad (3.21)$$

This yields the threshold functions

$$\begin{aligned} l_0^d(w) &= \ln \left(1 + \frac{1}{1+w} \right) + \hat{l}_0^d(w), \quad \hat{l}_0^d(w) = \int_0^1 dy y^{\frac{d}{2}-1} (y+1+w)^{-1}, \\ \hat{l}_0^2(w) &= \ln \left(1 + \frac{1}{1+w} \right), \quad \hat{l}_0^3(w) = 2 - 2\sqrt{1+w} \operatorname{arctg} \left(\frac{1}{\sqrt{1+w}} \right) \\ \hat{l}_0^4(w) &= 1 - (1+w) \ln \left(1 + \frac{1}{1+w} \right), \quad \hat{l}_0^{d+2}(w) = \frac{2}{d} - (1+w) \hat{l}_0^d(w) \end{aligned} \quad (3.22)$$

In order to get a more detailed overview, it is useful to discuss some other limiting cases for the choice of the cutoff. For $\gamma = 1$ the family of cutoffs (3.21) represents the exponential cutoff (15), for $\gamma \rightarrow 0$ one finds a masslike cutoff $R_k = Z_k k^2$ and for $\gamma \rightarrow \infty$ we recover the step-function cutoff (3.19). One may modify the step-function cutoff (3.19) to

$$R_k = Z_k k^2 \Theta(\alpha k^2 - q^2) \quad (3.23)$$

with

$$l_0^d(w) = \dots + \int_0^\alpha dy y^{\frac{d}{2}-1} (y+1+w)^{-1}. \quad (3.24)$$

In the limit $\alpha \rightarrow \infty$ one approaches again a masslike cutoff $R_k = Z_k k^2$. We observe that l_0^d does not remain finite in this limit. This reflects the fact that for a masslike cutoff the high momentum modes are not yet fully integrated out in the computation of Γ_k . However, for low enough dimensions suitable differences remain finite

$$l_0^3(w) - l_0^3(0) = \pi(\sqrt{1+w} - 1). \quad (3.25)$$

For $d < 4$ the masslike cutoff can be used except for an overall additive constant in the potential.

Another interesting extension of the step cutoff (3.19) is

$$R_k = Z_k k^2 \beta \Theta(k^2 - q^2) \quad (3.26)$$

such that

$$l_0^d(w) = \ln \frac{\beta + 1 + w}{1 + w} + \beta \hat{l}_0^d(w + \beta - 1) \quad (3.27)$$

It is instructive to consider the limit $\beta \rightarrow \infty$ which corresponds to a sharp momentum cutoff, where $r_k(y > 1) \rightarrow 0$ and $r_k(y < 1) \rightarrow \infty$. Although a sharp momentum cutoff leads to certain problems with analyticity, it is useful because of technical simplifications. The momentum integrals are now dominated by an extremely narrow range $q^2 \approx k^2$. (This holds except for a field-independent constant in $\partial_t \Gamma_k$.) We can therefore evaluate the two-point function in the rhs of $\partial_t U_k$ by its value for $q^2 = k^2$. In consequence, the correction $\Delta \zeta_k$ vanishes in this limit.

Furthermore, the threshold functions take a very simple form and one infers²⁴ from (3.22), (3.27)

$$l_0^d(w) = \ln \frac{1}{1+w} + \ln \beta + \frac{2}{d}, \quad l_1^d(w) = \frac{1}{1+w} \quad (3.28)$$

Actually, the constant part in l_0^d depends on the precise way how the sharp cutoff is defined. Nevertheless, this ambiguity does not affect the field-dependent part of the flow equation and the sharp cutoff limit obeys universally

$$l_1^d(w; \eta, z) = \frac{1}{z+w} \quad (3.29)$$

One ends in the sharp cutoff limit with a simple exact equation (up to an irrelevant constant)

$$\partial_t u = -du + (d-2+\eta)\tilde{\rho} u' - 2v_d \{ (N-1) \ln(z+u') + \ln(z+\tilde{\rho}\tilde{y}+u'+2\tilde{\rho}u'') \} \quad (3.30)$$

In leading order in the derivative expansion ($z=1, \tilde{y}=0$) and neglecting the anomalous dimension ($\eta=0$), this yields for $N=1, d=3$

$$\partial_t u = -3u + \tilde{\rho}u' - \frac{1}{4\pi^2} \ln(u'+2\tilde{\rho}u'') \quad (3.31)$$

which corresponds to the Wegner-Houghton equation [3] for the potential [33, 35, 34, 7, 110].

²⁴The functions $l_1^d(w)$ coincide with the sharp cutoff limit of a different family of threshold functions considered in [8].

3.3 Large- N expansion

In the limit $N \rightarrow \infty$ the exact flow equation for the average potential (3.8) can be solved analytically [113, 121]²⁵. In this limit the quantities η, \tilde{y} and $\Delta\zeta_k$ vanish and $z = 1$. Furthermore, the correction from $\tilde{\rho}u''$ in the second term in eq. (3.8) is suppressed by $1/N$. In consequence, the right-hand side of the flow equation for the potential only depends on u' (and $\tilde{\rho}$)

$$\partial_t u = -du + (d-2)\tilde{\rho}u' + 2v_d N l_0^d(u') \quad (3.32)$$

We can therefore use the exact solution (3.12), (3.13) with

$$\psi_k(u') = 2v_d N l_1^d(u') \quad (3.33)$$

In particular, for the sharp cutoff (3.29) the functions G, H obey the differential equation

$$\begin{aligned} \frac{\partial G(w)}{\partial w} &= v_d N w^{-d/2} (1+w)^{-1}, \\ \frac{\partial H(w)}{\partial w} &= v_d N w^{-d/2} (1-w)^{-1} \end{aligned} \quad (3.34)$$

Consider the three-dimensional models. For $d = 3$ the general solution reads

$$\begin{aligned} \frac{\tilde{\rho} - 2v_3 N}{\sqrt{u'}} - 2v_3 N \operatorname{arctg}(\sqrt{u'}) &= F_+(u'e^{2t}), \quad \text{for } u' > 0 \\ \frac{\tilde{\rho} - 2v_3 N}{\sqrt{-u'}} + v_3 N \ln \frac{1 + \sqrt{-u'}}{1 - \sqrt{-u'}} &= F_-(u'e^{2t}), \quad \text{for } u' < 0 \end{aligned} \quad (3.35)$$

The functions $F_{\pm}(w)$ are arbitrary. They are only fixed by the initial conditions at the microscopic scale $k = \Lambda$ ($t = 0$). As an example, consider the microscopic potential

$$u_{\Lambda} = \frac{1}{2} \lambda_{\Lambda} (\tilde{\rho} - \kappa_{\Lambda})^2 \quad (3.36)$$

Insertion into eq. (3.35) at $t = 0$ yields

$$\begin{aligned} F_+(w) &= \frac{1}{\sqrt{w}} \left(\frac{w}{\lambda_{\Lambda}} + \kappa_{\Lambda} - 2v_3 N \right) - 2v_3 N \operatorname{arctg}(\sqrt{w}) \\ F_-(w) &= -\frac{\sqrt{-w}}{\lambda_{\Lambda}} + \frac{\kappa_{\Lambda} - 2v_3 N}{\sqrt{-w}} + v_3 N \ln \frac{1 + \sqrt{-w}}{1 - \sqrt{-w}} \end{aligned} \quad (3.37)$$

where we note the consistency condition

$$u'_{\Lambda} > -1, \quad \lambda_{\Lambda} \kappa_{\Lambda} < 1 \quad (3.38)$$

In consequence, the exact solution for $u'(\tilde{\rho}, t)$ obeys for $u' > 0$

$$\begin{aligned} \tilde{\rho} - 2v_3 N &= 2v_3 N \sqrt{u'} \operatorname{arctg} \sqrt{u'} + \frac{u'}{\lambda_{\Lambda}} e^t \\ &\quad + (\kappa_{\Lambda} - 2v_3 N) e^{-t} - 2v_3 N \sqrt{u'} \operatorname{arctg}(\sqrt{u'} e^t) \end{aligned} \quad (3.39)$$

²⁵See also refs. [3, 119, 110, 122] for the large N limit of the Wegner-Houghton [3] and Polchinski equation [6].

Retranslating to the original variables $\rho = \tilde{\rho}k$, $U' = \partial U/\partial \rho = u'k^2$ and using $v_3 = 1/(8\pi^2)$, this reads

$$\rho - \rho_0(k) = \frac{N}{4\pi^2} \sqrt{U'} \left(\text{arctg} \left(\frac{\sqrt{U'}}{k} \right) - \text{arctg} \left(\frac{\sqrt{U'}}{\Lambda} \right) \right) + \frac{U'}{\lambda_\Lambda \Lambda}$$

with

$$\rho_0(k) = (\kappa_\Lambda - \frac{N}{4\pi^2})\Lambda + \frac{N}{4\pi^2}k \quad (3.40)$$

One sees how the average potential interpolates between the microscopic potential

$$U_\Lambda = \frac{1}{2} \lambda_\Lambda \Lambda (\rho - \kappa_\Lambda \Lambda)^2 \quad (3.41)$$

and the effective potential for $k \rightarrow 0$

$$U = \frac{1}{3} \left(\frac{8\pi}{N} \right)^2 (\rho - \rho_0)^3, \quad \rho_0 = \left(\kappa_\Lambda - \frac{N}{4\pi^2} \right) \Lambda \quad (3.42)$$

Here the last formula is an approximation valid for $U'/\Lambda^2 \ll \left(\frac{N\lambda_\Lambda}{8\pi}\right)^2$ and $U'/\Lambda^2 \ll (\pi/2)^2$ which can easily be replaced by the exact expression in the range of large U' . For vanishing source the model is in the symmetric phase for $\rho_0 < 0$ with masses of the excitations given by

$$M^2 = U'(0) = \left(\frac{8\pi}{N} \right)^2 \left(\kappa_\Lambda - \frac{N}{4\pi^2} \right)^2 \Lambda^2 \quad (3.43)$$

For $\rho_0 > 0$ spontaneous symmetry breaking occurs with order parameter (for $J = 0$)

$$\langle \varphi \rangle = \sqrt{2\rho_0} = (\kappa_\Lambda - \frac{N}{4\pi^2})^{1/2} (2\Lambda)^{1/2} \quad (3.44)$$

If we associate the deviation of κ_Λ from the critical value $\kappa_{\Lambda,c} = \frac{N}{4\pi^2}$ with a deviation from the critical temperature T_c

$$\kappa_\Lambda = \frac{N}{4\pi^2} + \frac{A}{\Lambda} (T_c - T), \quad \rho_0 = A(T_c - T) \quad (3.45)$$

it is straightforward to extract the critical exponents in the large N approximation

$$M \sim (T - T_c)^\nu, \quad \langle \varphi \rangle = (T_c - T)^\beta, \quad \nu = 1, \quad \beta = 0.5 \quad (3.46)$$

Eq. (3.42) constitutes the critical equation of state for the dependence of the magnetization φ on a homogeneous magnetic field J with

$$J = \frac{\partial U}{\partial \varphi} = \varphi U' = \left(\frac{4\pi}{N} \right)^2 \varphi (\varphi^2 - 2\rho_0)^2 \quad (3.47)$$

At the critical temperature one has $\rho_0 = 0$ and

$$J \sim \varphi^\delta, \quad \delta = 5 \quad (3.48)$$

whereas the susceptibility

$$\chi = \frac{\partial \varphi}{\partial J} = \left(\frac{N}{4\pi} \right)^2 (\varphi^2 - 2\rho_0)^{-1} (5\varphi^2 - 2\rho_0)^{-1} \quad (3.49)$$

obeys for $\rho_0 < 0$ at $J = 0$

$$\chi \sim (T - T_c)^{-\gamma} \quad , \quad \gamma = 2 \quad (3.50)$$

We note that the critical amplitudes (given by the proportionality constants in eqs. (3.46), (3.48) and (3.50)) are all given explicitly by eq. (3.42) once the proportionality constant A in eq. (3.45) is fixed. Universal amplitude ratios are those which do not depend on A . In the large N approximation the explicit solution $U(\rho, T)$ contains only one free constant instead of the usual two. This is related to the vanishing anomalous dimension and provides for an additional universal amplitude ratio. We finally may define the quartic coupling

$$\begin{aligned} \lambda_R &= U''(0) \quad \text{for} \quad \rho_0 \leq 0 \\ \lambda_R &= U''(\rho_0) \quad \text{for} \quad \rho_0 > 0 \end{aligned} \quad (3.51)$$

and observe the constant critical ratio in the symmetric phase

$$\frac{\lambda_R}{M} = \frac{16\pi}{N} \quad (3.52)$$

All this agrees with diagrammatic studies of the large N approximation [123] and numerical solutions of the flow equation [113, 109, 36] for the exponential cutoff function (2.17).

The solution for the region $u' < 0$ can be found along similar lines

$$\rho - \rho_0(k) = \frac{N}{8\pi^2} \sqrt{-U'} \left(\ln \frac{\Lambda + \sqrt{-U'}}{\Lambda - \sqrt{-U'}} - \ln \frac{k + \sqrt{-U'}}{k - \sqrt{-U'}} \right) + \frac{U'}{\lambda_\Lambda \Lambda} \quad (3.53)$$

Up to corrections involving inverse powers of Λ this yields the implicit relation

$$\sqrt{-U'} = k - (k + \sqrt{-U'}) \exp \left(-\frac{8\pi^2(\rho_0(k) - \rho)}{N\sqrt{-U'}} \right) \quad (3.54)$$

One infers that $\sqrt{-U'}$ is always smaller than k and maximal for $\rho = 0$. In the phase with spontaneous symmetry breaking where $\rho_0(k=0) = \rho_0 > 0$ the behavior near the origin is given for small k by

$$U'(\rho) = -k^2 \left[1 - 2 \exp \left(-\frac{8\pi^2(\rho_0 - \rho)}{Nk} \right) \right]^2 \quad (3.55)$$

For $k \rightarrow 0$ the validity of this region extends to the whole region $0 \leq \rho < \rho_0$. The “inner part” of the average potential becomes flat²⁶, in agreement with the general discussion of the approach to convexity above.

It is interesting to compare these results with the large N limit of the scaling solution which obeys

$$u' = \frac{1}{2} \left(\tilde{\rho} - \frac{N}{4\pi^2} \frac{1}{1+u'} \right) u'' \quad (3.56)$$

²⁶The exponential approach to the asymptotic form $U' = -k^2$ may cause problems for a numerical solution of the flow equation. The analytical information provided here can be useful in this respect.

For $u'(\kappa) = 0$ this yields for the minimum of u

$$\kappa = \frac{N}{4\pi^2} \quad (3.57)$$

Taking ρ -derivatives of eq. (3.56) and defining $\lambda = u''(\kappa)$, $\gamma = u'''(\kappa)$, we find

$$u''(1 - \frac{\kappa u''}{(1+u')^2}) = (\tilde{\rho} - \frac{\kappa}{1+u'})u''' \quad (3.58)$$

$$\lambda = \frac{1}{\kappa} = \frac{4\pi^2}{N}, \quad \gamma = \frac{2}{3}\lambda^2 = \frac{32\pi^4}{3N^2} \quad (3.59)$$

We emphasize that we have chosen the quartic potential (3.36) only for the simplicity of the presentation. The general solution can be evaluated equally well for other microscopic potentials (provided $u'_\Lambda > -1$). This can be used for an explicit demonstration of the universality of the critical behavior. It also may be employed for an investigation of tricritical behavior which can happen for more complicated forms of the microscopic potential. In summary, the exact solution of the flow equation for the average potential in the limit $N \rightarrow \infty$ provides a very detailed quantitative description for the “transition to complexity”.

3.4 Graphical representation and resummed perturbation theory

One is often interested in the flow equation for some particular n -point function $\Gamma_k^{(n)}$. Here $\Gamma^{(n)}$ is defined by the n -th functional derivative of Γ_k evaluated for a fixed field, as, for example, $\varphi = 0$. Correspondingly, the flow equation for $\Gamma^{(n)}$ can be obtained by taking n functional derivatives of the exact flow equation (2.19). We give here a simple prescription how the rhs of the flow equation can be computed from the usual perturbative Feynman graphs. Only one-loop diagrams are needed, but additional vertices are present and the propagators and vertices in the graphs correspond to full propagators and full vertices as derived by functional differentiation of Γ_k .

This purpose is achieved by writing eq. (2.19) formally in the form

$$\partial_t \Gamma_k = \frac{1}{2} \text{Tr} \tilde{\partial}_t \ln(\Gamma_k^{(2)} + R_k) \quad (3.60)$$

where the derivative $\tilde{\partial}_t$ acts only on R_k and not on Γ_k , i.e. $\tilde{\partial}_t = (\partial R_k / \partial t) \partial / \partial R_k$. If we forget for a moment possible problems of regularization, we may place $\tilde{\partial}_t$ in front of the trace so that

$$\partial_t \Gamma_k = \tilde{\partial}_t \hat{\Gamma}_k^{(1)} \quad (3.61)$$

where $\hat{\Gamma}_k^{(1)}$ is the one-loop expression with “renormalization group improvement”, i.e. full vertices and propagators instead of the classical ones. Functional derivatives commute with ∂_t and $\tilde{\partial}_t$. In consequence, the right-hand side of the exact flow equation for $\Gamma_k^{(n)}$ can be evaluated by the following procedure: 1) Write down the one-loop Feynman graphs for $\Gamma^{(n)}$. 2) Insert “renormalized” couplings instead of the classical ones. This also introduces a momentum dependence of the vertices which may not be present in the classical couplings. There may also

be contributions from higher vertices (e.g. six-point vertices) not present in the classical action. (The classical couplings vanish, the renormalized effective ones do not!) All renormalized vertices in the graphs correspond to appropriate functional derivatives of Γ_k . 3) Replace the propagators by the full average propagator $(\Gamma^{(2)} + R_k)^{-1}$ (evaluated at a fixed field). 4) Apply the formal differentiation $\tilde{\partial}_t$. More precisely, the derivative $\tilde{\partial}_t$ should act on the integrand of the one-loop momentum integral. This makes the expression finite so that regularization is of no worry. The result is the exact flow equation for $\Gamma_k^{(n)}$. An example is provided by eq. (2.30).

Standard perturbation theory can easily be recovered from an iterative solution of the flow equation (3.60). Starting from the leading or “classical” contribution $\Gamma_{k(0)} \equiv \Gamma_\Lambda$ one may insert this instead of Γ_k in the rhs of (3.60). Performing the t -integration generates the one-loop contribution

$$\Gamma_k - \Gamma_\Lambda = \frac{1}{2} \text{Tr} \left\{ \ln(\Gamma_\Lambda^{(2)} + R_k) - \ln(\Gamma_\Lambda^{(2)} + R_\Lambda) \right\}, \quad (3.62)$$

where we remind that $R_k \rightarrow 0$ for $k \rightarrow 0$. We observe that the momentum integration in the rhs of (3.62) is regularized in the ultraviolet through subtraction of $\ln(\Gamma_\Lambda^{(2)} + R_\Lambda)$. This is a type of implicit Pauli-Villars regularization with the heavy mass term replaced by a momentum-dependent piece R_Λ in the inverse propagator. With suitable chirally invariant R_Λ [81] this can be used for a regularization of models with chiral fermions. Also gauge theories can, in principle, be regularized in this way, but care is needed since Γ_Λ has to obey identities reflecting the gauge invariance [47, 11], [48]–[76]. Going further, the two-loop contribution is obtained by inserting the one-loop expression for $\Gamma_k^{(2)}$ as obtained from eq. (3.62) into the rhs of (3.60). It is easy to see that this generates two-loop integrals. Only the classical inverse propagator $\Gamma_\Lambda^{(2)}$ and its functional derivatives appear in the nested expressions. They are independent of k and the integration of the approximated flow equation is straightforward.

It is often useful to replace the perturbative iteration sketched above by a new one which involves full propagators and vertices instead of the classical ones. This will amount to a systematic resummed perturbation theory [124]. We start again with the lowest order term

$$\Gamma_{k(0)}[\varphi] = \Gamma_\Lambda[\varphi] \quad (3.63)$$

where Λ is now some conveniently chosen scale (not necessarily the ultraviolet cutoff). In the next step we write equation (3.60) in the form

$$\partial_t \Gamma_k = \frac{1}{2} \text{Tr} \partial_t \ln(\Gamma_k^{(2)} + R_k) - \frac{1}{2} \text{Tr} \left\{ \partial_t \Gamma_k^{(2)} (\Gamma_k^{(2)} + R_k)^{-1} \right\} \quad (3.64)$$

Here $\partial_t \Gamma_k^{(2)}$ can be inferred by taking the second functional derivative of eq. (3.60) with respect to the fields φ . Equation (3.64) can be taken as the starting point of a systematic loop expansion by counting any t -derivative acting only on Γ_k or its functional derivatives as an additional order in the number of loops. From (3.60) it is obvious that any such derivative involves indeed a new momentum loop. It will become clear below that in case of weak interactions it also involves a higher power in the coupling constants. The contribution from the first step of the iteration $\Gamma'_{k(1)}$ can now be defined by

$$\Gamma_k = \Gamma_{k(0)} + \Gamma'_{k(1)} \quad (3.65)$$

with

$$\Gamma'_{k(1)} = \frac{1}{2} \text{Tr} \left\{ \ln(\Gamma_k^{(2)} + R_k) - \ln(\Gamma_k^{(2)} + R_\Lambda) \right\} \quad (3.66)$$

In contrast to eq. (3.62) the rhs involves now the full (field-dependent) inverse propagator $\Gamma_k^{(2)}$, and, by performing suitable functional derivatives, the full proper vertices. Putting $k = 0$ the resummed one-loop expression (3.66) resembles a Schwinger-Dyson [108] or gap equation, but in contrast to those only full vertices appear! For example, for $k = 0$ the first iteration to the inverse propagator is obtained by taking the second functional derivative of eq. (3.66)

$$\begin{aligned} \left(\Gamma'_{(1)}^{(2)} \right)_{ab}(q, q') &= \frac{1}{2} \text{Tr} \left\{ (\Gamma^{(2)})^{-1} \frac{\delta^2 \Gamma^{(2)}}{\delta \varphi_a(q) \delta \bar{\varphi}_b(q')} \right\} \\ &\quad - \frac{1}{2} \text{Tr} \left\{ (\Gamma^{(2)})^{-1} \frac{\delta \Gamma^{(2)}}{\delta \varphi_a(q)} (\Gamma^{(2)})^{-1} \frac{\delta \Gamma^{(2)}}{\delta \bar{\varphi}_b(q')} \right\} \\ &\quad \text{--regulator terms} \end{aligned} \quad (3.67)$$

and involves the proper three- and four-point vertices. Adding the lowest order piece $\Gamma_{(0)}^{(2)}$ and approximating the vertices by their lowest order expressions, eq. (3.67) reduces to the standard gap equation for the propagator in a regularized form. Assuming that this is solved (for example numerically by an iterative procedure) we see that the resummed one-loop expression (3.67) involves already arbitrarily high powers in the coupling constant, and, in particular, contains part of the perturbative two-loop contribution. The remaining part of the perturbative two-loop contribution appears in the resummed two-loop contribution. Along these lines a systematic resummed perturbation theory (SRPT) can be developed [124].

Systematic resummed perturbation theory is particularly convenient for a computation of ultraviolet finite n -point functions (as the φ^6 coupling) or differences of n -point functions at different momenta. In this case the momentum integrals in the loop expansion are dominated by momenta for which renormalized vertices are appropriate²⁷. For $\Lambda \rightarrow \infty$ all dependence on the effective ultraviolet cutoff Λ is absorbed in the renormalized couplings. In this limit also the regulator terms vanish. In this context one can combine SRPT with approximate solutions of the flow equation. In fact, the ‘‘closure’’ of the flow equation by SRPT instead of truncation constitutes an interesting alternative: Eq. (3.60) is a functional differential equation which cannot be reduced to a closed system for a finite number of couplings (for finite N). For example, the beta function for the four-point vertex (the fourth functional derivative of the rhs of eq. (3.60)) involves not only two-, three- and four-point functions, but also up to six-point functions. Approximate solutions to the flow equation often proceed by truncation. For example, contributions involving the five- and six-point function could be neglected. As an alternative, these higher n -point functions can be evaluated by SRPT. We observe that the momentum integrals relevant for the higher n -point functions (also for differences of lower n -point functions at different momenta) are usually dominated by the low momentum modes with $q^2 \approx k^2$. This motivates the use of SRPT rather than standard perturbation theory for this purpose. A successful test of these ideas is provided by a computation of the β -function

²⁷A direct use of the ‘‘gap equation’’ (3.67) for the mass term is no improvement as compared to the standard Schwinger-Dyson equation since high momentum modes play an important role in the mass renormalization.

for the quartic scalar coupling for $d = 4$ via an evaluation of the momentum dependence of the vertices appearing in the flow equation by SRPT [156]. This resulted for small coupling in the universal two-loop β -function, without that two-loop momentum integrals had ever to be computed.

3.5 Exact flow of the propagator

We now turn to the exact flow equation for the propagator. This can be derived either by the graphical rules of the last subsection or by the functional derivatives sketched in eq. (2.30). We concentrate here on the inverse propagator in the Goldstone direction in a constant background field (see eq. (2.38))

$$G^{-1}(\rho, q^2) = Z_k(\rho, q^2)q^2 + U'_k(\rho) = M_0(\rho, q^2) - R_k(q) \quad (3.68)$$

According to eq. (2.30) its flow involves the three- and four-point functions. We notice that the three-point function $\Gamma_k^{(3)}$ vanishes for $\rho = 0$.

We parametrize the most general form of the inverse propagator in an arbitrary constant background φ_a by

$$\begin{aligned} \Gamma_{(2)k} &= \frac{1}{2} \int \frac{d^d q}{(2\pi)^d} \{ (U'_k(\rho) + Z_k(\rho, q^2)q^2) \varphi_a(q) \varphi_a(-q) \\ &\quad + \frac{1}{2} \varphi_a \varphi_b (2U''_k(\rho) + Y_k(\rho, q^2)q^2) \varphi_a(q) \varphi_b(-q) \}, \end{aligned} \quad (3.69)$$

and note that eq. (3.69) specifies all 1PI n -point functions with at most two nonvanishing momenta. Similarly the effective interactions which involve up to four fields with nonvanishing momentum are

$$\begin{aligned} \Gamma_{(3)k} &= \frac{1}{2} \int \frac{d^d q_1}{(2\pi)^d} \frac{d^d q_2}{(2\pi)^d} \{ \varphi_a \lambda_k^{(1)}(\rho; q_1, q_2) \varphi_a(q_1) \varphi_b(q_2) \varphi_b(-q_1 - q_2) \\ &\quad + \frac{1}{3} \varphi_a \varphi_b \varphi_c \gamma_k^{(1)}(\rho; q_1, q_2) \varphi_a(q_1) \varphi_b(q_2) \varphi_c(-q_1 - q_2) \}, \\ \Gamma_{(4)k} &= \frac{1}{8} \int \frac{d^d q_1}{(2\pi)^d} \frac{d^d q_2}{(2\pi)^d} \frac{d^d q_3}{(2\pi)^d} \{ \lambda_k^{(2)}(\rho; q_1, q_2, q_3) \varphi_a(q_1) \varphi_a(q_2) \varphi_b(q_3) \varphi_b(q_4) \\ &\quad + 2 \varphi_a \varphi_b \gamma_k^{(2)}(\rho; q_1, q_2, q_3) \varphi_a(q_1) \varphi_b(q_2) \varphi_c(q_3) \varphi_c(q_4) \\ &\quad + \frac{1}{3} \varphi_a \varphi_b \varphi_c \varphi_d \tau_k(\rho; q_1, q_2, q_3) \varphi_a(q_1) \varphi_b(q_2) \varphi_c(q_3) \varphi_d(q_4) \}, \end{aligned} \quad (3.70)$$

with $q_4 = -(q_1 + q_2 + q_3)$, $\rho = \frac{1}{2} \varphi_a \varphi_a$. The couplings $\lambda_k^{(i)}$, $\gamma_k^{(i)}$ and τ_k are appropriately symmetrized in the momenta (including symmetrization in the momentum of the last field, ie. q_4). The effective vertices are connected to U_k , Z_k and Y_k by continuity

$$\begin{aligned} \lambda_k^{(1)}(\rho; q_1, q_2) &= U''_k(\rho) + (q_2(q_1 + q_2)) Z'_k(\rho, (q_2(q_1 + q_2))) + \frac{1}{2} q_1^2 Y_k(\rho, q_1^2) + \Delta \lambda_k^{(1)}(\rho; q_1, q_2) \\ \lambda_k^{(2)}(\rho; q_1, q_2, q_3) &= U''_k(\rho) - (q_1 q_2) Z'_k(\rho, -(q_1 q_2)) - (q_3 q_4) Z'_k(\rho, -(q_3 q_4)) \\ &\quad + \frac{1}{2} (q_1 + q_2)^2 Y_k(\rho, (q_1 + q_2)^2) + \Delta \lambda_k^{(2)}(\rho; q_1, q_2, q_3) \end{aligned}$$

$$\begin{aligned}
\gamma_k^{(1)}(\rho; q_1, q_2) &= U_k'''(\rho) - \frac{1}{2}\{(q_1 q_2)Y_k'(\rho, -(q_1 q_2)) \\
&\quad + (q_1 \rightarrow -(q_1 + q_2)) + (q_2 \rightarrow -(q_1 + q_2))\} + \Delta\gamma_k^{(1)}(\rho; q_1, q_2) \\
\gamma_k^{(2)}(\rho; q_1, q_2, q_3) &= U_k'''(\rho) - (q_3 q_4)Z_k''(\rho, -(q_3 q_4)) \\
&\quad + \frac{1}{2}\{(q_1(q_1 + q_2))Y_k'(\rho, (q_1(q_1 + q_2)) + (q_1 \rightarrow q_2))\} \\
&\quad - \frac{1}{2}(q_1 q_2)Y_k'(\rho, -(q_1 q_2)) + \Delta\gamma_k^{(2)}(\rho; q_1, q_2, q_3) \\
\tau_k(\rho; q_1, q_2, q_3) &= U_k^{(4)}(\rho) - \frac{1}{2}\{(q_1, q_2)Y_k''(\rho, -(q_1 q_2)) + 5 \text{ permutations}\} + \Delta\tau_k(\rho; q_1, q_2, q_3)
\end{aligned} \tag{3.71}$$

In fact, we require that eq. (3.70) coincides with eq. (3.69) if only two of the momenta are nonvanishing, without that the corrections $\Delta\gamma, \Delta\lambda, \Delta\tau$ are involved. In particular, $\Delta\lambda_k^{(1)}$ and $\Delta\gamma_k^{(1)}$ vanish for $q_1 = 0, q_2 = 0$ or $(q_1 + q_2) = 0$, and, similarly, $\Delta\lambda_k^{(2)}, \Delta\gamma_k^{(2)}$ and $\Delta\tau_k$ vanish if two of the four momenta q_1, q_2, q_3 or q_4 are zero.

In terms of these couplings the exact flow equation for $G^{-1}(\rho, q^2)$ reads

$$\begin{aligned}
\partial_t G^{-1}(\rho, q^2) &= \frac{1}{2} \int \frac{d^d p}{(2\pi)^d} \partial_t R_k(p) \\
&\quad [4\rho\{M_1^{-2}(\rho, p^2)M_0^{-1}(\rho, (p+q)^2)(\lambda_k^{(1)}(\rho; p, q))^2 \\
&\quad + M_0^{-2}(\rho, p^2)M_1^{-1}(\rho, (p+q)^2)(\lambda_k^{(1)}(\rho; -q-p, q))^2\} \\
&\quad - M_0^{-2}(\rho, p^2)\{(N-1)\lambda_k^{(2)}(\rho; q, -q, p) + 2\lambda_k^{(2)}(\rho; q, p, -q)\} \\
&\quad - M_1^{-2}(\rho, p^2)\{\lambda_k^{(2)}(\rho; q, -q, p) + 2\rho\gamma_k^{(2)}(\rho; p, -p, q)\}] \\
&= -\frac{1}{2} \int \frac{d^d p}{(2\pi)^d} \tilde{\partial}_t \{ 4\rho(\lambda_k^{(1)}(\rho; -q-p, q))^2 M_0^{-1}(\rho, p^2) M_1^{-1}((q+p)^2) \\
&\quad - [(N-1)\lambda_k^{(2)}(\rho; q, -q, p) + 2\lambda_k^{(2)}(\rho; q, p, -q)] M_0^{-1}(\rho, p^2) \\
&\quad - [\lambda_k^{(2)}(\rho; q, -q, p) + 2\rho\gamma_k^{(2)}(\rho; p, -p, q)] M_1^{-1}(\rho, p^2) \}
\end{aligned} \tag{3.72}$$

Subtraction of the mass term in eq. (3.68) yields

$$\partial_t Z_k(\rho, q^2) = \frac{1}{q^2} (\partial_t G^{-1}(\rho, q^2) - \partial_t U_k'(\rho)) \equiv -\xi_k(\rho, \frac{q^2}{k^2}) Z_k \tag{3.73}$$

and the exact expression for the anomalous dimension is

$$\begin{aligned}
\eta &= -\frac{d}{dt} \ln Z_k(\rho_0(k), k^2) \\
&= \xi_k(\rho_0, 1) - \frac{2k^2}{Z_k} \frac{\partial}{\partial q^2} Z_k(\rho_0, q^2)|_{q^2=k^2} - \frac{\partial \rho_0}{\partial t} \frac{Z_k'(\rho_0, k^2)}{Z_k(\rho_0, k^2)}
\end{aligned} \tag{3.74}$$

Alternative definitions of η related to the flow of $Z_k(\rho_0, q^2 \rightarrow 0)$ will be discussed in later sections. Expressed in terms of the scaling variables the anomalous dimension can be equivalently extracted from the condition (3.4), i.e. $dz_k(\kappa)/dt = 0$ or

$$\partial_t z(\kappa) = -z_k'(\kappa) \partial_t \kappa \tag{3.75}$$

with $\kappa = Z_k k^{2-d} \rho_0$ the minimum of $u(\tilde{\rho})$. The flow of $z_k(\tilde{\rho})$ obeys

$$\partial_t z(\tilde{\rho}) = \eta z(\tilde{\rho}) + (d-2+\eta)\tilde{\rho} z'(\tilde{\rho}) - \xi_k(\tilde{\rho}, 1) + 2 \frac{\partial}{\partial y} \Delta z(\tilde{\rho}, y)|_{y=1} \quad (3.76)$$

and we note that for the scaling solution the rhs of eq. (3.75) vanishes since $\partial_t \kappa = 0$.

An exact expression for ξ_k is computed for a sharp cutoff in appendix B. Here we evaluate ξ_k in first order in the derivative expansion. In this order the momentum dependence of Z', Z'', Y and Y' is neglected and we can omit the terms $\Delta \lambda_k^{(i)}, \Delta \gamma_k^{(i)}$ and $\Delta \tau_k$. Inserting eq. (3.71) in (3.72) yields

$$\begin{aligned} \xi_k(\rho, \frac{q^2}{k^2}) &= \frac{1}{2} \int \frac{d^d p}{(2\pi)^d} Z^{-1} \tilde{\partial}_t \{ \rho(2U'' + p^2 Y)^2 \\ &M_0^{-1}(p^2)[M_1^{-1}((p+q)^2) - M_1^{-1}(p^2)]/q^2 \\ &+ \rho[(4U'' + 2p^2 Y)((1 + 2\frac{pq}{q^2})Y - 2\frac{pq}{q^2}Z') \\ &+ q^2((1 + 2\frac{pq}{q^2})Y - 2\frac{pq}{q^2}Z')^2] M_0^{-1}(p^2) M_1^{-1}((p+q)^2) \\ &- [(N-1)Z' + Y] M_0^{-1}(p^2) - (Z' + 2\rho Z'') M_1^{-1}(p^2) \} \end{aligned} \quad (3.77)$$

In this approximation we can also neglect the term $\partial \Delta z / \partial y$ in eq. (3.76) so that for the scaling solution ($\partial_t z(\tilde{\rho}) = 0$) the anomalous dimension is given by

$$\eta_{y_\eta} = \xi_k(\kappa, y_\eta) - (d-2+\eta_{y_\eta})\kappa z'(\kappa) \quad (3.78)$$

Here we show the freedom in the definition of η by the subscript y_η which indicates the value of q^2/k^2 for which Z_k is defined.

The optimal choice is presumably $y_\eta = 1$ (see above) which corresponds to the hybrid derivative expansion. An algebraic simplification occurs, however, for $y_\eta = 0$, corresponding to the “direct” derivative expansion. For a smooth cutoff the propagators $M_0^{-1}((p+q)^2)$ and $M_1^{-1}((p+q)^2)$ can be expanded for $q^2 \rightarrow 0$

$$\begin{aligned} M_0^{-1}((p+q)^2) &= M_0^{-1}(p^2) - (q^2 + 2pq)(Z + \dot{R}_k(p))M_0^{-2}(p^2) \\ &+ (q^2 + 2(pq))^2[(Z + \dot{R}_k(p))^2 M_0^{-3}(p^2) - \frac{1}{2}\ddot{R}_k(p)M_0^{-2}(p^2)] + \dots \end{aligned} \quad (3.79)$$

with $\dot{R}_k = \partial R_k / \partial p^2$ and Z replaced by $Z + \rho Y$ in a similar expression for $M_1^{-1}((p+q)^2)$. Since integrals over odd powers of p_μ vanish, one concludes that η_0 is well defined for a smooth cutoff. On the other hand, one observes [8] in the sharp cutoff limit a divergence in the derivative expansion $\lim_{y_\eta \rightarrow 0} \eta_{y_\eta} \sim (y_\eta)^{-1/2}$.

We emphasize that the dependence of η on the choice of y_η is a pure artifact of the truncation. Going beyond the derivative expansion, the scaling solution is characterized by the same anomalous dimension η independent of y_η . Nevertheless, for practical calculations some type of a derivative expansion is often crucial. For the direct derivative expansion it has been argued [102] that only smooth and rapidly falling cutoffs (like the exponential cutoff

(2.16)) and only the flow equations for Γ_k (as opposed to the one for the Wilsonian effective action) have satisfactory convergence properties. The constraints on the precise formulation seem, however, much less restrictive for the hybrid derivative expansion. This is strongly suggested by the computation of η for a sharp cutoff in appendix B. A detailed investigation is presented in [125].

The result for $\xi_k(\rho, 0)$ in first order in the derivative expansion can be found in [8, 42]. Here we present explicitly only the lowest order in the derivative expansion for which all terms $\sim Z', Z''$ and Y are neglected. One finds

$$\begin{aligned} \eta_0 = \xi_k(\kappa, 0) &= \frac{16v_d}{d} \lambda^2 \kappa m_{2,2}^d(0, 2\lambda\kappa) \\ m_{n_1, n_2}^d(w_1, w_2) &= -\frac{1}{2} k^{2(n_1+n_2-1)-d} Z_k^{n_1+n_2-2} \int_0^\infty dx x^{\frac{d}{2}} \tilde{\partial}_t \\ &\left\{ \dot{P}^2(x) (P(x) + Z_k k^2 w_1)^{-n_1} (P(x) + Z_k k^2 w_2)^{-n_2} \right\} \end{aligned} \quad (3.80)$$

where $P(x) = Z_k x + R_k(x)$ and $\dot{P} = \partial P / \partial x$. In particular, the limit $w_2 \gg 1$ is simple for all cutoff functions for which $\dot{R}_k(x)$ does not exceed Z_k by a large factor in some region of x , namely

$$\lim_{w_2 \rightarrow \infty} m_{n_1, n_2}^d(w_1, w_2) = w_2^{-n_2} m_{n_1, 0}^d(w_1) \quad (3.81)$$

For $d = 2$ and neglecting terms $\sim \eta$ one has the identity

$$\begin{aligned} m_{2,0}^2(0) &= -\frac{1}{2} \int_0^\infty dx x \tilde{\partial}_t \{ \dot{P}^2(x) / P^2(x) \} \\ &= \int_0^\infty dx \frac{d}{dx} \left\{ \frac{\dot{P}^2(x) x^2}{P^2(x)} \right\} = 1 \end{aligned} \quad (3.82)$$

One concludes for all cutoffs in this class

$$\lim_{\lambda\kappa \rightarrow \infty} \eta_0 = 2v_2 / \kappa = \frac{1}{4\pi\kappa} \quad (3.83)$$

This independence of the precise choice of the cutoff is directly related to the universality of the one-loop β -function for the two-dimensional nonlinear σ -models (cf. eq. (2.55)).

3.6 Approach to the convex potential for spontaneous symmetry breaking

For $k \rightarrow 0$ the effective potential U is a convex function of φ [126], i.e. $U'_0(\rho) \geq 0$. This is not only a formal property due to the Maxwell construction of thermodynamic potentials. The convexity reflects directly the effect of fluctuations. Indeed, as long as not all fluctuations are included the average potential U_k for $k > 0$ needs not to be convex – and it is actually not convex in case of spontaneous symmetry breaking. One therefore has to understand quantitatively how the fluctuations lead to an approach to convexity for $k \rightarrow 0$. The “flattening” of the nonconvex “inner region” of the potential is crucial to the computation of the nucleation rate in case of first-order phase transitions. This rate receives an exponential suppression factor from the free energy of the saddle point solution which interpolates between

two local minima of U_k and corresponds to tunneling through a (nonconvex!) potential barrier. We discuss this issue in detail in section 6. The discussion of this subsection is relevant for average potentials $U_k(\varphi)$ with several local minima for all $k > 0$, and not for the case where only a single minimum survives for small k (e.g. the symmetric phase of $O(N)$ models).

Different pictures can describe how fluctuations lead to a flattening of the potential. In a first approach [79] the average potential has been computed in a saddle point approximation. In the inner (nonconvex) region of the potential the relevant saddle point does not correspond to a constant field but rather to a spin wave (for $N > 1$) or a kink (for $N = 1$). Due to the existence of these nontrivial extrema the average potential shows in case of spontaneous symmetry breaking a generic behavior

$$U_k(\rho) = V(k) - pk^2\rho \quad (3.84)$$

for small ρ and k . (Here p is a positive constant and $V(k)$ is independent of ρ .) Similar nontrivial saddle points have been discussed [127] in the context of the exact Wegner-Houghton [3] equation. This ‘‘classical renormalization’’ confirms the generic behavior (3.84).

Since the flow equation (2.35) for the average potential is exact, there is, in principle, no need to investigate special non-perturbative saddle point solutions. The effects of all non-perturbative solutions like spin waves, kinks or instantons in appropriate models are fully included in the exact equation. For an appropriate truncation the solution of eq. (2.35) should therefore directly exhibit the approach to convexity. A first discussion of the flow of the curvature of U_k around the origin has indeed shown [80] the generic behavior (3.84). We extend this discussion here to the whole ‘‘inner region’’ of the potential. In this region the poles of the threshold functions for negative arguments dominate for small k . This leads indeed to a flattening of the average potential and to convexity for $k \rightarrow 0$, with the universal behavior (3.84).

The approach to convexity will be dominated by a pole of the threshold functions for negative arguments. This will allow us to find a solution of the flow equation which is valid for a restricted range of the field variable ρ . The way how convexity is approached depends only on a few characteristics of the infrared cutoff R_k and is otherwise model independent. We therefore need the behavior of the threshold functions for negative w . In order to become independent of truncations we generalize l_0^d for a momentum-dependent wave function renormalization²⁸

$$\begin{aligned} \bar{l}_0^d(w) &= \frac{1}{2} \int_0^\infty dy y^{\frac{d}{2}} s_k(y) (p(\tilde{\rho}, y) + w)^{-1} \\ p(\tilde{\rho}, y) &= (z(\tilde{\rho}, y) + r_k(y))y \end{aligned} \quad (3.85)$$

We consider here a class of infrared cutoffs with the property that for a given $\tilde{\rho}$ the function $p(\tilde{\rho}, y)$ has a minimum at $y_0 > 0$, with $p(\tilde{\rho}, y_0) = p_0(\tilde{\rho})$. For a range of $(\tilde{\rho}, w)$ for which

$$\epsilon = p_0 + w > 0 \quad (3.86)$$

²⁸Here we have not indicated in our notation the dependence of \bar{l}_0^d on η and the function $z(y, \tilde{\rho}) = z_k(\tilde{\rho}) + \Delta z_k(\tilde{\rho}, y)$. The exact flow equation for the potential is obtained then from eq. (2.63) by the replacement $l_0^d \rightarrow \bar{l}_0^d$, $\Delta\zeta_k = 0$.

and for small values of ϵ the integral (3.85) is dominated by the region $y \approx y_0$. In the vicinity of the minimum of $p(y)$ we can expand

$$p(y) = p_0 + a_2(y - y_0)^2 + \dots \quad (3.87)$$

and approximate the threshold function²⁹ (for $s_k(y_0) > 0$)

$$\begin{aligned} \bar{l}_0^d(w) &= \frac{1}{2} \int_0^\infty dy y_0^{d/2} s_k(y_0) [a_2(y - y_0)^2 + \epsilon]^{-1} \\ &= \frac{\pi}{2} y_0^{d/2} s_k(y_0) (a_2 \epsilon)^{-1/2} \end{aligned} \quad (3.88)$$

One concludes that \bar{l}_0^d has a singularity³⁰ $\sim \epsilon^{-1/2}$. This is the generic behavior³¹ for smooth threshold functions with sufficiently large $R_k(0)$.

For $N > 1$ the contribution of the radial mode can be at most as strong as the one from the Goldstone modes and the exact evolution equation for the potential can be approximated in the vicinity of the singularity at $u' = -p_0$ by

$$\partial_t u + du - (d - 2 + \eta) \tilde{\rho} u' = 2\tilde{c}(p_0 + u')^{-1/2} \quad (3.89)$$

In the range of its validity we can solve eq. (3.89) by the method of characteristics, using eqs. (2.56), (2.57) with

$$\psi_k(u') = \tilde{c}(p_0 + u')^{-\frac{3}{2}} \quad (3.90)$$

For $\eta = 0$ the most singular terms yield

$$(p_0 + u')^{-\frac{1}{2}} + \frac{1}{\tilde{c}} p_0^{d/2} \tilde{\rho} (-u')^{1-\frac{d}{2}} = f(u' e^{2t}) \quad (3.91)$$

Here f is fixed by the “initial value” $u'_0(\tilde{\rho})$ at t and reads

$$f(u' e^{2t}) = (p_0 + u' e^{2(t-t_0)})^{-\frac{1}{2}} + \frac{1}{\tilde{c}} p_0^{\frac{d}{2}} \hat{\rho}(u' e^{2(t-t_0)}) (-u')^{1-\frac{d}{2}} e^{(2-d)(t-t_0)} \quad (3.92)$$

where the function $\hat{\rho}$ is obtained by inversion of $u'_0(\tilde{\rho})$,

$$\hat{\rho}(u'_0(\tilde{\rho})) = \tilde{\rho} \quad (3.93)$$

For simplicity we consider here a linear approximation $u'_0(\tilde{\rho}) = \lambda_0(\tilde{\rho} - \kappa_0)$ with $\lambda_0 \kappa_0 = p_0 - \epsilon_0$, $0 < \epsilon_0 \ll 1$, or

$$\hat{\rho}(u' e^{2(t-t_0)}) = \frac{1}{\lambda_0} u' e^{2(t-t_0)} + \kappa_0 \quad (3.94)$$

²⁹See ref. [80] for a detailed discussion. The quantities p_0 and a_2 depend on $\tilde{\rho}$. If $w(\tilde{\rho})$ is monotonic in the appropriate range of $\tilde{\rho}$ we can consider them as functions of w and expand $p_0(w) = p_0(-p_0) + \epsilon p'_0 + \dots$, $a_2(w) = a_2(-p_0) + \epsilon a'_2 + \dots$. Up to higher orders in ϵ we can neglect the $\tilde{\rho}$ -dependence of p_0 and a_2 and use constants $p_0 \equiv p_0(-p_0)$, $a_2 \equiv a_2(-p_0)$.

³⁰Near the singularity the correction is $\sim \ln \epsilon$ or smaller.

³¹It is, however, not realized for a sharp cutoff for which the threshold function diverges only logarithmically.

For $d > 2$ the approximate expression for eq. (3.91) in the limit $k \ll k_0$ reads (with $e^{2(t-t_0)} = k^2/k_0^2$)

$$u' = -p_0 + \left(\frac{p_0\kappa_0}{\tilde{c}}\right)^{-2} \left(\frac{k}{k_0}\right)^{2(d-2)} \left(1 - \frac{\tilde{\rho}}{\kappa_0} \left(\frac{k}{k_0}\right)^{d-2} + \frac{\tilde{c}}{\kappa_0} p_0^{-\frac{3}{2}} \left(\frac{k}{k_0}\right)^{d-2}\right)^{-2} \quad (3.95)$$

We see that $u' + p_0$ remains always positive. The singularity is approached, but never crossed. (These features hold for generic $u'_0(\tilde{\rho}) > -p_0$.) In consequence, the derivative of the average potential is always larger than $-p_0k^2$

$$\frac{\partial U_k}{\partial \rho} > -p_0k^2 \quad (3.96)$$

and the potential becomes indeed convex for $k \rightarrow 0$. Furthermore, this implies that the region where eq. (3.96) is valid extends towards the potential minimum for $k \rightarrow 0$. For small k a reasonable approximate form for the phase with spontaneous symmetry breaking and $\rho < \rho_0(k)$ is

$$U_k(\rho) = \tilde{V}(k) - p_0k^2\rho + C\rho_0^2(k)k^{2(d-1)}(\rho_0(k) - \rho)^{-1} \quad (3.97)$$

where the constant C can be extracted by comparing with eq. (3.95). This agrees with eq. (3.84). The validity of the approximation (3.97) breaks down in a vicinity of $\rho_0(k)$ which shrinks to zero as $k \rightarrow 0$. In this vicinity the behavior for $\rho < \rho_0(k)$ is essentially determined by analytic continuation from the region $\rho \geq \rho_0(k)$.

For a nonvanishing constant anomalous dimension η we have to replace

$$d \rightarrow d_\eta = \frac{2d}{2-\eta}, \quad t \rightarrow t_\eta = \frac{2-\eta}{2}t, \quad \tilde{c} \rightarrow \tilde{c}_\eta = \frac{2}{2-\eta}\tilde{c} \quad (3.98)$$

This is important for $d = 2, N = 2$ where the anomalous dimension governs the approach to convexity. Indeed, at the Kosterlitz-Thouless phase transition (see section 3.9) or in the low temperature phase the anomalous dimension remains strictly positive for all values³² of k . The above discussion (3.95) of the approach to convexity remains valid, with $\left(\frac{k}{k_0}\right)^{d-2}$ replaced by $\left(\frac{k}{k_0}\right)^\eta$. We finally turn to the case $N = 1$ which we only discuss for $\eta = 0$. Near the pole at $\epsilon = u' + 2\tilde{\rho}u'' + p_0 \rightarrow 0$ the evolution equation for the potential is now approximated by

$$\partial_t u = -du + (d-2)\tilde{\rho}u' + 2\tilde{c}(p_0 + u' + 2\tilde{\rho}u'')^{-1/2} \quad (3.99)$$

For $d > 2$ and small k an iterative solution can be found for $|2\tilde{\rho}u''| \ll |p_0 + u'|$. In lowest order it is given by (3.95)

$$p_0 + u' = \left(\frac{p_0\kappa_0}{\tilde{c}}\right)^{-2} \left(\frac{k}{k_0}\right)^{2(d-2)} \left[1 - \frac{\tilde{\rho}}{\kappa_0} \left(\frac{k}{k_0}\right)^{d-2}\right]^{-2} \quad (3.100)$$

³²This is in contrast to $d = 3$ or $d = 2, N = 1$ where the anomalous dimension vanishes for $k \rightarrow 0$, except for the critical hypersurface of the phase transition.

and one finds that

$$\frac{2\tilde{\rho}u''}{p_0 + u'} = \frac{4\tilde{\rho}}{\kappa_0} \left(\frac{k}{k_0}\right)^{d-2} \left[1 - \frac{\tilde{\rho}}{\kappa_0} \left(\frac{k}{k_0}\right)^{d-2}\right]^{-1} \quad (3.101)$$

becomes indeed negligible for $k \rightarrow 0$. For this solution one obtains the same approach to convexity as for $N > 1$.

It is instructive to compare the “power law approach” (3.97) towards the asymptotic behavior for the “inner region” $U'_k = -p_0k^2$ with the “exponential approach” (3.55). It is obvious that the first is much easier to handle for numerical solutions. Indeed, already a tiny error in the numerical computation of (3.55) may lead to vanishing or negative values of $p_0k^2 + U'_k$ for which the threshold functions are ill defined. This is often a source of difficulties for numerical solutions of the partial differential equations. For numerical investigations of the approach to convexity it is advantageous to use threshold functions of the type (2.61) or corresponding smooth versions like (2.17) or (3.21) multiplied by $\beta > 1$, say $\beta = 4$. Then a simple truncation of the momentum dependence of the propagator like $\Gamma^{(2)} \sim Z_k q^2 + \text{const}$ obeys the conditions for a power-law approach (3.97), namely a minimum of $p(y)$ for $y_0 > 0$ (3.85) and $s_k(y_0) > 0$ (3.89). On the other hand, the above simple truncation fails to describe the appropriate approach to convexity for the cutoff (2.17). This is due to the fact that the minimum of $p(y)$ occurs for $y_0 = 0$ in this case. One learns that for this cutoff the simple truncation of the propagator is insufficient for the inner region of the potential. A correct reproduction of the exact bound $U'_k \geq -Z_k k^2$ (2.16) needs an extension of the truncation for the momentum dependence. For practical investigations of problems where the precise approach to convexity is not relevant one may use directly the knowledge of the exact result (2.16). Neglected effects of an insufficient truncation for the “inner region” may then be mimicked by a modification “by hand” of the threshold function in the immediate vicinity of the pole, for example by imposing the form (3.88).

Let us summarize the most important result of this subsection. The solution of the exact flow equation for the average potential leads in case of spontaneous symmetry breaking to a universal form $U'_k(\rho) \approx -p_0k^2$ for small ρ and k . As $k \rightarrow 0$ the region of validity of this behavior extends towards the minimum of the potential. Eq. (3.84) becomes valid in a range $0 \leq \rho < \rho_0(k) - \Delta(k)$ with $\Delta(k) > 0$ and $\lim_{k \rightarrow 0} \Delta(k) = 0$. The potential becomes therefore convex, in agreement with general properties and the exact bound (2.16).

4 $O(N)$ -symmetric scalar models

4.1 Introduction

In this section we study the N -component scalar model with $O(N)$ -symmetry in three and two dimensions. The case of four dimensional quantum field theories will be considered in section 8. The $O(N)$ model serves as a prototype for investigations concerning the restoration of a spontaneously broken symmetry at high temperature. For $N = 4$ the model describes the scalar sector of the electroweak standard model in the limit of vanishing gauge and Yukawa couplings. It is also used as an effective model for the chiral phase transition in QCD in the

limit of two quark flavors [24, 25, 26, 27], which will be discussed in section 8. In condensed matter physics $N = 3$ corresponds to the Heisenberg model used to describe the ferromagnetic phase transition. There are other applications like the helium superfluid transition ($N = 2$), liquid-vapor transition ($N = 1$) or statistical properties of long polymer chains ($N = 0$).

For three dimensions, we will concentrate on the computation of the equation of state near the critical temperature of the second order phase transition. The equation of state for a magnetic system is specified by the free energy density as a function of arbitrary magnetization ϕ and temperature T . All thermodynamic quantities can be derived from the function $U(\phi, T)$, which equals the free energy density for vanishing source (cf. eq. (2.2)). For example, the response of the system to a homogeneous magnetic field H follows from $\partial U/\partial\phi = H$. This permits the computation of ϕ for arbitrary H and T . There is a close analogy to quantum field theory at non-vanishing temperature. Here U corresponds to the temperature dependent effective potential as a function of a scalar field ϕ . For instance, in the $O(4)$ symmetric model for the chiral phase transition in two flavor QCD the meson field ϕ has four components. In this picture, the average light quark mass \hat{m} is associated with the source $H \sim \hat{m}$ and one is interested in the behavior during the phase transition (or crossover) for $H \neq 0$. The temperature and source dependent meson masses and zero momentum interactions are given by derivatives of U (cf. section 8).

The applicability of the $O(N)$ -symmetric scalar model to a wide class of very different physical systems in the vicinity of the critical temperature T_c is a manifestation of universality of critical phenomena. There exists a universal scaling form of the equation of state in the vicinity of the second order phase transition. The quantitative description of this scaling form will be the main topic here [36, 109]. The calculation of the effective potential $U(\phi, T)$ in the vicinity of the critical temperature of a second order phase transition is an old problem. One can prove through a general renormalization group analysis [2, 3] the Widom scaling form [128] of the equation of state³³

$$H = \phi^\delta \tilde{f}((T - T_c)/\phi^{1/\beta}). \quad (4.1)$$

Only the limiting cases $\phi \rightarrow 0$ and $\phi \rightarrow \infty$ are described by critical exponents and amplitudes.

For classical statistics in three dimensions we present in section 4.2 a computation of the effective potential $U_0 = \lim_{k \rightarrow 0} U_k = U/T$ from a derivative expansion of the effective average action with a uniform wave function renormalization factor. The approximation takes into account the most general field dependence of the potential term. This will allow us to compute the non-analytic behavior of U in the vicinity of the second order phase transition. From U the universal scaling form of the equation of state is extracted in section 4.3.

We demonstrate in section 4.4 that the non-universal aspects can be described by these methods as well. The example of carbon dioxide is worked out in detail. Going beyond the lowest order in a derivative expansion the approximation used in these sections takes into account the most general field dependence of the wave function renormalization factor.

³³We frequently suppress in our notation an appropriate power of a suitable “microscopic” length scale Λ^{-1} which is used to render quantities dimensionless.

Section 4.7 describes an application to the critical swelling of long polymer chains ($N = 0$). For two dimensions, we present in section 4.8 a quantitative description of the “Kosterlitz-Thouless” transition ($N = 2$).

4.2 The running average potential

In this section we compute the effective average potential $U_k(\rho)$ directly in three dimensions [36, 109]. Here $\rho = \frac{1}{2}\phi^a\phi_a$ and ϕ^a denotes the N -component real scalar field. For $k \rightarrow 0$ one obtains the effective potential $U_0(\rho) \equiv U(\rho)T^{-1}$, where we omit the factor T^{-1} in the following. It is related to the (Helmholtz) free energy density f_H by $f_H/T = U_0 - 2\rho\partial U_0/\partial\rho = U_0 - \phi H$. In the phase with spontaneous symmetry breaking the minimum of the potential occurs for $k = 0$ at $\rho_0 \neq 0$. In the symmetric phase the minimum of $U_k(\rho)$ ends at $\rho_0 = 0$ for $k = 0$. The two phases are separated by a scaling solution for which U_k/k^3 becomes independent of k once expressed in terms of a suitably rescaled field variable and the corresponding phase transition is of second order.

Our truncation is the lowest order in a derivative expansion of Γ_k ,

$$\Gamma_k = \int d^d x \{U_k(\rho) + \frac{1}{2}Z_k\partial^\mu\phi_a\partial_\mu\phi^a\}. \quad (4.2)$$

We keep for the potential term the most general $O(N)$ -symmetric form $U_k(\rho)$, whereas the wave function renormalization is approximated by one k -dependent parameter. We study the effects of a field dependent Z_k for the Ising model in section 4.4. Next order in the derivative expansion would be the generalization to a ρ -dependent wave function renormalization $Z_k(\rho)$ plus a function $Y_k(\rho)$ accounting for a possible different index structure of the kinetic term for $N \geq 2$. Going further would require the consideration of terms with four derivatives and so on. We employ in this section the exponential infrared cutoff (2.17).

For a study of the behavior in the vicinity of the phase transition it is convenient to work with dimensionless renormalized fields ³⁴

$$\begin{aligned} \tilde{\rho} &= Z_k k^{2-d} \rho, \\ u_k(\tilde{\rho}) &= k^{-d} U_k(\rho). \end{aligned} \quad (4.3)$$

The scaling form of the evolution equation for the effective potential has been derived in (3.1). With the truncation of eq. (4.2) the exact evolution equation for $u'_k \equiv \partial u_k / \partial \tilde{\rho}$ reduces then to the partial differential equation

$$\begin{aligned} \frac{\partial u'_k}{\partial t} = & \quad (-2 + \eta)u'_k + (d - 2 + \eta)\tilde{\rho}u''_k \\ & - 2v_d(N - 1)u''_k l_1^d(u'_k; \eta) - 2v_d(3u''_k + 2\tilde{\rho}u'''_k)l_1^d(u'_k + 2\tilde{\rho}u''_k; \eta), \end{aligned} \quad (4.4)$$

where $t = \ln(k/\Lambda)$, $v_3 = 1/8\pi^2$, primes denote derivatives with respect to $\tilde{\rho}$ and Λ is the ultraviolet cutoff of the theory. The “threshold” functions $l_n^d(w; \eta) \equiv l_n^d(w; \eta, z = 1)$ are discussed in section 3.2. We evaluate these functions numerically for the cutoff (2.17). Finally,

³⁴We keep the number of dimensions d arbitrary and specialize only later to $d = 3$.

the anomalous dimension is defined here by the q^2 -derivative of the inverse propagator at $q^2 = 0$. According to sect. 3.5 it is given in our truncation by³⁵ [42, 113, 109]

$$\eta(k) = \frac{16v_d}{d} \kappa \lambda^2 m_{2,2}^d(2\lambda\kappa), \quad (4.5)$$

with κ the location of the minimum of u_k and λ the quartic coupling

$$\begin{aligned} u'_k(\kappa) &= 0, \\ u''_k(\kappa) &= \lambda. \end{aligned} \quad (4.6)$$

The function $m_{2,2}^d$ is given by

$$\begin{aligned} m_{2,2}^d(w) &= \int_0^\infty dy y^{\frac{d}{2}-2} \frac{1+r+y\frac{\partial r}{\partial y}}{(1+r)^2 [(1+r)y+w]^2} \\ &\quad \left\{ 2y \frac{\partial r}{\partial y} + 2 \left(y \frac{\partial}{\partial y} \right)^2 r - 2y^2 \left(1+r+y\frac{\partial r}{\partial y} \right) \frac{\partial r}{\partial y} \left[\frac{1}{(1+r)y} + \frac{1}{(1+r)y+w} \right] \right\}. \end{aligned} \quad (4.7)$$

We point out that the argument $2\lambda\kappa$ turns out generically to be of order one for the scaling solution. Therefore, $\kappa \sim \lambda^{-1}$ and the mass effects are important, in contrast to perturbation theory where they are treated as small quantities $\sim \lambda$.

At a second order phase transition there is no mass scale present in the theory. In particular, one expects a scaling behavior of the rescaled effective average potential $u_k(\tilde{\rho})$. This can be studied by following the trajectory describing the scale dependence of $u_k(\tilde{\rho})$ as k is lowered from Λ to zero. Near the phase transition the trajectory spends most of the “time” t in the vicinity of the k -independent scaling solution of eq. (4.4) given by $\partial_t u'_*(\tilde{\rho}) = 0$. Only at the end of the running the “near-critical” trajectories deviate from the scaling solution. For $k \rightarrow 0$ they either end up in the symmetric phase with $\kappa = 0$ and positive constant mass term m^2 so that $u'_k(0) \sim m^2/k^2$; or they lead to a non-vanishing constant ρ_0 indicating spontaneous symmetry breaking with $\kappa \rightarrow Z_0 k^{2-d} \rho_0$. The equation of state involves the potential $U_0(\rho)$ for temperatures away from the critical temperature. Its computation requires the solution for the running away from the critical trajectory which involves the full partial differential equation (4.4).

In fig. 4.2 we present the results of the numerical integration of eq. (4.4) for $d = 3$ and $N = 1$. The function $u'_k(\tilde{\rho})$ is plotted for various values of $t = \ln(k/\Lambda)$. The evolution starts at $k = \Lambda$ ($t = 0$) where the average potential is equal to the classical potential (no effective integration of modes has been performed). We start with a quartic classical potential parameterized as

$$u'_\Lambda(\tilde{\rho}) = \lambda_\Lambda(\tilde{\rho} - \kappa_\Lambda). \quad (4.8)$$

We arbitrarily choose $\lambda_\Lambda = 0.1$ and fine tune κ_Λ so that a scaling solution is approached at later stages of the evolution. There is a critical value $\kappa_{cr} \simeq 6.396 \times 10^{-2}$ for which the

³⁵We neglect here for simplicity the implicit, linear η -dependence of the function $m_{2,2}^d$. We have numerically verified this approximation to have only a minor effect on the value of η .

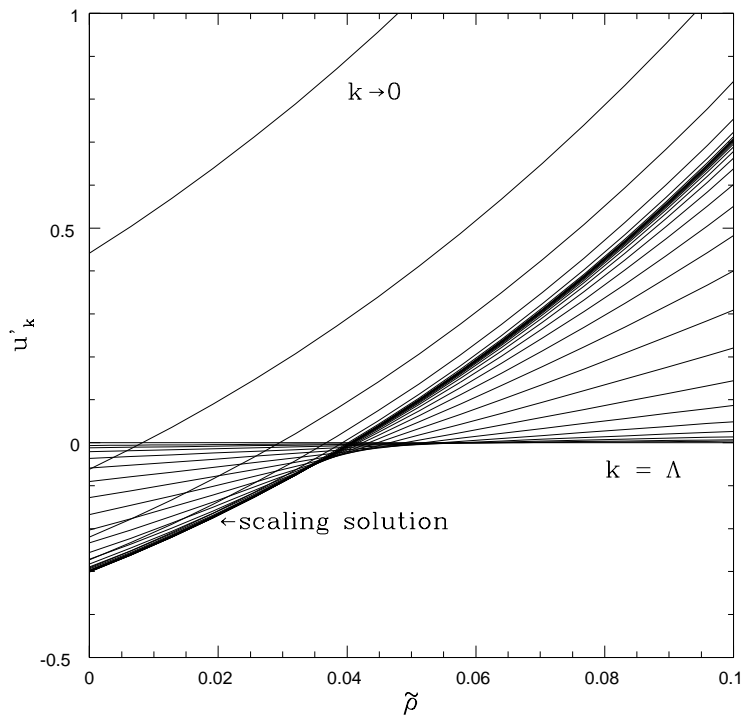


Figure 2: *The evolution of $u'_k(\tilde{\rho})$ as k is lowered from Λ to zero for $N = 1$. The initial conditions (bare couplings) have been chosen such that the scaling solution is approached before the system evolves towards the symmetric phase with $u'_k(0) > 0$. The concentration of lines near the scaling solution (flat diagonal line) indicates that the model is close to criticality. The scaling solution for $u(\tilde{\rho})$ has a minimum for $\tilde{\rho} \approx 0.04$.*

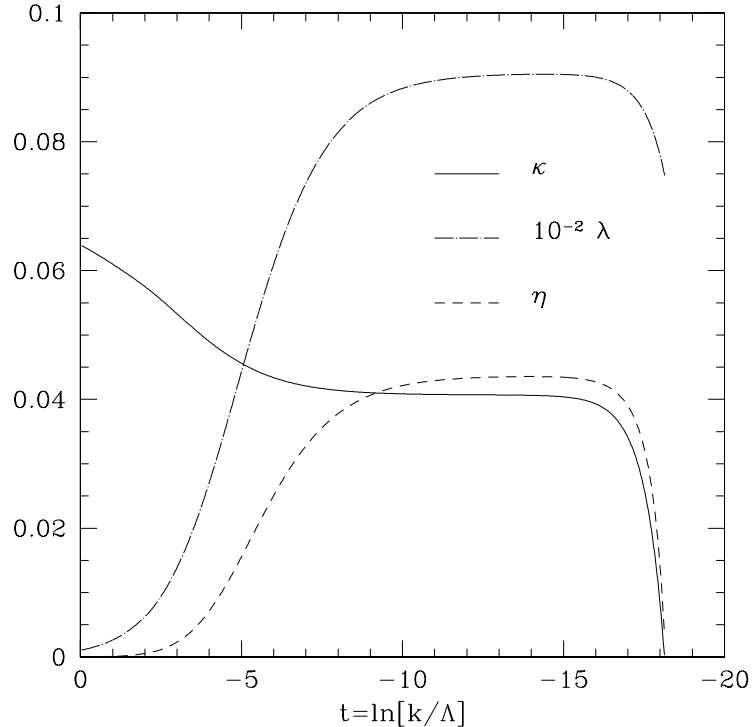


Figure 3: *The scale evolution of κ , λ and η for the initial conditions of Fig. 1. The plateaus correspond to the scaling solution.*

evolution leads to the scaling solution. For the results in fig. 4.2 a value κ_Λ slightly smaller than κ_{cr} is used. As k is lowered (and t turns negative), $u'_k(\tilde{\rho})$ deviates from its initial linear shape. Subsequently it evolves towards a form which is independent of k and corresponds to the scaling solution $\partial_t u'_*(\tilde{\rho}) = 0$. It spends a long “time” t – which can be rendered arbitrarily long through appropriate fine tuning of κ_Λ – in the vicinity of the scaling solution. During this “time”, the minimum of the potential $u'_k(\tilde{\rho})$ takes a fixed value κ_* , while the minimum of $U_k(\rho)$ evolves towards zero according to

$$\rho_0(k) = k\kappa_*/Z_k. \quad (4.9)$$

The longer $u'_k(\tilde{\rho})$ stays near the scaling solution, the smaller the resulting value of $\rho_0(k)$ when the system deviates from it. As this value determines the mass scale for the renormalized theory at $k = 0$, the scaling solution governs the behavior of the system very close to the phase transition, where the characteristic mass scale goes to zero. Another important property of the “near-critical” trajectories, which spend a long “time” t near the scaling solution, is that they become insensitive to the details of the classical theory which determine the initial conditions for the evolution. After $u'_k(\tilde{\rho})$ has evolved away from its scaling form $u'_*(\tilde{\rho})$, its shape is independent of the choice of λ_Λ for the classical theory. This property gives rise to the universal behavior near second order phase transitions. For the solution depicted in fig. 4.2, $u_k(\tilde{\rho})$ evolves in such a way that its minimum runs to zero with $u'_k(0)$ subsequently increasing. Eventually the theory settles down in the symmetric phase with a positive constant

renormalized mass term $m^2 = k^2 u'_k(0)$ as $k \rightarrow 0$. Another possibility is that the system ends up in the phase with spontaneous symmetry breaking. In this case κ grows in such a way that $\rho_0(k)$ approaches a constant value for $k \rightarrow 0$.

The approach to the scaling solution and the deviation from it can also be seen in fig. 4.2. The evolution of the running parameters $\kappa(t)$, $\lambda(t)$ starts with their initial classical values, leads to fixed point values κ_* , λ_* near the scaling solution, and finally ends up in the symmetric phase (κ runs to zero). Similarly the anomalous dimension $\eta(k)$, which is given by eq. (4.5), takes a fixed point value η_* when the scaling solution is approached. During this part of the evolution the wave function renormalization is given by

$$Z_k \sim k^{-\eta_*} \quad (4.10)$$

according to eq. (2.38). When the parts of the evolution towards and away from the fixed point become negligible compared to the evolution near the fixed point – that is, very close to the phase transition – eq. (4.10) becomes a very good approximation for sufficiently low k . This indicates that η_* can be identified with the critical exponent η . For the solution of fig. 2 ($N = 1$) we find $\kappa_* = 4.07 \times 10^{-2}$, $\lambda_* = 9.04$ and $\eta_* = 4.4 \times 10^{-2}$.

	κ_*	λ_*	$u_*^{(3)}$	η	ν
a	6.57×10^{-2}	11.5			0.745
b	8.01×10^{-2}	7.27	52.8		0.794
c	7.86×10^{-2}	6.64	42.0	3.6×10^{-2}	0.760
d	7.75×10^{-2}	6.94	43.5	3.8×10^{-2}	0.753
e	7.71×10^{-2}	7.03	43.4	3.8×10^{-2}	0.752
f	7.64×10^{-2}	7.07	44.2	3.8×10^{-2}	0.747
g	7.765×10^{-2}	6.26	39.46	4.9×10^{-2}	0.704

Table 1: *Truncation dependence of the scaling solution and critical exponents. The minimum κ of the potential $u_k(\tilde{\rho})$ and the quartic and six point couplings $\lambda = u''(\kappa)$, $u_k^{(3)}(\kappa)$ are given for the scaling solution. We also display the critical exponents η and ν , in various approximations: (a)-(e) from refs. [42, 113] and (f) from the present section [109, 36]. $N = 3$.*

- a) *Quartic truncation where only the evolution of κ and λ is considered and higher derivatives of the potential and the anomalous dimension are neglected (cf. section 2.5).*
- b) *Sixth order truncation with κ , λ , $u_k^{(3)}(\kappa)$ included.*
- c) *All couplings with canonical dimension ≥ 0 are included and η is approximated by eq. (4.5).*
- d) *Addition of $u_k^{(4)}(\kappa)$ which has negative canonical dimension.*
- e) *Additional estimate of $u_k^{(5)}(\kappa)$, $u_k^{(6)}(\kappa)$.*
- f) *The partial differential equation (4.4) for $u'_k(\tilde{\rho})$ is solved numerically and η is approximated by eq. (4.5).*
- g) *First order derivative expansion with field dependent wave function renormalizations z and y [130].*

As we have already mentioned the details of the renormalized theory in the vicinity of the phase transition are independent of the classical coupling λ_Λ . Also the initial form of the

potential does not have to be of the quartic form of eq. (4.8) as long as the symmetries are respected. Moreover, the critical theory can be parameterized in terms of critical exponents [129], an example of which is the anomalous dimension η . These exponents are universal quantities which depend only on the dimensionality of the system and its internal symmetries. For our three-dimensional theory they depend only on the value of N and can be easily extracted from our results. We concentrate here on the exponent ν , which parameterizes the behavior of the renormalized mass in the critical region. Other exponents are computed in the following sections along with the critical equation of state. The other exponents are not independent quantities, but can be determined from η and ν through universal scaling laws [129]. We define the exponent ν through the renormalized mass term in the symmetric phase

$$m^2 = \frac{1}{Z_k} \frac{dU_k(0)}{d\rho} = k^2 u'_k(0) \quad \text{for } k \rightarrow 0. \quad (4.11)$$

The behavior of m^2 in the critical region depends only on the distance from the phase transition, which can be expressed in terms of the difference of κ_Λ from the critical value κ_{cr} for which the renormalized theory has exactly $m^2 = 0$. The exponent ν is determined from the relation

$$m^2 \sim |\delta\kappa_\Lambda|^{2\nu} = |\kappa_\Lambda - \kappa_{cr}|^{2\nu}. \quad (4.12)$$

Assuming proportionality $\delta\kappa_\Lambda \sim T_c - T$ this yields the critical temperature dependence of the correlation length $\xi = m^{-1}$. For a determination of ν from our results we calculate m^2 for various values of κ_Λ near κ_{cr} . We subsequently plot $\ln(m^2)$ as a function of $\ln|\delta\kappa_\Lambda|$. This curve becomes linear for $\delta\kappa_\Lambda \rightarrow 0$ and we obtain ν from the constant slope.

Our numerical solution of the partial differential equation (4.4) corresponds to an infinite level of truncation in a Taylor expansion around the “running” minimum of the potential. This infinite system may be approximately solved by neglecting $\tilde{\rho}$ -derivatives of $u_k(\tilde{\rho})$ higher than a given order. The apparent convergence of this procedure can be observed from table 4.2. We present results obtained through the procedure of successive truncations and through our numerical solution of the partial differential equation for $N = 3$. We give the values of κ , λ , $u_k^{(3)}(\kappa)$ for the scaling solution and the critical exponents η , ν . We observe how the results stabilize as more $\tilde{\rho}$ -derivatives of $u_k(\tilde{\rho})$ at $\tilde{\rho} = \kappa$ and the anomalous dimension are taken into account. The last line gives the results of our numerical solution of eq. (4.4). By comparing with the previous line we conclude that the inclusion of all the $\tilde{\rho}$ -derivatives higher than $u_k^{(6)}(\kappa)$ and the term $\sim \eta$ in the “threshold” functions generates an improvement of less than 1 % for the results. This is smaller than the error induced by the omission of the higher derivative terms in the average action, which typically generates an uncertainty of the order of the anomalous dimension. A systematic comparison [103] between the expansion around κ presented here and an expansion around $\tilde{\rho} = 0$ reveals that only the first procedure shows this convergence.

In table 2 we compare our values for the critical exponents obtained from the numerical solution of the partial differential equation (4.4) and (4.5) with results obtained from other methods (such as the ϵ -expansion, perturbation series at fixed dimension, lattice high temperature expansions, Monte Carlo simulations and the $1/N$ -expansion). As expected η

N	ν		η	
0	0.589 ^f	0.5882(11) ^a 0.5875(25) ^b 0.5878(6) ^c 0.5877(6) ^e	0.040 ^f	0.0284(25) ^a 0.0300(50) ^b
1	0.643 ^f 0.6307 ^g	0.6304(13) ^a 0.6290(25) ^b 0.6315(8) ^c 0.6294(9) ^e	0.044 ^f 0.0467 ^g	0.0335(25) ^a 0.0360(50) ^b 0.0374(14) ^e
2	0.697 ^f 0.666 ^g	0.6703(15) ^a 0.6680(35) ^b 0.675(2) ^c 0.6721(13) ^e	0.042 ^f 0.049 ^g	0.0354(25) ^a 0.0380(50) ^b 0.042(2) ^e
3	0.747 ^f 0.704 ^g	0.7073(35) ^a 0.7045(55) ^b 0.716(2) ^c 0.7128(14) ^e	0.038 ^f 0.049 ^g	0.0355(25) ^a 0.0375(45) ^b 0.041(2) ^e
4	0.787 ^f 0.739 ^g	0.741(6) ^a 0.737(8) ^b 0.759(3) ^c 0.7525(10) ^e	0.034 ^f 0.047 ^g	0.0350(45) ^a 0.036(4) ^b 0.038(1) ^e
10	0.904 ^f	0.894(4) ^c 0.877 ^d	0.019 ^f	0.025 ^d
100	0.990 ^f	0.989 ^d	0.002 ^f	0.003 ^d

Table 2: Critical exponents ν and η for various values of N . For comparison we list results obtained with other methods as summarized in [131], [132] and [133]:

- a) From perturbation series at fixed dimension including seven-loop contributions.
- b) From the ϵ -expansion at order ϵ^5 .
- c) From lattice high temperature expansions [133] (see also [134, 135]).
- d) From the $1/N$ -expansion at order $1/N^2$.
- e) From lattice Monte Carlo simulations [136, 137].
- f) Average action in lowest order in the derivative expansion (present section).
- g) From first order in the derivative expansion for the average action with field dependent wave function renormalizations (for $N = 1$ see [38] and section 4.4, and [130] for $N > 1$).

is rather poorly determined since it is the quantity most seriously affected by the omission of the higher derivative terms in the average action. The exponent ν is in agreement with the known results at the 1-5 % level, with a discrepancy roughly equal to the value of η for various N . Our results compare well with those obtained by similar methods using a variety of forms for the infrared cutoff function [138, 110, 104, 87, 83].

In conclusion, the shape of the average potential is under good quantitative control for every scale k . This permits a quantitative understanding of the most important properties of the system at every length scale. We will exploit this in the following to extract the scaling form of the equation of state.

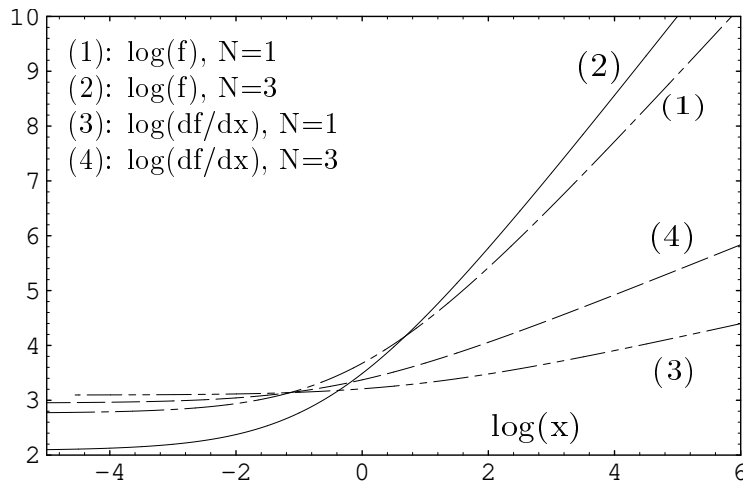


Figure 4: *Universal critical equation of state, symmetric phase: Logarithmic plot of f and df/dx for $x > 0$.*

4.3 Universal critical equation of state

In this section we extract the Widom scaling form of the equation of state from a solution [36] of eqs. (4.4), (4.5) for the three dimensional $O(N)$ model. Its asymptotic behavior yields the universal critical exponents and amplitude ratios. We also present fits for the scaling function for $N = 3$ and $N = 4$. A detailed discussion of the universal and non-universal aspects of the Ising model ($N = 1$) is given in section 4.4.

Eq. (4.1) establishes the scaling properties of the equation of state. The external field H is related to the derivative of the effective potential $U' = \partial U / \partial \rho$ by $H_a = U' \phi_a$. The critical equation of state, relating the temperature, the external field and the order parameter, can then be written in the scaling form ($\phi = \sqrt{2\rho}$)

$$\frac{U'}{\phi^{\delta-1}} = f(x), \quad x = \frac{-\delta\kappa_\Lambda}{\phi^{1/\beta}}, \quad (4.13)$$

with critical exponents δ and β . A measure of the distance from the phase transition is the difference $\delta\kappa_\Lambda = \kappa_\Lambda - \kappa_{cr}$. If κ_Λ is interpreted as a function of temperature, the deviation $\delta\kappa_\Lambda$ is proportional to the deviation from the critical temperature, i.e. $\delta\kappa_\Lambda = A(T)(T_{cr} - T)$ with $A(T_{cr}) > 0$. For $\phi \rightarrow \infty$ our numerical solution for U' obeys $U' \sim \phi^{\delta-1}$ with high accuracy. The inferred value of δ is displayed in table 4, and we have checked the scaling relation $\delta = (5 - \eta)/(1 + \eta)$. The value of the critical exponent η is obtained from eq. (4.4) for the scaling solution. We have also verified explicitly that f depends only on the scaling variable x for the value of β given in table 4. In figs. 1 and 2 we plot $\log(f)$ and $\log(df/dx)$ as a function of $\log|x|$ for $N = 1$ and $N = 3$. Fig. 1 corresponds to the symmetric phase ($x > 0$), and fig. 2 to the phase with spontaneous symmetry breaking ($x < 0$).

One can easily extract the asymptotic behavior from the logarithmic plots and compare with known values of critical exponents and amplitudes. The curves become constant, both for $x \rightarrow 0^+$ and $x \rightarrow 0^-$ with the same value, consistently with the regularity of $f(x)$ at $x = 0$.

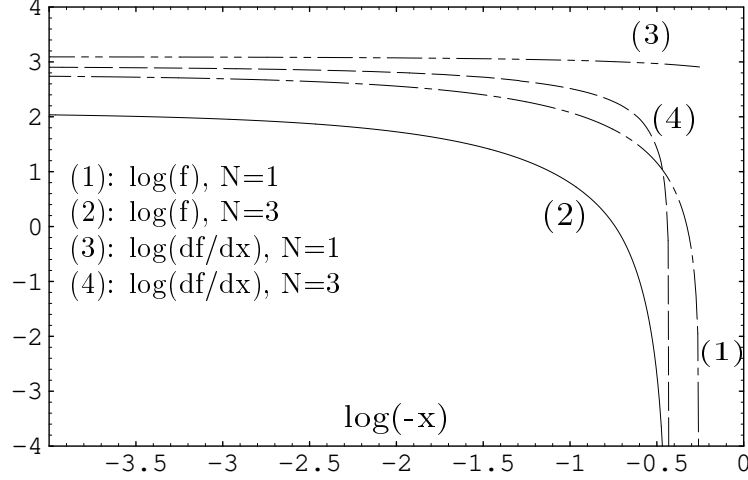


Figure 5: *Universal critical equation of state, spontaneous symmetry breaking: Logarithmic plot of f and df/dx for $x < 0$.*

For the universal function one obtains

$$\lim_{x \rightarrow 0} f(x) = D, \quad (4.14)$$

and $H = D\phi^\delta$ on the critical isotherm. For $x \rightarrow \infty$ one observes that $\log(f)$ becomes a linear function of $\log(x)$ with constant slope γ . In this limit the universal function takes the form

$$\lim_{x \rightarrow \infty} f(x) = (C^+)^{-1} x^\gamma. \quad (4.15)$$

The amplitude C^+ and the critical exponent γ characterize the behavior of the 'unrenormalized' squared mass or inverse susceptibility

$$\bar{m}^2 = \chi^{-1} = \lim_{\phi \rightarrow 0} \left(\frac{\partial^2 U}{\partial \phi^2} \right) = (C^+)^{-1} |\delta\kappa_\Lambda|^\gamma \phi^{\delta-1-\gamma/\beta}. \quad (4.16)$$

We have verified the scaling relation $\gamma/\beta = \delta - 1$ that connects γ with the exponents β and δ appearing in the Widom scaling form (4.1). One observes that the zero-field magnetic susceptibility, or equivalently the inverse unrenormalized squared mass $\bar{m}^{-2} = \chi$, is non-analytic for $\delta\kappa_\Lambda \rightarrow 0$ in the symmetric phase: $\chi = C^+ |\delta\kappa_\Lambda|^{-\gamma}$. In this phase we find that the correlation length $\xi = (Z_0\chi)^{1/2}$, which is equal to the inverse of the renormalized mass m_R , behaves as $\xi = \xi^+ |\delta\kappa_\Lambda|^{-\nu}$ with $\nu = \gamma/(2 - \eta)$.

The spontaneously broken phase is characterized by a nonzero value ϕ_0 of the minimum of the effective potential U with $H = (\partial U/\partial \phi)(\phi_0) = 0$. The appearance of spontaneous symmetry breaking below T_c implies that $f(x)$ has a zero $x = -B^{-1/\beta}$ and one observes a singularity of the logarithmic plot in fig. 2. In particular, according to eq. (4.1) the minimum behaves as $\phi_0 = B(\delta\kappa_\Lambda)^\beta$. Below the critical temperature, the longitudinal and transversal susceptibilities χ_L and χ_T are different for $N > 1$

$$\chi_L^{-1} = \frac{\partial^2 U}{\partial \phi^2} = \phi^{\delta-1} \left(\delta f(x) - \frac{x}{\beta} f'(x) \right), \quad \chi_T^{-1} = \frac{1}{\phi} \frac{\partial U}{\partial \phi} = \phi^{\delta-1} f(x) \quad (4.17)$$

(with $f' = df/dx$). This is related to the existence of massless Goldstone modes in the $(N-1)$ transverse directions, which causes the transversal susceptibility to diverge for vanishing external field. Fluctuations of these modes induce the divergence of the zero-field longitudinal susceptibility. This can be concluded from the singularity of $\log(f')$ for $N = 3$ in fig. 2. The first x -derivative of the universal function vanishes as $H \rightarrow 0$, i.e. $f'(x = -B^{-1/\beta}) = 0$ for $N > 1$. For $N = 1$ there is a non-vanishing constant value for $f'(x = -B^{-1/\beta})$ with a finite zero-field susceptibility $\chi = C^-(\delta\kappa_\Lambda)^{-\gamma}$, where $(C^-)^{-1} = B^{\delta-1-1/\beta} f'(-B^{-1/\beta})/\beta$. For a non-vanishing physical infrared cutoff k , the longitudinal susceptibility remains finite also for $N > 1$: $\chi_L \sim (k\rho_0)^{-1/2}$. For $N = 1$ in the ordered phase, the correlation length behaves as $\xi = \xi^-(\delta\kappa_\Lambda)^{-\nu}$, and the renormalized minimum $\rho_{0R} = Z_0\rho_0$ of the potential U scales as $\rho_{0R} = E(\delta\kappa_\Lambda)^\nu$.

The amplitudes of singularities near the phase transition D , C^\pm , ξ^\pm , B and E are given in table 4. They are not universal. All models in the same universality class can be related by a multiplicative rescaling of ϕ and $\delta\kappa_\Lambda$ or $(T_c - T)$. Accordingly there are only two independent amplitudes and exponents respectively. Ratios of amplitudes which are invariant under this rescaling are universal. We display the critical exponents and the universal combinations $R_\chi = C^+DB^{\delta-1}$, $\tilde{R}_\xi = (\xi^+)^{\beta/\nu}D^{1/(\delta+1)}B$ and ξ^+E for $N = 3, 4$ in tables 3 and 4.

N	β	γ	δ	ν	η
3	0.388	1.465	4.78	0.747	0.038
4	0.407	1.548	4.80	0.787	0.0344

Table 3: *Universal critical exponents for $N = 3, 4$.*

N	C^+	D	B	ξ^+	E	R_χ	\tilde{R}_ξ	ξ^+E
3	0.0743	8.02	1.180	0.263	0.746	1.11	0.845	0.196
4	2.79	1.82	7.41	0.270	0.814	1.02	0.852	0.220

Table 4: *Universal amplitude ratios R_χ , \tilde{R}_ξ and ξ^+E for $N = 3, 4$. The amplitudes C^+ , D , B , ξ^+ and E are not universal.*

The asymptotic behavior observed for the universal function can be used in order to obtain a semi-analytical expression for $f(x)$. We find that the following two-parameter fits for $N = 3, 4$ reproduce the numerical values for both f and df/dx with 1–2% accuracy:

$$f_{\text{fit}}(x) = D(1 + B^{1/\beta}x)^2(1 + \Theta x)^\Delta(1 + cx)^{\gamma-2-\Delta}, \quad (4.18)$$

with $c = (C^+DB^{2/\beta}\Theta^\Delta)^{-1/(\gamma-2-\Delta)}$. The fitting parameters are chosen as $\Theta = 1.312$ and $\Delta = -0.595$ for $N = 3$. For $N = 4$ we find the following fit,

$$f_{\text{fit}}(x) = 1.816 \cdot 10^{-4}(1 + 136.1x)^2(1 + 160.9\theta x)^\Delta(1 + 160.9(0.9446\theta^\Delta)^{-1/(\gamma-2-\Delta)}x)^{\gamma-2-\Delta} \quad (4.19)$$

with $\theta = 0.625$ (0.656), $\Delta = -0.490$ (-0.550) for $x > 0$ ($x < 0$) and γ as given in table 4.3.

The universal properties of the scaling function can be compared with results obtained by other methods for the three-dimensional $O(4)$ Heisenberg model. In figure 6 we display our results for $N = 4$ along with those obtained from lattice Monte Carlo simulation [139], second order epsilon expansion [140] and mean field theory.

In summary, our numerical solution of eq. (4.3) gives a very detailed picture of the critical equation of state of the three dimensional $O(N)$ model. The numerical uncertainties are estimated by comparison of results obtained through two independent integration algorithms [109, 37]. They are small, typically less than 0.3% for critical exponents. The scaling relations between the critical exponents are fulfilled within a deviation of 2×10^{-4} . The dominant quantitative error stems from the relatively crude approximation of the kinetic term in (4.2) and is related to the size of the anomalous dimension $\eta \simeq 4\%$. We emphasize that in contrast to most other analytical methods no scaling hypothesis is used as an input and no resummations of series are needed. The scaling behavior is simply a property of the solution of the flow equation.

In the following we improve on this approximation for the Ising model ($N = 1$). We allow for a most general field dependence of the wave function renormalization factor, and compare with the results of this section. The Ising model is analyzed with a particular short distance action relevant for carbon dioxide. This allows us to compare the non-universal aspects as well as the universal aspects of the liquid-gas phase transition in carbon dioxide with experiment.

4.4 Gas-liquid transition and the Ising universality class ³⁶

Field theoretical description

Many phase transitions are described near the critical temperature by a one-component ($N = 1$) scalar field theory without internal symmetries. A typical example is the water-vapor transition where the field $\varphi(x)$ corresponds to the average density field $n(x)$. At normal pressure one observes a first order transition corresponding to a jump in φ from high (water) to low (vapor) values as the temperature T is increased. With increasing pressure the first order transition line ends at some critical pressure p_* in an endpoint. For $p > p_*$ the phase transition is replaced by an analytical crossover.

This behaviour is common to many systems and characterizes the universality class of the Ising model. As another example from particle physics, the high temperature electroweak phase transition in the early universe is described by this universality class if the mass of the Higgs particle in the standard model is near the endpoint value $M_{H_*} \approx 72\text{GeV}$ [141]. An Ising type endpoint should also exist if the high temperature or high density chiral phase transition in QCD or the gas-liquid transition for nuclear matter are of first order in some region of parameter space.

Very often the location of the endpoint - e.g. the critical T_* , p_* and n_* for the liquid-gas transition - is measured quite precisely. The approach to criticality is governed by universal

³⁶Sections 4.4-4.6 are based on a collaboration with S. Seide [38].

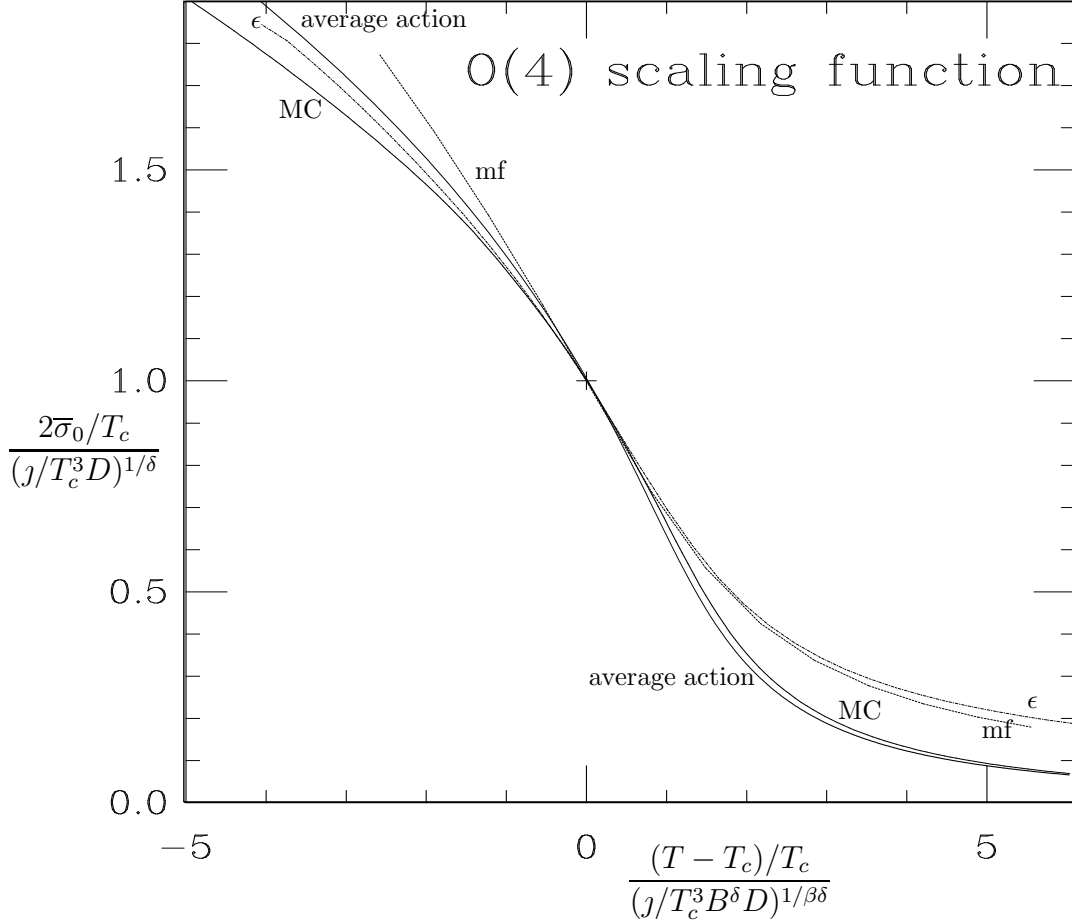


Figure 6: *Critical equation of state for the three-dimensional $O(4)$ Heisenberg model. We compare our results for the scaling function, denoted by “average action”, with results of other methods. We have labeled the axes in terms of the expectation value $\bar{\sigma}_0$ and the source j relevant for the chiral phase transition in QCD discussed in section 8. In this context they describe the dependence of the chiral condensate $\sim \bar{\sigma}_0$ on the quark mass $\sim j$ for two flavors of quarks. The constants B and D specify the non-universal amplitudes of the model. The curve labeled by “MC” represents a fit to lattice Monte Carlo data. The second order epsilon expansion [140] and mean field results are denoted by “ ϵ ” and “mf”, respectively. Apart from our results the curves are taken from ref. [139].*

scaling laws with critical exponents. Experimental information is also available about the non-universal amplitudes appearing in this scaling behaviour. These non-universal critical properties are specific for a given system, and the question arises how they can be used to gain precise information about the underlying microscopic physics. This problem clearly involves the difficult task of an explicit connection between the short distance physics and the collective behaviour leading to a very large correlation length.

So far renormalization group methods [1]–[7], [123] have established the structure of this relation and led to a precise determination of the universal critical properties. The non-perturbative flow equation (2.19) allows us to complete the task by mapping details of microscopic physics to non-universal critical quantities. A demonstration is given for the liquid-gas transition in carbon dioxide.

In the following, we will work with a truncation which includes the most general terms containing up to two derivatives,

$$\Gamma_k[\varphi] = \int d^3x \left\{ U_k(\varphi(x)) + \frac{1}{2} Z_k(\varphi(x)) \partial^\mu \varphi \partial_\mu \varphi \right\}. \quad (4.20)$$

In contrast to the ansatz (4.2) we now include the field dependence of the wave function renormalization factor $Z_k(\varphi(x))$. Our aim is the computation of the potential $U_0 \equiv U_{k \rightarrow 0} = U/T$ and the wave function renormalization $Z \equiv Z_{k \rightarrow 0}$ for a vanishing infrared cutoff. For the liquid gas transition the source J is linear in the chemical potential μ . For a homogeneous situation $U_0 T$ corresponds therefore to the free energy density. Indeed, expressing U_0 as a function of the density one finds for the liquid-gas system at a given chemical potential μ

$$\frac{\partial U_0}{\partial n} = \frac{\mu}{T}. \quad (4.21)$$

Equivalently, one may also use the more familiar form of the equation of state in terms of the pressure p ,

$$n^2 \frac{\partial}{\partial n} \left(\frac{U_0}{n} \right) = \frac{p}{T}. \quad (4.22)$$

(Here the additive constant in U_0 is fixed such that $U_0(n=0) = 0$). The wave function renormalization $Z(\varphi)$ contains the additional information needed for a determination of the two point correlation function at large distance for arbitrary pressure.

The computation of thermodynamic potentials, correlation length etc. is done in two steps: The first is the computation of a short distance free energy Γ_Λ . This does not involve large length scales and can be done by a variety of expansion methods or numerical simulations. This step is not the main emphasis here and we will use a relatively crude approximation for the gas-liquid transition. The second step is more difficult and will be addressed here. It involves the relation between Γ_Λ and Γ_0 , and has to account for possible complicated collective long distance fluctuations.

For a large infrared cutoff $k = \Lambda$ one may compute Γ_Λ perturbatively. For example, the lowest order in a virial expansion for the liquid-gas system yields

$$U_\Lambda(n) = -n \left(1 + \ln g + \frac{3}{2} \ln \frac{MT}{2\pi\Lambda^2} \right)$$

$$+n \ln \left(\frac{n}{(1 - b_0(\Lambda)n)\Lambda^3} \right) - \frac{b_1(\Lambda)}{T} n^2 + c_\Lambda. \quad (4.23)$$

Here Λ^{-1} should be of the order of a typical range of intermolecular interactions, M and g are the mass and the number of degrees of freedom of a molecule and b_0, b_1 parameterize the virial coefficient $B_2(T) = b_0 - b_1/T$.³⁷ (The (mass) density ρ is related to the particle density n by $\rho = Mn$.) We emphasize that the convergence of a virial expansion is expected to improve considerably in presence of an infrared cutoff Λ which suppresses the long distance fluctuations.

The field $\varphi(x)$ is related to the (space-dependent) particle density $n(x)$ by

$$\varphi(x) = K_\Lambda(n(x) - \hat{n}) \quad (4.24)$$

with \hat{n} some suitable fixed reference density. We approximate the wave function renormalization Z_Λ by a constant. It can be inferred from the correlation length $\hat{\xi}$, evaluated at some reference density \hat{n} and temperature \hat{T} away from the critical region, through

$$\hat{\xi}^{-2} = Z_\Lambda^{-1} \frac{\partial^2 U_0}{\partial \varphi^2} \Big|_{\hat{\varphi}, \hat{T}}. \quad (4.25)$$

For a suitable scaling factor

$$K_\Lambda = \left(\frac{1}{\hat{n}} + \frac{b_0(2 - b_0\hat{n})}{(1 - b_0\hat{n})^2} - \frac{2b_1}{\hat{T}} \right)^{1/2} \hat{\xi} \quad (4.26)$$

one has $Z_\Lambda = 1$.

We observe that the terms linear in n in eq. (4.23) play only a role for the relation between n and μ . It is instructive to subtract from U_Λ the linear piece in φ and to expand in powers of φ :

$$U_\Lambda(\varphi) = \frac{m_\Lambda^2}{2} \varphi^2 + \frac{\gamma_\Lambda}{6} \varphi^3 + \frac{\lambda_\Lambda}{8} \varphi^4 + \dots \quad (4.27)$$

with

$$\begin{aligned} m_\Lambda^2 &= K_\Lambda^{-2} \left(\frac{1}{\hat{n}} + \frac{b_0(2 - b_0\hat{n})}{(1 - b_0\hat{n})^2} - \frac{2b_1}{\hat{T}} \right) \\ \gamma_\Lambda &= K_\Lambda^{-3} \left(\frac{b_0^2(3 - b_0\hat{n})}{(1 - b_0\hat{n})^3} - \frac{1}{\hat{n}^2} \right) \\ \lambda_\Lambda &= \frac{2}{3} K_\Lambda^{-4} \left(\frac{b_0^3(4 - b_0\hat{n})}{(1 - b_0\hat{n})^4} + \frac{1}{\hat{n}^3} \right). \end{aligned} \quad (4.28)$$

For a convenient choice $\hat{n} = \frac{1}{3b_0}$, $\hat{T} = \frac{8}{11} \frac{b_1}{b_0}$ one has $\gamma_\Lambda = 0$ and

$$K_\Lambda = 2b_0^{1/2} \hat{\xi}, \quad m_\Lambda^2 = \left(\frac{27}{16} - \frac{b_1}{2b_0T} \right) \hat{\xi}^{-2}, \quad \lambda_\Lambda = \frac{243}{128} b_0 \hat{\xi}^{-4}. \quad (4.29)$$

³⁷The Van der Waals coefficients b_0, b_1 for real gases can be found in the literature. These values are valid for small densities. They also correspond to $k = 0$ rather than to $k = \Lambda$. Fluctuation effects lead to slightly different values for $b_i(\Lambda)$ and $b_i(k = 0)$ even away from the critical line. We find that these differences are small for $n \ll n_*$. Similarly, a constant c_Λ should be added to U_Λ so that $U_0(0) = 0$.

Carbon dioxide

In order to be specific we will discuss the equation of state for carbon dioxide near the endpoint of the critical line. Typical values of the parameters are $m_\Lambda^2/\Lambda^2 = -0.31$, $\lambda_\Lambda/\Lambda = 6.63$ for $\Lambda^{-1} = 5 \cdot 10^{-10} m$, $\hat{\xi} = 0.6 \Lambda^{-1}$. In the limit (4.27) one obtains a φ^4 -model. Our explicit calculations for carbon dioxide will be performed, however, for the microscopic free energy (4.23). The linear piece in the potential can be absorbed in the source term so that the equation of state reads ³⁸

$$\frac{\partial U_0}{\partial \varphi} = j \quad , \quad j = K_\Lambda^{-1} \left(\frac{\mu}{T} + 1 + \ln g + \frac{3}{2} \ln \frac{MT}{2\pi\Lambda^2} \right). \quad (4.30)$$

We emphasize that a polynomial microscopic potential (4.27) with equation of state $\partial U_0/\partial \varphi = j$ is a good approximation for a large variety of different systems. For the example of magnets φ corresponds to the magnetization and jT to the external magnetic field. For $\gamma_\Lambda = 0$ and $\lambda_\Lambda \rightarrow \infty$, with finite negative $m_\Lambda^2/\lambda_\Lambda$, this is the Z_2 -symmetric Ising model.

For values of φ for which the mass term $m^2(\varphi) = \frac{1}{Z} \frac{\partial^2 U}{\partial \varphi^2}$ is much larger than Λ^2 the microscopic approximation to Γ_k remains approximately valid also for $k \rightarrow 0$, i.e. $U(\varphi) \approx U_\Lambda(\varphi)$. The contribution of the long wavelength fluctuations is suppressed by the small correlation length or large mass. In the range where $m^2(\varphi) \ll \Lambda^2$, however, long distance fluctuations become important and perturbation theory loses its validity. Beyond the computation of universal critical exponents and amplitude ratios we want to establish an explicit connection between the universal critical equation of state and the microscopic free energy Γ_Λ .

In fig. 7 we plot the results for the equation of state near the endpoint of the critical line for carbon dioxide. For the microscopic scale we have chosen $\Lambda^{-1} = 0.5 nm$. For $\hat{\xi} = 0.6\Lambda^{-1}$, $b_0(\Lambda) = 34 cm^3 mol^{-1}$, $b_1(\Lambda) = 3.11 \cdot 10^6 bar cm^6 mol^{-2}$ one finds the location of the endpoint at $T_* = 307.4 K$, $p_* = 77.6 bar$, $\rho_* = 0.442 gcm^{-3}$. This compares well with the experimental values $T_* = 304.15 K$, $p_* = 73.8 bar$, $\rho_* = 0.468 gcm^{-3}$. Comparing with literature values $b_i(0)_{ld}$ for low density this yields $b_0(\Lambda)/b_0(0)_{ld} = 0.8$, $b_1(\Lambda)/b_1(0)_{ld} = 0.86$. We conclude that the microscopic free energy can be approximated reasonably well by a van der Waals form even for high densities near n_* . The coefficients of the virial expansion are shifted compared to this low density values by 15-20 per cent. The comparison between the ‘‘microscopic equation of state’’ (dashed lines) and the true equation of state (solid lines) in the plot clearly demonstrates the importance of the fluctuations in the critical region. Away from the critical region the fluctuation effects are less significant and could be computed perturbatively.

Flow equations

Our aim is a numerical solution of the flow equation for U_k with given initial conditions at the scale $k \approx \Lambda$. We introduce a dimensionless renormalized field

$$\tilde{\varphi} = k^{\frac{2-d}{2}} Z_{0,k}^{1/2} \varphi \quad (4.31)$$

³⁸Note that the source term is independent of k . The linear piece in the potential can therefore easily be added to $U_{k \rightarrow 0}$ once all fluctuation effects are included.

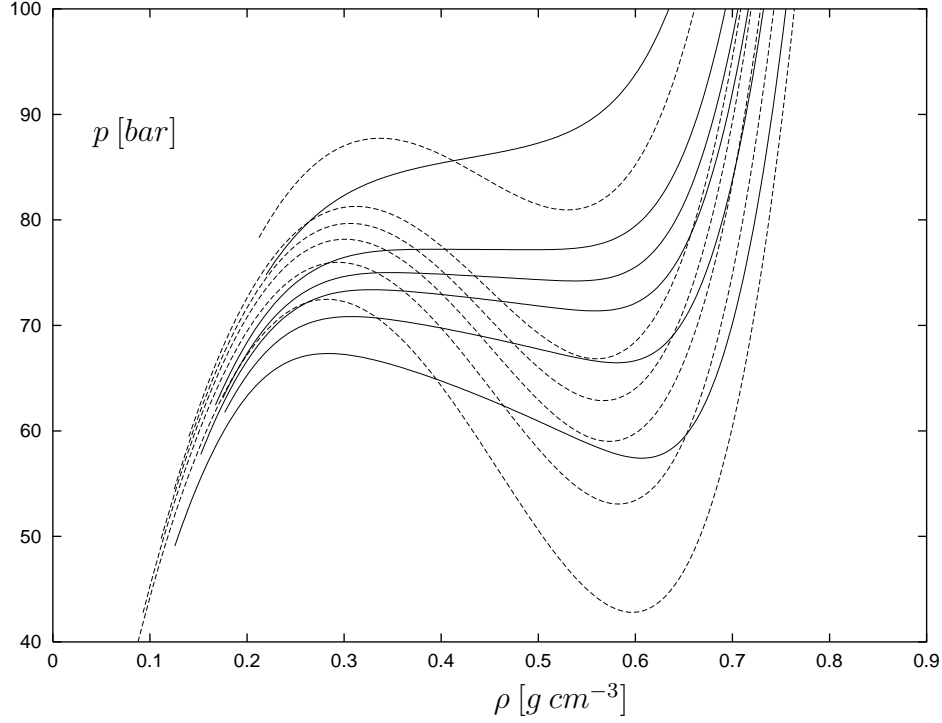


Figure 7: *Liquid-vapor transition for carbon dioxide. We display p - ρ -isotherms for $T = 295K$, $T = 300K$, $T = 303K$, $T = 305K$, $T = 307K$ and $T = 315K$. The dashed lines represent the virial expansion (at the scale $k = \Lambda$) in 2nd order with $b_0 = 34 \text{ cm}^3 \text{ mol}^{-1}$, $b_1 = 3.11 \cdot 10^6 \text{ bar cm}^6 \text{ mol}^{-2}$. The solid lines are the results at the scale $k = 0$ ($\hat{\xi}_\Lambda = 0.6$).*

with wave function renormalization $Z_{0,k} = Z_k(\varphi_0(k))$ taken at the global potential minimum $\varphi_0(k)$. We do not choose the field squared as a variable in order to facilitate the discussion of first order transitions below, where terms cubic in the field appear³⁹. We also use

$$\begin{aligned} u_k(\tilde{\varphi}) &= k^{-d} U_k(\varphi) \\ \tilde{z}_k(\tilde{\varphi}) &= Z_{0,k}^{-1} Z_k(\varphi) \end{aligned} \quad (4.32)$$

and denote here by u' , \tilde{z}' the derivatives with respect to $\tilde{\varphi}$. This yields the scaling form of the flow equation for u'_k :

$$\begin{aligned} \frac{\partial}{\partial t} u'_k(\tilde{\varphi}) &= -\frac{1}{2}(d+2-\eta_0) \cdot u'_k(\tilde{\varphi}) + \frac{1}{2}(d-2+\eta_0) \tilde{\varphi} \cdot u''_k(\tilde{\varphi}) \\ &\quad - 2v_d \tilde{z}'_k(\tilde{\varphi}) \cdot l_1^{d+2}(u''_k(\tilde{\varphi}); \eta_0, \tilde{z}_k(\tilde{\varphi})) - 2v_d u'''_k(\tilde{\varphi}) \cdot l_1^d(u''_k(\tilde{\varphi}); \eta_0, \tilde{z}_k(\tilde{\varphi})). \end{aligned} \quad (4.33)$$

Similarly, the evolution of \tilde{z}_k is described in the truncation (4.20) by

$$\begin{aligned} \frac{\partial}{\partial t} \tilde{z}_k(\tilde{\varphi}) &= \eta_0 \cdot \tilde{z}_k(\tilde{\varphi}) + \frac{1}{2}(d-2+\eta_0) \tilde{\varphi} \cdot \tilde{z}'_k(\tilde{\varphi}) \\ &\quad - \frac{4}{d} v_d \cdot u'''_k(\tilde{\varphi})^2 \cdot m_{4,0}^d(u''_k(\tilde{\varphi}); \eta_0, \tilde{z}_k(\tilde{\varphi})) \end{aligned}$$

³⁹A combination of eq. (3.8) with $\tilde{y} = 0$, $\Delta\zeta_k = 0$ with a suitable flow equation for $z(\bar{\rho})$ has led to identical results.

$$\begin{aligned}
& - \frac{8}{d} v_d \cdot u_k'''(\tilde{\varphi}) \tilde{z}'_k(\tilde{\varphi}) \cdot m_{4,0}^{d+2}(u_k''(\tilde{\varphi}); \eta_0, \tilde{z}_k(\tilde{\varphi})) \\
& - \frac{4}{d} v_d \cdot \tilde{z}'_k(\tilde{\varphi})^2 \cdot m_{4,0}^{d+4}(u_k''(\tilde{\varphi}); \eta_0, \tilde{z}_k(\tilde{\varphi})) - 2v_d \cdot \tilde{z}''_k(\tilde{\varphi}) \cdot l_1^d(u_k''(\tilde{\varphi}); \eta_0, \tilde{z}_k(\tilde{\varphi})) \\
& + 4v_d \cdot \tilde{z}'_k(\tilde{\varphi}) u_k'''(\tilde{\varphi}) \cdot l_2^d(u_k''(\tilde{\varphi}); \eta_0, \tilde{z}_k(\tilde{\varphi})) \\
& + \frac{2}{d} (1 + 2d) v_d \cdot \tilde{z}'_k(\tilde{\varphi})^2 \cdot l_2^{d+2}(u_k''(\tilde{\varphi}); \eta_0, \tilde{z}_k(\tilde{\varphi})) .
\end{aligned} \tag{4.34}$$

Here the mass threshold functions are

$$\begin{aligned}
l_n^d(u''; \eta_0, \tilde{z}) &= -\frac{1}{2} k^{2n-d} \cdot Z_{0,k}^n \cdot \int_0^\infty dx x^{\frac{d}{2}-1} \tilde{\partial}_t \left\{ \frac{1}{(P(x) + Z_{0,k} k^2 u'')^n} \right\} \\
m_{n,0}^d(u''; \eta_0, \tilde{z}) &= -\frac{1}{2} k^{2(n-1)-d} \cdot Z_{0,k}^{n-2} \cdot \int_0^\infty dx x^{\frac{d}{2}} \tilde{\partial}_t \left\{ \frac{\dot{P}^2(x)}{(P(x) + Z_{0,k} k^2 u'')^n} \right\}
\end{aligned} \tag{4.35}$$

(with $P(x) = \tilde{z} Z_{0,k} x + R_k(x)$, $\dot{P} \equiv \frac{dP}{dx}$ and $\tilde{\partial}_t$ acting only on R_k). The anomalous dimension

$$\eta_{0,k} \equiv -\frac{d}{dt} \ln Z_{0,k} = -Z_{0,k}^{-1} \frac{\partial}{\partial t} Z_k(\varphi_0) - Z_{0,k}^{-1} \cdot \frac{\partial Z_k}{\partial \varphi} \Big|_{\varphi_0} \cdot \frac{d\varphi_0}{dt} \tag{4.36}$$

is determined by the condition $d\tilde{z}(\tilde{\varphi}_0)/dt = 0$. It appears linearly in the threshold functions due to $\tilde{\partial}_t$ acting on $Z_{0,k}$ in R_k ,

$$R_k(x) = \frac{Z_{0,k} x}{\exp(x/k^2) - 1}. \tag{4.37}$$

For a computation of η_0 we need the evolution of the potential minimum $\varphi_0(k)$, which follows from the condition $\frac{d}{dt}(\partial U_k / \partial \varphi(\varphi_0(k))) = 0$, namely

$$\begin{aligned}
\frac{d\tilde{\varphi}_0}{dt} &= \frac{1}{2} (2 - d - \eta_0) \tilde{\varphi}_0 \\
&+ 2v_d \frac{\tilde{z}'_k(\tilde{\varphi}_0)}{u_k''(\tilde{\varphi}_0)} \cdot l_1^{d+2}(u_k''(\tilde{\varphi}_0); \eta_0, 1) + 2v_d \frac{u_k'''(\tilde{\varphi}_0)}{u_k''(\tilde{\varphi}_0)} \cdot l_1^d(u_k''(\tilde{\varphi}_0); \eta_0, 1).
\end{aligned} \tag{4.38}$$

One infers an implicit equation for the anomalous dimension $\eta_{0,k}$,

$$\begin{aligned}
\eta_0 &= \frac{4}{d} v_d \cdot u_k'''(\tilde{\varphi}_0)^2 \cdot m_{4,0}^d(u_k''(\tilde{\varphi}_0); \eta_0, 1) + \frac{8}{d} v_d \cdot u_k'''(\tilde{\varphi}_0) \tilde{z}'_k(\tilde{\varphi}_0) \cdot m_{4,0}^{d+2}(u_k''(\tilde{\varphi}_0); \eta_0, 1) \\
&+ \frac{4}{d} v_d \cdot \tilde{z}'_k(\tilde{\varphi}_0)^2 \cdot m_{4,0}^{d+4}(u_k''(\tilde{\varphi}_0); \eta_0, 1) + 2v_d \cdot \tilde{z}''_k(\tilde{\varphi}_0) \cdot l_1^d(u_k''(\tilde{\varphi}_0); \eta_0, 1) \\
&- 4v_d \cdot \tilde{z}'_k(\tilde{\varphi}_0) u_k'''(\tilde{\varphi}_0) \cdot l_2^d(u_k''(\tilde{\varphi}_0); \eta_0, 1) \\
&- \frac{2}{d} (1 + 2d) v_d \cdot \tilde{z}'_k(\tilde{\varphi}_0)^2 \cdot l_2^{d+2}(u_k''(\tilde{\varphi}_0); \eta_0, 1) \\
&- 2v_d \frac{\tilde{z}'_k(\tilde{\varphi}_0)}{u_k''(\tilde{\varphi}_0)} \cdot \left\{ \tilde{z}'_k(\tilde{\varphi}_0) l_1^{d+2}(u_k''(\tilde{\varphi}_0); \eta_0, 1) + u_k'''(\tilde{\varphi}_0) l_1^d(u_k''(\tilde{\varphi}_0); \eta_0, 1) \right\},
\end{aligned} \tag{4.39}$$

that can be solved by separating the threshold functions in η_0 -dependent and η_0 -independent parts (c.f. eq. (4.35)). Since η_0 will turn out to be only a few percent, the neglect

of contributions from higher derivative terms not contained in (4.20) induces a substantial *relative* error for η_0 , despite the good convergence of the derivative expansion. We believe that the missing higher derivative contributions to η_0 constitute the main uncertainty in the results.

For given initial conditions $U_\Lambda(\varphi)$, $Z_\Lambda(\varphi)$ the system of partial differential equations (4.33),(4.34),(4.38),(4.39) can be solved numerically. A description of the algorithm used can be found in [37].

4.5 Universal and non-universal critical properties

In order to make the discussion transparent we present here first results for polynomial initial conditions (4.27) with $\tilde{z}_\Lambda(\tilde{\varphi}) = 1$. The term linear in φ is considered as a source j . The special value $\gamma_\Lambda = 0$ realizes the Z_2 -symmetric Ising model. We start with the results for the universal critical behaviour for this case. For this particular purpose we hold λ_Λ fixed and measure the deviation from the critical temperature by

$$\delta m_\Lambda^2 = m_\Lambda^2 - m_{\Lambda,crit}^2 = S(T - T_c). \quad (4.40)$$

For the liquid-gas system one has $S = 2b_1/(K_\Lambda^2 T_c^2)$.

The anomalous dimension η determines the two point function at the critical temperature and equals $\eta_{0,k}$ for the scaling solution where $\partial_t u = \partial_t \tilde{z} = 0$. The results for the critical exponents are compared with those from other methods in table 5. We observe a very good agreement for ν whereas the relative error for η is comparatively large as expected. Comparison with the lowest order of the derivative expansion (f), used in section 4.2, shows a convincing apparent convergence of this expansion for ν . For η this convergence is hidden by the fact that in (4.5) a different determination of η was used. Employing the present definition would lead in lowest order of the derivative expansion to a value $\eta = 0.11$. As expected, the convergence of the derivative expansion is faster for the very effective exponential cutoff than for the powerlike cutoff (g) which would lead to unwanted properties of the momentum integrals in the next order.

In order to establish the quantitative connection between the short distance parameters m_Λ^2 and λ_Λ and the universal critical behaviour one needs the amplitudes C^\pm , ξ^\pm , etc. For $\lambda_\Lambda/\Lambda = 5$ we find $C^+ = 1.033$, $C^- = 0.208$, $\xi^+ = 0.981$, $\xi^- = 0.484$, $B = 0.608$, $E = 0.208$. Here and in the following all dimensionful quantities are quoted in units of Λ . The amplitude D is given by $\partial U_0/\partial\varphi = D \cdot \varphi^\delta$ on the critical isotherme and we obtain $D = 10.213$. In table 6 we present our results for the universal amplitude ratios C^+/C^- , ξ^+/ξ^- , $R_\chi = C^+ D B^{\delta-1}$, $\tilde{R}_\xi = (\xi^+)^{\beta/\nu} D^{1/(\delta+1)} B$.

The critical exponents and amplitudes only characterize the behaviour of $U_0(\varphi)$ in the limits $\varphi \rightarrow \varphi_0$ and $\varphi \rightarrow \infty$. Our method allows us to compute $U_0(\varphi)$ for arbitrary φ . As an example, the quartic coupling $\lambda_R = \frac{1}{3} \frac{\partial^4 U_0}{\partial \varphi_R^4}(0) = \frac{\partial^2 U_0}{\partial \rho_R^2}(0)$, $\hat{\lambda}_R = \frac{\partial^2 U_0}{\partial \rho_R^2}(\varphi_{0R})$, $\rho_R = \frac{1}{2} \varphi_R^2$, becomes in the critical region proportional to m_R . Our results for the universal couplings λ_R/m_R in the symmetric and $\hat{\lambda}_R/\hat{m}_R$ in the ordered phase can also be found in table 6. Here $m_R = \frac{\partial^2 U_0}{\partial \varphi_R^2} \Big|_{\varphi_R=0}$ in the symmetric and $\hat{m}_R = \frac{\partial^2 U_0}{\partial \varphi_R^2} \Big|_{\varphi_{0R}}$ in the ordered phase.

	ν	β	γ	η
(a)	0.6304(13)	0.3258(14)	1.2396(13)	0.0335(25)
(b)	0.6290(25)	0.3257(25)	1.2355(50)	0.0360(50)
(c)	0.6315(8)		1.2388(10)	
(d)	0.6294(9)			0.0374(14)
(f)	0.643	0.336	1.258	0.044
(g)	0.6181			0.054
(h)	0.6307	0.3300	1.2322	0.0467
(i)	0.625(6)	0.316 – 0.327	1.23 – 1.25	

Table 5: *Critical exponents of the ($d=3$)-Ising model, calculated with various methods.*

(a) *From perturbation series at fixed dimension $d = 3$ including seven-loop contributions [123, 131].*

(b) *ϵ -expansion in five loop order [123, 131].*

(c) *high temperature series [133] (see also [134, 135]).*

(d) *Monte Carlo simulation [137] (See also [142]- [144]).*

(f)-(h): *“exact” renormalization group equations.*

(f) *effective average action for the $O(N)$ -model, $N \rightarrow 1$, with uniform wave function renormalization [36] (see also [113]).*

(g) *scaling solution of equations analogous to (4.33), (4.34) with powerlike cutoff [120].*

(h) *effective average action for one-component scalar field theory with field-dependent wave function renormalization (present section).*

(i) *experimental data for the liquid-vapor system quoted from [123].*

We should emphasize that the shape of the potential in the low temperature phase depends on k in the “inner” region corresponding to $|\varphi| < \varphi_0$. This is due to the fluctuations which are responsible for making the potential convex in the limit $k \rightarrow 0$ [79, 80, 127]. We illustrate this by plotting the potential for different values of k in fig. 1. Our results for the scaling function $f(x)$ are shown in fig. 8, together with the asymptotic behaviour (dashed lines) as dictated by the critical exponents and amplitudes.

A different useful parameterization of the critical equation of state can be given in terms of nonlinearly rescaled fields $\hat{\varphi}_R$, using a φ -dependent wave function renormalization $Z(\varphi) = Z_{k \rightarrow 0}(\varphi)$,

$$\hat{\varphi}_R = Z(\varphi)^{1/2} \varphi. \quad (4.41)$$

Our numerical results can be presented in terms of a fit to the universal function

$$\hat{F}(\hat{s}) = m_R^{-5/2} \frac{\partial U_0}{\partial \hat{\varphi}_R}, \quad \hat{s} = \frac{\hat{\varphi}_R}{m_R^{1/2}} = \left(\frac{Z(\varphi)\varphi^2}{m_R} \right)^{1/2}, \quad (4.42)$$

$$\hat{F}_{Fit}(\hat{s}) = (a_0 \hat{s} + a_1 \hat{s}^3 + a_2 \hat{s}^5 + a_3 \hat{s}^7) \cdot f_\alpha(\hat{s}) + (1 - f_\alpha(\hat{s})) \cdot a_4 \hat{s}^5. \quad (4.43)$$

The factors f_α and $(1 - f_\alpha)$ interpolate between a polynomial expansion and the asymptotic

	C^+/C^-	ξ^+/ξ^-	R_χ	\tilde{R}_ξ	ξ^+E	λ_R/m_R	$\tilde{\lambda}_R/\hat{m}_R$
(a)	4.79 ± 0.10		1.669 ± 0.018			7.88	
(b)	4.73 ± 0.16		1.648 ± 0.036			9.33	
(c)	4.77 ± 0.02	1.96 ± 0.01	1.662 ± 0.005			7.9 – 8.15	
(d)	4.75 ± 0.03	1.95 ± 0.02				7.76	5.27
(f)	4.29	1.86	1.61	0.865	0.168	9.69	5.55
(h)	4.966	2.027	1.647	0.903	0.204	8.11	4.96
(i)	4.8 – 5.2		1.69 ± 0.14				

Table 6: *Universal amplitude ratios and couplings of the ($d=3$)-Ising model.*

(a) *perturbation theory at fixed dimension $d=3$ [131, 145].*

(b) *ϵ -expansion [131, 145].*

(c) *high temperature series. Amplitude ratios from [146, 123], λ_R/m_R from [134, 135, 149].*

(d) *Monte Carlo simulations. Amplitude ratios from [144], λ_R/\hat{m}_R from [143], λ_R/m_R from [142].*

(f) *effective average action for the $O(N)$ -model, $N \rightarrow 1$, with uniform wave function renormalization [36].*

(h) *present section with field-dependent wave function renormalization.*

(i) *experimental data for the liquid-vapor system [147].*

behaviour for large arguments. We use

$$f_\alpha(x) = \alpha^{-2}x^2 \cdot \frac{\exp(-\frac{x^2}{\alpha^2})}{1 - \exp(-\frac{x^2}{\alpha^2})}. \quad (4.44)$$

A similar fit can be given for

$$\tilde{z}(s) = \frac{\lim_{k \rightarrow 0} Z_k(\varphi)}{Z_0}, \quad s = \frac{\varphi_R}{m_R^{1/2}} = \left(\frac{Z_0 \varphi^2}{m_R} \right)^{1/2} = \tilde{z}^{-1/2} \hat{s}, \quad (4.45)$$

$$\tilde{z}_{Fit}(s) = (b_0 + b_1 s^2 + b_2 s^4 + b_3 s^6 + b_4 s^8) \cdot f_\beta(s) + (1 - f_\beta(s)) \cdot b_5 |s|^{-\frac{2\eta}{1+\eta}}. \quad (4.46)$$

In the symmetric phase one finds (with $\eta = 0.0467$) $\alpha = 1.012$, $a_0 = 1.0084$, $a_1 = 3.1927$, $a_2 = 9.7076$, $a_3 = 0.5196$, $a_4 = 10.3962$ and $\beta = 0.5103$, $b_0 = 1$, $b_1 = 0.3397$, $b_2 = -0.8851$, $b_3 = 0.8097$, $b_4 = -0.2728$, $b_5 = 1.0717$, whereas the fit parameters for the phase with spontaneous symmetry breaking are $\alpha = 0.709$, $a_0 = -0.0707$, $a_1 = -2.4603$, $a_2 = 11.8447$, $a_3 = -1.3757$, $a_4 = 10.2115$ and $\beta = 0.486$, $b_0 = 1.2480$, $b_1 = -1.4303$, $b_2 = 2.3865$, $b_3 = -1.7726$, $b_4 = 0.4904$, $b_5 = 0.8676$ (our fit parameters are evaluated for this phase for $(\partial^2 U_k / \partial \varphi_R^2)(\varphi_{R,max})/k^2 = -0.99$). One observes that the coefficients a_2 and a_4 are large and of comparable size. A simple polynomial form $\hat{F} = \tilde{a}_0 \hat{s} + \tilde{a}_1 \hat{s}^3 + \tilde{a}_2 \hat{s}^5$ is not too far from the more precise result. We conclude that in terms of the rescaled field $\hat{\varphi}_R$ (4.41) the potential is almost a polynomial φ^6 -potential.

In fig. 9 we show \tilde{z} as a function of s both for the symmetric and ordered phase. Their shape is similar to the scaling solution found in [120]. Nevertheless, the form of \tilde{z} for $k = 0$

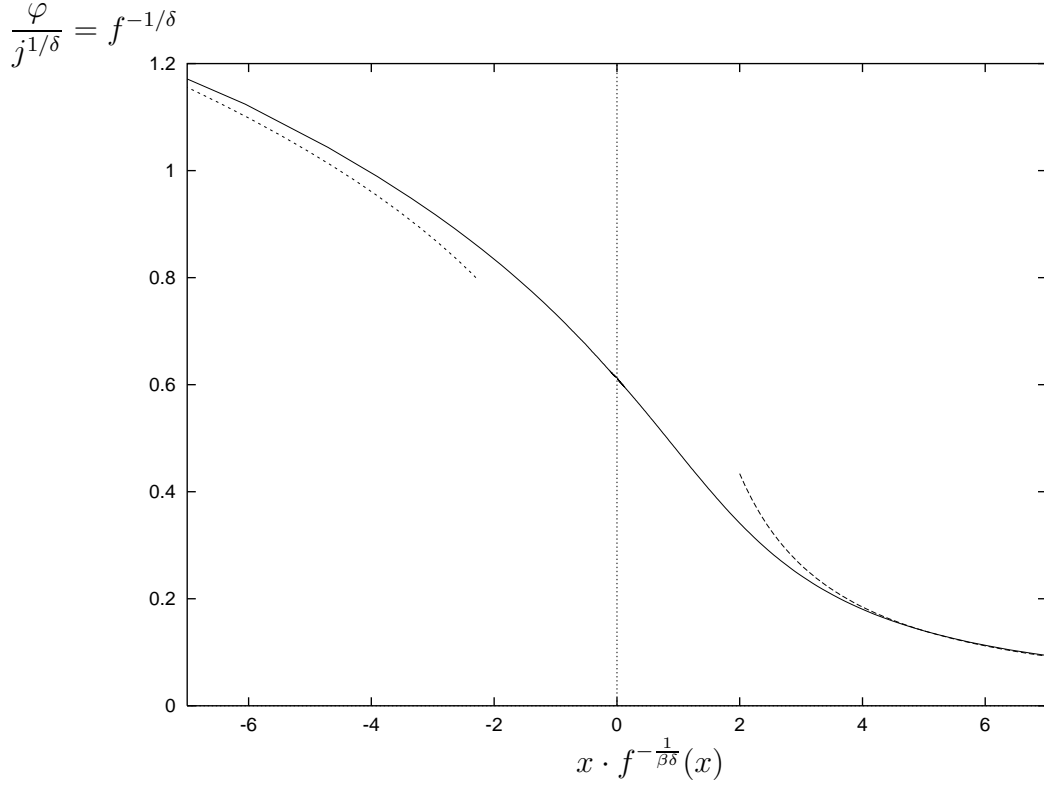


Figure 8: *Widom scaling function $f(x)$ of the $(d = 3)$ -Ising model. (The present curve is generated for a quartic short distance potential U_Λ with $\lambda_\Lambda/\Lambda = 5$). The dashed lines indicate extrapolations of the limiting behaviour as given by the critical exponents.*

which expresses directly information about the physical system should not be confounded with the scaling solution which depends on the particular infrared cutoff. For the low temperature phase one sees the substantial dependence of \tilde{z}_k on the infrared cutoff k for small values $s < s_0$. Again this corresponds to the “inner region” between the origin ($s=0$) and the minimum of the potential ($s_0=0.449$) where the potential finally becomes convex for $k \rightarrow 0$.

Knowledge of U_0 and \tilde{z} permits the computation of the (renormalized) propagator for low momenta with arbitrary sources j . It is given by

$$G(q^2) = \left(\frac{\partial^2 U_0(\varphi_R)}{\partial \varphi_R^2} + \tilde{z}(\varphi_R) q^2 \right)^{-1} \quad (4.47)$$

for $\tilde{z} q^2 \lesssim \partial^2 U_0 / \partial \varphi_R^2$. Here φ_R obeys $\partial U_0 / \partial \varphi_R = Z_0^{-1/2} j$. We emphasize that the correlation length $\xi(\varphi_R) = \tilde{z}^{1/2}(\varphi_R) (\partial^2 U_0 / \partial \varphi_R^2)^{-1/2}$ at given source j requires information about \tilde{z} . For the gas-liquid transition $\xi(\varphi_R)$ is directly connected to the density dependence of the correlation length. For magnets, it expresses the correlation length as a function of magnetization. The factor $\tilde{z}^{1/2}$ is often omitted in other approaches. From

$$\xi^{-2} = m_R^2 \left\{ \left(1 + \frac{1}{2} \frac{\partial \ln \tilde{z}}{\partial \ln s} \right)^2 \frac{\partial \hat{F}}{\partial \hat{s}} + \frac{1}{2} \left[\frac{\partial \ln \tilde{z}}{\partial \ln s} + \frac{1}{2} \left(\frac{\partial \ln \tilde{z}}{\partial \ln s} \right)^2 + \frac{\partial^2 \ln \tilde{z}}{(\partial \ln s)^2} \right] \frac{\hat{F}}{\hat{s}} \right\} \quad (4.48)$$

one can extract the behavior for $|\varphi| \rightarrow \infty$ for the high and low temperature phases

$$\xi = L^\pm |\varphi|^{-\lambda} \quad (4.49)$$

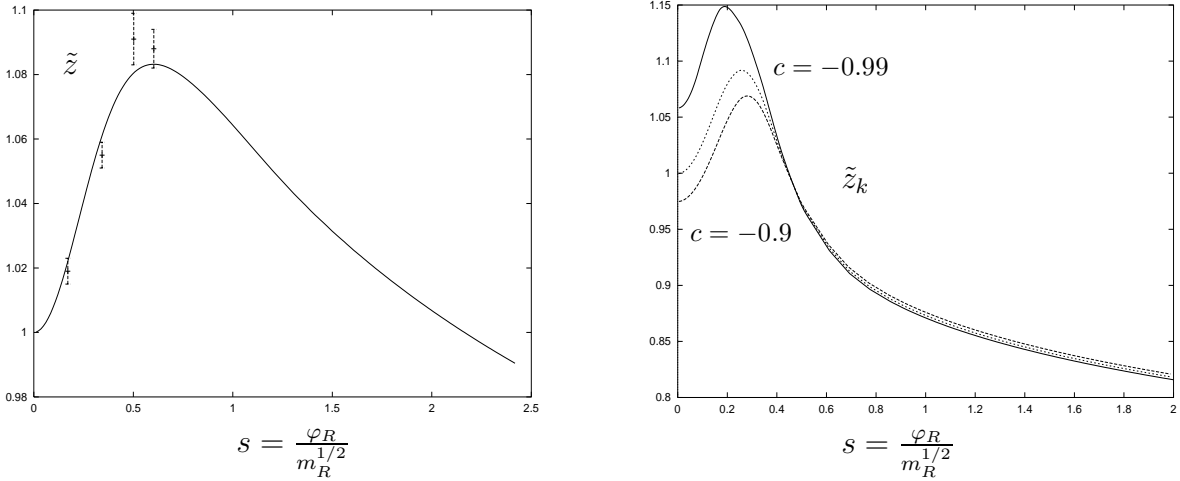


Figure 9: *Universal rescaled wave function renormalization \tilde{z} in the symmetric and ordered phase of the $(d=3)$ -Ising model. In the low temperature phase the plots are for different k with $\frac{1}{k^2} \frac{\partial^2 U}{\partial \varphi_R^2}(\varphi_{R,max}) = c$ ($c = -0.9, -0.95, -0.99$). Here $\varphi_{R,max}$ is the location of the local maximum of the potential in the inner (non-convex) region. In the graph for the high temperature phase we have inserted Monte Carlo results by M. Tsypin (private communication).*

Critical equations of state for the Ising model have been computed earlier with several methods. They are compared with our result for the phase with spontaneous symmetry breaking in fig. 10 and for the symmetric phase in fig. 11. For this purpose we use $F(\tilde{s}) = m_R^{-5/2} \partial U_0 / \partial \varphi_R$ with $\tilde{s} = \frac{\varphi_R}{\varphi_{0R}}$ in the phase with spontaneous symmetry breaking (note $\tilde{s} \sim s$). The constant c_F is chosen such that $\frac{1}{c_F} \frac{\partial F}{\partial \tilde{s}}(\tilde{s} = 1) = 1$. In the symmetric phase we take instead $\tilde{s} = \frac{\varphi_R}{m_R^{1/2}}$ so that $\frac{\partial F}{\partial \tilde{s}}(\tilde{s} = 0) = 1$. One expects for large \tilde{s} an inaccuracy of our results due to the error in η .

	$m_{\Lambda,crit}^2$	C^+	D
$\lambda_\Lambda = 0.1$	$-6.4584 \cdot 10^{-3}$	0.1655	5.3317
$\lambda_\Lambda = 1$	$-5.5945 \cdot 10^{-2}$	0.485	7.506
$\lambda_\Lambda = 5$	-0.22134	1.033	10.213
$\lambda_\Lambda = 20$	-0.63875	1.848	16.327

Table 7: *The critical values $m_{\Lambda,crit}^2$ and the non-universal amplitudes C^+, D as a function of the quartic short distance coupling λ_Λ (all values expressed in units of Λ). Other non-universal amplitudes can be calculated from the universal quantities of table 6.*

In summary of this section we may state that the non-perturbative flow equations in second order in a derivative expansion lead to a critical equation of state which is well compatible with high order expansions within other methods. In addition, it allows to establish an explicit connection between the parameters appearing in the microscopic free energy Γ_Λ and the universal long distance behaviour. For a quartic polynomial potential this involves in addition to the non-universal amplitudes the value of $m_{\Lambda,crit}^2$. We have listed these

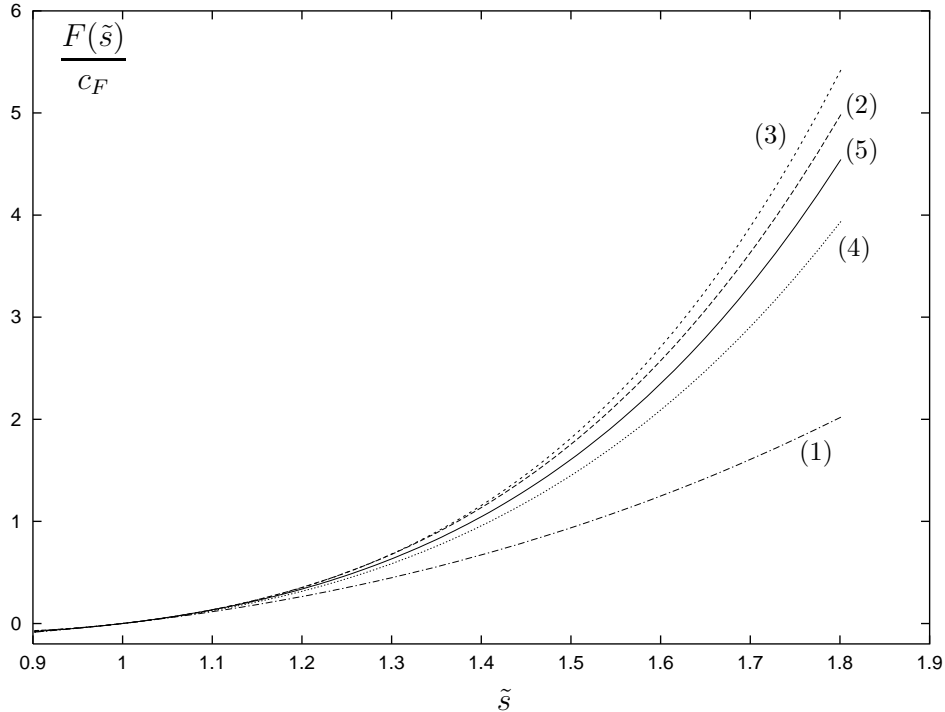


Figure 10: *The critical equation of state in the ordered phase.*

(1) *mean field approximation.*

(2) *effective average action with uniform wave function renormalization [36].*

(3) *Monte Carlo simulation [143].*

(4) *resummed ϵ -expansion in $O(\epsilon^3)$, five loop perturbative expansion and high temperature series [145].*

(5) *present section.*

quantities for different values of λ_Λ in table 7. Finally, the temperature scale is established by $S = \partial m_\Lambda^2 / \partial T |_{T_c}$.

4.6 Equation of state for first order transitions

Our method is not restricted to a microscopic potential with discrete Z_2 -symmetry. The numerical code works for arbitrary initial potentials. We have investigated the polynomial potential (4.27) with $\gamma_\Lambda \neq 0$. The numerical solution of the flow equations (4.33),(4.34) shows the expected first order transition (in case of vanishing linear term j). Quite generally, the universal critical equation of state for first order transitions will depend on two scaling parameters (instead of one for second order transitions) since the jump in the order parameter or the mass introduces a new scale. This has been demonstrated in [37] for a scalar matrix model and is discussed in more detail in section 5. The degree to which universality applies depends on the properties of a given model and its parameters. For a φ^4 -model with cubic term (4.27) one can relate the equation of state to the Ising model by an appropriate mapping. This allows us to compute the universal critical equation of state for arbitrary first order phase transitions in the Ising universality class from the critical equation of state for the second order

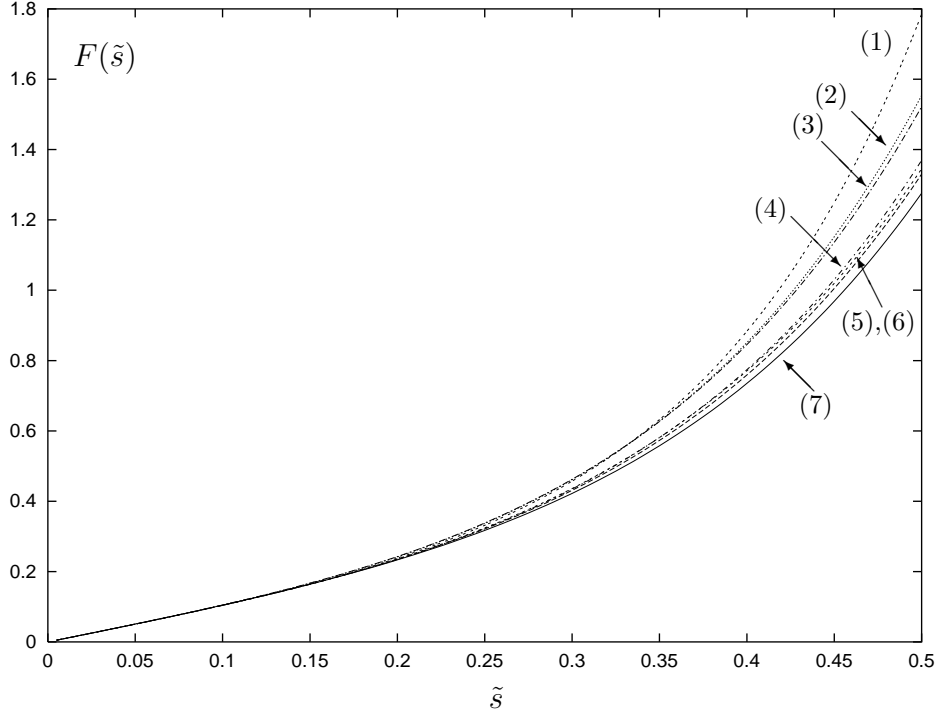


Figure 11: *The critical equation of state in the symmetric phase.*

- (1) Monte Carlo simulation [148], (2) ϵ -expansion [145].
(3) effective average action with uniform wave function renormalization [36].
(4) Monte Carlo simulation [142], (5),(6) high temperature series [149],[135].
(7) present section.

phase transition in the Ising model. For other universality classes a simple mapping to a second order equation of state is not always possible - its existence is particular to the present model.

By a variable shift

$$\sigma = \varphi + \frac{\gamma_\Lambda}{3\lambda_\Lambda} \quad (4.50)$$

we can bring the short distance potential (4.27) into the form

$$U_\Lambda(\sigma) = -J_\gamma\sigma + \frac{\mu_\Lambda^2}{2}\sigma^2 + \frac{\lambda_\Lambda}{8}\sigma^4 + c_\Lambda \quad (4.51)$$

with

$$\begin{aligned} J_\gamma &= \frac{\gamma_\Lambda}{3\lambda_\Lambda}m_\Lambda^2 - \frac{\gamma_\Lambda^3}{27\lambda_\Lambda^2} \\ \mu_\Lambda^2 &= m_\Lambda^2 - \frac{\gamma_\Lambda^2}{6\lambda_\Lambda}. \end{aligned} \quad (4.52)$$

We can now solve the flow equations in terms of σ and reexpress the result in terms of φ by eq. (4.50) at the end. The exact flow equation (2.19) does not involve the linear term $\sim J_\gamma\sigma$ in the rhs (also the constant c_Λ is irrelevant). Therefore the effective potential ($k = 0$) is given

by

$$U_0 = U^{Z_2}(\sigma) - J_\gamma \sigma + c_\Lambda = U^{Z_2}\left(\varphi + \frac{\gamma_\Lambda}{3\lambda_\Lambda}\right) - \left(\varphi + \frac{\gamma_\Lambda}{3\lambda_\Lambda}\right)J_\gamma + c_\Lambda, \quad (4.53)$$

where U^{Z_2} is the effective potential of the Ising type model with quartic coupling λ_Λ and mass term μ_Λ^2 . The equation of state $\partial U/\partial\varphi = j$ or, equivalently

$$\frac{\partial U^{Z_2}}{\partial\varphi} \Big|_{\varphi+\frac{\gamma_\Lambda}{3\lambda_\Lambda}} = j + J_\gamma, \quad (4.54)$$

is therefore known explicitly for arbitrary m_Λ^2 , γ_Λ and λ_Λ (cf. eq. (4.13) for the universal part). This leads immediately to the following conclusions:

- i) First order transitions require that the combination $U_0(\varphi) - j\varphi$ has two degenerate minima. This happens for $J_\gamma + j = 0$ and $\mu_\Lambda^2 < \mu_{\Lambda,crit}^2$ or

$$j = -\frac{\gamma_\Lambda}{3\lambda_\Lambda} \left(m_\Lambda^2 - \frac{\gamma_\Lambda^2}{9\lambda_\Lambda} \right) \quad (4.55)$$

$$m_\Lambda^2 < \mu_{\Lambda,crit}^2 + \frac{\gamma_\Lambda^2}{6\lambda_\Lambda}. \quad (4.56)$$

Here $\mu_{\Lambda,crit}^2$ is the critical mass term of the Ising model.

- ii) The boundary of this region for

$$m_\Lambda^2 = \mu_{\Lambda,crit}^2 + \frac{\gamma_\Lambda^2}{6\lambda_\Lambda} \quad (4.57)$$

is a line of second order phase transitions with vanishing renormalized mass or infinite correlation length.

For $j = 0$ (e.g. magnets with polynomial potential in absence of external fields) the equations (4.55), (4.57) have the solutions

$$\gamma_{\Lambda;1} = 0 \quad , \quad \gamma_{\Lambda;2,3} = \pm(-18\lambda_\Lambda\mu_{\Lambda,crit}^2)^{1/2}. \quad (4.58)$$

The second order phase transition for $\gamma_\Lambda \neq 0$ can be described by Ising models for shifted fields σ . For a given model, the way how a phase transition line is crossed as the temperature is varied follows from the temperature dependence of j , m_Λ^2 , γ_Λ and λ_Λ . For the gas-liquid transition both j and m_Λ^2 depend on T .

In the vicinity of the boundary of the region of first order transitions the long range fluctuations play a dominant role and one expects universal critical behaviour. The detailed microscopic physics is only reflected in two non-universal amplitudes. One reflects the relation between the renormalized and unrenormalized fields as given by Z_0 . The other is connected to the renormalization factor for the mass term. Expressed in terms of renormalized fields and mass the potential U loses all memory about the microphysics.

The critical equation of state of the non-symmetric model ($\gamma_\Lambda \neq 0$) follows from the Ising model (4.5). With $\frac{\partial U^{Z_2}}{\partial \varphi} |_\varphi = |\varphi|^\delta f(x)$, the scaling form of the equation of state $j = \frac{\partial U}{\partial \varphi}$ for the model with cubic coupling can be written as

$$j = |\varphi + \frac{\gamma_\Lambda}{3\lambda_\Lambda}|^\delta f(x) - \left(\frac{\gamma_\Lambda}{3\lambda_\Lambda} \mu_{\Lambda, \text{crit}}^2 + \frac{\gamma_\Lambda^3}{54\lambda_\Lambda^2} \right) - \frac{\gamma_\Lambda}{3\lambda_\Lambda} \delta \mu_\Lambda^2, \quad (4.59)$$

where $x = \frac{\delta \mu_\Lambda^2}{|\varphi + \frac{\gamma_\Lambda}{3\lambda_\Lambda}|^{1/\beta}}$ and $\delta \mu_\Lambda^2 = m_\Lambda^2 - \frac{\gamma_\Lambda^2}{6\lambda_\Lambda} - \mu_{\Lambda, \text{crit}}^2$. One may choose

$$y = \frac{\gamma_\Lambda}{3\lambda_\Lambda} \left(\mu_{\Lambda, \text{crit}}^2 + \frac{\gamma_\Lambda^2}{18\lambda_\Lambda} + \delta \mu_\Lambda^2 \right) |\varphi + \frac{\gamma_\Lambda}{3\lambda_\Lambda}|^{-\delta} \quad (4.60)$$

as the second scaling variable. For small symmetry breaking cubic coupling γ_Λ one notes $y \sim \gamma_\Lambda$. The scaling form of the equation of state for the non-symmetric model reads

$$j = |\varphi + \frac{\gamma_\Lambda}{3\lambda_\Lambda}|^\delta \{f(x) - y\}. \quad (4.61)$$

This universal form of the equation of state is relevant for a large class of microscopic free energies, far beyond the special polynomial form used for its derivation.

It is often useful to express the universal equation of state in terms of renormalized fields and masses. We use the variables

$$\tilde{s} = \frac{\varphi_R}{\varphi_{0R}} \quad ; \quad v = \frac{m_R}{m_R^{Z_2}}, \quad (4.62)$$

where $m_R = \left(\frac{\partial^2 U}{\partial \varphi_R^2} |_{\varphi_{0R}} \right)^{1/2}$ is the renormalized mass at the minimum φ_{0R} of $U(\varphi_R)$ whereas $m_R^{Z_2}$ is the renormalized mass at the minimum of the corresponding Z_2 -symmetric effective potential obtained for vanishing cubic coupling $\gamma_\Lambda = 0$. Then the critical temperature corresponds to $v = 1$. In this parameterization the universal properties of the equation of state for the Ising type first order transition can be compared with transitions in other models - e.g. matrix models [37] - where no simple mapping to a second order phase transition exists (see section 5).

A convenient universal function $G(\tilde{s}, v)$ for weak first order transitions can be defined as

$$G(\tilde{s}, v) := \frac{U_0(\varphi_R)}{\varphi_{0R}^6}. \quad (4.63)$$

We plot $G(\tilde{s}, v)$ in fig. 12 as a function of \tilde{s} for different values of v . For the present model all information necessary for a universal description of first order phase transitions is already contained in eqs. (4.53) or (4.54). The function $G(\tilde{s}, v)$ can serve, however, for a comparison with other models, for which a simple relation to a second order phase transition does not exist. We discuss the function G for matrix models in sect. 5.6 (cf. fig. 25). At this place we mention that we have actually computed the potential U both by solving the flow equations with initial values where $\gamma_\Lambda \neq 0$ and by a shift from the Ising model results. We found good agreement between the two approaches.

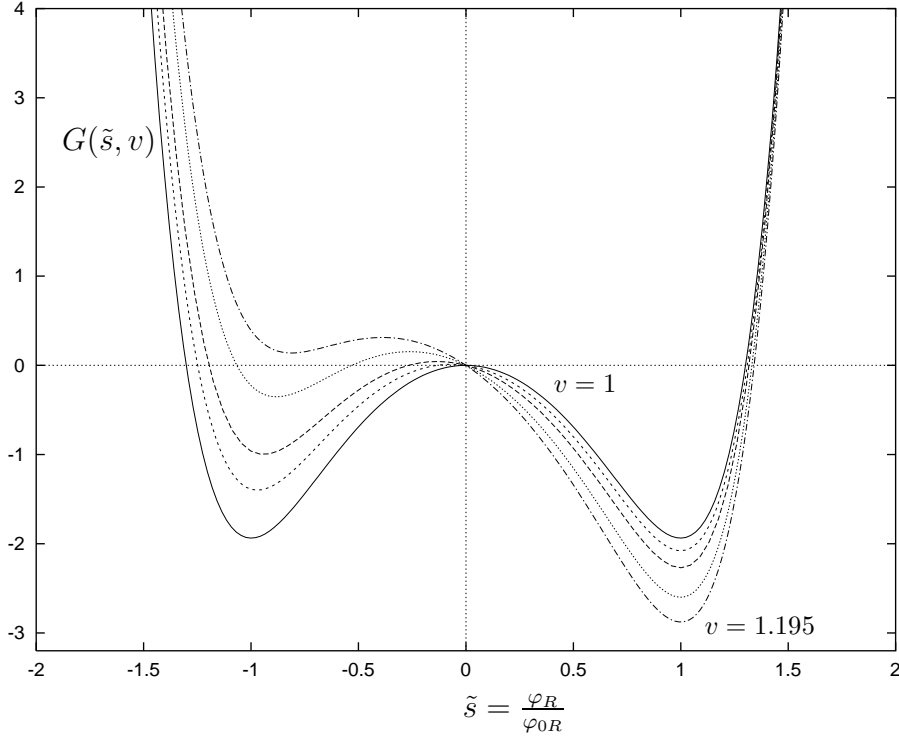


Figure 12: *Universal critical equation of state for a first order transition. We display $G(\tilde{s}, v)$ for $v = 1$, $v = 1.037$, $v = 1.072$, $v = 1.137$ and $v = 1.195$.*

In conclusion, we have employed non-perturbative flow equations in order to compute explicitly the equation of state. We have first studied models where the microscopic free energy can be approximated by a polynomial approximation with terms up to quartic order. This covers second order as well as first order transitions, both for the universal and non-universal features. The same method can be used away from the critical hypersurface, allowing therefore for an explicit connection between critical and non-critical observations.

The ability of the method to deal also with a microscopic free energy which is not of a polynomial form is demonstrated by a particular example, namely the equation of state for carbon dioxide. In the vicinity of the endpoint of the critical line we can give an explicit formula for the free energy density $U(n, T)T$. Using the fits (3.15), ((3.18), for $\hat{F}(\hat{s})$ and $\tilde{z}(s)$ one finds⁴⁰

$$U_0(n, T) = U^{Z_2}(\hat{\varphi}_R(n, T), m_R(T)) + J(T)(n - n_*) - K(T) \quad (4.64)$$

$$U^{Z_2} = \frac{1}{2}\tilde{a}_0 m_R^2 \hat{\varphi}_R^2 + \frac{1}{4}\tilde{a}_1 m_R \hat{\varphi}_R^4 + \frac{1}{6}\tilde{a}_2 \hat{\varphi}_R^6 \quad (4.65)$$

with $\tilde{a}_i \approx a_i$ and

$$\hat{\varphi}_R(n, T) = \tilde{z} \left(\frac{\varphi_R(n, T)}{m_R^{1/2}(T)} \right) \varphi_R(n, T)$$

⁴⁰Note that n_* is somewhat different from \hat{n} and therefore φ_R is defined slightly different from eq. (1.7). This variable shift (similar to (4.1) reflects the fact that eq. (1.6) contains higher than quartic interactions and cannot be reduced to a φ^4 -potential even for $\gamma_\Lambda = 0$.

$$\begin{aligned}
\varphi_R(n, T) &= H_{\pm} \left| \frac{T - T_*}{T_*} \right|^{-\eta\nu} (n - n_*) \\
m_R(T) &= \xi_{T\pm} \left| \frac{T - T_*}{T_*} \right|^{\nu}
\end{aligned} \tag{4.66}$$

The two non-universal functions $J(T)$ and $K(T)$ enter in the determination of the chemical potential and the critical line.

In particular, the non-universal amplitudes governing the behaviour near the endpoint of the critical line can be extracted from the equation of state: In the vicinity of the endpoint we find for $T = T_*$

$$\rho_{>} - \rho_* = \rho_* - \rho_{<} = D_p^{-1} \left(\frac{|p - p_*|}{p_*} \right)^{1/\delta} \tag{4.67}$$

with $D_p = 2.8 \text{ g}^{-1} \text{ cm}^3$, where $\rho_{>} > \rho_*$ and $\rho_{<} < \rho_*$ refer to the density in the high and low density region respectively. At the critical temperature $T_c < T_*$ and pressure $p_c < p_*$ for a first order transition one finds for the discontinuity in the density between the liquid (ρ_l) and gas (ρ_g) phase

$$\Delta\rho = \rho_l - \rho_g = B_p \left(\frac{p_* - p_c}{p_*} \right)^{\beta} = B_T \left(\frac{T_* - T_c}{T_*} \right)^{\beta} \tag{4.68}$$

with $B_p = 0.85 \text{ g cm}^{-3}$, $B_T = 1.5 \text{ g cm}^{-3}$. This relation also defines the slope of the critical line near the endpoint.

There is no apparent limitation for the use of the flow equation for an arbitrary microscopic free energy. This includes the case where U_{Λ} has several distinct minima and, in particular, the interesting case of a tricritical point. At present, the main inaccuracy arises from a simplification of the q^2 -dependence of the four point function which reflects itself in an error in the anomalous dimension η . The simplification of the momentum dependence of the effective propagator in the flow equation plays presumably only a secondary role. In summary, the non-perturbative flow equation appears to be a very efficient tool for the establishment of an explicit quantitative connection between the microphysical interactions and the long-range properties of the free energy.

4.7 Critical behavior of polymer chains

The large scale properties of isolated polymer chains can be computed from the critical behaviour of the $O(N)$ -symmetric scalar theory using a variant of the so-called replica limit: the statistics of polymer chains can be described by the N -component field theory in the limit $N \rightarrow 0$ [150].

In polymer theory critical behavior occurs when the size of an isolated swollen polymer becomes infinite. The size of a chain can be defined by its mean square distance $\langle (\vec{r}(\lambda) - \vec{r}(0))^2 \rangle$. Here λ denotes the distance along the chain between the end points with position $\vec{r}(\lambda)$ and $\vec{r}(0)$. The scaling behaviour of the mean square distance is characterized by the exponent ν ,

$$\langle (\vec{r}(\lambda) - \vec{r}(0))^2 \rangle \sim \lambda^{2\nu} . \tag{4.69}$$

The exponent ν for the polymer system corresponds to the correlation length exponent of the N -component field theory in the limit $N \rightarrow 0$. There are two independent critical exponents for the $O(N)$ model near its second order phase transition. In polymer theory, the exponent γ characterizes the asymptotic behaviour of the number of configurations $N(\lambda)$ of the self avoiding chains

$$N(\lambda) \sim \lambda^{\gamma-1}. \quad (4.70)$$

For a chain with independent links one has $\gamma = 1$. The exponent γ corresponds to the critical exponent that describes the behaviour of the magnetic susceptibility in the zero component field theory.

We compute the critical exponents ν and γ , as well as the anomalous dimension η , for the $O(N)$ model in the limit $N \rightarrow 0$ using the lowest order of the derivative expansion of the effective average action (4.2). The flow equations for the scale dependent effective potential U_k and wave function renormalization Z_k (or equivalently the anomalous dimension η) are derived for integer N . The results are given in eqs. (4.4) and (4.5). We analytically continue the evolution equations to non-integer values of N . We explicitly verify that the limit $N \rightarrow 0$ is continuously connected to the results for integer N by computing the exponents for numbers of components N between one and zero. The case $N = 1$ is also useful in polymer theory. It belongs to the universality class that describes the point at the top of the coexistence curve of a polymer solution [150]. The first table 8 below shows the results for the critical exponents ν, γ and η for several (non-integer) values of N [151].

N	ν	γ	$\eta [10^{-2}]$
0	0.589	1.155	4.06
0.1	0.594	1.165	4.12
0.2	0.600	1.175	4.18
0.3	0.605	1.185	4.22
0.4	0.610	1.195	4.26
0.5	0.616	1.205	4.30
0.6	0.621	1.216	4.32
0.7	0.626	1.226	4.34
0.8	0.632	1.237	4.36
0.9	0.637	1.247	4.37
1.0	0.643	1.258	4.37

Table 8: *Critical exponents for $0 \leq N \leq 1$*

In the following table 9 we compare our results for $N = 0$ with the epsilon expansion [131], perturbation series at fixed dimension [131], lattice Monte Carlo [136], high temperature series [133] and experiment [152]. The comparison shows a rather good agreement of these results.

$N = 0$	ν	γ	η
Average action	0.589	1.155	0.0406
ϵ -expansion	0.5875(25)	1.1575(60)	0.0300(50)
$d = 3$ expansion	0.5882(11)	1.1596(20)	0.0284(25)
lattice MC	0.5877(6)		
HT series	0.5878(6)	1.1594(8)	
Experiment	0.586(4)		

Table 9: *Critical exponents for polymer chains: Comparison between average action, epsilon expansion [131], perturbation series at fixed dimension [131], lattice Monte Carlo [136], high temperature series [133] and experiment [152].*

4.8 Two dimensional models and the Kosterlitz-Thouless transition

We investigate the $O(N)$ -symmetric linear σ -model in two dimensions. Apart from their physical relevance, two dimensional systems provide a good testing ground for non-perturbative methods. Let us consider first the $O(N)$ model in the limit $N \rightarrow 0$ motivated in the previous section. In this limit the two dimensional model exhibits a second order phase transition. The critical exponent ν describes the critical swelling of long polymer chains [150]. The value of this exponent is known exactly, $\nu_{\text{exact}} = 0.75$ [123]. To compare with the exact result, we study the $N = 0$ model using the lowest order derivative expansion (4.2) of the effective average action. We obtain the result $\nu = 0.782$ [151] which already compares rather well to the exact result. It points out that the present techniques allow us to give a unified description of the $O(N)$ model in two and in three dimensions, as well as four dimensions which will be discussed in section 8. In the following, we extend the discussion in two dimensions and show that for $N = 2$ one obtains a good picture of the Kosterlitz-Thouless phase transition⁴¹.

To evaluate the equation for the potential we make a further approximation and expand around the minimum of u_k for non-zero field squared $\tilde{\rho} = \kappa$ up to the quadratic order in $\tilde{\rho}$:

$$u_k(\tilde{\rho}) = u_k(\kappa) + \frac{1}{2}\lambda(\tilde{\rho} - \kappa)^2. \quad (4.71)$$

The condition $\partial u / \partial \tilde{\rho}|_{\tilde{\rho}=\kappa} = 0$ holds independent of t and gives us the evolution equation for the location of the minimum of the potential parametrized by κ . A similar evolution equation can be derived [113] for the symmetric regime where $\kappa = 0$ and an appropriate variable is $\partial u / \partial \tilde{\rho}|_{\tilde{\rho}=0}$. The flow equations for κ and λ read

$$\begin{aligned} \beta_\kappa &\equiv \frac{d\kappa}{dt} = -(d-2+\eta)\kappa + 2v_d(N-1)l_1^d(0) + 6v_d l_1^d(2\lambda\kappa) \\ \beta_\lambda &\equiv \frac{d\lambda}{dt} = (d-4+2\eta)\lambda + 2v_d(N-1)\lambda^2 l_2^d(0) + 18v_d \lambda^2 l_2^d(2\lambda\kappa). \end{aligned} \quad (4.72)$$

where the ‘‘threshold functions’’ are defined in 3.2. The theory is in the symmetric phase if $\kappa(0) = 0$ – this happens if κ reaches zero for some nonvanishing $k_s > 0$. On the

⁴¹For investigations in two dimensions using similar methods see also refs. [153, 154].

other hand, the phase with spontaneous symmetry breaking corresponds to $\rho_0(0) > 0$ where $\rho_0(k) = k^{d-2} Z_k^{-1} \kappa(k)$. A second order phase transition is characterized by a scaling solution corresponding to fixed points for κ and λ . For small deviations from the fixed point there is typically one infrared unstable direction which is related to the relevant mass parameter. The phase transition can be studied as a function of $\kappa(\Lambda)$ with a critical value $\kappa(\Lambda) = \kappa_c$. The difference $\kappa(\Lambda) - \kappa_c$ can be assumed to be proportional to $T_c - T$, with T_c the critical temperature. This allows to define and compute critical exponents in a standard way. We should mention a particular possibility for $d = 2$, namely that $\kappa(0)$ remains strictly positive whereas $\rho_0(0)$ vanishes due to $\lim_{k \rightarrow 0} Z_k \rightarrow \infty$. This is a somewhat special form of spontaneous symmetry breaking, where the renormalized expectation value, which determines the renormalized mass, is different from zero whereas the expectation value of the unrenormalized field vanishes. We will see that this scenario is indeed realized for $d = 2, N = 2$. The phase with this special form of spontaneous symmetry breaking exhibits a massive radial and a massless Goldstone boson – and remains nevertheless consistent with the Mermin-Wagner theorem [112] that the expectation value of the (unrenormalized) field ϕ_a must vanish for $N \geq 2$. The Kosterlitz-Thouless phase transition [111] describes the transition from this phase to the standard symmetric phase of the linear σ -model, i.e. the phase where $\kappa(0) = 0$ with a spectrum of two degenerate massive modes.

In order to solve the flow equation (4.72) we further need the anomalous dimension η which is given in our truncation by eq. (4.5). We specialize to the two dimensional linear σ -model ($d = 2$). We observe that the flow equations can be solved analytically in the limiting case of a large mass $\omega = 2\lambda\kappa$ of the radial mode. The threshold functions vanish with powers of ω^{-1} and for $N > 1$ the leading contributions to the β -functions are those from the Goldstone modes. Therefore this limit is called the Goldstone regime. In this approximation the β -functions can be expanded in powers of ω^{-1} . In particular, the leading order of the anomalous dimension can be extracted immediately from (4.2):

$$\eta = \frac{1}{4\pi\kappa} + \mathcal{O}(\kappa^{-2}). \quad (4.73)$$

Inserting this result in (4.72) we have

$$\beta_\kappa = \frac{(N-2)}{4\pi} + \mathcal{O}(\kappa^{-1}) \quad (4.74)$$

and the leading order of β_λ is

$$\beta_\lambda = -2\lambda + \frac{(N-1)\ln 2}{2\pi} \lambda^2 + \mathcal{O}(\kappa^{-1}). \quad (4.75)$$

Eq. (4.75) has a fixed point solution $\lambda_* = \frac{4\pi}{(N-1)\ln 2} \approx 18.13/(N-1)$.

For $N > 2$ there exists a simple relation between the linear and the nonlinear σ -model: The effective coupling between the Goldstone bosons of the nonabelian nonlinear σ -model can be extracted directly from (4.2) and reads in an appropriate normalization [155]

$$g^2 = \frac{1}{2\kappa}. \quad (4.76)$$

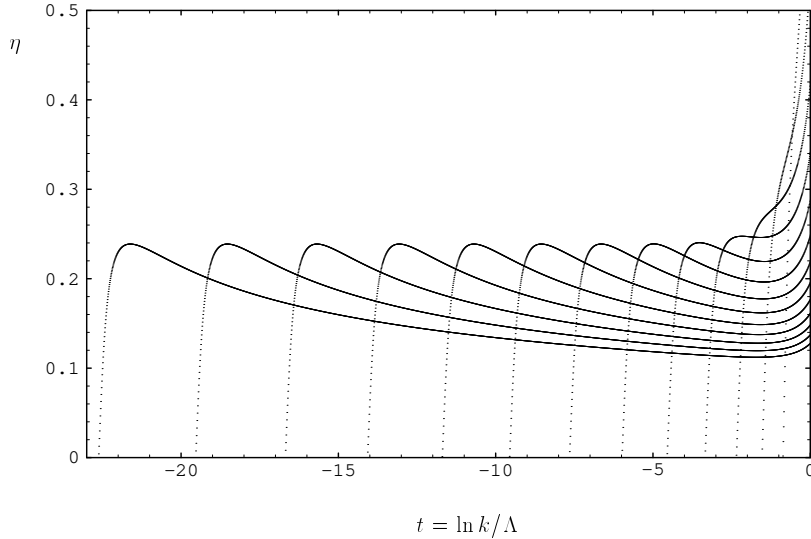


Figure 13: *The scale dependent anomalous dimension $\eta(t)$ for a series of initial potentials U_Λ approaching the phase transition.*

The lowest order contribution to β_κ (4.74) coincides with the one loop expression for the running of g^2 as computed in the nonlinear σ -model. We emphasize in this context the importance of the anomalous dimension η which changes the factor $(N - 1)$ appearing in (4.72) into the appropriate factor $(N - 2)$ in (4.74). In correspondence with the universality of the two loop β -function for g^2 in the nonlinear σ -model we expect the next to leading term $\sim \kappa^{-1}$ in β_κ (4.74) to be also proportional to $(N - 2)$. In order to verify this one has to go beyond the truncation (4.2) and systematically keep all terms contributing in the appropriate order of κ^{-1} . (This calculation is similar to the extraction of the two loop β -function of the linear σ -model in four dimensions by means of an “improved one loop calculation” using the flow equation (2.19) [156].) We have calculated the expansion of β_κ up to the order $\mathcal{O}(\kappa^{-1})$ for the most general two derivative action, i.e. neglecting only the momentum dependence of Z_k and Y_k . The result agrees with the two loop term of the nonlinear σ -model within a few per cent, and the discrepancy should be attributed to the neglected momentum dependence of the wave function renormalization. The issue of the contribution to β_κ in order κ^{-2} is less clear: Of course, the direct contribution of the Goldstone bosons (combined with their contribution to η) should always vanish for $N = 2$ since no nonabelian coupling exists in this case. The radial mode however, could generate a contribution which is not proportional to $(N - 2)$. This contribution is possibly nonanalytic in κ^{-1} and would correspond to a non-perturbative contribution in the language of the nonlinear σ -model.

Let us now turn to the two dimensional abelian model ($d = 2, N = 2$) for which we want to describe the Kosterlitz-Thouless phase transition. In the limit of vanishing β_κ for large enough κ the location of the minimum of $u_k(\tilde{\rho})$ (4.71) is independent of the scale k . Therefore the parameter κ , or, alternatively, the temperature difference $T_c - T$, can be viewed as a free parameter. If we go beyond the lowest order estimate (4.75) the fixed point for λ remains, but λ_* becomes dependent on κ . This implies that the system has a line of fixed

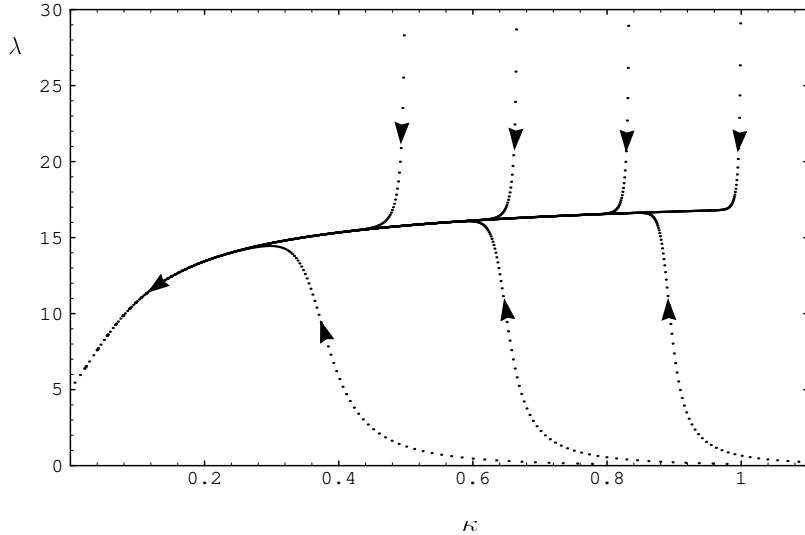


Figure 14: *Flow of the quartic coupling λ and the minimum κ for different t . One observes the (pseudo) critical line $\lambda(\kappa)$ as an (approximate) line of fixed points.*

points which is parametrized by κ as suggested by results obtained from calculations with the nonlinear σ -model [157]. In particular, the anomalous dimension η depends on the temperature $T_c - T$ (4.73). Even if this picture is not fully accurate for nonvanishing β_κ , it is a very good approximation for large κ : The possible running of κ is extremely slow, especially if β_κ vanishes in order κ^{-1} . We associate the low temperature or large κ phase with the phase of vortex condensation in the nonlinear σ -model. The correlation length is always infinite due to the Goldstone boson. Since $\eta > 0$ we expect the inverse propagator of this Goldstone degree of freedom $\sim (q^2)^{1-\eta/2}$, thus avoiding Coleman's no go theorem [117] for free massless particles in two dimensions. On the other hand, for small values of $\lambda\kappa$ the threshold functions can be expanded in powers of $\lambda\kappa$. The anomalous dimension is small and κ is driven to zero for $k_s > 0$. This corresponds to the symmetric phase of the linear σ -model with a massive complex scalar field. We associate this high temperature phase with the phase of vortex disorder in the picture of the nonlinear σ -model. The transition between the behaviour for large and small κ is described by the Kosterlitz-Thouless transition. In the language of the linear σ -model it is the transition from a special type of spontaneous symmetry breaking to symmetry restoration.

Finally we give a summary of the results obtained from the numerical integration of the evolution equations (4.72) and (4.5) for the special case $d = 2, N = 2$ ⁴². We use a Runge-Kutta method starting at $t = 0$ with arbitrary initial values for κ and λ and solve the flow equations for large negative values of t . Results are shown in figs.1-4 where we plot typical trajectories. The distance between points corresponds to equal steps in t such that very dense points or lines indicate the very slow running in the vicinity of fixed points.

The understanding of the trajectories needs a few comments: The work of Kosterlitz and

⁴²This work has also been done for $d = 2, N = 1$. There we find a fixed point which corresponds to the second order phase transition in the Ising model.

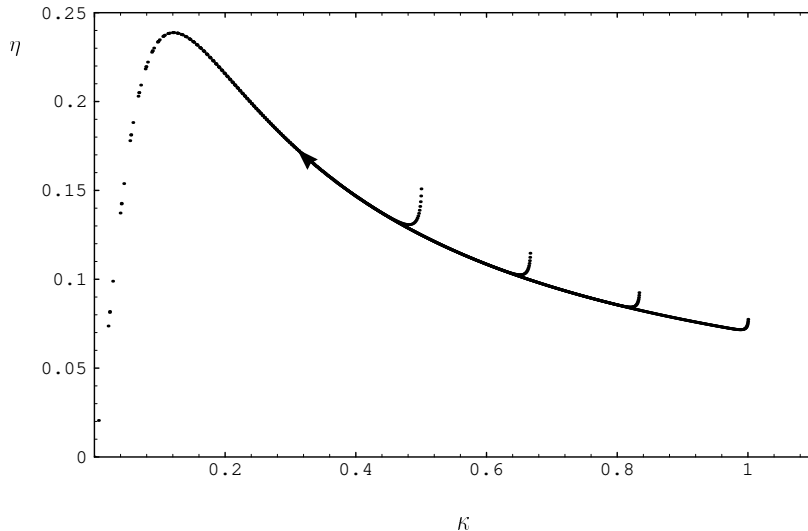


Figure 15: *Flow of the anomalous dimension η and the minimum κ . One observes (approximate) scaling solutions with the universal function $\eta(\kappa)$.*

Thouless [111] suggests that the correlation length is divergent for all temperatures below a critical temperature T_c and that the critical exponent η depends on temperature. The consequence for our model is that above a critical value for κ all β - functions should vanish for a line of fixed points parametrized by κ . From the results in the Goldstone regime and from earlier calculations [157] we conclude that β_κ should vanish faster than κ^{-1} for large κ . Our truncation (4.2), however, yields a function β_κ which vanishes only like κ^{-1} . The consequence is that even if the system reaches the supposed line of fixed points the parameter κ decreases very slowly until the transition to the symmetric regime is reached. The anomalous dimension first grows with decreasing κ (4.73) until the critical value is reached. Then the system runs into the symmetric regime and η vanishes. So we expect that η reaches a maximum near the phase transition. We use this as a criterion for the critical value κ_c . In summary, the truncation (4.2) smoothens the phase transition and this prevents a very accurate determination of the critical value κ_c and the corresponding anomalous dimension η_c . From the numerical point of view the absence of a true phase transition in the truncation (4.2) makes life easier: One particular trajectory can show both the features of the low and the high temperature phase since it crosses from one to the other.

The numerical results fulfill our expectations. Fig.13 shows the evolution of the anomalous dimension with decreasing t for several different initial values $\kappa(\Lambda), \lambda(\Lambda)$. The maximum is reached with $\eta_c = 0.24$ which has to be compared with the result of Kosterlitz and Thouless $\eta_c = 0.25$ [111]. The approximate “line of fixed points” for $\kappa > \kappa_c$ ($\eta < \eta_c$) is demonstrated by the self-similarity of the curves for large $-t$. Trajectories with different initial conditions hit the line of fixed points at different κ . Subsequently they follow the line of fixed points. Except for the value of $\kappa(k)$ all “memory” of the initial conditions is lost for $t \leq -3$. Another manifestation of the line of fixed points in the (κ, λ) plane is demonstrated in fig. 14. After some fast “initial running” (dotted parts of the trajectories) all trajectories with large enough

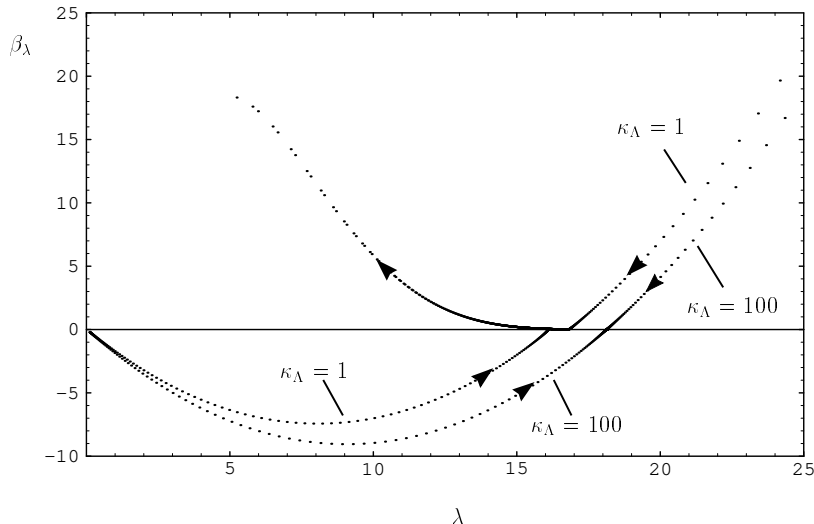


Figure 16: *The beta function for the quartic coupling β_λ for different initial κ_Λ (see text).*

$\kappa(\Lambda)$ follow this line independent of the initial $\lambda(\Lambda)$. We emphasize that the nonlinear σ -model corresponds to $\lambda(\Lambda) \rightarrow \infty$. Our investigation shows that the linear σ -model is in the same universality class, even for very small $\lambda(\Lambda)$. In fig.15 we plot $\eta(\kappa)$. Along the line of fixed points we find perfect agreement with the analytical estimate (4.73) for large κ . For $\kappa = 0.3$ the deviation from the lowest order result is 34% in the present truncation. Finally we show in fig.16 the value of β_λ for different trajectories. The dense parts of the “ingoing curves” show the fixed point behaviour at $\lambda_*(\kappa_1)$ where κ_1 denotes the value of κ where the line of fixed points is hit. (For small $\kappa(\Lambda)$ there is a substantial difference between κ_1 and $\kappa(\Lambda)$ which depends also on $\lambda(\Lambda)$. This can be seen from the curves with $\kappa(\Lambda) = 1$.) After hitting the line of fixed points the trajectories stay for a large t -interval at β_λ very close to zero. Subsequently, the “outgoing curve” indicates the transition to the symmetric phase.

In conclusion, both the analytical and the numerical investigations demonstrate all important characteristics of the Kosterlitz-Thouless phase transition for the linear σ -model. This belongs to the same universality class as the nonlinear σ -model and we have demonstrated a close correspondence between the linear and the nonlinear σ -model with abelian symmetry. In particular, the phase with vortex disorder in the nonlinear σ -model corresponds simply to the symmetric phase of the linear σ -model. We emphasize that we have never needed the explicit investigation of vortex configurations. The exact non-perturbative flow equation includes automatically all configurations. Its ability to cope with the infrared problems of perturbation theory is confirmed by the present work.

Despite the simple and clear qualitative picture arising from the truncation (4.2) this letter only constitutes a first step for a quantitative investigation. It is not excluded that the coincidence of our critical $\eta_c \approx 0.24$ with $1/4$ is somewhat accidental. In order to answer this question one needs to go beyond the truncation (4.2). In view of the relatively large value of η_c we expect in particular that the momentum dependence of the wave function renormalization Z_k (or the deviation of the inverse propagator from q^2) could play an important role at the

phase transition. This effect should be included in a more detailed quantitative investigation.

5 Scalar matrix models

5.1 Introduction

Matrix models are extensively discussed in statistical physics. Beyond the $O(N)$ -symmetric Heisenberg models (“vector models”), which we have discussed in the previous sections, they correspond to the simplest scalar field theories. There is a wide set of different applications as the metal insulator transition [158] or liquid crystals [159] or strings and random surfaces [160]. The universal behavior of these models in the vicinity of a second order or weak first order phase transition is determined by the symmetries and the field content of the corresponding field theories. We will consider here [37] models with $U(N) \times U(N)$ symmetry with a scalar field in the (\bar{N}, N) representation, described by an arbitrary complex $N \times N$ matrix φ .⁴³ We do not impose nonlinear constraints for φ a priori but rather use a “classical” potential. This enforces nonlinear constraints in certain limiting cases. Among those, our model describes a nonlinear matrix model for unitary matrices or one for singular 2×2 matrices. The universal critical behavior does not depend on the details of the classical potential and there is no difference between the linear and nonlinear models in the vicinity of the limiting cases. We concentrate here on three dimensions, relevant for statistical physics and critical phenomena in high temperature field theory.

The cases $N = 2, 3$ have a relation to high temperature strong interaction physics. At vanishing temperature the four dimensional models can be used for a description of the pseudoscalar and scalar mesons for N quark flavors. For $N = 3$ the antihermitean part of φ describes here the pions, kaons, η and η' whereas the hermitean part accounts for the nonet of scalar 0^{++} mesons.⁴⁴ For nonzero temperature T the effects of fluctuations with momenta $p^2 \lesssim (\pi T)^2$ are described by the corresponding three dimensional models. These models account for the long distance physics and are obtained by integrating out the short distance fluctuations. In particular, the three dimensional models embody the essential dynamics in the immediate vicinity of a second order or weak first order chiral phase transition [24, 25, 26, 27]. The four dimensional models at nonvanishing temperature have also been used for investigations of the temperature dependence of meson masses [161, 162]. The simple model investigated in this section is not yet realistic for QCD – it neglects the effect of the axial anomaly which reduces the chiral flavor symmetry to $SU(N) \times SU(N) \times U(1)$. In the present section we also neglect the fluctuations of fermions (quarks). They play no role for the universal aspects near the phase transition. They are needed, however, for a realistic connection with QCD and will be included in sect. 8. For simplicity we will concentrate here on $N = 2$, but our methods can be generalized to $N = 3$ and the inclusion of the axial anomaly.

⁴³The methods presented here have recently been applied also to the principle chiral model with $SO(3) \times O(3)$ symmetry [163] and to Heisenberg frustrated magnets with $O(N) \times O(2)$ symmetry [164].

⁴⁴See ref. [165, 166] for a phenomenological analysis.

The case $N = 2$ also has a relation to the electroweak phase transition in models with two Higgs doublets. Our model corresponds here to the critical behavior in a special class of left-right symmetric theories in the limit where the gauge couplings are neglected. Even though vanishing gauge couplings are not a good approximation for typical realistic models one would like to understand this limiting case reliably.

For the present matrix models one wants to know if the phase transition becomes second order in certain regions of parameter space. In the context of flow equations this is equivalent to the question if the system of running couplings admits a fixed point which is infrared stable (except one relevant direction corresponding to $T - T_c$). We find that the phase transition for the investigated matrix models with $N = 2$ and symmetry breaking pattern $U(2) \times U(2) \rightarrow U(2)$ is always (fluctuation induced) first order, except for a boundary case with enhanced $O(8)$ symmetry. For a large part of parameter space the transition is weak and one finds large renormalized dimensionless couplings near the critical temperature. If the running of the couplings towards approximate fixed points (there are no exact fixed points) is sufficiently fast the large distance physics loses memory of the details of the short distance or classical action. In this case the physics near the phase transition is described by an universal equation of state. This new universal critical equation of state for first order transitions involves two (instead of one for second order transitions) scaling variables.

In section 5.2 we define the $U(2) \times U(2)$ symmetric matrix model and we establish the connection to a matrix model for unitary matrices and to one for singular complex 2×2 matrices. There we also give an interpretation of the model as the coupled system of two $SU(2)$ -doublets for the weak interaction Higgs sector. The evolution equation for the average potential U_k and its scaling form is computed in section 5.3. A detailed account on the renormalization group flow is presented in section 5.4. Section 5.5 is devoted to an overview over the phase structure and the coarse-grained effective potential U_k for the three dimensional theory. We compute the universal form of the equation of state for weak first order phase transitions in section 5.6 and we extract critical exponents and the corresponding index relations.

5.2 Scalar matrix model with $U(2) \times U(2)$ symmetry

We consider a $U(2) \times U(2)$ symmetric effective action for a scalar field φ which transforms in the $(2, 2)$ representation with respect to the subgroup $SU(2) \times SU(2)$. Here φ is represented by a complex 2×2 matrix and the transformations are

$$\begin{aligned}\varphi &\rightarrow U\varphi V^\dagger, \\ \varphi^\dagger &\rightarrow V\varphi^\dagger U^\dagger\end{aligned}\tag{5.1}$$

where U and V are unitary 2×2 matrices corresponding to the two distinct $U(2)$ factors.

We classify the invariants for the construction of the effective average action by the number of derivatives. The lowest order is given by

$$\Gamma_k = \int d^d x \{U_k(\varphi, \varphi^\dagger) + Z_k \partial_\mu \varphi_{ab}^* \partial^\mu \varphi^{ab}\} \quad (a, b = 1, 2).\tag{5.2}$$

The term with no derivatives defines the scalar potential U_k which is an arbitrary function of traces of powers of $\varphi^\dagger\varphi$. The most general $U(2) \times U(2)$ symmetric scalar potential can be expressed as a function of only two independent invariants,

$$\begin{aligned}\rho &= \text{tr}(\varphi^\dagger\varphi) \\ \tau &= 2\text{tr}\left(\varphi^\dagger\varphi - \frac{1}{2}\rho\right)^2 = 2\text{tr}(\varphi^\dagger\varphi)^2 - \rho^2.\end{aligned}\tag{5.3}$$

Here we have used for later convenience the traceless matrix $\varphi^\dagger\varphi - \frac{1}{2}\rho$ to construct the second invariant. Higher invariants, $\text{tr}(\varphi^\dagger\varphi - \frac{1}{2}\rho)^n$ for $n > 2$, can be expressed as functions of ρ and τ [167].

For the derivative part we consider a standard kinetic term with a scale dependent wave function renormalization constant Z_k . The first correction to the kinetic term would include field dependent wave function renormalizations $Z_k(\rho, \tau)$ plus functions not specified in eq. (5.2) which account for a different index structure of invariants with two derivatives. The wave function renormalizations may be defined at zero momentum or for $q^2 = k^2$ in the hybrid derivative expansion. The next level involves invariants with four derivatives and so on. We define here Z_k at the minimum ρ_0, τ_0 of U_k and at vanishing momenta q^2 ,

$$Z_k = Z_k(\rho = \rho_0, \tau = \tau_0; q^2 = 0).\tag{5.4}$$

The factor Z_k appearing in the definition of the infrared cutoff R_k in eq. (2.7) is identified with (5.4). The k dependence of this function is given by the anomalous dimension

$$\eta(k) = -\frac{d}{dt} \ln Z_k.\tag{5.5}$$

If the ansatz (5.2) is inserted into the flow equation for the effective average action (2.19) one obtains flow equations for the effective average potential $U_k(\rho, \tau)$ and for the wave function renormalization constant Z_k (or equivalently the anomalous dimension η). This is done in section 5.3. These flow equations have to be integrated starting from some short distance scale Λ and one has to specify U_Λ and Z_Λ as initial conditions. The short distance potential is taken to be a quartic potential which is parametrized by two quartic couplings $\bar{\lambda}_{1\Lambda}, \bar{\lambda}_{2\Lambda}$ and a mass term. We start in the spontaneously broken regime where the minimum of the potential occurs at a nonvanishing field value and there is a negative mass term at the origin of the potential ($\bar{\mu}_\Lambda^2 > 0$),

$$U_\Lambda(\rho, \tau) = -\bar{\mu}_\Lambda^2\rho + \frac{1}{2}\bar{\lambda}_{1\Lambda}\rho^2 + \frac{1}{4}\bar{\lambda}_{2\Lambda}\tau\tag{5.6}$$

and $Z_\Lambda = 1$. The potential is bounded from below provided $\bar{\lambda}_{1\Lambda} > 0$ and $\bar{\lambda}_{2\Lambda} > -2\bar{\lambda}_{1\Lambda}$. For $\bar{\lambda}_{2\Lambda} > 0$ one observes the potential minimum for the configuration $\varphi_{ab} = \varphi\delta_{ab}$ corresponding to the spontaneous symmetry breaking down to the diagonal $U(2)$ subgroup of $U(2) \times U(2)$. For negative $\bar{\lambda}_{2\Lambda}$ the potential is minimized by the configuration $\varphi_{ab} = \varphi\delta_{a1}\delta_{ab}$ which corresponds to the symmetry breaking pattern $U(2) \times U(2) \longrightarrow U(1) \times U(1) \times U(1)$. In the special case $\bar{\lambda}_{2\Lambda} = 0$ the theory exhibits an enhanced $O(8)$ symmetry. This constitutes the boundary between two phases with different symmetry breaking patterns.

The limits of infinite couplings correspond to nonlinear constraints in the matrix model. For $\bar{\lambda}_{1\Lambda} \rightarrow \infty$ with fixed ratio $\bar{\mu}_\Lambda^2/\bar{\lambda}_{1\Lambda}$ one finds the constraint $\text{tr}(\varphi^\dagger\varphi) = \bar{\mu}_\Lambda^2/\bar{\lambda}_{1\Lambda}$. By a convenient choice of Z_Λ (rescaling of φ) this can be brought to the form $\text{tr}(\varphi^\dagger\varphi) = 2$. On the other hand, the limit $\bar{\lambda}_{2\Lambda} \rightarrow +\infty$ enforces the constraint $\varphi^\dagger\varphi = \frac{1}{2}\text{tr}(\varphi^\dagger\varphi)$. Combining the limits $\bar{\lambda}_{1\Lambda} \rightarrow \infty$, $\bar{\lambda}_{2\Lambda} \rightarrow \infty$ the constraint reads $\varphi^\dagger\varphi = 1$ and we deal with a matrix model for unitary matrices. (These considerations generalize to arbitrary N .) Another interesting limit is obtained for $\bar{\lambda}_{1\Lambda} = -\frac{1}{2}\bar{\lambda}_{2\Lambda} + \Delta_\lambda$, $\Delta_\lambda > 0$ if $\bar{\lambda}_{2\Lambda} \rightarrow -\infty$. In this case the nonlinear constraint reads $(\text{tr}\varphi^\dagger\varphi)^2 = \text{tr}(\varphi^\dagger\varphi)^2$ which implies for $N = 2$ that $\det \varphi = 0$. This is a matrix model for singular complex 2×2 matrices.

One can also interpret our model as the coupled system of two $SU(2)$ -doublets for the weak interaction Higgs sector. This is simply done by decomposing the matrix φ_{ab} into two two-component complex fundamental representations of one of the $SU(2)$ subgroups, $\varphi_{ab} \rightarrow \varphi_{1b}, \varphi_{2b}$. The present model corresponds to a particular left-right symmetric model with interactions specified by

$$\rho = \varphi_1^\dagger\varphi_1 + \varphi_2^\dagger\varphi_2 \quad (5.7)$$

$$\tau = \left(\varphi_1^\dagger\varphi_1 - \varphi_2^\dagger\varphi_2\right)^2 + 4\left(\varphi_1^\dagger\varphi_2\right)\left(\varphi_2^\dagger\varphi_1\right). \quad (5.8)$$

We observe that for a typical weak interaction symmetry breaking pattern the expectation values of φ_1 and φ_2 should be aligned in the same direction or one of them should vanish. In the present model this corresponds to the choice $\bar{\lambda}_{2\Lambda} < 0$. The phase structure of a related model without the term $\sim (\varphi_1^\dagger\varphi_2)(\varphi_2^\dagger\varphi_1)$ has been investigated previously [168] and shows second or first order transitions⁴⁵. Combining these results with the outcome of this work leads already to a detailed qualitative overview over the phase pattern in a more general setting with three independent couplings for the quartic invariants $(\varphi_1^\dagger\varphi_1 + \varphi_2^\dagger\varphi_2)^2$, $(\varphi_1^\dagger\varphi_1 - \varphi_2^\dagger\varphi_2)^2$ and $(\varphi_1^\dagger\varphi_2)(\varphi_2^\dagger\varphi_1)$. We also note that the special case $\bar{\lambda}_{2\Lambda} = 2\bar{\lambda}_{1\Lambda}$ corresponds to two Heisenberg models interacting only by a term sensitive to the alignment between φ_1 and φ_2 , i.e. a quartic interaction of the form $(\varphi_1^\dagger\varphi_1)^2 + (\varphi_2^\dagger\varphi_2)^2 + 2(\varphi_1^\dagger\varphi_2)(\varphi_2^\dagger\varphi_1)$.

The model is now completely specified and it remains to extract the flow equations for U_k and Z_k .

5.3 Scale dependence of the effective average potential

To obtain U_k we evaluate the flow equation for the average action (2.19) for a constant field with $\Gamma_k = \Omega U_k$ where Ω denotes the volume. With the help of $U(2) \times U(2)$ transformations the matrix field φ can be turned into a standard diagonal form with real nonnegative eigenvalues. Without loss of generality the evolution equation for the effective potential can therefore be obtained by calculating the trace in (2.19) for small field fluctuations χ_{ab} around a constant background configuration which is real and diagonal,

$$\varphi_{ab} = \varphi_a \delta_{ab}, \quad \varphi_a^* = \varphi_a. \quad (5.9)$$

⁴⁵First order phase transitions and coarse graining have also been discussed in a multi-scalar model with Z_2 symmetry [169].

We separate the fluctuation field into its real and imaginary part, $\chi_{ab} = \frac{1}{\sqrt{2}}(\chi_{Rab} + i\chi_{Iab})$ and perform the second functional derivatives of Γ_k with respect to the eight real components. For the constant configuration (5.9) it turns out that $\Gamma_k^{(2)}$ has a block diagonal form because mixed derivatives with respect to real and imaginary parts of the field vanish. The remaining submatrices $\delta^2\Gamma_k/\delta\chi_R^{ab}\delta\chi_R^{cd}$ and $\delta^2\Gamma_k/\delta\chi_I^{ab}\delta\chi_I^{cd}$ can be diagonalized in order to find the inverse of $\Gamma_k^{(2)} + R_k$ under the trace occurring in eq. (2.19). Here the momentum independent part of $\Gamma_k^{(2)}$ defines the mass matrix by the second functional derivatives of U_k . The eight eigenvalues of the mass matrix are

$$\begin{aligned}(M_1^\pm)^2 &= U'_k + 2(\rho \pm (\rho^2 - \tau)^{1/2})\partial_\tau U_k, \\ (M_2^\pm)^2 &= U'_k \pm 2\tau^{1/2}\partial_\tau U_k\end{aligned}\tag{5.10}$$

corresponding to second derivatives with respect to χ_I and

$$\begin{aligned}(M_3^\pm)^2 &= (M_1^\pm)^2, \\ (M_4^\pm)^2 &= U'_k + \rho U''_k + 2\rho\partial_\tau U_k + 4\tau\partial_\tau U'_k + 4\rho\tau\partial_\tau^2 U_k \\ &\quad \pm \left\{ \tau (U''_k + 4\partial_\tau U_k + 4\rho\partial_\tau U'_k + 4\tau\partial_\tau^2 U_k)^2 \right. \\ &\quad \left. + (\rho^2 - \tau) (U''_k - 2\partial_\tau U_k - 4\tau\partial_\tau^2 U_k)^2 \right\}^{1/2}\end{aligned}\tag{5.11}$$

corresponding to second derivatives with respect to χ_R . Here the eigenvalues are expressed in terms of the invariants ρ and τ using

$$\varphi_1^2 = \frac{1}{2}(\rho + \tau^{1/2}), \quad \varphi_2^2 = \frac{1}{2}(\rho - \tau^{1/2})\tag{5.12}$$

and we adopt the convention that a prime on $U_k(\rho, \tau)$ denotes the derivative with respect to ρ at fixed τ and k and $\partial_\tau^n U_k \equiv \partial^n U_k / (\partial\tau)^n$.

The flow equation for the effective average potential is simply expressed in terms of the mass eigenvalues

$$\begin{aligned}\frac{\partial}{\partial t} U_k(\rho, \tau) &= \frac{1}{2} \int \frac{d^d q}{(2\pi)^d} \frac{\partial}{\partial t} R_k(q) \\ &\quad \left\{ \frac{2}{P_k(q) + (M_1^+(\rho, \tau))^2} + \frac{2}{P_k(q) + (M_1^-(\rho, \tau))^2} + \frac{1}{P_k(q) + (M_2^+(\rho, \tau))^2} \right. \\ &\quad \left. + \frac{1}{P_k(q) + (M_2^-(\rho, \tau))^2} + \frac{1}{P_k(q) + (M_4^+(\rho, \tau))^2} + \frac{1}{P_k(q) + (M_4^-(\rho, \tau))^2} \right\}.\end{aligned}\tag{5.13}$$

In the rhs of the evolution equation appears the (massless) inverse average propagator

$$P_k(q) = Z_k q^2 + R_k(q) = \frac{Z_k q^2}{1 - e^{-q^2/k^2}}\tag{5.14}$$

which incorporates the infrared cutoff function R_k given by eq. (2.17). The only approximation so far is due to the derivative expansion (5.2) of Γ_k which enters into the flow equation (5.13) through the form of P_k . The mass eigenvalues (5.10) and (5.11) appearing in the above flow

equation are exact since we have kept for the potential the most general form $U_k(\rho, \tau)$.

Spontaneous symmetry breaking and mass spectra

In the following we consider spontaneous symmetry breaking patterns and the corresponding mass spectra for a few special cases. For the origin at $\varphi_{ab} = 0$ all eigenvalues equal $U'_k(0, 0)$. If the origin is the absolute minimum of the potential we are in the symmetric regime where all excitations have mass squared $U'_k(0, 0)$.

Spontaneous symmetry breaking to the diagonal $U(2)$ subgroup of $U(2) \times U(2)$ can be observed for a field configuration which is proportional to the identity matrix, i.e. $\varphi_{ab} = \varphi\delta_{ab}$. The invariants (5.3) take on values $\rho = 2\varphi^2$ and $\tau = 0$. The relevant information for this symmetry breaking pattern is contained in $U_k(\rho) \equiv U_k(\rho, \tau = 0)$. In case of spontaneous symmetry breaking there is a nonvanishing value for the minimum ρ_0 of the potential. With $U'_k(\rho_0) = 0$ one finds the expected four massless Goldstone bosons with $(M_1^-)^2 = (M_2^\pm)^2 = (M_3^-)^2 = 0$. In addition there are three massive scalars in the adjoint representation of the unbroken diagonal $SU(2)$ with mass squared $(M_1^+)^2 = (M_3^+)^2 = (M_4^-)^2 = 4\rho_0\partial_\tau U_k$ and one singlet with mass squared $(M_4^+)^2 = 2\rho_0 U''_k$. The situation corresponds to chiral symmetry breaking in two flavor QCD in absence of quark masses and the chiral anomaly. The Goldstone modes are the pseudoscalar pions and the η (or η'), the scalar triplet has the quantum numbers of a_0 and the singlet is the so-called σ -field.

Another interesting case is the spontaneous symmetry breaking down to a residual $U(1) \times U(1) \times U(1)$ subgroup of $U(2) \times U(2)$ which can be observed for the configuration $\varphi_{ab} = \varphi\delta_{a1}\delta_{ab}$ ($\rho = \varphi^2$, $\tau = \varphi^4 = \rho^2$). Corresponding to the number of broken generators one observes the five massless Goldstone bosons $(M_1^\pm)^2 = (M_2^+)^2 = (M_3^\pm)^2 = 0$ for the minimum of the potential at $U'_k + 2\rho_0\partial_\tau U_k = 0$. In addition there are two scalars with mass squared $(M_2^-)^2 = (M_4^-)^2 = U'_k - 2\rho_0\partial_\tau U_k$ and one with $(M_4^+)^2 = U'_k + 2\rho_0 U''_k + 6\rho_0\partial_\tau U_k + 8\rho_0^2\partial_\tau U'_k + 8\rho_0^3\partial_\tau^2 U_k$.

We finally point out the special case where the potential is independent of the second invariant τ . In this case there is an enhanced $O(8)$ symmetry instead of $U(2) \times U(2)$. With $\partial_\tau^n U_k \equiv 0$ and $U'_k(\rho_0) = 0$ one observes the expected seven massless Goldstone bosons and one massive mode with mass squared $2\rho_0 U''_k$.

Scaling form of the flow equations

For the $O(8)$ symmetric model in the limit $\bar{\lambda}_{2\Lambda} = 0$ one expects a region of the parameter space which is characterized by renormalized masses much smaller than the ultraviolet cutoff or inverse microscopic length scale of the theory. In particular, in the absence of a mass scale one expects a scaling behavior of the effective average potential U_k . The behavior of U_k at or near a second order phase transition is most conveniently studied using the scaling form of the evolution equation. This form is also appropriate for an investigation that has to deal with weak first order phase transitions as encountered in the present model for $\bar{\lambda}_{2\Lambda} > 0$. The remaining part of this subsection is devoted to the derivation of the scaling form (5.18) of the flow equation (5.13).

In the present form of eq. (5.13) the rhs shows an explicit dependence on the scale k once the momentum integration is performed. By a proper choice of variables we cast the

evolution equation into a form where the scale no longer appears explicitly. We introduce a dimensionless potential $u_k = k^{-d}U_k$ and express it in terms of dimensionless renormalized fields

$$\begin{aligned}\tilde{\rho} &= Z_k k^{2-d} \rho, \\ \tilde{\tau} &= Z_k^2 k^{4-2d} \tau.\end{aligned}\tag{5.15}$$

The derivatives of u_k are given by

$$\partial_{\tilde{\tau}}^n u_k^{(m)}(\tilde{\rho}, \tilde{\tau}) = Z_k^{-2n-m} k^{(2n+m-1)d-4n-2m} \partial_{\tau}^n U_k^{(m)}(\rho, \tau).\tag{5.16}$$

(Note that $u_k^{(m)}$ denotes m derivatives with respect to $\tilde{\rho}$ at fixed $\tilde{\tau}$ and k , while $U_k^{(m)}$ denotes m derivatives with respect to ρ at fixed τ and k). With

$$\begin{aligned}\frac{\partial}{\partial t} u_k(\tilde{\rho}, \tilde{\tau})|_{\tilde{\rho}, \tilde{\tau}} &= -du_k(\tilde{\rho}, \tilde{\tau}) + (d-2+\eta)\tilde{\rho}u'_k(\tilde{\rho}, \tilde{\tau}) + (2d-4+2\eta)\tilde{\tau}\partial_{\tilde{\tau}}u_k(\tilde{\rho}, \tilde{\tau}) \\ &\quad + k^{-d}\frac{\partial}{\partial t}U_k(\rho(\tilde{\rho}), \tau(\tilde{\tau}))|_{\rho, \tau}\end{aligned}\tag{5.17}$$

one obtains from (5.13) the evolution equation for the dimensionless potential. Here the anomalous dimension η arises from the t -derivative acting on Z_k and is given by eq. (5.5). Using the notation $l_0^d(w; \eta, z=1) = l_0^d(w; \eta)$ for the threshold functions defined in section A (see also section 3.2) one obtains

$$\begin{aligned}\frac{\partial}{\partial t} u_k(\tilde{\rho}, \tilde{\tau}) &= -du_k(\tilde{\rho}, \tilde{\tau}) + (d-2+\eta)\tilde{\rho}u'_k(\tilde{\rho}, \tilde{\tau}) + (2d-4+2\eta)\tilde{\tau}\partial_{\tilde{\tau}}u_k(\tilde{\rho}, \tilde{\tau}) \\ &\quad + 4v_d l_0^d((m_1^+(\tilde{\rho}, \tilde{\tau}))^2; \eta) + 4v_d l_0^d((m_1^-(\tilde{\rho}, \tilde{\tau}))^2; \eta) + 2v_d l_0^d((m_2^+(\tilde{\rho}, \tilde{\tau}))^2; \eta) \\ &\quad + 2v_d l_0^d((m_2^-(\tilde{\rho}, \tilde{\tau}))^2; \eta) + 2v_d l_0^d((m_4^+(\tilde{\rho}, \tilde{\tau}))^2; \eta) + 2v_d l_0^d((m_4^-(\tilde{\rho}, \tilde{\tau}))^2; \eta)\end{aligned}\tag{5.18}$$

where the dimensionless mass terms are related to (5.11) according to

$$(m_i^\pm(\tilde{\rho}, \tilde{\tau}))^2 = \frac{(M_i^\pm(\rho(\tilde{\rho}), \tau(\tilde{\tau})))^2}{Z_k k^2}.\tag{5.19}$$

Eq. (5.18) is the scaling form of the flow equation we are looking for. For a $\tilde{\tau}$ -independent potential it reduces to the evolution equation for the $O(8)$ symmetric model [113, 120] given by eq. (3.8) with $z=1, \tilde{y}=0, \Delta\zeta_k=0$. The potential u_k at a second order phase transition is given by a k -independent (scaling) solution $\partial u_k/\partial t = 0$ [113, 120]. For this solution all the k -dependent functions in the rhs of eq. (5.18) become independent of k . For a weak first order phase transition these functions will show a weak k dependence for k larger than the inherent mass scale of the system (cf. section 5.4). There is no particular advantage of the scaling form of the flow equation for strong first order phase transitions.

Eq. (5.18) describes the scale dependence of the effective average potential u_k by a nonlinear partial differential equation for the three variables $t, \tilde{\rho}$ and $\tilde{\tau}$. We concentrate in the following on spontaneous symmetry breaking with a residual $U(2)$ symmetry group. As we have already

pointed out in section 5.2 this symmetry breaking can be observed for a configuration which is proportional to the identity and we have $\tilde{\tau} = 0$. In this case the eigenvalues (5.10) and (5.11) of the mass matrix with (5.19) are given by

$$\begin{aligned} (m_1^-)^2 &= (m_2^\pm)^2 = (m_3^-)^2 = u'_k, \\ (m_1^+)^2 &= (m_3^+)^2 = (m_4^-)^2 = u'_k + 4\tilde{\rho}\partial_{\tilde{\tau}}u_k, \\ (m_4^+)^2 &= u'_k + 2\tilde{\rho}u''_k \end{aligned} \quad (5.20)$$

and in the rhs of the partial differential equation (5.18) for $u_k(\tilde{\rho}) \equiv u_k(\tilde{\rho}, \tilde{\tau} = 0)$ only the functions $u'_k(\tilde{\rho})$, $u''_k(\tilde{\rho})$ and $\partial_{\tilde{\tau}}u_k(\tilde{\rho})$ appear. We determine these functions through the use of flow equations which are obtained by taking the derivative in eq. (5.18) with respect to $\tilde{\rho}$ and $\tilde{\tau}$ evaluated at $\tilde{\tau} = 0$. Since we are interested in the $\tilde{\rho}$ -dependence of the potential at $\tilde{\tau} = 0$ we shall use a truncated expansion in $\tilde{\tau}$ with

$$\partial_{\tilde{\tau}}^n u_k(\tilde{\rho}, \tilde{\tau} = 0) = 0 \quad \text{for } n \geq 2. \quad (5.21)$$

In three space dimensions the neglected ($\tilde{\rho}$ -dependent) operators have negative canonical mass dimension. We make no expansion in terms of $\tilde{\rho}$ since the general $\tilde{\rho}$ -dependence allows a description of a first order phase transition where a second local minimum of $u_k(\tilde{\rho})$ appears. The approximation (5.21) only affects the flow equations for $\partial_{\tilde{\tau}}u_k$. The form of the flow equation for u'_k is not affected by the truncation. From u'_k we obtain the effective average potential u_k by simple integration. We have tested the sensitivity of our results for u'_k to a change in $\partial_{\tilde{\tau}}u_k$ by neglecting the $\tilde{\rho}$ -dependence of the $\tilde{\tau}$ -derivative. We observed no qualitative change of the results. We expect that the main truncation error is due to the derivative expansion (5.2) for the effective average action.

To simplify notation we introduce

$$\begin{aligned} \epsilon(\tilde{\rho}) &= u'_k(\tilde{\rho}, \tilde{\tau} = 0), \\ \lambda_1(\tilde{\rho}) &= u''_k(\tilde{\rho}, \tilde{\tau} = 0), \\ \lambda_2(\tilde{\rho}) &= 4\partial_{\tilde{\tau}}u_k(\tilde{\rho}, \tilde{\tau} = 0). \end{aligned} \quad (5.22)$$

Higher derivatives are denoted by primes on the $\tilde{\rho}$ -dependent quartic ‘‘couplings’’, i.e. $\lambda'_1 = u'''_k$, $\lambda'_2 = \partial_{\tilde{\tau}}u'_k$ etc. It is convenient to introduce two-parameter functions $l_{n_1, n_2}^d(w_1, w_2; \eta)$ [167]. For $n_1 = n_2 = 1$ their relation to the functions $l_n^d(w; \eta)$ can be expressed as

$$\begin{aligned} l_{1,1}^d(w_1, w_2; \eta) &= \frac{1}{w_2 - w_1} [l_1^d(w_1; \eta) - l_1^d(w_2; \eta)] \quad \text{for } w_1 \neq w_2, \\ l_{1,1}^d(w, w; \eta) &= l_2^d(w; \eta) \end{aligned} \quad (5.23)$$

and

$$l_{n_1+1, n_2}^d(w_1, w_2; \eta) = -\frac{1}{n_1} \frac{\partial}{\partial w_1} l_{n_1, n_2}^d(w_1, w_2; \eta), \quad l_{n_1, n_2}^d(w_1, w_2; \eta) = l_{n_2, n_1}^d(w_2, w_1; \eta). \quad (5.24)$$

With the help of these functions the scale dependence of ϵ is described by

$$\begin{aligned} \frac{\partial \epsilon}{\partial t} &= (-2 + \eta)\epsilon + (d - 2 + \eta)\tilde{\rho}\lambda_1 - 6v_d(\lambda_1 + \lambda_2 + \tilde{\rho}\lambda'_2)l_1^d(\epsilon + \tilde{\rho}\lambda_2; \eta) \\ &\quad - 2v_d(3\lambda_1 + 2\tilde{\rho}\lambda'_1)l_1^d(\epsilon + 2\tilde{\rho}\lambda_1; \eta) - 8v_d\lambda_1 l_1^d(\epsilon; \eta) \end{aligned} \quad (5.25)$$

and for λ_1 one finds

$$\begin{aligned}
\frac{\partial \lambda_1}{\partial t} &= (d-4+2\eta)\lambda_1 + (d-2+\eta)\tilde{\rho}\lambda'_1 \\
&+ 6v_d [(\lambda_1 + \lambda_2 + \tilde{\rho}\lambda'_2)^2 l_2^d(\epsilon + \tilde{\rho}\lambda_2; \eta) - (\lambda'_1 + 2\lambda'_2 + \tilde{\rho}\lambda''_2) l_1^d(\epsilon + \tilde{\rho}\lambda_2; \eta)] \\
&+ 2v_d [(3\lambda_1 + 2\tilde{\rho}\lambda'_1)^2 l_2^d(\epsilon + 2\tilde{\rho}\lambda_1; \eta) - (5\lambda'_1 + 2\tilde{\rho}\lambda''_1) l_1^d(\epsilon + 2\tilde{\rho}\lambda_1; \eta)] \\
&+ 8v_d [(\lambda_1)^2 l_2^d(\epsilon; \eta) - \lambda'_1 l_1^d(\epsilon; \eta)].
\end{aligned} \tag{5.26}$$

Similarly the scale dependence of λ_2 is given by

$$\begin{aligned}
\frac{\partial \lambda_2}{\partial t} &= (d-4+2\eta)\lambda_2 + (d-2+\eta)\tilde{\rho}\lambda'_2 - 4v_d(\lambda_2)^2 l_{1,1}^d(\epsilon + \tilde{\rho}\lambda_2, \epsilon; \eta) \\
&+ 2v_d [3(\lambda_2)^2 + 12\lambda_1\lambda_2 + 8\tilde{\rho}\lambda'_2(\lambda_1 + \lambda_2) + 4\tilde{\rho}^2(\lambda'_2)^2] l_{1,1}^d(\epsilon + \tilde{\rho}\lambda_2, \epsilon + 2\tilde{\rho}\lambda_1; \eta) \\
&- 14v_d\lambda_2' l_1^d(\epsilon + \tilde{\rho}\lambda_2; \eta) - 2v_d(5\lambda'_2 + 2\tilde{\rho}\lambda''_2) l_1^d(\epsilon + 2\tilde{\rho}\lambda_1; \eta) \\
&+ 2v_d [(\lambda_2)^2 l_2^d(\epsilon; \eta) - 4\lambda'_2 l_1^d(\epsilon; \eta)].
\end{aligned} \tag{5.27}$$

For the numerical solution we evaluate the above flow equations at different points $\tilde{\rho}_i$ for $i = 1, \dots, l$ and use a set of matching conditions that are described in ref. [109]. If there is a minimum of the potential at nonvanishing $\kappa \equiv \tilde{\rho}_0$, the condition $\epsilon(\kappa) = 0$ can be used to obtain the scale dependence of $\kappa(k)$:

$$\begin{aligned}
\frac{d\kappa}{dt} &= -[\lambda_1(\kappa)]^{-1} \frac{\partial \epsilon}{\partial t} \Big|_{\tilde{\rho}=\kappa} \\
&= -(d-2+\eta)\kappa + 6v_d \left(1 + \frac{\lambda_2(\kappa) + \kappa\lambda'_2(\kappa)}{\lambda_1(\kappa)} \right) l_1^d(\kappa\lambda_2(\kappa); \eta) \\
&+ 2v_d \left(3 + \frac{2\kappa\lambda'_1(\kappa)}{\lambda_1(\kappa)} \right) l_1^d(2\kappa\lambda_1(\kappa); \eta) + 8v_d l_1^d(0; \eta).
\end{aligned} \tag{5.28}$$

To make contact with β -functions for the couplings at the potential minimum κ we point out the relation

$$\frac{d\lambda_{1,2}^{(m)}(\kappa)}{dt} = \frac{\partial \lambda_{1,2}^{(m)}}{\partial t} \Big|_{\tilde{\rho}=\kappa} + \lambda_{1,2}^{(m+1)}(\kappa) \frac{d\kappa}{dt}. \tag{5.29}$$

It remains to compute the anomalous dimension η defined in (5.5) which describes the scale dependence of the wave function renormalization Z_k . We consider a space dependent distortion of the constant background field configuration (5.9) of the form

$$\varphi_{ab}(x) = \varphi_a \delta_{ab} + [\delta\varphi e^{-iQx} + \delta\varphi^* e^{iQx}] \Sigma_{ab}. \tag{5.30}$$

Insertion of the above configuration into the parametrization (5.2) of Γ_k yields

$$Z_k = Z_k(\rho, \tau, Q^2 = 0) = \frac{1}{2} \frac{1}{\Sigma_{ab}^* \Sigma_{ab}} \lim_{Q^2 \rightarrow 0} \frac{\partial}{\partial Q^2} \frac{\delta \Gamma_k}{\delta(\delta\varphi \delta\varphi^*)} \Big|_{\delta\varphi=0}. \tag{5.31}$$

To obtain the flow equation of the wave function renormalization one expands the effective

average action around a configuration of the form (5.30) and evaluates the rhs of eq. (2.19). This computation has been done in ref. [167] for a ‘‘Goldstone’’ configuration with

$$\Sigma_{ab} = \delta_{a1}\delta_{b2} - \delta_{a2}\delta_{b1} \quad (5.32)$$

and $\varphi_a\delta_{ab} = \varphi\delta_{ab}$ corresponding to a symmetry breaking pattern with residual $U(2)$ symmetry. The result of ref. [167] can be easily generalized to arbitrary fixed field values of $\tilde{\rho}$ and we find

$$\eta(k) = 4\frac{v_d}{d}\tilde{\rho} [4(\lambda_1)^2 m_{2,2}^d(\epsilon, \epsilon + 2\tilde{\rho}\lambda_1; \eta) + (\lambda_2)^2 m_{2,2}^d(\epsilon, \epsilon + \tilde{\rho}\lambda_2; \eta)]. \quad (5.33)$$

The definition of the threshold function

$$m_{2,2}^d(w_1, w_2; \eta) = m_{2,2}^d(w_1, w_2) - \eta \hat{m}_{2,2}^d(w_1, w_2) \quad (5.34)$$

can be found in appendix A. For vanishing arguments the functions $m_{2,2}^d$ and $\hat{m}_{2,2}^d$ are of order unity. They are symmetric with respect to their arguments and in leading order $m_{2,2}^d(0, w) \sim \hat{m}_{2,2}^d(0, w) \sim w^{-2}$ for $w \gg 1$. According to eq. (5.4) we use $\tilde{\rho} = \kappa$ to define the uniform wave function renormalization

$$Z_k \equiv Z_k(\kappa). \quad (5.35)$$

We point out that according to our truncation of the effective average action with eq. (5.33) the anomalous dimension η is exactly zero at $\tilde{\rho} = 0$. This is an artefact of the truncation and we expect the symmetric phase to be more affected by truncation errors than the spontaneously broken phase. We typically observe small values for $\eta(k) = -d(\ln Z_k)/dt$ (of the order of a few per cent). The smallness of η is crucial for our approximation of a uniform wave function renormalization to give quantitatively reliable results for the equation of state. For the universal equation of state given in section 5.6 one has $\eta = 0.022$ as given by the corresponding index of the $O(8)$ symmetric ‘‘vector’’ model.

5.4 Renormalization group flow of couplings

To understand the detailed picture of the phase structure, which is presented in section 5.5, we will consider the flow of some characteristic quantities for the effective average potential as the infrared cutoff k is lowered. The short distance potential U_Λ given in eq. (5.6) is parametrized by quartic couplings,

$$\bar{\lambda}_{1\Lambda}, \bar{\lambda}_{2\Lambda} > 0 \quad (5.36)$$

and the location of its minimum is given by

$$\rho_{0\Lambda} = \bar{\mu}_\Lambda^2 / \bar{\lambda}_{1\Lambda}. \quad (5.37)$$

We integrate the flow equation for the effective average potential U_k for a variety of initial conditions $\rho_{0\Lambda}$, $\bar{\lambda}_{1\Lambda}$ and $\bar{\lambda}_{2\Lambda}$. In particular, for general $\bar{\lambda}_{1\Lambda}, \bar{\lambda}_{2\Lambda} > 0$ we are able to find a critical value $\rho_{0\Lambda} = \rho_{0c}$ for which the system exhibits a first order phase transition. In this case the evolution of U_k leads at some scale $k_2 < \Lambda$ to the appearance of a second local minimum at

the origin of the effective average potential and both minima become degenerate in the limit $k \rightarrow 0$. If $\rho_0(k) > 0$ denotes the k -dependent outer minimum of the potential ($U'_k(\rho_0) = 0$), where the prime on U_k denotes the derivative with respect to ρ at fixed k) at a first order phase transition one has

$$\lim_{k \rightarrow 0} (U_k(0) - U_k(\rho_0)) = 0. \quad (5.38)$$

A measure of the distance from the phase transition is the difference $\delta\kappa_\Lambda = (\rho_{0\Lambda} - \rho_{0c})/\Lambda$. If $\bar{\mu}_\Lambda^2$ and therefore $\rho_{0\Lambda}$ is interpreted as a function of temperature, the deviation $\delta\kappa_\Lambda$ is proportional to the deviation from the critical temperature T_c , i.e. $\delta\kappa_\Lambda = A(T)(T_c - T)$ with $A(T_c) > 0$.

We will always consider in this subsection the trajectories for the critical “temperature”, i.e. $\delta\kappa_\Lambda = 0$, and we follow the flow for different values of the short distance parameters $\lambda_{1\Lambda}$ and $\lambda_{2\Lambda}$. The discussion for sufficiently small $\delta\kappa_\Lambda$ is analogous. In particular, we compare the renormalization group flow of these quantities for a weak and a strong first order phase transition. In some limiting cases their behavior can be studied analytically. For the discussion we will frequently consider the flow equations for the quartic “couplings” $\lambda_1(\tilde{\rho})$, $\lambda_2(\tilde{\rho})$ eqs. (5.26), (5.27) and for the minimum κ eq. (5.28).

In fig. 17, 18 we follow the flow of the dimensionless renormalized minimum κ and the radial mass term $\tilde{m}^2 = 2\kappa\lambda_1(\kappa)$ in comparison to their dimensionful counterparts $\rho_{0R} = k\kappa$ and $m_R^2 = k^2\tilde{m}^2$ in units of the momentum scale Λ . We also consider the dimensionless renormalized mass term $\tilde{m}_2^2 = \kappa\lambda_2(\kappa)$ corresponding to the curvature of the potential in the direction of the second invariant $\tilde{\tau}$. The height of the potential barrier $U_B(k) = k^3 u_k(\tilde{\rho}_B)$ with $u'_k(\tilde{\rho}_B) = 0$, $0 < \tilde{\rho}_B < \kappa$, and the height of the outer minimum $U_0(k) = k^3 u_k(\kappa)$ is also displayed. Fig. 17 shows these quantities as a function of $t = \ln(k/\Lambda)$ for $\lambda_{1\Lambda} = 2$, $\lambda_{2\Lambda} = 0.1$. One observes that the flow can be separated into two parts. The first part ranging from $t = 0$ to $t \simeq -6$ is characterized by $\kappa \simeq \text{const}$ and small \tilde{m}_2^2 . It is instructive to consider what happens in the case $\tilde{m}_2^2 \equiv 0$. In this case $\lambda_2 \equiv 0$ and the flow is governed by the Wilson-Fisher fixed point of the $O(8)$ symmetric theory. At the corresponding second order phase transition the evolution of u_k leads to the scaling solution of (5.18) which is obtained for $\partial u_k / \partial t = 0$. As a consequence u_k becomes a k -independent function that takes on constant (fixed point) values. In particular, the minimum κ of the potential takes on its fixed point value $\kappa(k) = \kappa_*$. The fixed point is not attractive in the $U(2) \times U(2)$ symmetric theory and $\lambda_{2\Lambda}$ is an additional relevant parameter for the system. For small λ_2 the evolution is governed by an anomalous dimension $d\lambda_2/dt = A\lambda_2$ with $A < 0$, leading to the increasing \tilde{m}_2^2 as k is lowered.

The system exhibits scaling behavior only for sufficiently small λ_2 . As \tilde{m}_2^2 increases the quartic coupling λ_1 and therefore the radial mass term \tilde{m}^2 is driven to smaller values as can be observed from fig. 17. For nonvanishing λ_2 the corresponding qualitative change in the flow equation (5.26) for λ_1 is the occurrence of a term $\sim \lambda_2^2$. It allows to drive λ_1 to negative values in a certain range of $\tilde{\rho} < \kappa$ and, therefore, to create a potential barrier inducing a first order phase transition. We observe from the plot that at $t \lesssim -9.5$ a second minimum arises ($U_B \neq 0$). The corresponding value of $k = \Lambda e^t = k_2$ sets a characteristic scale for the first order phase transition. Below this scale the dimensionless, renormalized quantities approximately scale according to their canonical dimension. The dimensionful quantities like

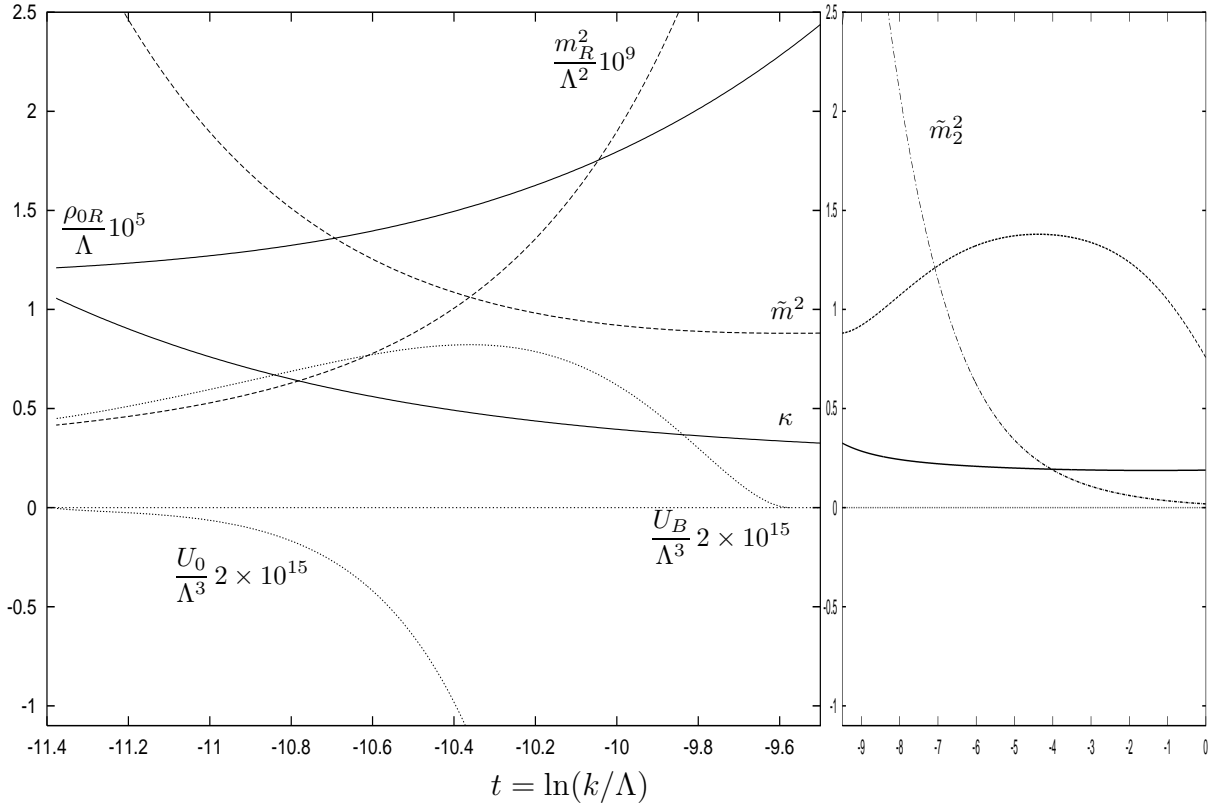


Figure 17: *Running couplings for a weak first order transition. We show the scale dependence of the dimensionless renormalized masses \tilde{m}^2 , \tilde{m}_2^2 , minimum κ and dimensionful counterparts $m_R^2 = k^2 \tilde{m}^2$, $\rho_{0R} = k\kappa$ in units of Λ . We also show $U_B(k)$ and $U_0(k)$, the value of the potential at the top of the potential barrier and at the minimum ρ_{0R} , respectively. The short distance parameters are $\lambda_{1\Lambda} = 2$, $\lambda_{2\Lambda} = 0.1$ and $\delta\kappa_\Lambda = 0$. The right panel shows the approximate scaling solution.*

ρ_{0R} or m_R^2 show only a weak scale dependence in this range. In contrast to the above example of a weak first order phase transition with characteristic renormalized masses much smaller than Λ , fig. 18 shows the flow of the corresponding quantities for a strong first order phase transition. The short distance parameters employed are $\lambda_{1\Lambda} = 0.1$, $\lambda_{2\Lambda} = 2$. Here the range with $\kappa \simeq \text{const}$ is absent and one observes no approximate scaling behavior.

In the discussion of the phase structure of the model in the next section we distinguish between the range $\lambda_{2\Lambda}/\lambda_{1\Lambda} \ll 1$ and $\lambda_{2\Lambda}/\lambda_{1\Lambda} \gg 1$ to denote the weak and the strong first order region. For $\lambda_{2\Lambda}/\lambda_{1\Lambda} \ll 1$ the initial renormalization group flow is dominated by the Wilson-Fisher fixed point of the $O(8)$ symmetric theory. In this range the irrelevant couplings are driven close to the fixed point for some “time” $|t| = -\ln(k/\Lambda)$, losing their memory on the initial conditions given by the short distance potential u_Λ . As a consequence we are able to observe universal behavior as is demonstrated in fig. 23.

To discuss the case $\lambda_{2\Lambda}/\lambda_{1\Lambda} \gg 1$ we consider the flow equations for the couplings at the minimum $\kappa \neq 0$ of the potential given by (5.28) and (5.29) with (5.26), (5.27). In the limit of an infinite mass term $\tilde{m}_2^2 = \kappa\lambda_2(\kappa) \rightarrow \infty$ the β -functions for $\lambda_1(\kappa)$ and κ become independent from $\lambda_2(\kappa)$ due to the threshold functions, with $l_n^3(\kappa\lambda_2) \sim (\kappa\lambda_2)^{-(n+1)}$ for large $\kappa\lambda_2(\kappa)$. As a

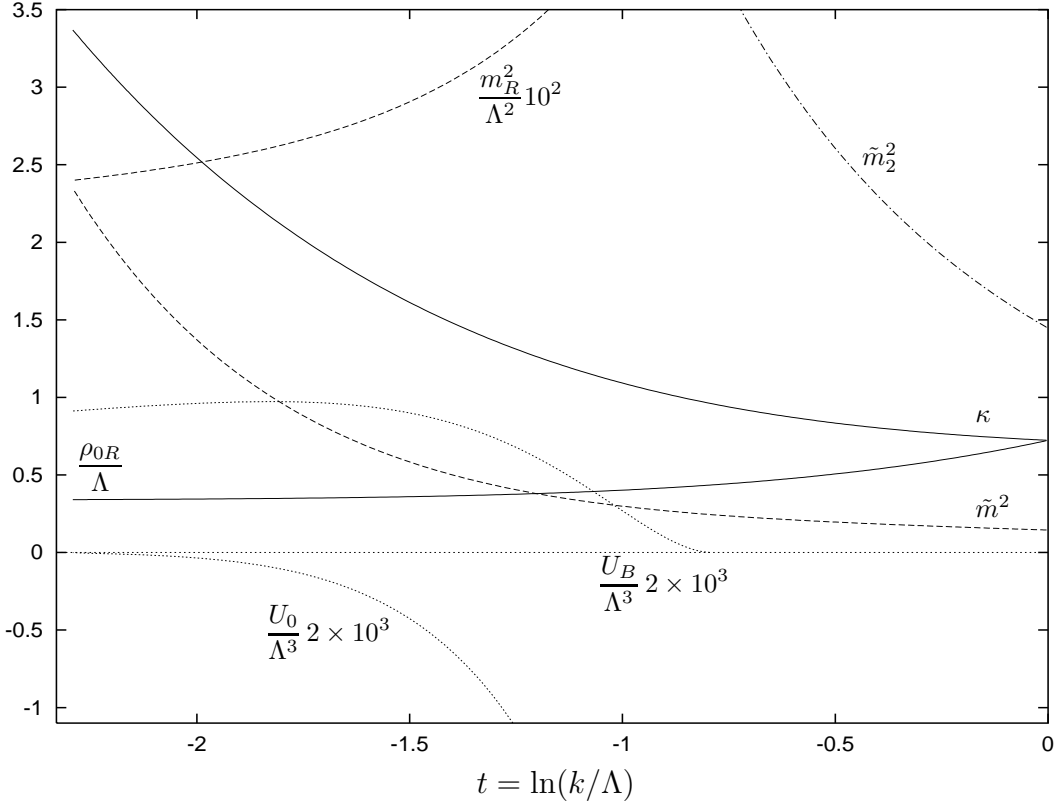


Figure 18: *Running couplings for a strong first order transition. We plot the same couplings as in fig. 17 for $\lambda_{1\Lambda} = 0.1$ and $\lambda_{2\Lambda} = 2$. No approximate scaling solution is reached.*

consequence β_{λ_1} and β_{κ} equal the β -functions for an $O(5)$ symmetric model. We argue in the following that in this large coupling limit fluctuations of massless Goldstone bosons lead to an attractive fixed point for $\lambda_2(\kappa)$. We take the flow equation (5.29), (5.27) for $\lambda_2(\kappa)$ keeping only terms with positive canonical mass dimension for a qualitative discussion. (This amounts to the approximation $\lambda_1^{(n)}(\kappa) = \lambda_2^{(n)}(\kappa) = 0$ for $n \geq 1$.) To be explicit, one may consider the case for given $\lambda_{1\Lambda} = 2$. The critical cutoff value for the potential minimum is $\kappa_{\Lambda} \simeq 0.2$ for $\lambda_{2\Lambda} \gg 1$. For $\kappa\lambda_2(\kappa) \gg 1$ and taking $\eta \simeq 0$ the β -function for $\lambda_2(\kappa)$ is to a good approximation given by ($d = 3$)

$$\frac{d\lambda_2(\kappa)}{dt} = -\lambda_2(\kappa) + 2v_3(\lambda_2(\kappa))^2 l_2^3(0). \quad (5.39)$$

The second term in the rhs of eq. (5.39) is due to massless Goldstone modes which give the dominant contribution in the considered range. The solution of (5.39) implies an attractive fixed point for $\lambda_2(\kappa)$ with a value

$$\lambda_{2*}(\kappa) = \frac{1}{2v_3 l_2^3(0)} \simeq 4\pi^2. \quad (5.40)$$

Starting from $\lambda_{2\Lambda}$ one finds for the “time” $|t|$ necessary to reach a given $\lambda_2(\kappa) > \lambda_{2*}(\kappa)$

$$|t| = -\ln \frac{\lambda_2(\kappa) - \lambda_{2*}(\kappa)}{\lambda_2(\kappa) \left(1 - \frac{\lambda_{2*}(\kappa)}{\lambda_{2\Lambda}}\right)}. \quad (5.41)$$

This converges to a finite value for $\lambda_{2\Lambda} \rightarrow \infty$. The further evolution therefore becomes insensitive to the initial value for $\lambda_{2\Lambda}$ in the large coupling limit. The flow of $\lambda_1(\kappa)$ and κ is not affected by the initial running of $\lambda_2(\kappa)$ and quantities like $\Delta\rho_{0R}/\Lambda$ or $m_R/\Delta\rho_{0R}$ become independent of $\lambda_{2\Lambda}$ if the coupling is sufficiently large. This qualitative discussion is confirmed by the numerical solution of the full set of equations presented in figs. 22 and 23 of section 5.5. For the fixed point value we obtain $\lambda_{2\star}(\kappa) = 38.02$. We point out that an analogous discussion for the large coupling region of $\lambda_{1\Lambda}$ cannot be made. This can be seen by considering the mass term at the origin of the short distance potential (5.6) given by $u'_\Lambda(0,0) = -\kappa_\Lambda\lambda_{1\Lambda}$. Due to the pole of $l_n^3(w,\eta)$ at $w = -1$ for $n > 1/2$ [37] one obtains the constraint

$$\kappa_\Lambda\lambda_{1\Lambda} < 1 \quad . \quad (5.42)$$

In the limit $\lambda_{1\Lambda} \rightarrow \infty$ the mass term $2\kappa_\Lambda\lambda_{1\Lambda}$ at the minimum κ of the potential at the critical temperature therefore remains finite.

5.5 Phase structure of the $U(2) \times U(2)$ model

We study the phase structure of the $U(2) \times U(2)$ symmetric model in three space dimensions. We concentrate here on the spontaneous symmetry breaking with a residual $U(2)$ symmetry group. We consider in the following the effective average potential U_k for a nonzero scale k . This allows to observe the nonconvex part of the potential. As an example we show in fig. 19 the effective average potential $U_{k=k_f}$ for $\lambda_{1\Lambda} = \bar{\lambda}_{1\Lambda}/\Lambda = 0.1$ and $\lambda_{2\Lambda} = \bar{\lambda}_{2\Lambda}/\Lambda = 2$ as a function of the renormalized field $\varphi_R = (\rho_R/2)^{1/2}$ with $\rho_R = Z_{k=k_f}\rho$. The scale k_f is some characteristic scale below which the location of the minimum $\rho_0(k)$ becomes essentially independent of k . Its precise definition is given below. We have normalized U_{k_f} and φ_R to powers of the renormalized minimum $\varphi_{0R}(k_f) = (\rho_{0R}(k_f)/2)^{1/2}$ with $\rho_{0R}(k_f) = Z_{k_f}\rho_0(k_f)$. The potential is shown for various values of deviations from the critical temperature or $\delta\kappa_\Lambda$. For the given examples $\delta\kappa_\Lambda = -0.03, -0.015$ the minimum at the origin becomes the absolute minimum and the system is in the symmetric (disordered) phase. Here φ_{0R} denotes the minimum in the metastable ordered phase. In contrast, for $\delta\kappa_\Lambda = 0.04, 0.1$ the absolute minimum is located at $\varphi_R/\varphi_{0R} = 1$ which characterizes the spontaneously broken phase. For large enough $\delta\kappa_\Lambda$ the local minimum at the origin vanishes. For $\delta\kappa_\Lambda = 0$ the two distinct minima are degenerate in height⁴⁶. As a consequence the order parameter makes a discontinuous jump at the phase transition which characterizes the transition to be first order. It is instructive to consider some characteristic values of the effective average potential. In fig. 20 we consider for $\lambda_{1\Lambda} = 0.1, \lambda_{2\Lambda} = 2$ the value of the renormalized minimum $\rho_{0R}(k_f)$ and the radial mass term as a function of $-\delta\kappa_\Lambda$ or temperature. In the spontaneously broken phase the renormalized radial mass squared is given by

$$m_R^2(k_f) = 2Z_{k_f}^{-1}\rho_0 U''_{k_f}(\rho_0), \quad (5.43)$$

⁴⁶We note that the critical temperature is determined by condition (5.38) in the limit $k \rightarrow 0$. Nevertheless for the employed nonvanishing scale $k = k_f$ the minima of U_k become almost degenerate at the critical temperature.

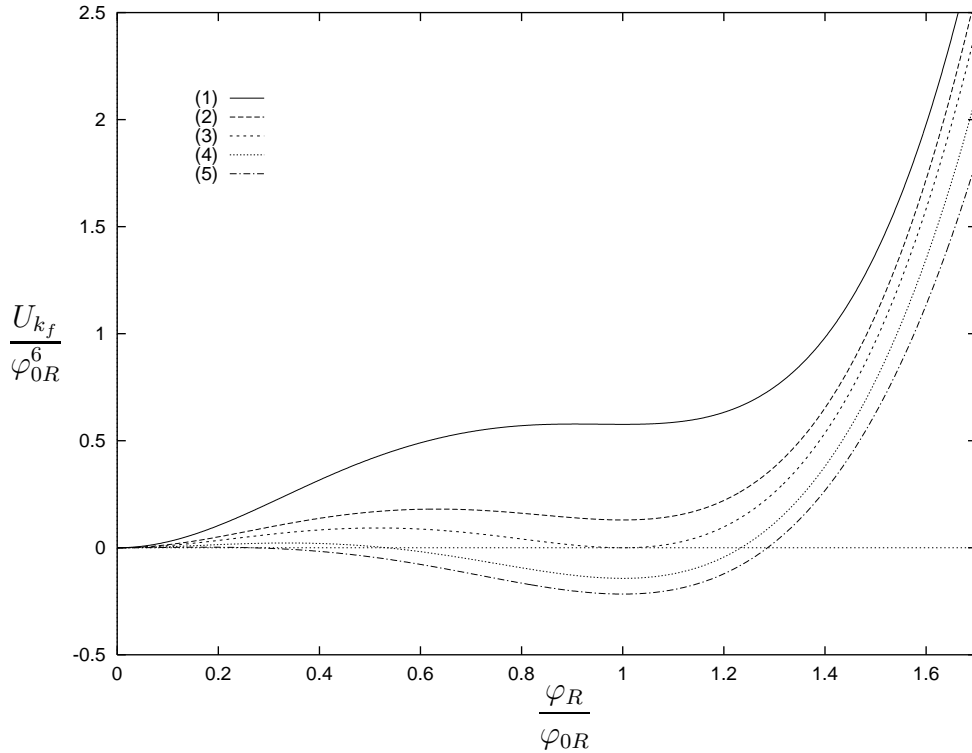


Figure 19: The effective average potential $U_{k=k_f}$ as a function of the renormalized field φ_R . The potential is shown for various values of $\delta\kappa_\Lambda \sim T_c - T$. The parameters for the short distance potential U_Λ are (1) $\delta\kappa_\Lambda = -0.03$, (2) $\delta\kappa_\Lambda = -0.015$, (3) $\delta\kappa_\Lambda = 0$, (4) $\delta\kappa_\Lambda = 0.04$, (5) $\delta\kappa_\Lambda = 0.1$ and $\lambda_{1\Lambda} = 0.1$, $\lambda_{2\Lambda} = 2$.

whereas in the symmetric phase the renormalized mass term reads

$$m_{0R}^2(k_f) = Z_{k_f}^{-1} U'_{k_f}(0). \quad (5.44)$$

At the critical temperature ($\delta\kappa_\Lambda = 0$) one observes the discontinuity $\Delta\rho_{0R} = \rho_{0R}(k_f)$ and the jump in the mass term $\Delta m_R = m_R(k_f) - m_{0R}(k_f) = m_R^c - m_{0R}^c$. (Here the index “c” denotes $\delta\kappa_\Lambda = 0$). The ratio $\Delta\rho_{0R}/\Lambda$ is a rough measure for the “strength” of the first order transition. For $\Delta\rho_{0R}/\Lambda \ll 1$ the phase transition is weak in the sense that typical masses are small compared to Λ . In consequence, the long-wavelength fluctuations play a dominant role and the system exhibits universal behavior, i.e. it becomes largely independent of the details at the short distance scale Λ^{-1} . We will discuss the universal behavior in more detail below.

In order to characterize the strength of the phase transition for arbitrary positive values of $\lambda_{1\Lambda}$ and $\lambda_{2\Lambda}$ we consider lines of constant $\Delta\rho_{0R}/\Lambda$ in the $\lambda_{1\Lambda}, \lambda_{2\Lambda}$ plane. In fig. 21 this is done for the logarithms of these quantities. For fixed $\lambda_{2\Lambda}$ one observes that the discontinuity at the phase transition weakens with increased $\lambda_{1\Lambda}$. On the other hand for given $\lambda_{1\Lambda}$ one finds a larger jump in the order parameter for increased $\lambda_{2\Lambda}$. This is true up to a saturation point where $\Delta\rho_{0R}/\Lambda$ becomes independent of $\lambda_{2\Lambda}$. In the plot this can be observed from the vertical part of the line of constant $\ln(\Delta\rho_{0R}/\Lambda)$. This phenomenon occurs for arbitrary nonvanishing $\Delta\rho_{0R}/\Lambda$ in the strong $\lambda_{2\Lambda}$ coupling limit as discussed in section 5.4.

In the following we give a detailed quantitative description of the first order phase

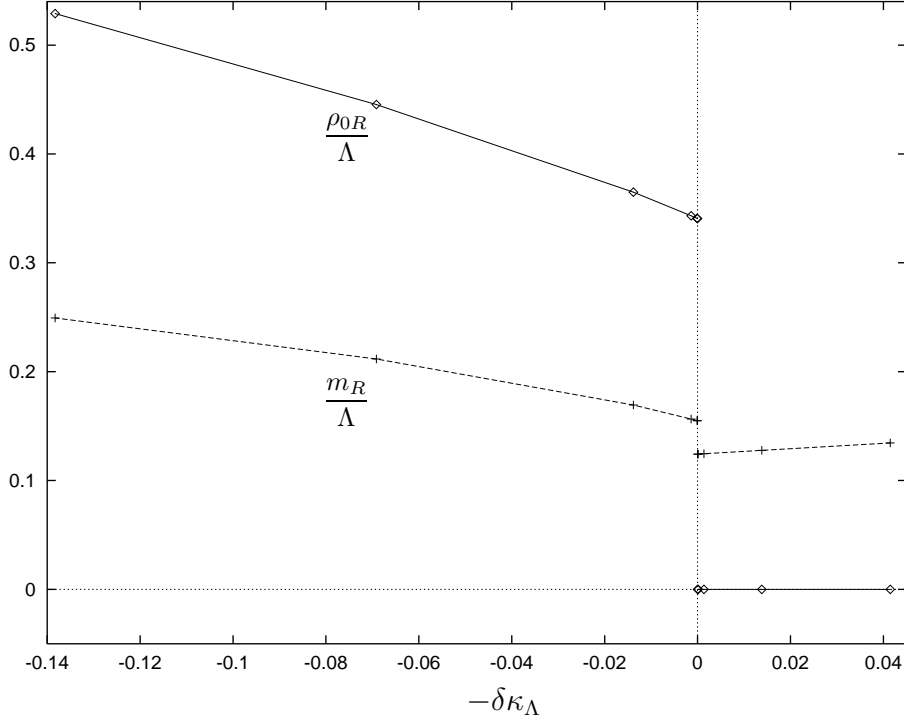


Figure 20: The minimum ρ_{0R} and the mass term m_R in units of the momentum scale Λ as a function of $-\delta\kappa_\Lambda$ or temperature ($\lambda_{1\Lambda} = 0.1$, $\lambda_{2\Lambda} = 2$, $k = k_f$). For $\delta\kappa_\Lambda = 0$ one observes the jump in the renormalized order parameter $\Delta\rho_{0R}$ and mass Δm_R .

transitions and a separation in weak and strong transitions. We consider some characteristic quantities for the effective average potential in dependence on the short distance parameters $\lambda_{1\Lambda}$ and $\lambda_{2\Lambda}$ for $\delta\kappa_\Lambda = 0$. We consider the discontinuity in the renormalized order parameter $\Delta\rho_{0R}$ and the inverse correlation lengths (mass terms) m_R^c and m_{0R}^c in the ordered and the disordered phase respectively. Fig. 22 shows the logarithm of $\Delta\rho_{0R}$ in units of Λ as a function of the logarithm of the initial coupling $\lambda_{2\Lambda}$. We have connected the calculated values obtained for various fixed $\lambda_{1\Lambda} = 0.1$, 2 and $\lambda_{1\Lambda} = 4$ by straight lines.

For $\lambda_{2\Lambda}/\lambda_{1\Lambda} \lesssim 1$ the curves show constant positive slope. In this range $\Delta\rho_{0R}$ follows a power law behavior

$$\Delta\rho_{0R} = R(\lambda_{2\Lambda})^\theta, \quad \theta = 1.93. \quad (5.45)$$

The critical exponent θ is obtained from the slope of the curve in fig. 22 for $\lambda_{2\Lambda}/\lambda_{1\Lambda} \ll 1$. The exponent is universal and, therefore, does not depend on the specific value for $\lambda_{1\Lambda}$. On the other hand, the amplitude R grows with decreasing $\lambda_{1\Lambda}$. For vanishing $\lambda_{2\Lambda}$ the order parameter changes continuously at the transition point and one observes a second order phase transition as expected for the $O(8)$ symmetric vector model. As $\lambda_{2\Lambda}/\lambda_{1\Lambda}$ becomes larger than one the curves deviate substantially from the linear behavior. The deviation depends on the specific choice of the short distance potential. For $\lambda_{2\Lambda}/\lambda_{1\Lambda} \gg 1$ the curves flatten. In this range $\Delta\rho_{0R}$ becomes insensitive to a variation of the quartic coupling $\lambda_{2\Lambda}$.

In addition to the jump in the order parameter we present the mass terms m_R^c and m_{0R}^c which we normalize to $\Delta\rho_{0R}$. In fig. 23 these ratios are plotted versus the logarithm of the

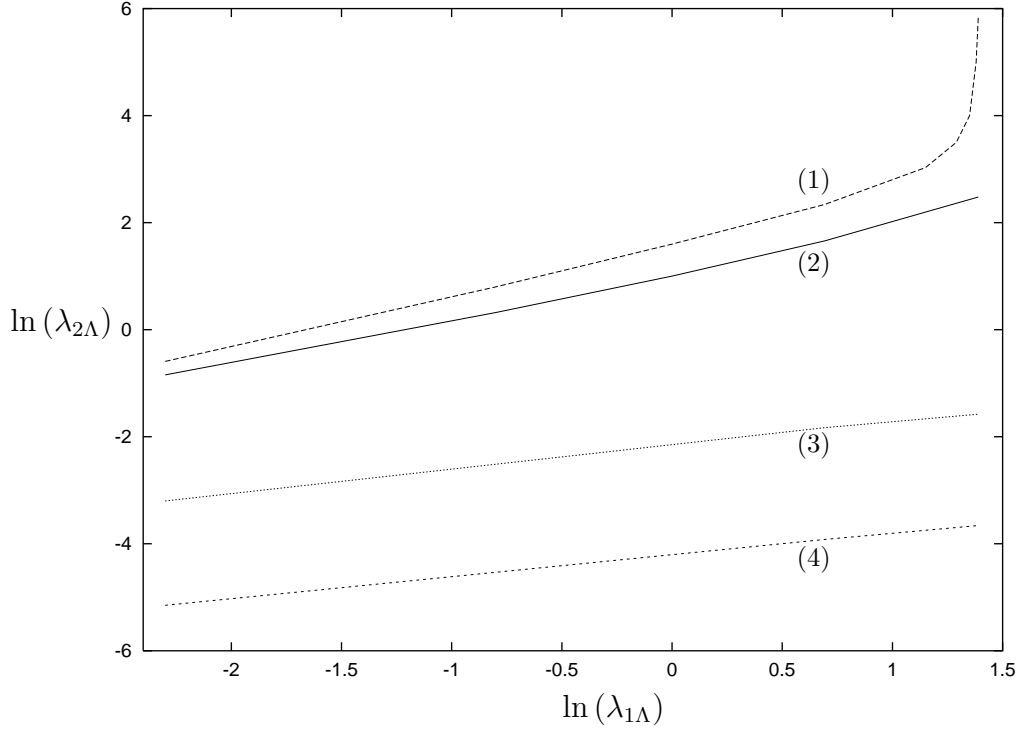


Figure 21: Lines of constant jump of the renormalized order parameter $\Delta\rho_{0R}/\Lambda$ at the phase transition in the $\ln(\lambda_{1\Lambda}), \ln(\lambda_{2\Lambda})$ plane. The curves correspond to (1) $\ln(\Delta\rho_{0R}/\Lambda) = -4.0$, (2) $\ln(\Delta\rho_{0R}/\Lambda) = -4.4$, (3) $\ln(\Delta\rho_{0R}/\Lambda) = -10.2$, (4) $\ln(\Delta\rho_{0R}/\Lambda) = -14.3$.

ratio of the initial quartic couplings $\lambda_{2\Lambda}/\lambda_{1\Lambda}$. Again values obtained for fixed $\lambda_{1\Lambda} = 0.1, 2$ and $\lambda_{1\Lambda} = 4$ are connected by straight lines. The universal range is set by the condition $m_R^c/\Delta\rho_{0R} \simeq \text{const}$ (equivalently for $m_{0R}^c/\Delta\rho_{0R}$). The universal ratios are $m_R^c/\Delta\rho_{0R} = 1.69$ and $m_{0R}^c/\Delta\rho_{0R} = 1.26$. For the given curves universality holds approximately for $\lambda_{2\Lambda}/\lambda_{1\Lambda} \lesssim 0.5$ and becomes “exact” in the limit $\lambda_{2\Lambda}/\lambda_{1\Lambda} \rightarrow 0$. In this range we obtain

$$m_R^c = S(\lambda_{2\Lambda})^\theta, \quad m_{0R}^c = \tilde{S}(\lambda_{2\Lambda})^\theta. \quad (5.46)$$

The universal features of the system are not restricted to the weak coupling region of $\lambda_{2\Lambda}$. This is demonstrated in fig. 23 for values up to $\lambda_{2\Lambda} \simeq 2$. The ratios $m_R^c/\Delta\rho_{0R}$ and $m_{0R}^c/\Delta\rho_{0R}$ deviate from the universal values as $\lambda_{2\Lambda}/\lambda_{1\Lambda}$ is increased. For fixed $\lambda_{2\Lambda}$ a larger $\lambda_{1\Lambda}$ results in a weaker transition concerning $\Delta\rho_{0R}/\Lambda$. The ratio $m_R^c/\Delta\rho_{0R}$ increases with $\lambda_{1\Lambda}$ for small fixed $\lambda_{2\Lambda}$ whereas in the asymptotic region, $\lambda_{2\Lambda}/\lambda_{1\Lambda} \gg 1$, one observes from fig. 23 that this tendency is reversed and $m_R^c/\Delta\rho_{0R}, m_{0R}^c/\Delta\rho_{0R}$ start to decrease at about $\lambda_{1\Lambda} \simeq 2$.

In summary, the above results show that though the short distance potential U_Λ indicates a second order phase transition, the transition becomes first order once fluctuations are taken into account. This fluctuation induced first order phase transition is known in four dimensions as the Coleman-Weinberg phenomenon [170]. The question of the order of the phase transition of the three dimensional $U(2) \times U(2)$ symmetric model has been addressed also using the ϵ -expansion [171, 24], in lattice studies [172] and in high-temperature expansion [173]. All studies are consistent with the first order nature of the transition and with the absence of

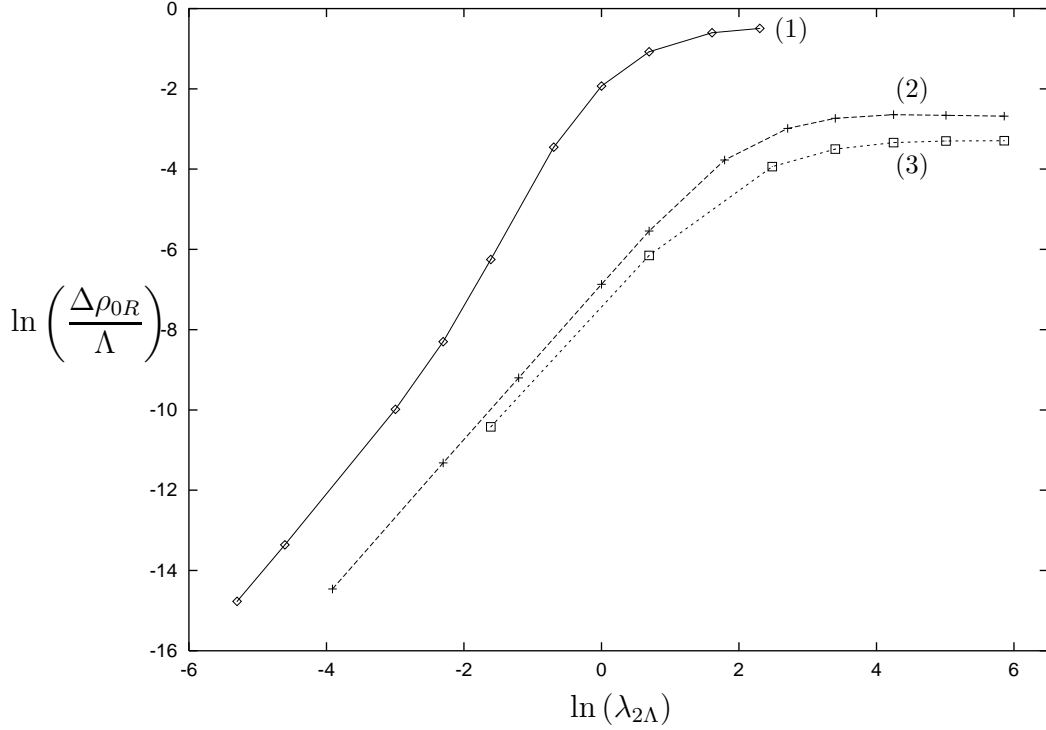


Figure 22: *Strength of the first order phase transition.* We plot the logarithm of the discontinuity of the renormalized order parameter $\Delta\rho_{0R}/\Lambda$ as a function of $\ln(\lambda_{2\Lambda})$. Data points for fixed (1) $\lambda_{1\Lambda} = 0.1$, (2) $\lambda_{1\Lambda} = 2$, (3) $\lambda_{1\Lambda} = 4$ are connected by straight lines. One observes a universal slope for small $\lambda_{2\Lambda}$ which is related to a critical exponent.

non-perturbative infrared stable fixed points. Our method gives here a clear and unambiguous answer and allows a detailed quantitative description of the phase transition. The universal form of the equation of state for weak first order phase transitions is presented in section 5.6.

In the following we specify the scale k_f for which we have given the effective average potential U_k . We observe that U_k depends strongly on the infrared cutoff k as long as k is larger than the scale k_2 where the second minimum of the potential appears. Below k_2 the two minima start to become almost degenerate for T near T_c and the running of $\rho_0(k)$ stops rather soon. The nonvanishing value of k_2 induces a physical infrared cutoff and represents a characteristic scale for the first order phase transition. We stop the integration of the flow equation for the effective average potential at a scale $k_f < k_2$ which is determined in terms of the curvature (mass term) at the top of the potential barrier that separates the two local minima of U_k at the origin and at $\rho_0(k)$. The top of the potential barrier at $\rho_B(k)$ is determined by

$$U'_k(\rho_B) = 0 \quad (5.47)$$

for $0 < \rho_B(k) < \rho_0(k)$ and for the renormalized mass term at $\rho_B(k)$ one obtains

$$m_{B,R}^2(k) = 2Z_k^{-1}\rho_B U''_k(\rho_B) < 0. \quad (5.48)$$

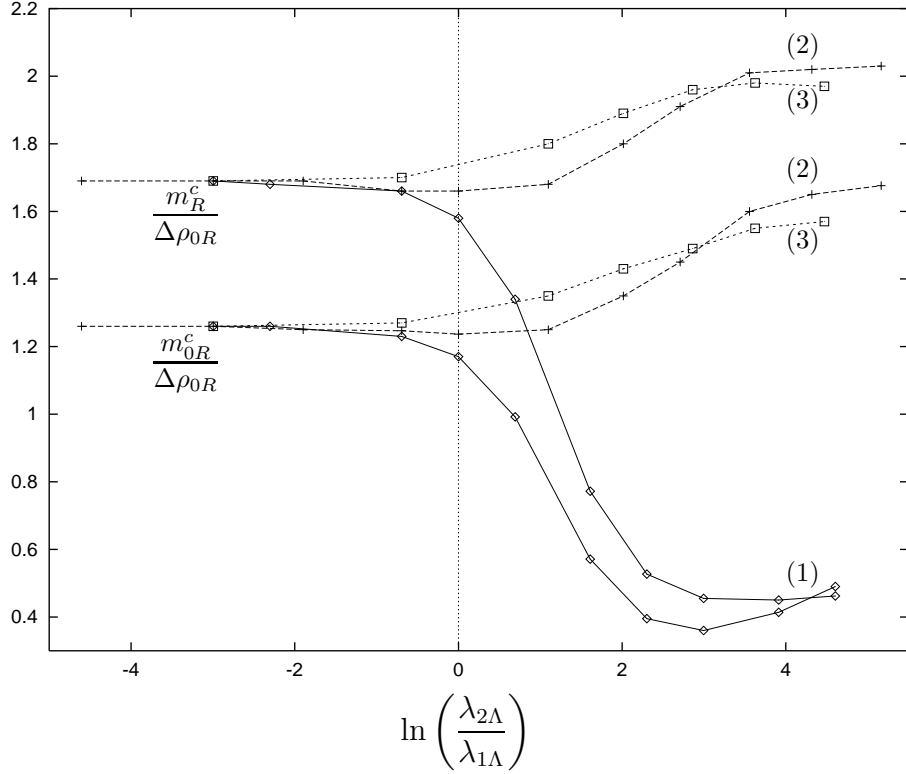


Figure 23: *The inverse correlation lengths m_R^c and m_{0R}^c in the ordered and the disordered phase respectively. They are normalized to $\Delta\rho_{0R}$ and given as a function of $\ln(\lambda_{2\Lambda}/\lambda_{1\Lambda})$. Data points for fixed (1) $\lambda_{1\Lambda} = 0.1$, (2) $\lambda_{1\Lambda} = 2$, (3) $\lambda_{1\Lambda} = 4$ are connected by straight lines. One observes universality for small ratios $\lambda_{2\Lambda}/\lambda_{1\Lambda}$.*

We fix our final value for the running by

$$\frac{k_f^2 - |m_{B,R}^2(k_f)|}{k_f^2} = 0.01 \quad (5.49)$$

For this choice the coarse-grained effective potential U_{k_f} essentially includes all fluctuations with momenta larger than the mass $|m_{B,R}|$ at the top of the potential barrier. It is a nonconvex function which is the appropriate quantity for the study of physical processes such as tunneling or inflation.

5.6 Universal equation of state for weak first order phase transitions

We presented in section 5.5 some characteristic quantities for the effective average potential which become universal at the phase transition for a sufficiently small quartic coupling $\lambda_{2\Lambda} = \bar{\lambda}_{2\Lambda}/\Lambda$ of the short distance potential U_Λ (5.6). The aim of this section is to generalize this observation and to find a universal scaling form of the equation of state for weak first order phase transitions. The equation of state relates the derivative of the free energy $U = \lim_{k \rightarrow 0} U_k$ to an external source, $\partial U/\partial\varphi = j$. Here the derivative has to be evaluated in the outer convex region of the potential. For instance, for the meson model of strong interactions the source j

is proportional to the average quark mass [24, 174] and the equation of state permits to study the quark mass dependence of properties of the chiral phase transition. We will compute the equation of state for a nonzero coarse graining scale k . It therefore contains information for quantities like the “classical” bubble surface tension in the context of Langer’s theory of bubble formation which will be discussed in section 6.

In three dimensions the $U(2) \times U(2)$ symmetric model exhibits a second order phase transition in the limit of a vanishing quartic coupling $\lambda_{2\Lambda}$ due to an enhanced $O(8)$ symmetry. In this case there is no scale present in the theory at the critical temperature. In the vicinity of the critical temperature (small $|\delta\kappa_\Lambda| \sim |T_c - T|$) and for small enough $\lambda_{2\Lambda}$ one therefore expects a scaling behavior of the effective average potential U_k and accordingly a universal scaling form of the equation of state. At the second order phase transition in the $O(8)$ symmetric model there are only two independent scales corresponding to the deviation from the critical temperature and to the external source or φ . As a consequence the properly rescaled potential U/ρ_R^3 or $U/\rho^{(\delta+1)/2}$ (with the usual critical exponent δ) can only depend on one dimensionless ratio. A possible set of variables to represent the two independent scales are the renormalized minimum of the potential $\varphi_{0R} = (\rho_{0R}/2)^{1/2}$ (or the renormalized mass for the symmetric phase) and the renormalized field $\varphi_R = (\rho_R/2)^{1/2}$. The rescaled potential will then only depend on the scaling variable $\tilde{s} = \varphi_R/\varphi_{0R}$ [36]. Another possible choice is the Widom scaling variable $x = -\delta\kappa_\Lambda/\varphi^{1/\beta}$ [128]. In the $U(2) \times U(2)$ symmetric theory $\lambda_{2\Lambda}$ is an additional relevant parameter which renders the phase transition first order and introduces a new scale, e.g. the nonvanishing value for the jump in the renormalized order parameter $\Delta\varphi_{0R} = (\Delta\rho_{0R}/2)^{1/2}$ at the critical temperature or $\delta\kappa_\Lambda = 0$. In the universal range we therefore observe three independent scales and the scaling form of the equation of state will depend on two dimensionless ratios.

The rescaled potential U/φ_{0R}^6 can then be written as a universal function G

$$\frac{U}{\varphi_{0R}^6} = G(\tilde{s}, \tilde{v}) \quad (5.50)$$

which depends on the two scaling variables

$$\tilde{s} = \frac{\varphi_R}{\varphi_{0R}}, \quad \tilde{v} = \frac{\Delta\varphi_{0R}}{\varphi_{0R}}. \quad (5.51)$$

The relation (5.50) is the scaling form of the equation of state we are looking for. At a second order phase transition the variable \tilde{v} vanishes and $G(\tilde{s}, 0)$ describes the scaling equation of state for the model with $O(8)$ symmetry [36]. The variable \tilde{v} accounts for the additional scale present at the first order phase transition. We note that $\tilde{s} = 1$ corresponds to a vanishing source and $G(1, \tilde{v})$ describes the temperature dependence of the free energy for $j = 0$. In this case $\tilde{v} = 1$ denotes the critical temperature T_c whereas for $T < T_c$ one has $\tilde{v} < 1$. Accordingly $\tilde{v} > 1$ is obtained for $T > T_c$ and φ_{0R} describes here the local minimum corresponding to the metastable ordered phase. The function $G(\tilde{s}, 1)$ accounts for the dependence of the free energy on j for $T = T_c$.

We consider the scaling form (5.50) of the equation of state for a nonzero coarse graining scale k with renormalized field given by $\varphi_R = Z_k^{1/2}\varphi$. As we have pointed out in section 5.5

there is a characteristic scale k_2 for the first order phase transition where the second local minimum of the effective average potential appears. For weak first order phase transitions one finds $\rho_{0R} \sim k_2$. To observe the scaling form of the equation of state the infrared cutoff k has to run below k_2 with $k \ll k_2$. For the scale k_f defined in eq. (5.49) we observe universal behavior to high accuracy (cf. fig. 23 for small $\lambda_{2\Lambda}/\lambda_{1\Lambda}$). The result for the universal function $U_{k_f}/\varphi_{0R}^6 = G_{k_f}(\tilde{s}, \tilde{v})$ is presented in fig. 24. For $\tilde{v} = 1$ one has $\varphi_{0R}(k_f) = \Delta\varphi_{0R}(k_f)$ which

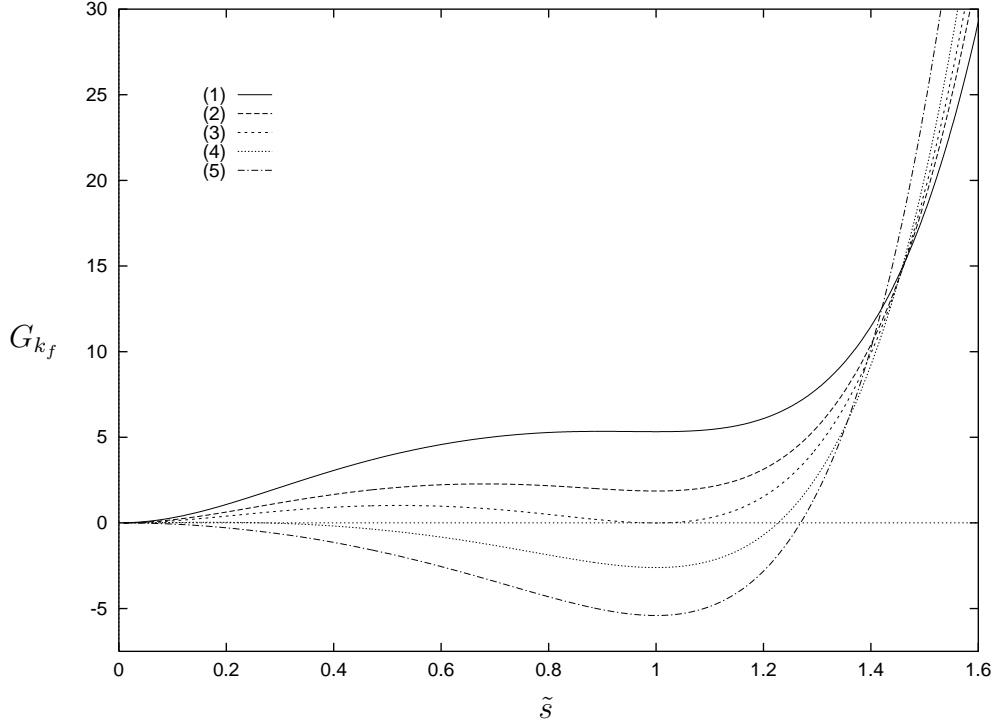


Figure 24: *Universal shape of the coarse-grained potential ($k = k_f$) as a function of the scaling variable $\tilde{s} = \varphi_R/\varphi_{0R} = (\rho_R/\rho_{0R})^{1/2}$ for different values of $\tilde{v} = \Delta\varphi_{0R}/\varphi_{0R} = (\Delta\rho_{0R}/\rho_{0R})^{1/2}$. The employed values for \tilde{v} are (1) $\tilde{v} = 1.18$, (2) $\tilde{v} = 1.07$, (3) $\tilde{v} = 1$, (4) $\tilde{v} = 0.90$, (5) $\tilde{v} = 0.74$. For vanishing sources one has $\tilde{s} = 1$. In this case $\tilde{v} = 1$ denotes the critical temperature T_c . Similarly $\tilde{v} > 1$ corresponds to $T > T_c$ with φ_{0R} denoting the minimum in the metastable ordered phase. The function G is symmetric for $\tilde{s} \rightarrow -\tilde{s}$ and one notes the qualitative difference with fig. 12.*

denotes the critical temperature. Accordingly $\tilde{v} > 1$ denotes temperatures above and $\tilde{v} < 1$ temperatures below the critical temperature. One observes that $G_{k_f}(\tilde{s}, 1)$ shows two almost degenerate minima. (They become exactly degenerate in the limit $k \rightarrow 0$). For the given examples $\tilde{v} = 1.18, 1.07$ the minimum at the origin becomes the absolute minimum and the system is in the symmetric phase. In contrast, for $\tilde{v} = 0.90, 0.74$ the absolute minimum is located at $\tilde{s} = 1$ which characterizes the spontaneously broken phase. For small enough \tilde{v} the local minimum at the origin vanishes.

We have explicitly verified that the universal function G_{k_f} depends only on the scaling variables \tilde{s} and \tilde{v} by choosing various values for $\delta\kappa_\Lambda$ and for the quartic couplings of the short distance potential, $\lambda_{1\Lambda}$ and $\lambda_{2\Lambda}$. We have seen in section 5.5 that the model shows universal behavior for a certain range of the parameter space. For given $\lambda_{1\Lambda}$ and small enough

$\lambda_{2\Lambda}$ one always observes universal behavior. For $\lambda_{1\Lambda} = 0.1, 2$ and 4 it is demonstrated that (approximate) universality holds for $\lambda_{2\Lambda}/\lambda_{1\Lambda} \lesssim 1/2$ (cf. fig. 23). For $\lambda_{1\Lambda}$ around 2 one observes from figs. 22, 23 that the system is to a good accuracy described by its universal properties for even larger values of $\lambda_{2\Lambda}$. The corresponding phase transitions cannot be considered as particularly weak first order. The universal function G_{k_f} therefore accounts for a quite large range of the parameter space.

We emphasize that the universal form of the effective potential given in fig. 24 depends on the scale k_f where the integration of the flow equations is stopped (cf. eq. (5.49)). A different prescription for k_f will, in general, lead to a different form of the effective potential in the “inner region”. We may interpret this as a scheme dependence describing the effect of different coarse graining procedures. This is fundamentally different from non-universal corrections since G_{k_f} is independent of details of the short distance or classical action and in this sense universal. Also the “outer region” for $\tilde{s} \geq 1$ is not affected by the approach to convexity and becomes independent of the choice of k_f . A more quantitative discussion of this scheme dependence will be presented in section 6. Since fluctuations on scales $k < k_f$ do not influence substantially the location of the minima of the coarse-grained potential and the form of $U_k(\varphi_R)$ for $\varphi_R > \varphi_{0R}$ one has $\partial U_{k_f}/\partial\varphi = j(k_f)$ with $j(k_f) \approx \lim_{k \rightarrow 0} j(k) = j$.⁴⁷

Let us consider the renormalized minimum φ_{0R} in two limits which are denoted by $\Delta\varphi_{0R} = \varphi_{0R}(\delta\kappa_\Lambda = 0)$ and $\varphi_{0R}^0 = \varphi_{0R}(\lambda_{2\Lambda} = 0)$. The behavior of $\Delta\varphi_{0R}$ is described in terms of the exponent θ according to eq. (5.45),

$$\Delta\varphi_{0R} \sim (\lambda_{2\Lambda})^{\theta/2}, \quad \theta = 1.93. \quad (5.52)$$

The dependence of the minimum φ_{0R}^0 of the $O(8)$ symmetric potential on the temperature is characterized by the critical exponent ν ,

$$\varphi_{0R}^0 \sim (\delta\kappa_\Lambda)^{\nu/2}, \quad \nu = 0.882. \quad (5.53)$$

The exponent ν for the $O(8)$ symmetric model is determined analogously to θ as described in section 22⁴⁸. We can also introduce a critical exponent ζ for the jump of the unrenormalized order parameter

$$\Delta\varphi_0 \sim (\lambda_{2\Lambda})^\zeta, \quad \zeta = 0.988. \quad (5.54)$$

With

$$\varphi_0^0 \sim (\delta\kappa_\Lambda)^\beta, \quad \beta = 0.451 \quad (5.55)$$

it is related to θ and ν by the additional index relation

$$\frac{\theta}{\zeta} = \frac{\nu}{\beta} = 1.95. \quad (5.56)$$

We have verified this numerically. For the case $\delta\kappa_\Lambda = \lambda_{2\Lambda} = 0$ one obtains

$$j \sim \varphi^\delta. \quad (5.57)$$

⁴⁷The role of massless Goldstone boson fluctuations for the universal form of the effective average potential in the limit $k \rightarrow 0$ has been discussed previously for the $O(8)$ symmetric model [36].

⁴⁸For the $O(8)$ symmetric model ($\lambda_{2\Lambda} = 0$) we consider the minimum φ_{0R}^0 at $k = 0$.

The exponent δ is related to the anomalous dimension η via the usual index relation $\delta = (5 - \eta)/(1 + \eta)$. From the scaling solution of eq. (5.33) we obtain $\eta = 0.0224$.

With the help of the above relations one immediately verifies that for $\lambda_{2\Lambda} = 0$

$$\tilde{s} \sim (-x)^{-\beta}, \quad \tilde{v} = 0 \quad (5.58)$$

and for $\delta\kappa_\Lambda = 0$

$$\tilde{s} \sim y^{-\zeta}, \quad \tilde{v} = 1. \quad (5.59)$$

Here we have used the Widom scaling variable x and the new scaling variable y given by

$$x = \frac{-\delta\kappa_\Lambda}{\varphi^{1/\beta}}, \quad y = \frac{\lambda_{2\Lambda}}{\varphi^{1/\zeta}}. \quad (5.60)$$

5.7 Summary

We have presented a detailed investigation of the phase transition in three dimensional models for complex 2×2 matrices. They are characterized by two quartic couplings $\bar{\lambda}_{1\Lambda}$ and $\bar{\lambda}_{2\Lambda}$. In the limit $\bar{\lambda}_{1\Lambda} \rightarrow \infty$, $\bar{\lambda}_{2\Lambda} \rightarrow \infty$ this also covers the model of unitary matrices. The picture arising from this study is unambiguous:

(1) One observes two symmetry breaking patterns for $\bar{\lambda}_{2\Lambda} > 0$ and $\bar{\lambda}_{2\Lambda} < 0$ respectively. The case $\bar{\lambda}_{2\Lambda} = 0$ denotes the boundary between the two phases with different symmetry breaking patterns. In this special case the theory exhibits an enhanced $O(8)$ symmetry. The phase transition is always first order for the investigated symmetry breaking $U(2) \times U(2) \rightarrow U(2)$ ($\bar{\lambda}_{2\Lambda} > 0$). For $\bar{\lambda}_{2\Lambda} = 0$ the $O(8)$ symmetric Heisenberg model is recovered and one finds a second order phase transition.

(2) The strength of the phase transition depends on the size of the classical quartic couplings $\bar{\lambda}_{1\Lambda}/\Lambda$ and $\bar{\lambda}_{2\Lambda}/\Lambda$. They describe the short distance or classical action at a momentum scale Λ . The strength of the transition can be parametrized by m_R^c/Λ with m_R^c a characteristic inverse correlation length at the critical temperature. For fixed $\bar{\lambda}_{2\Lambda}$ the strength of the transition decreases with increasing $\bar{\lambda}_{1\Lambda}$. This is analogous to the Coleman-Weinberg effect in four dimensions.

(3) For a wide range of classical couplings the critical behavior near the phase transition is universal. This means that it becomes largely independent of the details of the classical action once everything is expressed in terms of the relevant renormalized parameters. In particular, characteristic ratios like $m_R^c/\Delta\rho_{0R}$ (critical inverse correlation length in the ordered phase over discontinuity in the order parameter) or $m_{0R}^c/\Delta\rho_{0R}$ (same for the disordered phase) are not influenced by the addition of new terms in the classical action as far as the symmetries are respected.

(4) The range of short distance parameters $\bar{\lambda}_{1\Lambda}$, $\bar{\lambda}_{2\Lambda}$ for which the phase transition exhibits universal behavior is not only determined by the strength of the phase transition as measured by m_R^c/Λ . For a given $\bar{\lambda}_{1\Lambda}/\Lambda$ and small enough $\bar{\lambda}_{2\Lambda}/\Lambda$ one always observes universal behavior. In the range of small $\bar{\lambda}_{1\Lambda}/\Lambda$ the essential criterion for universal behavior is given by the size of $\bar{\lambda}_{2\Lambda}/\bar{\lambda}_{1\Lambda}$, with approximate universality for $\bar{\lambda}_{2\Lambda} < \bar{\lambda}_{1\Lambda}$. For strong couplings universality extends to larger $\bar{\lambda}_{2\Lambda}/\bar{\lambda}_{1\Lambda}$ and occurs for much larger m_R^c/Λ .

(5) We have investigated how various characteristic quantities like the discontinuity in the order parameter $\Delta\rho_0$ or the corresponding renormalized quantity $\Delta\rho_{0R}$ or critical correlation lengths depend on the classical parameters. In particular, at the critical temperature one finds universal critical exponents for not too large $\bar{\lambda}_{2\Lambda}$,

$$\begin{aligned}\Delta\rho_{0R} &\sim (\bar{\lambda}_{2\Lambda})^\theta, & \theta &= 1.93, \\ \Delta\rho_0 &\sim (\bar{\lambda}_{2\Lambda})^{2\zeta}, & \zeta &= 0.988.\end{aligned}\tag{5.61}$$

These exponents are related by a scaling relation to the critical correlation length and order parameter exponents ν and β of the $O(8)$ symmetric Heisenberg model according to $\theta/\zeta = \nu/\beta = 1.95$ ($\nu = 0.882$, $\beta = 0.451$ in our calculation for $\bar{\lambda}_{2\Lambda} = 0$). Small values of $\bar{\lambda}_{2\Lambda}$ can be associated with a perturbation of the $O(8)$ symmetric model and θ, ζ are related to the corresponding crossover exponents. On the other hand, $\Delta\rho_{0R}$ ($\Delta\rho_0$) becomes independent of $\bar{\lambda}_{2\Lambda}$ in the infinite coupling limit.

(6) We have computed the universal equation of state for the first order transition. It depends on two scaling variables, e.g. $\tilde{s} = (\rho_R/\rho_{0R})^{1/2}$ and $\tilde{v} = (\Delta\rho_{0R}/\rho_{0R})^{1/2}$. The equation of state relates the derivative of the free energy U to an external source, $\partial U/\partial\varphi = j$. From there one can extract universal ratios e.g. for the jump in the order parameter ($\Delta\rho_{0R}/m_R^c = 0.592$) or for the ratios of critical correlation lengths in the disordered (symmetric) and ordered (spontaneously broken) phase ($m_{0R}^c/m_R^c = 0.746$). It specifies critical couplings ($\lambda_{1R}/m_R^c = 0.845$, $\lambda_{2R}/m_R^c = 15.0$). The universal behavior of the potential for large field arguments $\rho \gg \rho_0$ is $U \sim \rho^{3/(1+\eta)}$ provided ρ_R is sufficiently small as compared to Λ . Here the critical exponent η which characterizes the dependence of the potential on the unrenormalized field ρ is found to be $\eta = 0.022$. For large ρ the universal equation of state equals the one for the $O(8)$ symmetric Heisenberg model and η specifies the anomalous dimension or the critical exponent $\delta = (5 - \eta)/(1 + \eta)$. In contrast to the Ising universality class (section 5.6) the first order universal equation of state cannot be reduced to the universal equation of state for the $O(8)$ model for general ρ .

Finally, we should mention that our approach can be extended to systems with reduced $SU(N) \times SU(N)$ symmetry. They obtain by adding to the classical potential a term involving the invariant $\xi = \det\varphi + \det\varphi^\dagger$. (Note that ξ is not invariant with respect to $U(N) \times U(N)$). This will give an even richer pattern of phase transitions and permits a close contact to realistic meson models in QCD where the axial anomaly is incorporated. Finally one can extend the three dimensional treatment to a four dimensional study of field theories at nonvanishing temperature. How this can be used to approach the chiral phase transition in QCD is presented in section 8.

6 Spontaneous nucleation and coarse graining ⁴⁹

6.1 Introduction

Let us consider a slow change with time of the “parameters” of the model that describes a physical system. This concerns, for example, the change in temperature in the early universe or a variation of the magnetic field in an experiment with ferromagnets. We assume that the time scale of the parameter change is much larger than the characteristic equilibration time t_{eq} of the system, so that the system can follow adiabatically in (approximate) local equilibrium. (For the example of the early universe the ratio of time scales involves the age of the universe H^{-1} , i.e. the characteristic small quantity is Ht_{eq} .) A second-order phase transition can proceed under these circumstances without major non-equilibrium effects. In this section we consider first-order phase transitions. Due to the discontinuity in the order parameter no continuous equilibrium evolution through the phase transition is possible. Near the phase transition the effective average potential U_k is characterized by two separate local minima. In the course of the evolution the minimum corresponding to the “true vacuum” (for late times) becomes lower than the one corresponding to the “false vacuum”. However, the system may not adapt immediately to the new equilibrium situation, and we encounter the familiar phenomena of supercooling or hysteresis. As vapor is cooled below the critical temperature, local droplets form and grow until the transition is completed. The inverse evolution proceeds by the formation of vapor bubbles in a liquid. The transition in ferromagnets is characterized by the formation of local Weiss domains with the magnetization corresponding to the late time equilibrium.

The formation of “bubbles” of the new vacuum is similar to a tunneling process and typically exponentially suppressed at the early stages of the transition. The reason is the “barrier” between the local minima. The transition requires at least the action of the saddle-point corresponding to the configuration with lowest action on the barrier. One therefore encounters a Boltzmann factor involving the action of this “critical bubble” that leads to exponential suppression.

A quantitative understanding of this important process is difficult both from the experimental and theoretical side. The theory deals mainly with pure systems, whereas in an experiment the exponentially suppressed rate of “spontaneous nucleation” has to compete with processes where impurities act as seeds for the formation of bubbles. As long as the exponential suppression is substantial, the theoretical treatment may separate the dynamics (which involves the growth of bubbles etc.) from the computation of the exponential suppression factor. The latter can be computed from equilibrium properties. Its quantitative determination is by itself a hard theoretical problem for which we propose a solution in this section. We also discuss carefully the range of applicability of this solution.

The problem of calculating nucleation rates during first-order phase transitions has a long history. (For reviews with an extensive list of references, see refs. [175, 176].) Our present understanding of the phenomenon of nucleation is based largely on the work of Langer [177].

⁴⁹This section is based on a collaboration with A. Strumia [39, 40].

His approach has been applied to relativistic field theory by Coleman [178] and Callan [179] and extended by Affleck [180] and Linde [181] to finite-temperature quantum field theory. The basic quantity in this approach is the nucleation rate I , which gives the probability per unit time and volume to nucleate a certain region of the stable phase (the true vacuum) within the metastable phase (the false vacuum). The calculation of I relies on a semiclassical approximation around a dominant saddle-point that is identified with the critical bubble. This is a static configuration (usually assumed to be spherically symmetric) within the metastable phase whose interior consists of the stable phase. It has a certain radius that can be determined from the parameters of the underlying theory. Bubbles slightly larger than the critical one expand rapidly, thus converting the metastable phase into the stable one.

The nucleation rate is exponentially suppressed by a suitable effective action of the critical bubble. Possible deformations of the critical bubble generate a static pre-exponential factor. The leading contribution to it has the form of a ratio of fluctuation determinants and corresponds to the first-order correction to the semiclassical result. Apart from the static prefactor, the nucleation rate includes a dynamical prefactor that takes into account the expansion of bubbles after their nucleation. In this review we concentrate only on the static aspects of the problem and neglect the dynamical prefactor. Its calculation requires the extension of our formalism to real time nonequilibrium dynamics.

For a four-dimensional theory of a real scalar field at temperature T , the nucleation rate is given by [177]–[181]

$$I = \frac{E_0}{2\pi} \left(\frac{\Gamma_b}{2\pi} \right)^{3/2} \left| \frac{\det'[\delta^2\Gamma/\delta\phi^2]_{\phi=\phi_b}}{\det[\delta^2\Gamma/\delta\phi^2]_{\phi=0}} \right|^{-1/2} \exp(-\Gamma_b). \quad (6.1)$$

Here Γ is the effective action (see sects. 1.2 and 2.1) of the system for a given configuration of the field ϕ that acts as the order parameter of the problem. The action of the critical bubble is $\Gamma_b = \Gamma[\phi_b(r)] - \Gamma[0]$, where $\phi_b(r)$ is the spherically-symmetric bubble configuration and $\phi = 0$ corresponds to the false vacuum. The fluctuation determinants are evaluated either at $\phi = 0$ or around $\phi = \phi_b(r)$. The prime in the fluctuation determinant around the bubble denotes that the three zero eigenvalues of the operator $[\delta^2\Gamma/\delta\phi^2]_{\phi=\phi_b}$ have been removed. Their contribution generates the factor $(\Gamma_b/2\pi)^{3/2}$ and the volume factor that is absorbed in the definition of I (nucleation rate per unit volume). The quantity E_0 is the square root of the absolute value of the unique negative eigenvalue.

In field theory, the rescaled free energy density of a system for homogeneous configurations is identified with the temperature-dependent effective potential. This is often evaluated through some perturbative scheme, such as the loop expansion [170]. In this way, the profile and the action of the bubble are determined through the potential. This approach, however, faces three fundamental difficulties:

- a) The effective potential, being the Legendre transform of the generating functional for the connected Green functions, is a convex function of the field. Consequently, it does not seem to be the appropriate quantity for the study of tunneling, as no structure with more than one minima separated by a barrier exists⁵⁰.

⁵⁰It has been argued in ref. [183] that the appropriate quantity for the study of tunneling is the generating

- b) The fluctuation determinants in the expression for the nucleation rate have a form completely analogous to the one-loop correction to the potential. The question of double-counting the effect of fluctuations (in the potential and the prefactor) must be properly addressed. This point is particularly important in the case of radiatively induced first-order phase transitions. These are triggered by the appearance of a new vacuum state in the theory as a result of the integration of (quantum or thermal) fluctuations [170]. A radiatively induced first-order phase transition takes place in theories for which the tree-level potential has only one minimum, while a second minimum appears at the level of radiative corrections⁵¹.
- (c) Another difficulty concerns the ultraviolet divergences that are inherent in the calculation of the fluctuation determinants in the prefactor. An appropriate regularization scheme must be employed in order to control them (for other approaches see refs. [185]–[188]). Moreover, this scheme must be consistent with the one employed for the absorption of the divergences appearing in the calculation of the potential that determines the action of the critical bubble.

In ref. [182] it was argued that all the above issues can be resolved through the implementation of the notion of coarse graining in the formalism, in agreement with Langer’s philosophy. The problem of computing the difference of the effective action between the critical bubble and the false vacuum may be divided into three steps: In the first step, one only includes fluctuations with momenta larger than a scale k which is of the order of the typical gradients of $\phi_b(r)$. For this step one can consider approximately constant fields ϕ and use a derivative expansion for the resulting coarse-grained free energy $\Gamma_k[\phi]$. The second step searches for the configuration $\phi_b(r)$ which is a saddle point of Γ_k . The quantity Γ_b in eq. (6.1 is identified with $\Gamma_k[\phi_b] - \Gamma_k[0]$. Finally, the remaining fluctuations with momenta smaller than k are evaluated in a saddle-point approximation around $\phi_b(r)$. This yields the ratio of fluctuation determinants with an ultraviolet cutoff k . Indeed, Langer’s approach corresponds to a one-loop approximation around the dominant saddle point for fluctuations with momenta smaller than a coarse-graining scale k . We solve here the problem of how to determine the coarse-grained free energy Γ_k in a consistent way. This is crucial for any quantitative treatment of the nucleation rate since Γ_k appears in an exponential.

functional of the 1PI Green functions (calculated perturbatively), which differs from the effective potential in the non-convex regions. However, as we discuss in the following, the consistent picture must rely on the notion of coarse graining and on the separation of the high-frequency fluctuations that may be responsible for the non-convexity of the potential, from the low-frequency ones that are relevant for tunneling. Such notions cannot be easily implemented in the context of perturbation theory.

⁵¹In ref. [184] an alternative procedure was suggested for the treatment of radiatively-induced first-order phase transitions: The fields whose fluctuations are responsible for the appearance of the new vacuum are integrated out first, so that an “effective” potential with two minima is generated for the remaining fields. Our philosophy is different: We integrate out high-frequency fluctuations of all fields, so that we obtain an effective low-energy action which we use for the calculation of the nucleation rate. Our procedure involves an explicit infrared cutoff in the calculation of the low-energy action. This prevents the appearance of non-localities arising from integrating out massless fields, which may be problematic for the approach of ref. [184]. For example, the fields that generate the new vacuum in radiatively-induced (fluctuation-driven) first-order phase transitions are usually massless or very light at the origin of the potential.

In the following subsections we review studies of nucleation based on the formalism of the effective average action Γ_k , which can be identified with the free energy, rescaled by the temperature, at a given coarse-graining scale k . In the simplest case, we consider a statistical system with one space-dependent degree of freedom described by a real scalar field $\phi(x)$. For example, $\phi(x)$ may correspond to the density for the gas/liquid transition, or to a difference in concentrations for chemical phase transitions, or to magnetization for the ferromagnetic transition. Our discussion also applies to a quantum field theory in thermal quasi-equilibrium. As we will see in sect. 7, an effective three-dimensional description applies for a thermal quantum field theory at scales k below the temperature T . We assume that Γ_{k_0} has been computed (for example perturbatively) for $k_0 = T$ [42, 44] and concentrate here on the three-dimensional (effective) theory.

We compute Γ_k by solving the flow equation between k_0 and k . For this purpose we approximate Γ_k by a standard kinetic term and a general potential U_k . This corresponds to the first level of the derivative expansion of eq. (2.14), where we set $Z_{\Phi,k}(\rho) = 1$ and neglect the higher derivative terms. Our approximation is expected to be a good one for the models we consider, because the deviations of $Z_{\Phi,k}(\rho)$ from 1 and the size of the higher-derivative terms are related to the anomalous dimension of the field, and this is small ($\eta \simeq 0.04$). The long-range collective fluctuations are not yet important at a short-distance scale⁵² $k_0^{-1} = T^{-1}$. For this reason, we assume here a polynomial potential

$$U_{k_0}(\phi) = \frac{1}{2}m_{k_0}^2\phi^2 + \frac{1}{6}\gamma_{k_0}\phi^3 + \frac{1}{8}\lambda_{k_0}\phi^4. \quad (6.2)$$

The parameters $m_{k_0}^2, \gamma_{k_0}$ and λ_{k_0} depend on T . This potential has the typical form relevant for first-order phase transitions in statistical systems with asymmetric potentials or in four-dimensional quantum field theories at high temperature [42, 44]. The two first-order critical lines are located at $\gamma_{k_0}^2 = 9\lambda_{k_0}m_{k_0}^2$ and $\gamma_{k_0} = 0$, with endpoints at $m_{k_0}^2 = -2\mu_{\text{cr}}^2$, $\gamma_{k_0}^2 = -18\lambda_{k_0}\mu_{\text{cr}}^2$ and $m_{k_0}^2 = \mu_{\text{cr}}^2$, $\gamma_{k_0} = 0$ respectively. Here μ_{cr}^2 is the critical mass term of the Ising model ($\mu_{\text{cr}}^2/k_0^2 \approx -0.0115$ for $\lambda_{k_0}/k_0 = 0.1$). We point out that, for fixed $m_{k_0}^2$ and λ_{k_0} , opposite values of γ_{k_0} result in potentials related through $\phi \leftrightarrow -\phi$. Also a model with $m_{k_0}^2 < 0$ can be mapped onto the equivalent model with $m_{k_0}^2 > 0$ by the shift $\phi \rightarrow \phi + c$, $\lambda_{k_0}c^2 + \gamma_{k_0}c = -2m_{k_0}^2$, where $m_{k_0}^2 = -2m_{k_0}^2 - \frac{1}{2}\gamma_{k_0}c$, $\gamma'_{k_0} = \gamma_{k_0} + 3\lambda_{k_0}c$.

As we have seen in section 4.6 a different shift $\phi \rightarrow \phi + \tilde{c}$ can eliminate the cubic term in favor of a term linear in ϕ . Therefore, the potential (6.2) also describes statistical systems of the Ising universality class in the presence of an external magnetic field. For a Hamiltonian

$$H = \int d^3x \left\{ \frac{\hat{\lambda}}{8} (\chi^2 - 1)^2 - B\chi + \frac{\zeta}{2} \partial_i \chi \partial^i \chi \right\}, \quad (6.3)$$

the parameters are $m_{k_0}^2 = \hat{\lambda}(3y^2 - 1)/2\zeta$, $\gamma_{k_0} = 3\hat{\lambda}T^{1/2}y/\zeta^{3/2}$, $\lambda_{k_0} = \hat{\lambda}T/\zeta^2$, with y given by $y(y^2 - 1) = 2B/\hat{\lambda}$. For real magnets k_0 must be taken somewhat below the inverse lattice distance, so that effective rotation and translation symmetries apply. Correspondingly, χ

⁵²In a three dimensional picture k_0 plays the role of the microscopic scale Λ .

and H are the effective normalized spin field and the effective Hamiltonian at this scale. We emphasize that our choice of potential encompasses a large class of field-theoretical and statistical systems. The universal critical behavior of these systems has been discussed extensively in section 4. In a different context, our results can also be applied to the problem of quantum tunneling in a (2+1)-dimensional theory at zero temperature. In this case k_0, m^2, γ and λ bear no relation to temperature.

We compute the form of the potential U_k at scales $k \leq k_0$ by integrating the evolution equation (2.37) with $Z_k(\rho, q^2) = \tilde{Z}_k(\rho, q^2) = 1$ in eqs. (2.38). The form of U_k changes as the effect of fluctuations with momenta above the decreasing scale k is incorporated in the effective couplings of the theory. We consider an arbitrary form of U_k which, in general, is not convex for non-zero k . U_k approaches the convex effective potential only in the limit $k \rightarrow 0$. In the region relevant for a first-order phase transition, U_k has two distinct local minima, where one is lower than the other away from the phase transition at $\gamma_{k_0} = 0$ or $|\gamma_{k_0}| = 3\sqrt{|\lambda_{k_0} m_{k_0}^2|}$. The nucleation rate should be computed for k larger than or around the scale k_f at which U_k starts receiving important contributions from field configurations that interpolate between the two minima. This happens when the negative curvature at the top of the barrier becomes approximately equal to $-k^2$ [79, 80] (see subsect. 3.6). Another consistency check for the above choice of k is the typical length scale of a thick-wall critical bubble which is $\gtrsim 1/k$ for $k > k_f$. The use of U_k at a non-zero value of k resolves the first fundamental difficulty in the calculation of bubble-nucleation rates that we mentioned earlier.

The other two difficulties are overcome as well. In our approach the pre-exponential factor in eq. (6.1) is well-defined and finite, as an ultraviolet cutoff of order k must be implemented in the calculation of the fluctuation determinants. The cutoff must guarantee that fluctuations with characteristic momenta $q^2 \gtrsim k^2$ do not contribute to the determinants. This is natural, as all fluctuations with typical momenta above k are already incorporated in the form of U_k . The choice of the ultraviolet cutoff must be consistent with the infrared cutoff procedure that determines Γ_k and, therefore, U_k . In the following subsection we show how this is achieved. It is clear that our approach resolves then automatically the problem of double-counting the effect of the fluctuations.

As a test of the validity of the approach, the result for the rate I must be independent of the coarse-graining scale k , because the latter should be considered only as a technical device. In the following we show that this is indeed the case when the expansion around the saddle point is convergent and the calculation of the nucleation rate reliable. Moreover, the residual k dependence of the rate can be used as a measure of the contribution of the next order in the saddle-point expansion.

6.2 Calculation of the nucleation rate

In all our calculations of bubble-nucleation rates we employ a mass-like infrared cutoff k for the fluctuations that are incorporated in Γ_k . This corresponds to the choice $R_k = k^2$ for the cutoff function defined in eq. (2.6). The reason for our choice is that the evaluation of the fluctuation determinants is technically simplified for this type of cutoff. In three dimensions

and for our approximation of neglecting the effects of wave function renormalization, the threshold function $l_0^3(w)$, defined in eqs. (3.16), is⁵³ $l_0^3(w) = \pi\sqrt{1+w}$. The evolution equation (3.5) for the potential can now be written as

$$\frac{\partial}{\partial k^2} [U_k(\phi) - U_k(0)] = -\frac{1}{8\pi} \left[\sqrt{k^2 + U_k''(\phi)} - \sqrt{k^2 + U_k''(0)} \right]. \quad (6.4)$$

In this entire section primes denote derivatives with respect to ϕ , similar to sections 4.4-4.6. In order to avoid confusion with the notation of other previous sections, in which primes denote derivatives with respect to $\rho = \phi^2/2$, we display explicitly the argument of the function with respect to which we differentiate.

In order to implement the appropriate ultraviolet cutoff $\sim k$ in the fluctuation determinant, let us look at the first step of an iterative solution for U_k , discussed in subsection 3.4

$$U_k^{(1)}(\phi) - U_k^{(1)}(0) = U_{k_0}(\phi) - U_{k_0}(0) + \frac{1}{2} \ln \left[\frac{\det[-\partial^2 + k^2 + U_k''(\phi)] \det[-\partial^2 + k_0^2 + U_k''(0)]}{\det[-\partial^2 + k_0^2 + U_k''(\phi)] \det[-\partial^2 + k^2 + U_k''(0)]} \right]. \quad (6.5)$$

For $k \rightarrow 0$, this solution is a regularized one-loop approximation to the effective potential. Due to the ratio of determinants, only momentum modes with $k^2 < q^2 < k_0^2$ are effectively included in the momentum integrals. The form of the infrared cutoff in eq. (6.4) suggests that we should implement the ultraviolet cutoff for the fluctuation determinant in the nucleation rate (6.1) as

$$I \equiv A_k \exp(-S_k) \\ A_k = \frac{E_0}{2\pi} \left(\frac{S_k}{2\pi} \right)^{3/2} \left| \frac{\det' [-\partial^2 + U_k''(\phi_b(r))]}{\det [-\partial^2 + k^2 + U_k''(\phi_b(r))]} \frac{\det [-\partial^2 + k^2 + U_k''(0)]}{\det [-\partial^2 + U_k''(0)]} \right|^{-1/2}. \quad (6.6)$$

where we switch the notation to $S_k = \Gamma_k[\phi_b] - \Gamma_k[0]$ instead of Γ_b in order to make the k -dependence in the exponential suppression factor explicitly visible. A comparison between eqs. (6.5) and (6.6) shows that the explicitly k -dependent regulator terms drop out for the combination $S_k - \ln A_k$. Our computation of U_k also includes contributions beyond eq. (6.5). The residual k -dependence of the nucleation rate will serve as a test for the validity of our approximations.

The critical bubble configuration $\phi_b(r)$ is an SO(3)-invariant solution of the classical equations of motion which interpolates between the local maxima of the potential $-U_k(\phi)$. It satisfies the equation

$$\frac{d^2 \phi_b}{dr^2} + \frac{2}{r} \frac{d\phi_b}{dr} = U_k'(\phi_b), \quad (6.7)$$

with the boundary conditions $\phi_b \rightarrow 0$ for $r \rightarrow \infty$ and $d\phi_b/dr = 0$ for $r = 0$. The bubble action S_k is given by

$$S_k = 4\pi \int_0^\infty \left[\frac{1}{2} \left(\frac{d\phi_b(r)}{dr} \right)^2 + U_k(\phi_b(r)) - U_k(0) \right] r^2 dr \equiv S_k^t + S_k^v, \quad (6.8)$$

⁵³We have neglected an infinite w -independent contribution to the threshold function that affects only the absolute normalization of the potential. As we are interested only in relative values of the potential for various field expectation values, this contribution is irrelevant for our discussion.

where the kinetic and potential contributions, S_k^t and S_k^v respectively, satisfy $S_k^v/S_k^t = -1/3$.

The computation of the fluctuation determinants A_k is more complicated. The differential operators that appear in eq. (6.6) have the general form

$$\mathcal{W}_{\kappa\alpha} = -\partial^2 + m_\kappa^2 + \alpha W_k(r), \quad (6.9)$$

where $m_\kappa^2 \equiv U_k''(0) + \kappa k^2$ and $W_k(r) \equiv U_k''(\phi_b(r)) - U_k''(0)$, with $\kappa, \alpha = 0$ or 1 . It is convenient to express the eigenfunctions ψ in terms of spherical harmonics: $\psi(r, \theta, \varphi) = Y_{\ell m}(\theta, \varphi)u(r)/r$ [185, 186]. Here ℓ and m are the usual angular momentum quantum numbers. The Laplacian operator ∂^2 takes the form

$$-\partial^2 \rightarrow \frac{1}{r} \left[-\frac{d^2}{dr^2} + \frac{\ell(\ell+1)}{r^2} \right] r \equiv -\frac{1}{r} \nabla_\ell^2 r, \quad (6.10)$$

so that

$$\begin{aligned} \det \mathcal{W}_{\kappa\alpha} &= \prod_{\ell=0}^{\infty} (\det \mathcal{W}_{\ell\kappa\alpha})^{2\ell+1} \\ \mathcal{W}_{\ell\kappa\alpha} &= -\nabla_\ell^2 + m_\kappa^2 + \alpha W_k(r). \end{aligned} \quad (6.11)$$

We recall that $\det \mathcal{W}_{\ell\kappa\alpha}$ is defined as the product of all eigenvalues λ that lead to solutions of $\mathcal{W}_{\ell\kappa\alpha}u(r) = \lambda u(r)$, with the function $u(r)$ vanishing at $r = 0$ and $r \rightarrow \infty$. The computation of such complicated determinants is made possible by a powerful theorem [193, 185] that relates ratios of determinants to solutions of ordinary differential equations. In particular, we have

$$g_{\ell\kappa} \equiv \frac{\det \mathcal{W}_{\ell\kappa 1}}{\det \mathcal{W}_{\ell\kappa 0}} = \frac{\det[-\nabla_\ell^2 + m_\kappa^2 + 1 \cdot W_k(r)]}{\det[-\nabla_\ell^2 + m_\kappa^2 + 0 \cdot W_k(r)]} = \frac{y_{\ell\kappa 1}(r \rightarrow \infty)}{y_{\ell\kappa 0}(r \rightarrow \infty)}, \quad (6.12)$$

where $y_{\ell\kappa\alpha}(r)$ is the solution of the differential equation

$$\left[-\frac{d^2}{dr^2} + \frac{\ell(\ell+1)}{r^2} + m_\kappa^2 + \alpha W_k(r) \right] y_{\ell\kappa\alpha}(r) = 0, \quad (6.13)$$

with the behaviour $y_{\ell\kappa\alpha}(r) \propto r^{\ell+1}$ for $r \rightarrow 0$. Such equations can be easily solved numerically. Special care is required for the treatment of the negative eigenvalue of the operator \mathcal{W}_{001} and the zero eigenvalues of \mathcal{W}_{101} . The details are given in ref. [39].

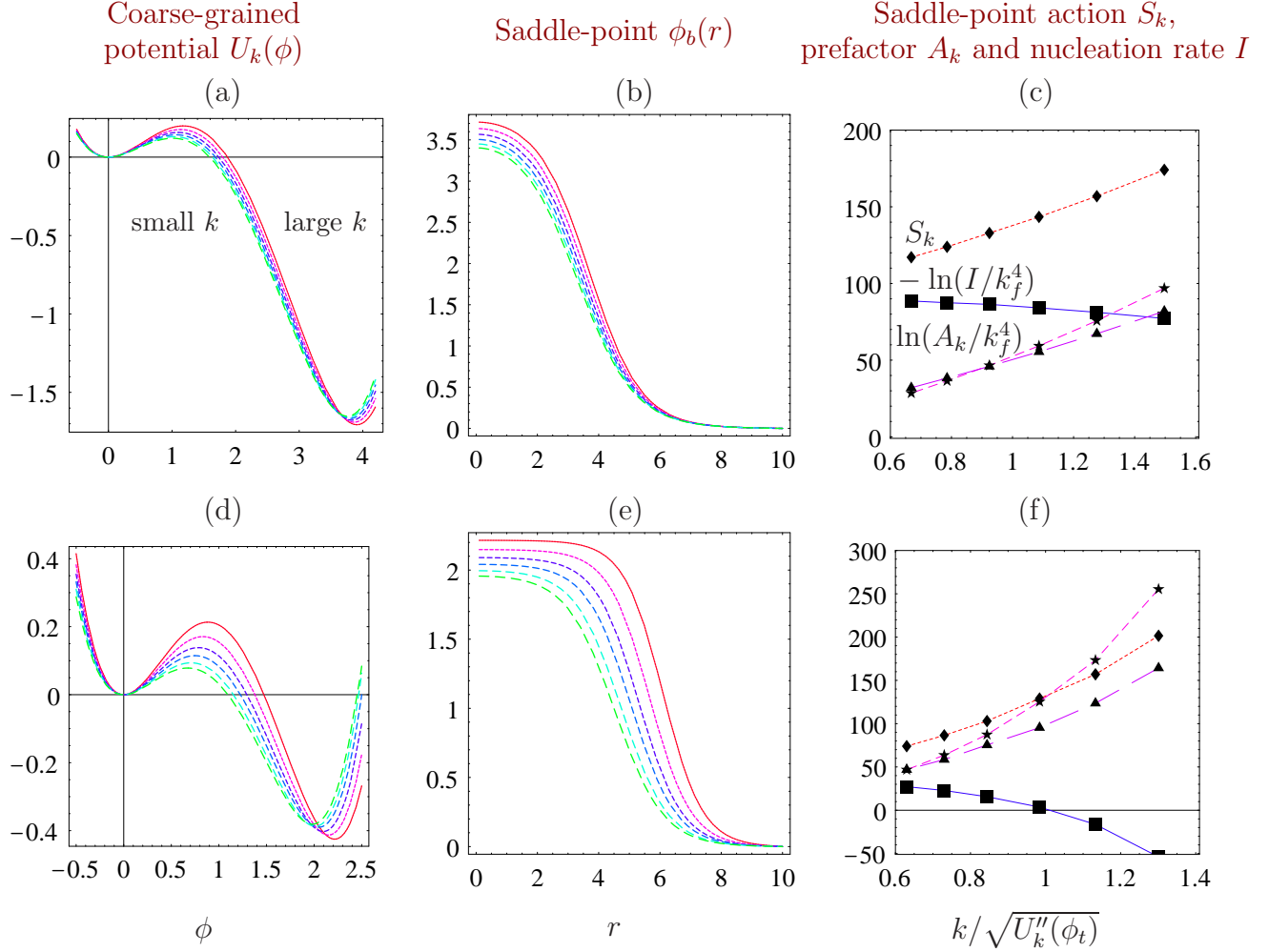


Figure 25: *Dependence of effective potential, critical bubble and nucleation rate on the coarse graining scale k . The parameters are $\lambda_{k_0} = 0.1 \cdot k_0$, $m_{k_0}^2 = -0.0433 \cdot k_0^2$, $\gamma_{k_0} = -0.0634 k_0^{3/2}$ (figs. a-c) and $m_{k_0}^2 = -0.013 \cdot k_0^2$, $\gamma_{k_0} = -1.61 \cdot 10^{-3} k_0^{3/2}$ (figs. d-f). All dimensional quantities are given in units of k_f , equal to $0.223 \cdot k_0$ in the first series and to $0.0421 \cdot k_0$ in the second series.*

Sample computations are presented in fig. 25. The potential U_k is determined through the numerical integration of eq. (6.4) between the scales k_0 and k , using algorithms from ref. [109]. The initial condition for the integration is given by eq. (6.2). Figs. 25a-25c correspond to a model with $m_{k_0}^2 = -0.0433 k_0^2$, $\gamma_{k_0} = -0.0634 k_0^{3/2}$, $\lambda_{k_0} = 0.1 k_0$. We first show in fig. 25a the evolution of the potential $U_k(\phi)$ as the scale k is lowered. (We always shift the metastable vacuum to $\phi = 0$.) The solid line corresponds to $k/k_0 = 0.513$ while the line with longest dashes (that has the smallest barrier height) corresponds to $k_f/k_0 = 0.223$. At the scale k_f the negative curvature at the top of the barrier is slightly larger than $-k_f^2$ and we stop the evolution. The potential and the field have been normalized with respect to k_f . As k is lowered from k_0 to k_f , the absolute minimum of the potential settles at a non-zero value of ϕ , while a significant barrier separates it from the metastable minimum at $\phi = 0$. The

profile of the critical bubble $\phi_b(r)$ is plotted in fig. 25b in units of k_f for the same sequence of scales. For $k \simeq k_f$ the characteristic length scale of the bubble profile and $1/k$ are comparable. This is expected, because the form of the profile is determined by the barrier of the potential, whose curvature is $\simeq -k^2$ at this point. This is an indication that we should not proceed to coarse-graining scales below k_f . We observe a significant variation of the value of the field ϕ in the interior of the bubble for different k .

Our results for the nucleation rate are presented in fig. 25c. The horizontal axis corresponds to $k/\sqrt{U_k''(\phi_t)}$, i.e. the ratio of the scale k to the square root of the positive curvature (equal to the mass of the field) at the absolute minimum of the potential located at ϕ_t . Typically, when k crosses below this mass, the massive fluctuations of the field start decoupling. The evolution of the convex parts of the potential slows down and eventually stops. The dark diamonds give the values of the action S_k of the critical bubble. We observe a strong k dependence of this quantity, which is expected from the behaviour in figs. 25a, 25b. The stars in fig. 25c indicate the values of $\ln(A_k/k_f^4)$. Again a substantial decrease with decreasing k is observed. This is expected, because k acts as the effective ultraviolet cutoff in the calculation of the fluctuation determinants in A_k . The dark squares give our results for $-\ln(I/k_f^4) = S_k - \ln(A_k/k_f^4)$. It is remarkable that the k dependence of this quantity almost disappears for $k/\sqrt{U_k''(\phi_t)} \lesssim 1$. The small residual dependence on k can be used to estimate the contribution of the next order in the expansion around the saddle point. It is reassuring that this contribution is expected to be smaller than $\ln(A_k/k_f^4)$.

This behaviour confirms our expectation that the nucleation rate should be independent of the scale k that we introduced as a calculational tool. It also demonstrates that all the configurations plotted in fig. 25b give equivalent descriptions of the system, at least for the lower values of k . This indicates that the critical bubble should not be associated only with the saddle point of the semiclassical approximation, whose action is scale dependent. It is the combination of the saddle point and its possible deformations in the thermal bath that has physical meaning.

For smaller values of $|m_{k_0}^2|$ the dependence of the nucleation rate on k becomes more pronounced. We demonstrate this in the second series of figs. 25d–25f where $\lambda_{k_0}/(-m_{k_0}^2)^{1/2} = 0.88$ (instead of 0.48 for figs. 25a–25c). The value of λ_{k_0} is the same as before, whereas $\gamma_{k_0} = -1.61 \cdot 10^{-3} k_0^{3/2}$ and $k_f/k_0 = 0.0421$. The strong k dependence is caused by the larger value of the dimensionless renormalized quartic coupling for the second parameter set [182]. Higher-loop contributions to A_k become important and the expansion around the saddle point does not converge any more. There are two clear indications of the breakdown of the expansion:

- a) The values of the leading and subleading contributions to the nucleation rate, S_k and $\ln(A_k/k_f^4)$ respectively, become comparable.
- b) The k dependence of $\ln(I/k_f^4)$ is strong and must be canceled by the higher-order contributions.

We point out that the discontinuity in the order parameter at the phase transition is approximately 5 times smaller in the second example than in the first one. As a result,

the second phase transition can be characterized as weaker. Typically, the breakdown of the saddle-point approximation is associated with weak first-order phase transitions.

It is apparent from figs. 25c and 25f that the leading contribution to the pre-exponential factor increases the total nucleation rate. This behaviour, related to the fluctuations of the field whose expectation value serves as the order parameter, is observed in multi-field models as well. The reason can be traced to the form of the differential operators in the prefactor of eq. (6.6). This prefactor involves the ratio $\det' [-\partial^2 + U_k''(\phi_b(r))] / \det [-\partial^2 + U_k''(0)]$ before regularization. The function $U_k''(\phi_b(r))$ always has a minimum away from $r = 0$ where it takes negative values (corresponding to the negative curvature at the top of the barrier), while $U_k''(0)$ is always positive. As a result the lowest eigenvalues of the operator $\det' [-\partial^2 + U_k''(\phi_b(r))]$ are smaller than those of $\det [-\partial^2 + U_k''(0)]$. The elimination of the very large eigenvalues through regularization does not affect this fact and the prefactor is always larger than 1. Moreover, for weak first-order phase transitions it becomes exponentially large because of the proliferation of low eigenvalues of the first operator. In physical terms, this implies the existence of a large class of field configurations of free energy comparable to that of the saddle-point. Despite the fact that they are not saddle points of the free energy (they are rather deformations of a saddle point) and are, therefore, unstable, they result in an important increase of the nucleation rate. This picture is very similar to that of “subcritical bubbles” of ref. [194].

In figs. 25c and 25f we also display the values of $\ln(A_k/k_f^4)$ (dark triangles) predicted by the approximate expression

$$\ln \frac{A_k}{k_f^4} \approx \frac{\pi k}{2} \left[- \int_0^\infty r^3 [U_k''(\phi_b(r)) - U_k''(0)] dr \right]^{1/2}. \quad (6.14)$$

This expression is based on the behaviour of the ratio of determinants (6.12) for large ℓ , for which an analytical treatment is possible [39, 40]. It is apparent from figs. 25c and 25f that eq. (6.14) gives a good approximation to the exact numerical results, especially near k_f . It can be used for quick checks of the validity of the expansion around the saddle point.

6.3 Region of validity of homogeneous nucleation theory

It is useful to obtain some intuition on the behaviour of the nucleation rate by using the approximate expression (6.14). We assume that the potential has a form similar to eq. (6.2) even near k_f , i.e.

$$U_{k_f}(\phi) \approx \frac{1}{2} m_{k_f}^2 \phi^2 + \frac{1}{6} \gamma_{k_f} \phi^3 + \frac{1}{8} \lambda_{k_f} \phi^4. \quad (6.15)$$

(Without loss of generality we take $m_{k_f}^2 > 0$.) For systems not very close to the endpoint of the first-order critical line, our assumption is supported by the numerical data, as can be verified from fig. 25. The scale k_f is determined by the relation

$$k_f^2 \approx \max \left| U_{k_f}''(\phi) \right| = \frac{\gamma_{k_f}^2}{6\lambda_{k_f}} - m_{k_f}^2. \quad (6.16)$$

Through the rescalings $r = \tilde{r}/m_{k_f}$, $\phi = 2\tilde{\phi} m_{k_f}^2 / \gamma_{k_f}$, the potential can be written as $\tilde{U}(\tilde{\phi}) = \tilde{\phi}^2/2 - \tilde{\phi}^3/3 + h\tilde{\phi}^4/18$, with $h = 9\lambda_{k_f} m_{k_f}^2 / \gamma_{k_f}^2$. For $h \approx 1$ the two minima of the

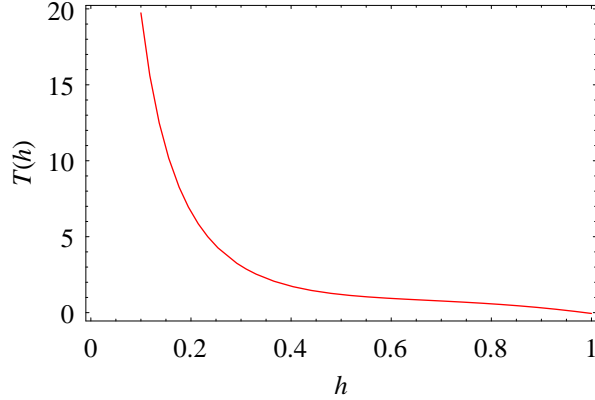


Figure 26: *The parameter $T(h)$, defined in eq. (6.19), as a function of h .*

potential have approximately equal depth. The action of the saddle point can be expressed as

$$S_{k_f} = \frac{4}{9} \frac{m_{k_f}}{\lambda_{k_f}} h \tilde{S}(h), \quad (6.17)$$

where $\tilde{S}(h)$ must be determined numerically through $\tilde{U}(\tilde{\phi})$. Similarly, the pre-exponential factor can be estimated through eq. (6.14) as

$$\begin{aligned} \ln \frac{A_{k_f}}{k_f^4} &\approx \frac{\pi}{2} \sqrt{\frac{3}{2h} - 1} \tilde{A}(h), \\ \tilde{A}^2(h) &= \int_0^\infty \left[\tilde{U}''(\tilde{\phi}_b(\tilde{r})) - 1 \right] \tilde{r}^3 d\tilde{r}, \end{aligned} \quad (6.18)$$

with $\tilde{A}(h)$ computed numerically. Finally, the relative importance of the fluctuation determinant is given by

$$R = \frac{\ln(A_{k_f}/k_f^4)}{S_{k_f}} \approx \frac{9\pi}{8} \frac{1}{h} \sqrt{\frac{3}{2h} - 1} \frac{\tilde{A}(h)}{\tilde{S}(h)} \frac{\lambda_{k_f}}{m_{k_f}} = T(h) \frac{\lambda_{k_f}}{m_{k_f}}. \quad (6.19)$$

The ratio R can be used as an indicator for the validity of the saddle point expansion, which is valid only for $R \lesssim 1$.

In fig. 26 we plot $T(h)$ as a function of h in the interval $(0, 1)$. It diverges for $h \rightarrow 0$. For $h \rightarrow 1$, our estimate of the prefactor predicts $T(h) \rightarrow 0$. The reason is that, for our approximate potential of eq. (6.15), the field masses at the two minima are equal in this limit. As a result, the integrand in eq. (6.14) vanishes, apart from the surface of the bubble. The small surface contribution is negligible for $h \rightarrow 1$, because the critical bubbles are very large in this limit. This behaviour is not expected to persist for more complicated potentials. Instead, we expect a constant value of $T(h)$ for $h \rightarrow 1$. However, we point out that the approximate expression (6.14) has not been tested for very large critical bubbles. The divergence of the saddle-point action in this limit results in low accuracy for our numerical analysis. Typically, our results are reliable for $\tilde{S}(h)$ less than a few thousand. Also, eq. (6.14) relies on a large- ℓ

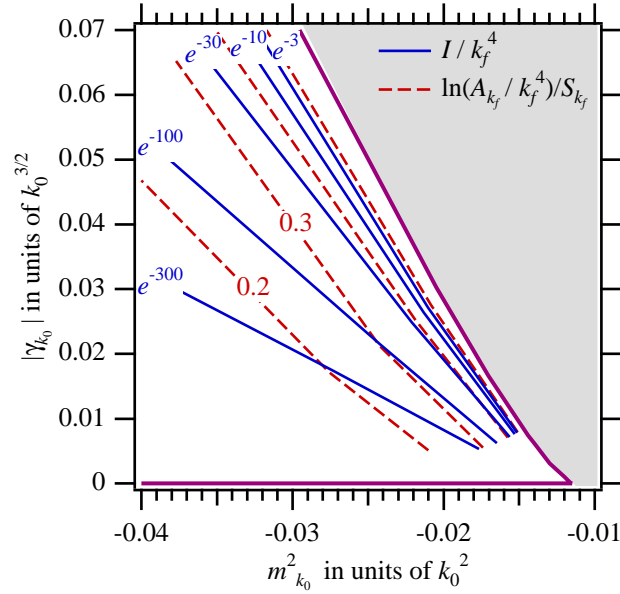


Figure 27: Contour plots of the nucleation rate I/k_f^4 and of $R = \ln(A_{k_f}/k_f^4)/S_{k_f}$ in the plane $(m_{k_0}^2, \gamma_{k_0})$, for $\lambda_{k_0}/k_0 = 0.1$. Regions to the right of the spinodal line (only one minimum) are shaded. The dashed lines correspond to $R = \{0.2, 0.3, 0.5, 1\}$ and the solid lines to I/k_f^4 .

approximation and is not guaranteed to be valid for large bubbles. We have checked that both our numerical and approximate results are reliable for $h \lesssim 0.9$.

The estimate of eq. (6.19) suggests two cases in which the expansion around the saddle point is expected to break down:

- a) For fixed λ_{k_f}/m_{k_f} , the ratio R becomes larger than 1 for $h \rightarrow 0$. In this limit the barrier becomes negligible and the system is close to the spinodal line.
- b) For fixed h , R can be large for sufficiently large λ_{k_f}/m_{k_f} . This is possible even for h close to 1, so that the system is far from the spinodal line. This case corresponds to weak first-order phase transitions, as can be verified by observing that the saddle-point action (6.17), the location of the true vacuum

$$\frac{\phi_t}{\sqrt{m_{k_f}}} = \frac{2}{3} \sqrt{h} \tilde{\phi}_t(h) \sqrt{\frac{m_{k_f}}{\lambda_{k_f}}}, \quad (6.20)$$

and the difference in free-energy density between the minima

$$\frac{\Delta U}{m_{k_f}^3} = \frac{4}{9} h \Delta \tilde{U}(h) \frac{m_{k_f}}{\lambda_{k_f}} \quad (6.21)$$

go to zero in the limit $m_{k_f}/\lambda_{k_f} \rightarrow 0$ for fixed h . This is in agreement with the discussion of fig. 25 in the previous subsection.

The breakdown of homogeneous nucleation theory in both the above cases is confirmed through the numerical computation of the nucleation rates [40]. In fig. 27 we show contour plots

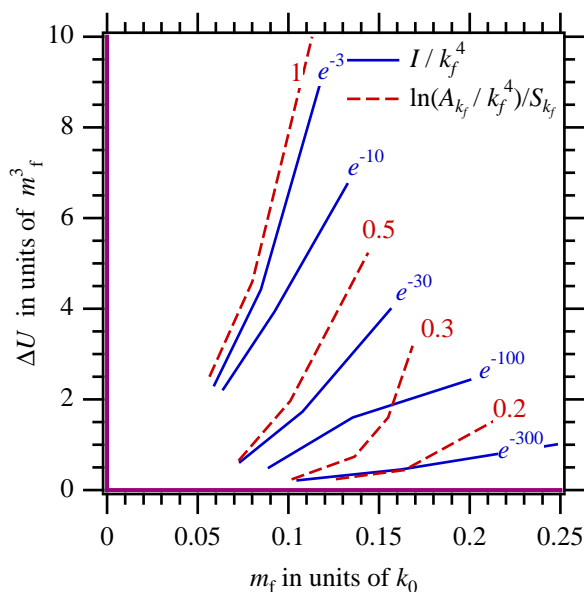


Figure 28: Nucleation rate as function of thermodynamic variables. We show the contour plots of fig. 27 in the plane $(m_f, \Delta U)$, where m_f^{-1} is the correlation length in the metastable phase and ΔU is the difference in free-energy density between the metastable and stable phase. The spinodal line corresponds to the vertical axis.

for I/k_f^4 and for $R = \ln(A_{k_f}/k_f^4)/S_{k_f}$ in the $(m_{k_0}^2, \gamma_{k_0})$ plane for fixed $\lambda_{k_0}/k_0 = 0.1$. One can see the decrease of the rate as the first-order critical line $\gamma_{k_0} = 0$ is approached. The spinodal line (end of the shaded region), on which the metastable minimum of U_k becomes unstable, is also shown. The nucleation rate becomes large before the spinodal line is reached. For $-\ln(I/k_f^4)$ of order 1, the exponential suppression of the nucleation rate disappears. Langer’s approach can no longer be applied and an alternative picture for the dynamical transition must be developed [195]. In the region between the contour $I/k_f^4 = e^{-3}$ and the spinodal line, one expects a smooth transition from nucleation to spinodal decomposition. The spinodal and critical lines meet at the endpoint in the lower right corner, which corresponds to a second order phase transition. The figure exhibits an increasing rate as the endpoint is approached at a fixed distance from the critical line.

The ratio R is a better measure of the validity of the semiclassical approximation. For $R \approx 1$ the fluctuation determinant is as important as the “classical” exponential factor e^{-S_k} . There is no reason to assume that higher loop contributions from the fluctuations around the critical bubble can be neglected anymore. Near the endpoint in the lower right corner, Langer’s semiclassical picture breaks down, despite the presence of a discontinuity in the order parameter. Requiring $I/k_f^4 \lesssim e^{-3}$, $R \lesssim 1$, gives a limit of validity for Langer’s theory. For a fixed value of the nucleation rate (solid lines in fig. 27), the ratio R grows as the endpoint in the lower right corner is approached. This indicates that Langer’s theory is not applicable for weak first-order phase transitions, even if the predicted rate is exponentially suppressed. The concept of nucleation of a region of the stable phase within the metastable phase may still be relevant. However, a quantitative estimate of the nucleation rate requires taking into account

fluctuations of the system that are not described properly by the semiclassical approximation [194].

The parameter region discussed here may be somewhat unusual since the critical line of the phase transition is approached by varying γ_{k_0} from negative or positive values towards zero. We have chosen it only for making the graph more transparent. However, the results of fig. 27 can be mapped by a shift $\phi \rightarrow \phi + c$ to another region with $m_{k_0}^2 > 0$, for which the first-order phase transition can be approached by varying $m_{k_0}^2$ at fixed γ_{k_0} . As opposite values of γ_{k_0} result in potentials related by $\phi \leftrightarrow -\phi$, we can always choose $\gamma_{k_0} < 0$. Then the phase transition proceeds from a metastable minimum at the origin to a stable minimum along the positive ϕ -axis (as in fig. 25a). Potentials with $m_{k_0}^2 > 0$, $\gamma_{k_0} < 0$ are relevant for cosmological phase transitions, such as the electroweak phase transition.

The microscopic parameters at the scale k_0 are often not known in statistical systems. In order to facilitate the interpretation of possible experiments where the nucleation rate would be measured together with the correlation length and the latent heat, we also give I as a function of renormalized parameters. In fig. 28 we depict the region of validity of homogeneous nucleation theory in terms of parameters of the low-energy theory at the scale k_f . The contours correspond to the same quantities as in fig. 27. They are now plotted as a function of the renormalized mass at the false vacuum $m_f = \sqrt{U_{k_f}''(0)}$ in units of k_0 and the difference in free-energy density between the two vacua in units of m_f^3 . Here m_f^{-1} corresponds to the correlation length in the false vacuum and $\Delta U/m_{k_f}^3$ can be related to observable quantities like the jump in the order parameter or the latent heat if λ_{k_0}/k_0 is kept fixed. Furthermore, for given λ_{k_f}/m_{k_f} , we can relate $\Delta U/m_{k_f}^3$ to h in the approximation of eq. (6.15) using eq. (6.21) and compute the observables from the explicit form of the free energy density (6.15). The spinodal line corresponds to the vertical axis, as for $m_f = 0$ the origin of the potential turns into a maximum. The critical line corresponds to the horizontal axis. The origin is the endpoint of the critical line. All the potentials we have studied have an approximate form similar to eq. (6.15) with $h \lesssim 0.9$. From our discussion in the previous subsection and fig. 26 we expect that R is approximately given by eq. (6.14) with $T(h) \gtrsim 0.3$ for $h \lesssim 0.9$. This indicates that $R \gtrsim 1$ for $m_f/k_0 \lesssim 0.05$ even far from the spinodal line. This expectation is confirmed by fig. 28. Even for theories with a significant exponential suppression for the estimated nucleation rate we expect $R \sim 1$ near $m_f/k_0 \approx 0.05$.

Finally, we point out that realistic statistical systems often have large dimensionless couplings $\lambda_{k_0}/k_0 \sim 10$. Our results indicate that Langer's homogeneous nucleation theory breaks down for such systems even for small correlation lengths in the metastable phase ($m_f/k_0 \sim 1$). For a large correlation length the universal behavior of the potential has been discussed in sect. 4.6. One obtains a large value $\lambda_{k_f}/m_f \approx 5$, independently of the short-distance couplings [38]. Therefore, a saddle-point approximation for the fluctuations around the critical bubble will not give accurate results in the universal region.

6.4 Radiatively induced first-order phase transitions

We now turn to a more complicated system, a theory of two scalar fields. It provides a framework within which we can test the reliability of our approach in the case of two fluctuating fields. The evolution equation for the potential resembles very closely the ones appearing in gauged Higgs theories, with the additional advantage that the approximations needed in the derivation of this equation are more transparent. We expect the qualitative conclusions for the region of validity of Langer's picture of homogeneous nucleation to be valid for gauged Higgs theories as well. The most interesting feature of the two-scalar models is the presence of radiatively induced first-order phase transitions. Such transitions usually take place when the mass of a certain field is generated through the expectation value of another. The fluctuations of the first field can induce the appearance of new minima in the potential of the second, resulting in first-order phase transitions [170]. As we have already discussed, the problem of double-counting the effect of fluctuations is particularly acute in such situations. The introduction of a coarse-graining scale k resolves this problem, by separating the high-frequency fluctuations of the system which may be responsible for the presence of the second minimum through the Coleman-Weinberg mechanism, from the low-frequency ones which are relevant for tunneling.

Similarly to the one-field case, we approximate the effective average action as

$$\Gamma_k = \int d^3x \left\{ \frac{1}{2} (\partial^\mu \phi_1 \partial_\mu \phi_1 + \partial^\mu \phi_2 \partial_\mu \phi_2) + U_k(\phi_1, \phi_2) \right\}. \quad (6.22)$$

The evolution equation for the potential can be written in the form [40, 168]

$$\begin{aligned} \frac{\partial}{\partial k^2} [U_k(\phi_1, \phi_2) - U_k(0, 0)] &= -\frac{1}{8\pi} \left[\sqrt{k^2 + M_1^2(\phi_1, \phi_2)} - \sqrt{k^2 + M_1^2(0, 0)} + \right. \\ &\quad \left. + \sqrt{k^2 + M_2^2(\phi_1, \phi_2)} - \sqrt{k^2 + M_2^2(0, 0)} \right], \end{aligned} \quad (6.23)$$

where $M_{1,2}^2(\phi_1, \phi_2)$ are the two eigenvalues of the field-dependent mass matrix, given by

$$M_{1,2}^2(\phi_1, \phi_2) = \frac{1}{2} \left[U_{11} + U_{22} \pm \sqrt{(U_{11} - U_{22})^2 + 4U_{12}^2} \right], \quad (6.24)$$

with $U_{ij} \equiv \partial^2 U_k / \partial \phi_i \partial \phi_j$. The only neglected corrections to eq. (6.23) are related to the wave-function renormalization of the fields. We expect these corrections to be small, as the anomalous dimension is $\eta \approx 0.035 - 0.04$. We consider models with the symmetry $\phi_2 \leftrightarrow -\phi_2$ throughout this paper. This means that the expressions for the mass eigenvalues simplify along the ϕ_1 -axis: $M_1^2 = \partial^2 U_k / \partial \phi_1^2$, $M_2^2 = \partial^2 U_k / \partial \phi_2^2$.

We always choose parameters such that minima of the potential are located along the ϕ_1 -axis. The saddle-point configuration satisfies eq. (6.7) along the ϕ_1 -axis and has $\phi_2 = 0$. The bubble-nucleation rate is derived in complete analogy to the one-field case and is given by

$$I = A_{1k} A_{2k} \exp(-S_k)$$

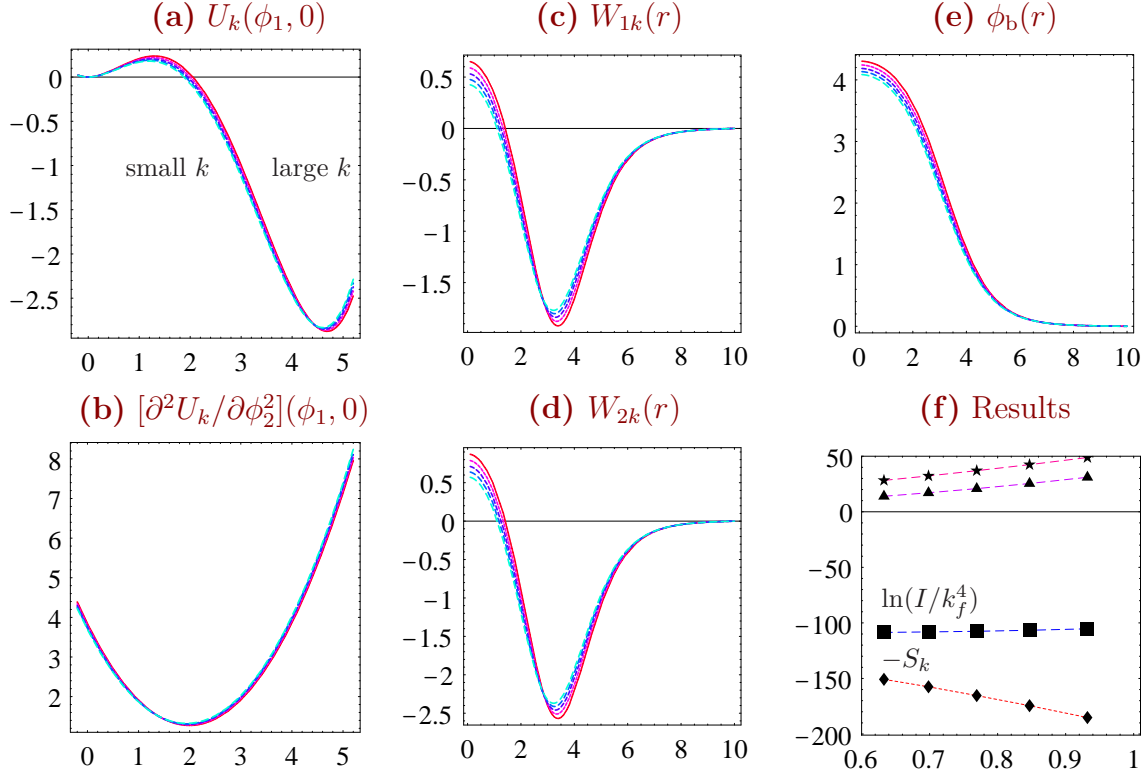


Figure 29: Nucleation rate for multicomponent models. We show the scale dependence of various quantities necessary for the computation of the nucleation rate. The microscopic potential is given by eq. (6.26) with $m_{2k_0}^2 = -m_{1k_0}^2 = 0.1 k_0^2$, $\lambda_{k_0} = g_{k_0} = 0.1 k_0$, $J_{k_0} = 0.6 k_0^{5/2}$. The coarse graining scale k varies between $k_i = e^{-0.8} k_0$ and $k_f = e^{-1.2} k_0$. All dimensionful quantities are given in units of k_f . In fig. 29f we plot the saddle-point action (diamonds), the two prefactors $\ln(A_{1k}/k_f^4)$ (stars) and $\ln(A_{2k})$ (triangles), and the nucleation rate $\ln(I/k_f^4)$ (squares) as a function of $k/\sqrt{U_{11}(\phi_t, 0)}$.

$$\begin{aligned}
A_{1k} &= \frac{E_0}{2\pi} \left(\frac{S_k}{2\pi} \right)^{3/2} \left| \frac{\det' [-\partial^2 + U_{11}(\phi_b(r))]}{\det [-\partial^2 + k^2 + U_{11}(\phi_b(r))]} \frac{\det [-\partial^2 + k^2 + U_{11}(0)]}{\det [-\partial^2 + U_{11}(0)]} \right|^{-1/2}, \\
A_{2k} &= \left| \frac{\det [-\partial^2 + U_{22}(\phi_b(r))]}{\det [-\partial^2 + k^2 + U_{22}(\phi_b(r))]} \frac{\det [-\partial^2 + k^2 + U_{22}(0)]}{\det [-\partial^2 + U_{22}(0)]} \right|^{-1/2}.
\end{aligned} \tag{6.25}$$

The calculation of the various determinants proceeds very similarly to the previous subsection. The details are given in ref. [189].

In fig. 29 we present results for a class of models defined through the potential

$$U_{k_0}(\phi_1, \phi_2) = -J_{k_0} \phi_1 + \frac{1}{2} m_{1k_0}^2 \phi_1^2 + \frac{1}{2} m_{2k_0}^2 \phi_2^2 + \frac{1}{8} \lambda_{k_0} (\phi_1^4 + \phi_2^4) + g_{k_0} \phi_1^2 \phi_2^2. \tag{6.26}$$

The term linear in ϕ_1 can be removed through an appropriate shift of ϕ_1 . This would introduce additional terms $\sim \phi_1^3$ and $\sim \phi_1 \phi_2^2$. In fig. 29a we present the evolution of $U_k(\phi_1) \equiv U_k(\phi_1, 0)$ for $m_{1k_0}^2 = -0.1 k_0^2$, $m_{2k_0}^2 = 0.1 k_0^2$, $\lambda_{k_0} = g_{k_0} = 0.1 k_0$ and $J_{k_0} = 0.6 k_0^{5/2}$. We always shift the

location of the false vacuum to zero. The evolution of $U_{22}(\phi_1) \equiv \partial^2 U_k / \partial \phi_2^2(\phi_1, 0)$ is displayed in fig. 29b. The solid lines correspond to $k_i/k_0 = e^{-0.8}$, while the line with longest dashes (that has the smallest barrier height) corresponds to $k_f/k_0 = e^{-1.2}$. The potential and the field have been normalized with respect to k_f , so that they are of order 1. The profile of the critical bubble $\phi_b(r)$ is plotted in fig. 29e in units of k_f for the same sequence of scales. The quantities $W_{1k}(r) = U_{11}(\phi_b(r)) - U_{11}(0)$ and $W_{2k}(r) = U_{22}(\phi_b(r)) - U_{22}(0)$ are plotted in figs. 29c and 29d respectively.

Our results for the nucleation rate are presented in fig. 29f. The horizontal axis corresponds to $k/\sqrt{U_{11}(\phi_t)}$, i.e. the ratio of the scale k to the square root of the positive curvature of the potential along the ϕ_1 -axis at the true vacuum. The latter quantity gives the mass of the field ϕ_1 at the absolute minimum. Typically, when k crosses below this mass the massive fluctuations of the fields start decoupling (in all the examples we present the mass of ϕ_2 is of the same order or larger than that of ϕ_1 at the absolute minimum) and the evolution of the convex parts of the potential slows down and eventually stops. The dark diamonds give the negative of the action S_k of the saddle point at the scale k . We observe a strong k dependence of this quantity. The stars in fig. 29d indicate the values of $\ln(A_{1k}/k_f^4)$ and the triangles those of $\ln(A_{2k})$, where the two prefactors A_{1k} , A_{2k} are defined in eqs. (6.25). Again a significant k dependence is observed. The dark squares give our results for $\ln(I/k_f^4) = -S_k + \ln(A_{1k}A_{2k}/k_f^4)$. This quantity has a very small k dependence, which confirms our expectation that the nucleation rate should be independent of the scale k . The small residual dependence on k can be used to estimate the contribution of the next order in the expansion around the saddle point. This contribution is expected to be smaller than the first-order correction $\ln(A_{1k}A_{2k}/k_f^4)$.

We now turn to the discussion of radiatively induced first-order phase transitions. An example can be observed in a model with a potential

$$U_{k_0}(\phi_1, \phi_2) = \frac{\lambda_{k_0}}{8} [(\phi_1^2 - \phi_{0k_0}^2)^2 + (\phi_2^2 - \phi_{0k_0}^2)^2] + \frac{g_{k_0}}{4} \phi_1^2 \phi_2^2, \quad (6.27)$$

with $\phi_{0k_0}^2 = 1.712 k_0$, $\lambda_{k_0} = 0.01 k_0$ and $g_{k_0} = 0.2 k_0$. Since $J_{k_0} = 0$, in this case the ‘‘classical potential’’ U_{k_0} only shows second-order transitions independence on the classical parameters $\phi_{0k_0}^2, \lambda_{k_0}, g_{k_0}$. Our results for this model are presented in fig. 30. In fig. 30a we plot a large part of the evolution of $U_k(\phi_1)$. The initial potential has only one minimum along the positive ϕ_1 -axis (and the equivalent ones under the the symmetries $\phi_1 \leftrightarrow -\phi_1$, $\phi_2 \leftrightarrow -\phi_2$, $\phi_1 \leftrightarrow \phi_2$) and a maximum at the origin. In the sequence of potentials depicted by dotted lines we observe the appearance of a new minimum at the origin at some point in the evolution (at $k/k_0 \approx e^{-4.4}$). This minimum is generated by the integration of fluctuations of the ϕ_2 field, whose mass depends on ϕ_1 through the last term in eq. (6.27) (the Coleman-Weinberg mechanism). In fig. 30b it can be seen that the mass term of the ϕ_2 field at the origin turns positive at the same value of k . This is a consequence of the $\phi_1 \leftrightarrow \phi_2$ symmetry of the potential. We calculate the nucleation rate using the potentials of the last stages of the evolution. The solid lines correspond to $k_i/k_0 = e^{-4.7}$, while the line with longest dashes corresponds to $k_f/k_0 = e^{-5.2}$. In figs. 30b–30e we observe that the mass of the ϕ_2 fluctuations in the interior of the critical bubble is much larger than the other mass scales of the problem, which are comparable to k_f .

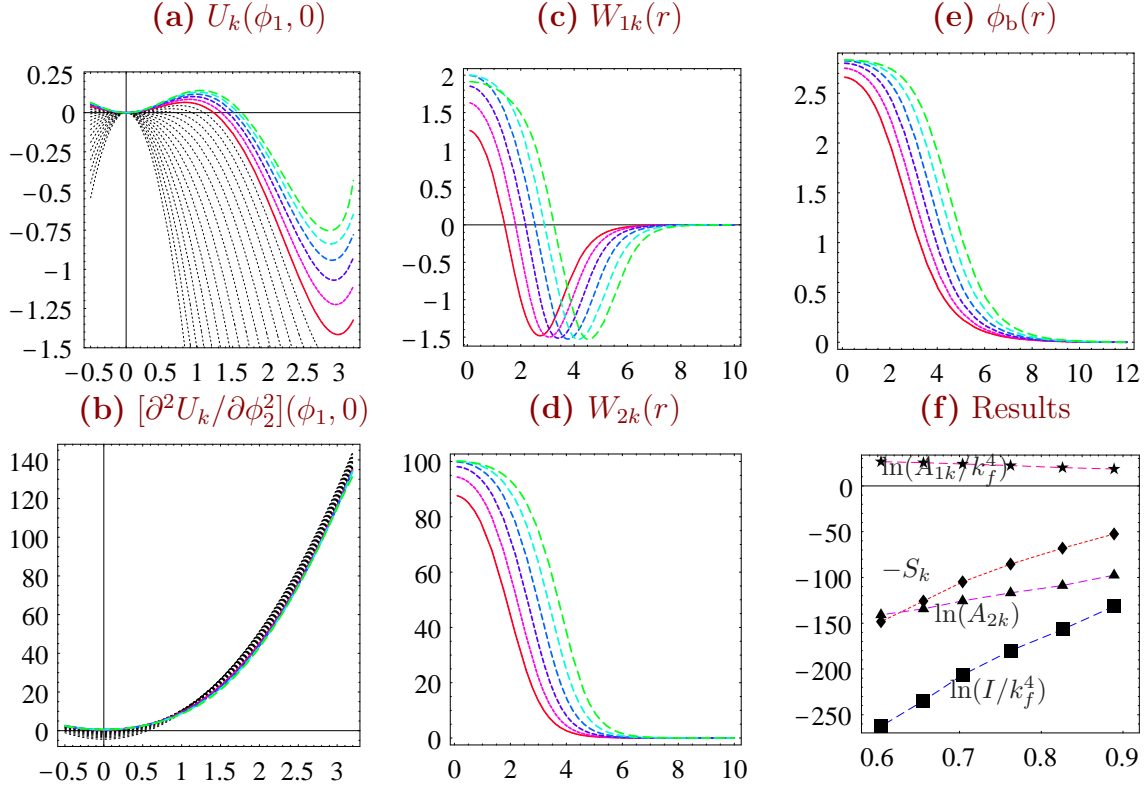


Figure 30: Nucleation rate for a fluctuation induced first order transition. We show the same quantities as in fig. 29 for a model with initial potential given by eq. (6.27) with $\phi_{0k_0}^2 = 1.712 k_0$, $\lambda_{k_0} = 0.01 k_0$ and $g_{k_0} = 0.2 k_0$. The calculation is performed between the scales $k_i = e^{-4.7} k_0$ and $k_f = e^{-5.2} k_0$. All dimensionful quantities are given in units of k_f . The strong scale dependence of the nucleation rate indicates the limits of this calculation.

This is a consequence of our choice of couplings $g/\lambda = 20$. Such a large ratio of g/λ is necessary for a strongly first-order phase transition to be radiatively induced. Unfortunately, this range of couplings also leads to large values for the ϕ_2 mass and, as a result, to values of $|\ln(A_{2k})|$ that are comparable or larger than the saddle-point action S_k , even though $\ln(A_{1k}/k_f^4)$ remains small. As a result, the saddle-point approximation breaks down and the predicted nucleation rate I/k_f^4 is strongly k dependent.

One may wonder if it is possible to obtain a convergent expansion around the saddle point by considering models with smaller values of g . This question was addressed in ref. [189]. For smaller values of the ratio g/λ , a weaker first-order phase transition is observed. The expansion around the saddle point is more problematic in this case. Not only $|\ln(A_{2k})|$ is larger than the saddle-point action S_k , but the prefactor $\ln(A_{1k}/k_f^4)$, associated with the fluctuations of the ϕ_1 field, becomes now comparable to S_k . No region of the parameter space that leads to a convergent saddle-point expansion for the nucleation rate was found.

The above results are not surprising. The radiative corrections to the potential and the pre-exponential factor have a very similar form of fluctuation determinants. When the radiative

corrections are large enough to modify the bare potential and generate a new minimum, the pre-exponential factor should be expected to be important also. More precisely, the reason for this behaviour can be traced to the form of the differential operators in the prefactor. The prefactor associated with the field ϕ_2 involves the ratio $\det(-\partial^2 + m_2^2 + W_{2k}(r)) / \det(-\partial^2 + m_2^2)$, with $m_2^2 = U_{22}(0)$ and $W_{2k}(r) = U_{22}(\phi_b(r)) - U_{22}(0)$. In units in which $\phi_b(r)$ is of order 1, the function $W_{2k}(r)$ takes very large positive values near $r = 0$ (see figs. 30). This is a consequence of the large values of g that are required for the appearance of a new minimum in the potential. As a result, the lowest eigenvalues of the operator $\det(-\partial^2 + m_2^2 + W_{2k}(r))$ are much larger than those of $\det(-\partial^2 + m_2^2)$. This induces a large suppression of the nucleation rate. In physical terms, this implies that the deformations of the critical bubble in the ϕ_2 direction cost excessive amounts of free energy. As these fluctuations are inherent to the system, the total nucleation rate is suppressed when they are taken into account properly. The implications for these finding for cosmological phase transitions, such as the electroweak, were discussed in refs. [189, 191].

6.5 Testing the approach through numerical simulations

As a final application of our formalism we consider (2+1)-dimensional theories at non-zero temperature. These theories provide a test of several points of our approach that depend strongly on the dimensionality, such as the form of the evolution equation of the potential, the nature of the ultraviolet divergences of the fluctuation determinants, and the k dependence of the saddle-point action and prefactor. The complementarity between the k dependence of S_k and A_k is a crucial requirement for the nucleation rate I to be k independent. Another strong motivation stems from the existence of lattice simulations of nucleation for (2+1)-dimensional systems [196].

As before, we work within an effective model after dimensional reduction. In two dimensions the evolution equation for the potential takes the form [190]

$$\frac{\partial}{\partial k^2} [U_k(\phi) - U_k(0)] = -\frac{1}{8\pi} \left[\ln \left(1 + \frac{U_k''(\phi)}{k^2} \right) - \ln \left(1 + \frac{U_k''(0)}{k^2} \right) \right]. \quad (6.28)$$

An approximate solution of this equation is given by

$$U_k(\phi) \approx V(\phi) + \frac{1}{8\pi} V''(\phi) - \frac{1}{8\pi} (k^2 + V''(\phi)) \ln \left(\frac{k^2 + V''(\phi)}{m^2} \right). \quad (6.29)$$

The potential $V(\phi)$ is taken

$$V(\phi) = \frac{m^2}{2} \phi^2 + \frac{\gamma}{6} \phi^3 + \frac{\lambda}{8} \phi^4, \quad (6.30)$$

with

$$\frac{\gamma}{m^2} = -\sqrt{\theta}, \quad \frac{\lambda}{m^2} = \frac{1}{3} \theta \hat{\lambda}, \quad (6.31)$$

in order to match the parameters θ and $\hat{\lambda}$ of the renormalized theory simulated in ref. [196]. The potential of the simulated model is calculated through lattice perturbation theory. The dimensionless coupling that controls the validity of the perturbative expansion is $\hat{\theta}\hat{\lambda}/3$. As

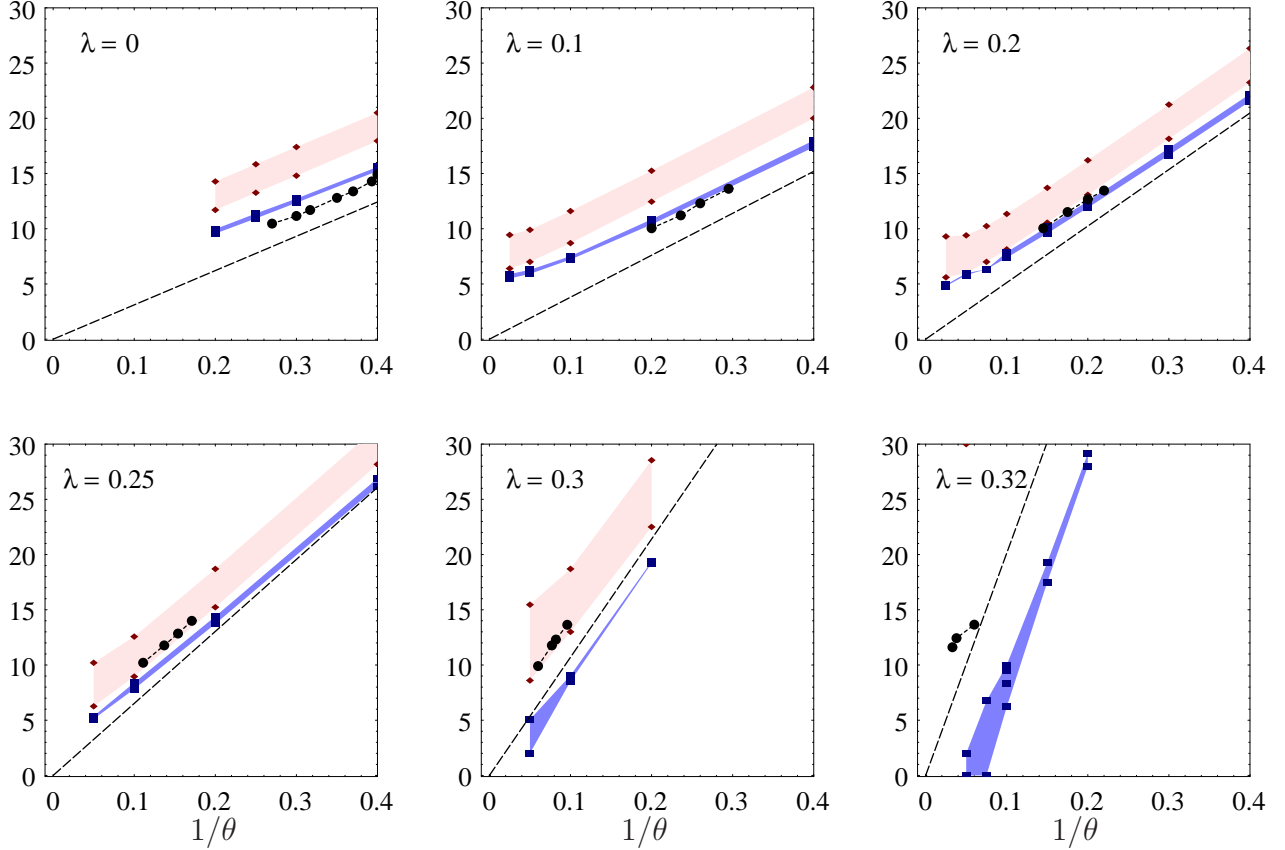


Figure 31: Comparison of our method with lattice studies: Diamonds denote the saddle-point action S_k and squares the bubble-nucleation rate $-\ln(I/m^3)$ for $k = 1.2 k_f$ and $2 k_f$ (shaded regions). Dark circles denote the results for the nucleation rate from the lattice study of ref. [196]. Finally, the dashed straight lines correspond to the action of the saddle point computed from the potential of eq. (6.30).

a result, this expansion is expected to break down for $\hat{\theta} \gtrsim 3/\hat{\lambda}$. Similarly, eq. (6.29) is an approximate solution of eq. (6.28) only for $\hat{\theta} \gtrsim 3/\hat{\lambda}$.

The calculation of bubble-nucleation rates proceeds in complete analogy to the (3+1)-dimensional case at non-zero temperature. The technical details are given in ref. [190]. In fig. 31 we present a comparison of results obtained through our method with the lattice results of fig. 1 of ref. [196]. For each of several values of $\hat{\lambda}$ we vary the parameter θ and determine the couplings γ , λ according to eqs. (6.31). The coarse-grained potential is then given by eq. (6.29) for $k \geq k_f$. The diamonds denote the saddle-point action S_k . For every choice of $\hat{\lambda}$, θ we determine S_k at two scales: $1.2 k_f$ and $2 k_f$. The light-grey region between the corresponding points gives an indication of the k dependence S_k . The bubble-nucleation rate $-\ln(I/m^3)$ is denoted by dark squares. The dark-grey region between the values obtained at $1.2 k_f$ and $2 k_f$ gives a good check of the convergence of the expansion around the saddle point. If this region is thin, the prefactor is in general small and cancels the k dependence of

the action. The dark circles denote the results for the nucleation rate from the lattice study of ref. [196]. The dashed straight lines correspond to the action of the saddle point computed from the ‘tree-level’ potential of eq. (6.30).

For $\hat{\lambda} = 0$ the values of $-\ln(I/m^3)$ computed at $1.2k_f$ and $2k_f$ are equal to a very good approximation. This confirms the convergence of the expansion around the saddle-point and the reliability of the calculation. The k dependence of the saddle-point action is canceled by the prefactor, so that the total nucleation rate is k independent. Moreover, the prefactor is always significantly smaller than the saddle-point action. The circles indicate the results of the lattice simulations of ref. [196]. The agreement with the lattice predictions is good. More specifically, it is clear that the contribution of the prefactor is crucial for the correct determination of the total bubble-nucleation rate. Similar conclusions can be drawn for $\hat{\lambda} = 0.1$ and $\hat{\lambda} = 0.2$.

For larger values of $\hat{\lambda}$ the lattice simulations have been performed only for θ significantly larger than 1. For smaller θ , nucleation events become too rare to be observable on the lattice. Also the matching between the lattice and the renormalized actions becomes imprecise for large θ . This indicates that we should expect deviations of our results from the lattice ones. These deviations start becoming apparent for the value $\hat{\lambda} = 0.25$, for which the lattice simulations were performed with $\theta \sim 10$ – 20 . For $\hat{\lambda} \geq 0.3$ the lattice results are in a region in which the expansion around the saddle point is not reliable any more.

For $\hat{\lambda} = 0.32$ the breakdown of the expansion around the saddle point is apparent for $1/\theta \lesssim 0.12$. The k dependence of the predicted bubble-nucleation rate is strong⁵⁴. The prefactor becomes comparable to the saddle-point action and the higher-order corrections are expected to be large. The k dependence of S_k is very large. For this reason we have not given values of S_k in this case.

The comparison of our results with data from lattice simulations constitutes a stringent quantitative test of our method. In the region where the renormalized action for the lattice model is known, the data of fig. 31, provide a strong confirmation of the reliability of our approach. Another test has been carried out as well. In ref. [192] a comparison has been made with the results of the thin-wall approximation in three dimensions. Very good agreement has been found, which provides additional support for the validity of the method.

7 Quantum statistics for fermions and bosons

7.1 Quantum universality

At low temperature the characteristic energies are near the ground state energy. Only a few states are important and one expects the effects of quantum mechanical coherence to become important. The low temperature region is therefore the quantum domain. In particular, the limit $T \rightarrow 0$ projects on the ground state and single excitations of it. In particle physics this is the vacuum, and the single excitations correspond to the particles. The opposite is classical statistics. For large T many excitations contribute in thermal equilibrium. These thermal fluctuations destroy the quantum mechanical coherence. The high temperature region is the

⁵⁴The additional squares for $1/\theta = 0.1$ correspond to results from the numerical integration of eq. (6.23).

classical domain. This also holds for quantum field theories. Their properties in thermal equilibrium are dominated by classical aspects for high T .

For bosons (and vanishing chemical potential μ) there is another interesting limit. If the characteristic length scale of a physical process becomes very large, many individual local modes must be involved. Again, the quantum mechanical coherence becomes unimportant and classical physics should prevail. Translated to characteristic momenta \vec{q} one concludes that the limit $|\vec{q}| \rightarrow 0$ belongs to the classical domain, typically well described by classical fields.

In thermodynamic equilibrium a characteristic length scale is given by the correlation length $\xi = m_R^{-1}$. This provides us with a dimensionless combination ξT for an assessment of the relevance of quantum statistics. For $\xi T \gg 1$ a classical treatment should be appropriate, whereas for $\xi T \ll 1$ quantum statistics becomes important. For second-order phase transitions the correlation length diverges. The universal critical phenomena are therefore always described by classical statistics! This extends to first-order transitions with small enough ξT . On the other hand the temperature may be much smaller than the microphysical momentum scale Λ . The modes with momenta $(\pi T)^2 < q^2 < \Lambda^2$ are governed by quantum statistics. Correspondingly, the renormalization flow in the range $(\pi T)^2 < k^2 < \Lambda^2$ is determined by the partial fixed points of the quantum system. This introduces a new type of universality since much of the microscopic information is lost in the running from Λ to πT . Subsequently, the difference in the flow for $k > \pi T$ and $k < \pi T$ leads to a crossover phenomenon⁵⁵ to classical statistics. For second-order phase transitions and $m_R \ll T \ll \Lambda$ not only the standard universal critical exponents and amplitude ratios can be computed. Also the (classically non-universal) critical amplitudes can be predicted as a consequence of the new type of universality. One may call this phenomenon “quantum universality”.

More formally, one can express the quantum trace in the partition function (1.1) by a functional integral in $D+1$ dimensions, with D the number of space dimensions of the classical theory. The basic ingredient is Feynman’s path integral in Euclidean space. Using insertions of a complete set of eigenstates

$$1 = \int d\chi_n |\chi_n\rangle\langle\chi_n| \quad (7.1)$$

one has (for a single degree of freedom)

$$Z = \text{tr} e^{-\beta H} = \prod_{n=0}^{N-1} \int d\chi_n \langle\chi_n|e^{-\frac{\beta}{N}H}|\chi_{n+1}\rangle \quad (7.2)$$

with $\chi_N \equiv \chi_0$. Introducing the Euclidean time $\tau = n\beta/N$, $\chi_n \equiv \chi(\tau)$, $\chi(\beta) = \chi(0)$ one obtains for $N \rightarrow \infty$, $d\tau = \beta/N$ a functional integral representation of Z

$$Z = \int D\chi e^{-S[\chi]} \\ e^{-S[\chi]} = \prod_n \langle\chi(\tau)|e^{-Hd\tau}|\chi(\tau+d\tau)\rangle \quad (7.3)$$

⁵⁵Such crossover phenomena have also been discussed in the framework of “environmentally friendly renormalization” [201].

This formulation is easily generalized to the case where χ carries additional indices or depends on coordinate or momentum variables. If χ is a field in D dimensions, we encounter a $D + 1$ dimensional functional integral. The additional dimension corresponds to the Euclidean time τ and is compactified on a torus with circumference $\beta = 1/T$. The action $S[\chi]$ can be evaluated by standard methods for the limit $d\tau \rightarrow 0$. For the example of a Hamiltonian depending on coordinate and momentum-type operators Q, P with $[Q(\vec{x}), P(\vec{y})] = i\delta(\vec{x} - \vec{y})$

$$H = \int d^3x \left\{ \frac{1}{2} P^2(x) + V(Q(x)) + \frac{1}{2} \vec{\nabla} Q(x) \vec{\nabla} Q(x) \right\} \quad (7.4)$$

one finds

$$S = \int d^4x \left\{ \frac{1}{2} \partial_\mu \chi(x) \partial_\mu \chi(x) + V(\chi(x)) \right\} \quad (7.5)$$

with $x = (\tau, \vec{x})$, $\partial_\mu = (\partial_\tau, \vec{\nabla})$. Up to the dimensionality this is identical to eq. (1.4) if V is a quartic polynomial. In particular, eqs. (7.4), (7.5) describe the Hamiltonian and the action for a scalar quantum field theory.

Bosonic fields obey the periodicity condition $\chi(\vec{x}, \beta) = \chi(\vec{x}, 0)$ and can therefore be expanded in ‘‘Matsubara modes’’ with $j \in \mathbb{Z}$

$$\chi(\vec{x}, \tau) = \sum_j \chi_j(\vec{x}) e^{\frac{2\pi i}{\beta} j \tau} \quad (7.6)$$

Correspondingly, the zero components of the momenta $q_\mu = (q_0, \vec{q})$ are given by the discrete Matsubara frequencies

$$q_0 = 2\pi j T \quad (7.7)$$

This discreteness is the only difference between quantum field theory in thermal equilibrium and in the vacuum. (For the vacuum $T \rightarrow 0$ and q_0 becomes a continuous variable.) Eq. (7.7) is the only point where the temperature enters into the quantum field theoretical formalism. Furthermore, the discreteness of q_0 constitutes the only difference between quantum statistics for a system in D space dimensions and classical statistics for a corresponding system in $D + 1$ dimensions.

In thermal equilibrium a characteristic value of q_0 may be associated with $m_R = \xi^{-1}$, where m_R is the smallest renormalized mass of the system. For $T/m_R \ll 1$ the discreteness of q_0 may be neglected and the quantum system is essentially determined by the ground state. According to our general discussion the opposite limit $T/m_R \gg 1$ should be dominated by classical statistics, at least for the ‘‘infrared sensitive’’ quantities (i.e. except for the relevant parameters in critical phenomena). For the action (7.5) this is easily seen in perturbation theory by realizing that the propagator

$$(q_\mu q_\mu + m_R^2)^{-1} = (\vec{q}^2 + (2\pi j T)^2 + m_R^2)^{-1} \quad (7.8)$$

has a masslike term $\sim T^2$ for all $j \neq 0$. For large T the contributions from the $j \neq 0$ Matsubara modes are therefore strongly suppressed in the momentum integrals for the fluctuation effects and may be neglected. In the limit where only the $j = 0$ mode contributes in the functional

integral (7.3), we are back to a classical functional integral in D dimensions. (The τ -integration in eq. (7.8) results in a simple factor β which can be reabsorbed by a rescaling of χ .) This “dimensional reduction” [202] from $D + 1$ to D dimensions is characteristic for the crossover from the quantum domain to the classical domain as the characteristic momenta given by m_R fall below T . We will see in section 7.3 how the flow equations realize this transition in a simple and elegant way.

We also want to discuss the quantum statistics of fermionic systems. They can be treated in parallel to the bosonic system, with one major modification: The classical fields $\chi(\vec{x})$ are replaced by anticommuting Grassmann variables $\psi(\vec{x})$

$$\{\psi_a(\vec{x}), \psi_b(\vec{y})\} = 0 \quad (7.9)$$

Correspondingly, they are antiperiodic in β , i. e. $\psi(\vec{x}, \beta) = -\psi(\vec{x}, 0)$. In the next subsection 7.2 we generalize the exact renormalization group equation to Grassmann variables. Applications of

7.2 Exact flow equation for fermions

The exact flow equation (2.19) can be extended to fermions in a straightforward way except for one important minus sign [81, 82]. We write the fermionic infrared cutoff term as

$$\Delta S_k^{(F)} = \int \frac{d^d q}{(2\pi)^d} \bar{\zeta}(q) R_{kF}(q) \zeta(q) \quad (7.10)$$

where $\bar{\zeta}, \zeta$ are euclidean Dirac or Weyl spinors in even dimensions and all spinor indices have been suppressed. (There appears an additional factor of $1/2$ in the rhs of (7.10) if $\bar{\zeta}$ and ζ are related or obey constraints, as for the case of Majorana and Majorana-Weyl spinors in those dimensions where this is possible. For Dirac spinors or the standard $2^{d/2-1}$ component Weyl spinors this factor is absent.)

In complete analogy to the case of bosonic fields χ (cf. sections 2.1, 2.2) we add the infrared cutoff term (7.10) to the classical action S

$$S_k[\chi, \bar{\zeta}, \zeta] = S[\chi, \bar{\zeta}, \zeta] + \Delta S_k[\chi] + \Delta S_k^{(F)}[\bar{\zeta}, \zeta]. \quad (7.11)$$

The generating functional of connected Green functions $W_k[J, \bar{\eta}, \eta]$ is now a generating functional of the Grassmann valued sources $\bar{\eta}$ and η in addition to the scalar sources J already contained in (2.5). The effective average action is then defined as

$$\begin{aligned} \Gamma_k[\phi, \bar{\psi}, \psi,] &= -W_k[J, \bar{\eta}, \eta] + \int d^d x [J(x)\phi(x) + \bar{\eta}(x)\psi(x) - \bar{\psi}(x)\eta(x)] \\ &\quad - \Delta S_k[\phi] - \Delta S_k^{(F)}[\bar{\psi}, \psi,] \end{aligned} \quad (7.12)$$

with

$$\psi(x) = \frac{\delta W_k[J, \bar{\eta}, \eta]}{\delta \bar{\eta}(x)}, \quad \bar{\psi}(x) = \frac{\delta W_k[J, \bar{\eta}, \eta]}{\delta \eta(x)}. \quad (7.13)$$

The matrix $\Gamma_k^{(2)}[\phi, \bar{\psi}, \psi]$ of second functional derivatives of Γ_k has a block substructure in boson-antifermion-fermion space which we abbreviate as $B - \bar{F} - F$:

$$\Gamma_k^{(2)} = \begin{pmatrix} \Gamma_{k,BB}^{(2)} & \Gamma_{k,B\bar{F}}^{(2)} & \Gamma_{k,BF}^{(2)} \\ \Gamma_{k,\bar{F}B}^{(2)} & \Gamma_{k,\bar{F}\bar{F}}^{(2)} & \Gamma_{k,\bar{F}F}^{(2)} \\ \Gamma_{k,FB}^{(2)} & \Gamma_{k,F\bar{F}}^{(2)} & \Gamma_{k,FF}^{(2)} \end{pmatrix}$$

where

$$\Gamma_{k,BB}^{(2)} = \frac{\delta^2 \Gamma_k}{\delta \phi \delta \phi}, \quad \Gamma_{k,B\bar{F}}^{(2)} = \frac{\delta^2 \Gamma_k}{\delta \phi \delta \bar{\psi}}, \quad \Gamma_{k,\bar{F}F}^{(2)} = -\frac{\delta^2 \Gamma_k}{\delta \bar{\psi} \delta \psi}, \quad \text{etc.} \quad (7.14)$$

It is now straightforward to generalize the exact flow equation (2.19) to include fermions and one finds

$$\begin{aligned} \frac{\partial}{\partial k} \Gamma_k[\phi, \bar{\psi}, \psi] &= \frac{1}{2} \text{STr} \left\{ \left[\Gamma_k^{(2)}[\phi, \bar{\psi}, \psi] + \mathbf{R}_k \right]^{-1} \frac{\partial}{\partial k} \mathbf{R}_k \right\} \\ &= \frac{1}{2} \text{Tr} \left\{ \left[\Gamma_k^{(2)}[\phi, \bar{\psi}, \psi] + \mathbf{R}_k \right]_{BB}^{-1} \frac{\partial}{\partial k} R_k \right\} \\ &\quad - \text{Tr} \left\{ \left[\Gamma_k^{(2)}[\phi, \bar{\psi}, \psi] + \mathbf{R}_k \right]_{\bar{F}\bar{F}}^{-1} \frac{\partial}{\partial k} R_{kF} \right\} \end{aligned} \quad (7.15)$$

where the block structure of \mathbf{R}_k in $B - \bar{F} - F$ space is given by

$$\mathbf{R}_k = \begin{pmatrix} R_k & 0 & 0 \\ 0 & 0 & R_{kF} \\ 0 & -R_{kF} & 0 \end{pmatrix} \quad (7.16)$$

and the minus sign in the fermionic trace arises from the anticommutation of fermions in the step corresponding to eq. (2.27). We observe that the infrared cutoff does not mix bosons and fermions. For purely bosonic background fields the inverse propagator $\Gamma_k^{(2)}$ is also block diagonal, and one obtains separate contributions from fermions and bosons. This is not true any more for fermionic background fields since the inverse propagator has now off-diagonal pieces. Again, the right-hand side of the flow equation can be expressed as the formal derivative $\tilde{\partial}_t$ acting on the IR-cutoff in a one-loop diagram.

The infrared cutoff for fermions has to meet certain requirements for various reasons. First of all, chiral fermions do not allow a mass term. In order to remain consistent with chiral symmetries (a necessity for neutrinos, for example), the infrared cutoff must have the same Lorentz structure as the kinetic term, i.e. $R_{kF} \sim \gamma^\mu q_\mu$ [81] or, at least, not mix left-handed and right-handed fermions, e.g. $R_k \sim \gamma^\mu \gamma^5 q_\mu$.⁵⁶ On the other hand, for $q^2 \rightarrow 0$ the infrared cutoff should behave as $R_{kF} \sim k$, e.g. $R_{kF} \sim k \gamma^\mu q_\mu / \sqrt{q^2}$. The nonanalyticity of $\sqrt{q^2}$ may then be a cause of problems. We will discuss here a few criteria for a chirally invariant infrared cutoff and present an explicit example which is suitable for practical calculations.

First of all, the fermionic infrared cutoff term $\Delta S_k^{(F)}$ should be quadratic in the fermion fields as in (7.10). We next require that $\Delta S_k^{(F)}$ should respect all symmetries of

⁵⁶We use a Euclidean convention with $\{\gamma^\mu, \gamma^\nu\} = 2\delta^{\mu\nu}$ and $\gamma^5 = -\gamma^0 \gamma^1 \gamma^2 \gamma^3$ in four dimensions.

the kinetic term for free fermions. We will include here chiral symmetries and Lorentz invariance. (Gauge symmetries may be implemented by covariant derivatives in a background gauge field [47].) The symmetry requirement implies in a momentum space representation ($\psi(x) = \int \frac{d^d q}{(2\pi)^d} e^{iqx} \psi(q)$)

$$\Delta S_k^{(F)} = - \int \frac{d^d q}{(2\pi)^d} \bar{\psi}(q) Z_{\psi,k} \not{q} r_F \left(\frac{q^2}{k^2} \right) \psi(q) , \quad (7.17)$$

i.e. $R_{kF} \equiv -Z_{\psi,k} \not{q} r_F$, where $\bar{\psi}$, ψ are Dirac spinors and $\not{q} = q_\mu \gamma^\mu$. The wave-function renormalization Z_ψ is chosen for convenience such that it matches with a fermion kinetic term of the form

$$\Gamma_k^{\text{kin}}[\bar{\psi}, \psi] = - \int \frac{d^d q}{(2\pi)^d} \bar{\psi}(q) Z_{\psi,k} \not{q} \psi(q) . \quad (7.18)$$

The third condition requires that $\Delta S_k^{(F)}$ acts effectively as an infrared cutoff. This means that for $k \rightarrow \infty$ the combination $Z_\psi r_F \left(\frac{q^2}{k^2} \right)$ should diverge for all values of q^2 . This divergence should also occur for finite k and $q^2/k^2 \rightarrow 0$ and be at least as strong as $(k^2/q^2)^{1/2}$. As a fourth point we remark that Γ_k becomes the effective action in the limit $k \rightarrow 0$ only if $\lim_{k \rightarrow 0} \Delta S_k^{(F)} = 0$. This should hold for all Fourier modes separately, i.e. for $\lim_{k \rightarrow 0} Z_{\psi,k} = \text{const.}$ one requires

$$\lim_{k \rightarrow 0} r_F \left(\frac{q^2}{k^2} \right) \not{q} = 0 . \quad (7.19)$$

We furthermore request that (7.19) also holds in the limit $q^2 \rightarrow 0$. Together with the third condition this implies exactly

$$\lim_{q^2/k^2 \rightarrow 0} r_F \left(\frac{q^2}{k^2} \right) \sim \left(\frac{q^2}{k^2} \right)^{-\frac{1}{2}} . \quad (7.20)$$

The requirement (7.20) implies a smooth behavior of R_{kF} for $q^2/k^2 \rightarrow 0$. However, the nonanalyticity of r_F at $q^2 = 0$ requires a careful choice of r_F in order to circumvent problems. We note that r_F appears in connection with the fermion propagator from Γ_k . The combination which will appear in calculations is

$$P_F = q^2 (1 + r_F)^2 . \quad (7.21)$$

Up to the wave-function renormalization, P_F corresponds to the squared inverse propagator of a free massless fermion in the presence of the infrared cutoff. We will require that P_F and therefore $(1 + r_F)^2$ is analytic in q^2 for all $q^2 \geq 0$. A reasonable choice is

$$P_F = \frac{q^2}{1 - \exp \left\{ -\frac{q^2}{k^2} \right\}} . \quad (7.22)$$

We will employ this choice in the treatment of Nambu–Jona-Lasinio type models in section 8, where we also discuss another choice for P_F .

7.3 Thermal equilibrium and dimensional reduction

The extension of the flow equations to non-vanishing temperature T is straightforward [42]. The (anti-)periodic boundary conditions for (fermionic) bosonic fields in the Euclidean time direction [203] leads to the replacement

$$\int \frac{d^d q}{(2\pi)^d} f(q^2) \rightarrow T \sum_{j \in \mathbb{Z}} \int \frac{d^{d-1} \vec{q}}{(2\pi)^{d-1}} f(q_0^2(j) + \vec{q}^2) \quad (7.23)$$

in the trace of the flow equation (2.36) when represented as a momentum integration. One encounters a discrete spectrum of Matsubara frequencies for the zero component $q_0(j) = 2j\pi T$ for bosons and $q_0(j) = (2j+1)\pi T$ for fermions. Hence, for $T > 0$ a four-dimensional QFT can be interpreted as a three-dimensional model with each bosonic or fermionic degree of freedom now coming in an infinite number of copies labeled by $j \in \mathbb{Z}$ (Matsubara modes). Each mode acquires an additional temperature dependent effective mass term $q_0^2(j)$ except for the bosonic zero mode for which $q_0^2(0)$ vanishes. At high temperature all massive Matsubara modes decouple from the dynamics of the system. In this case, one therefore expects to observe an effective three-dimensional theory with the bosonic zero mode as the only relevant degree of freedom. One may visualize this behavior by noting that for a given characteristic length scale l much larger than the inverse temperature β the compact Euclidean “time” dimension cannot be resolved anymore.

This phenomenon of dimensional reduction can be observed directly from the non-perturbative flow equations. The replacement (7.23) in (2.36) manifests itself in the flow equations only through a change to T -dependent threshold functions. For instance, the dimensionless threshold functions $l_n^d(w; \eta_\Phi)$ defined in eq. (3.16) are replaced by

$$l_n^d\left(w, \frac{T}{k}; \eta_\Phi\right) \equiv \frac{n + \delta_{n,0}}{4} v_d^{-1} k^{2n-d} T \sum_{j \in \mathbb{Z}} \int \frac{d^{d-1} \vec{q}}{(2\pi)^{d-1}} \left(\frac{1}{Z_{\Phi,k}} \frac{\partial R_k(q^2)}{\partial t} \right) \frac{1}{[P(q^2) + k^2 w]^{n+1}} \quad (7.24)$$

where $q^2 = q_0^2 + \vec{q}^2$ and $q_0 = 2\pi j T$. In the limit $k \gg T$ the sum over Matsubara modes approaches the integration over a continuous range of q_0 and we recover the zero temperature threshold function $l_n^d(w; \eta_\Phi)$. In the opposite limit $k \ll T$ the massive Matsubara modes ($j \neq 0$) are suppressed and we expect to find a $d-1$ dimensional behavior of l_n^d . In fact, one obtains from (7.24)

$$\begin{aligned} l_n^d(w, T/k; \eta_\Phi) &\simeq l_n^d(w; \eta_\Phi) && \text{for } T \ll k, \\ l_n^d(w, T/k; \eta_\Phi) &\simeq \frac{T}{k} \frac{v_{d-1}}{v_d} l_n^{d-1}(w; \eta_\Phi) && \text{for } T \gg k. \end{aligned} \quad (7.25)$$

For the choice of the infrared cutoff function R_k eq. (2.17) for bosons and eq. (7.22) for fermions the contribution of the temperature-dependent massive Matsubara modes to $l_n^d(w, T/k; \eta_\Phi)$ is exponentially suppressed for $T \ll k$. Nevertheless, all bosonic threshold functions are proportional to T/k for $T \gg k$ whereas those with fermionic contributions vanish in this limit. This behavior is demonstrated [28] in figure 32 where we have plotted

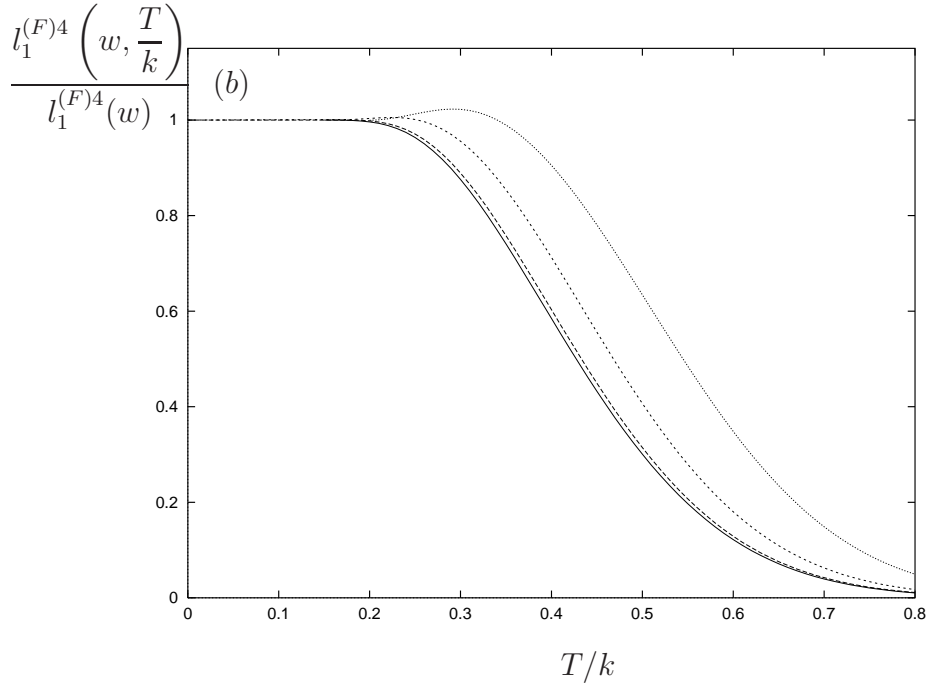
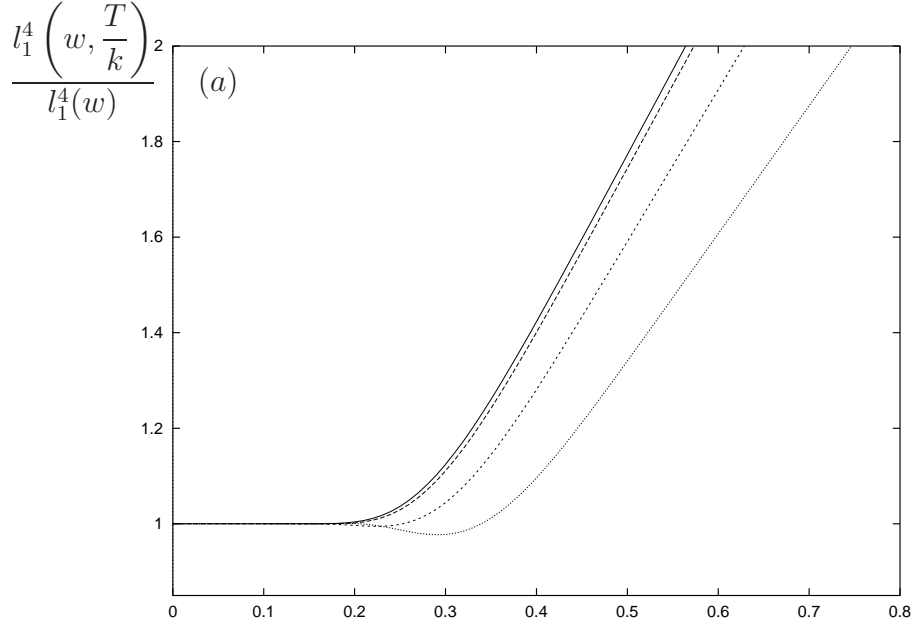


Figure 32: *Effective dimensional reduction: The plot shows the temperature dependence of the bosonic (a) and the fermionic (b) threshold functions $l_1^4(w, T/k)$ and $l_1^{(F)4}(w, T/k)$, respectively, for different values of the dimensionless mass term w . We have normalized them to the $T = 0$ threshold functions. The solid line corresponds to $w = 0$ whereas the dotted ones correspond to $w = 0.1$, $w = 1$ and $w = 10$ with decreasing size of the dots. For $T \gg k$ the bosonic threshold function becomes proportional to T/k whereas the fermionic one tends to zero. In this range the theory with properly rescaled variables behaves as a classical three-dimensional theory.*

the quotients $l_1^4(w, T/k)/l_1^4(w)$ and $l_1^{(F)4}(w, T/k)/l_1^{(F)4}(w)$ of bosonic and fermionic threshold functions, respectively. One observes that for $k \gg T$ both threshold functions essentially behave as for zero temperature. For growing T or decreasing k this changes as more and more Matsubara modes decouple until finally all massive modes are suppressed. The bosonic threshold function l_1^4 shows for $k \ll T$ the linear dependence on T/k derived in eq. (7.25). In particular, for the bosonic excitations the threshold function for $w \ll 1$ can be approximated with reasonable accuracy by $l_n^4(w; \eta_\Phi)$ for $T/k < 0.25$ and by $(4T/k)l_n^3(w; \eta_\Phi)$ for $T/k > 0.25$. The fermionic threshold function $l_1^{(F)4}$ tends to zero for $k \ll T$ since there is no massless fermionic zero mode, i.e. in this limit all fermionic contributions to the flow equations are suppressed. On the other hand, the fermions remain quantitatively relevant up to $T/k \simeq 0.6$ because of the relatively long tail in figure 32b. The formalism of the average action automatically provides the tools for a smooth decoupling of the massive Matsubara modes as the momentum scale k is lowered from $k \gg T$ to $k \ll T$. It therefore allows one to directly link the four-dimensional quantum field theory at low T to the effective three-dimensional high- T -theory.

Whereas for $k \gg T$ the theory is most efficiently described in terms of standard four-dimensional fields Φ a choice of rescaled three-dimensional variables $\Phi_3 = \Phi/\sqrt{T}$ becomes better adapted for $k \ll T$. Accordingly, for high temperatures one will use the rescaled dimensionless potential

$$u_3(t, \tilde{\rho}_3) = \frac{k}{T}u(t, \tilde{\rho}) ; \quad \tilde{\rho}_3 = \frac{k}{T}\tilde{\rho} . \quad (7.26)$$

For numerical calculations at non-vanishing temperature one can exploit the discussed behavior of the threshold functions by using the zero temperature flow equations in the range, say, $k \geq 10T$. For smaller values of k one can approximate the infinite Matsubara sums (cf. eq. (7.24)) by a finite series so that the numerical uncertainty at $k = 10T$ is better than a given value. This approximation becomes exact in the limit $k \ll 10T$.

7.4 The high-temperature phase transition for the ϕ^4 quantum field theory

The formalism of the previous sections can be applied to the phase transition of the four-dimensional $O(N)$ -symmetric ϕ^4 theory at non-vanishing temperature [42, 204] (see also [201, 205, 206, 207, 208] for studies using similar techniques). We consider models with spontaneous symmetry breaking at zero temperature, and investigate the restoration of symmetry as the temperature is raised. We specify the action together with some high momentum cutoff $\Lambda \gg T$ so that the theory is properly regulated. We then solve the evolution equation for the average potential for different values of the temperature. For $k \rightarrow 0$ this solution provides all the relevant features of the temperature-dependent effective potential. In order not to complicate our discussion, we neglect the wave-function renormalization and consider a very simple ansatz for the potential, in which we keep only the quadratic and quartic terms. Improved accuracy can be obtained by using more extended truncations of the average action. The flow equations for the rescaled minimum of the potential $\kappa(k, T) = \rho_0(k, T)/k^2$

and the quartic coupling $\lambda(k, T)$ are

$$\partial_t \kappa = \beta_\kappa = -2\kappa + \frac{1}{16\pi^2} \left\{ 3l_1^4 \left(2\lambda\kappa, \frac{T}{k} \right) + (N-1)l_1^4 \left(\frac{T}{k} \right) \right\} \quad (7.27)$$

$$\partial_t \lambda = \beta_\lambda = \frac{1}{16\pi^2} \lambda^2 \left\{ 9l_2^4 \left(2\lambda\kappa, \frac{T}{k} \right) + (N-1)l_2^4 \left(\frac{T}{k} \right) \right\}. \quad (7.28)$$

The initial conditions are determined by the “short distance values” $\rho_0(k = \Lambda)$ and $\lambda(k = \Lambda)$ that correspond to the minimum and the quartic coupling of the bare potential. We then have to compute the evolution, starting at $k = \Lambda$ and following the renormalization flow towards $k = 0$. This procedure has to be followed for $T = 0$ and then to be repeated for $T \neq 0$ in order to relate the zero and non-zero temperature effective potential of the same theory. Since the running of the parameters is the same in the zero and non-zero temperature case for $k \gg T$ we actually do not need to compute the evolution in this range of k . Our strategy is equivalent to the following procedure: We start with the zero-temperature theory at $k = 0$ taking the renormalized parameters as input. We subsequently integrate the zero-temperature flow equations “up” to $k = T/\theta_1$, where θ_1 is chosen such that $l_n^4(w, T/k) = l_n^4(w)$ to a good approximation for $k > T/\theta_1$. For bosons $\theta_1 \lesssim 0.1$ is sufficient. We can now use the values of the running parameters at $k = T/\theta_1$ as initial conditions for the non-zero temperature flow equations and integrate them “down” to $k = 0$. In this way we obtain the renormalized parameters at non-zero temperature in terms of the renormalized parameters at zero temperature.

As we discussed in the previous subsection, the threshold functions simplify considerably for $k < T/\theta_2$, with $\theta_2 \simeq 0.4$ for bosons. In this range $l_n^4(w, T/k) = 4l_n^3(w)T/k$ to a good approximation and we expect an effective three-dimensional evolution. We can define the dimensionless quantities

$$\begin{aligned} \tilde{\kappa}(k, T) &= \frac{\rho'(k, T)}{k} = \frac{\rho_0(k, T)}{kT} \\ \tilde{\lambda}(k, T) &= \frac{\lambda'(k, T)}{k} = \lambda(k, T) \frac{T}{k}. \end{aligned} \quad (7.29)$$

where ρ' and λ' have the canonical three-dimensional normalization. In terms of these quantities the flow equations read for $k < T/\theta_2$:

$$\frac{d\tilde{\kappa}}{dt} = -\tilde{\kappa} + \frac{1}{4\pi^2} \{ (N-1)l_1^3 + 3l_1^3(2\tilde{\lambda}\tilde{\kappa}) \} \quad (7.30)$$

$$\frac{d\tilde{\lambda}}{dt} = -\tilde{\lambda} + \frac{1}{4\pi^2} \tilde{\lambda}^2 \{ (N-1)l_2^3 + 9l_2^3(2\tilde{\lambda}\tilde{\kappa}) \}. \quad (7.31)$$

The main qualitative difference of the last equations from those of the zero-temperature theory arises from the term $-\tilde{\lambda}$ in the rhs of eq. (7.31), which is due to the dimensions of λ' . In consequence, the dimensionless quartic coupling $\tilde{\lambda}$ is not infrared free. Its behaviour with $k \rightarrow 0$ is characterized by an approximate fixed point for the region where $\tilde{\kappa}$ varies only slowly. Taken together, the pair of differential equations for $(\tilde{\lambda}, \tilde{\kappa})$ has an exact fixed point $(\tilde{\kappa}_*, \tilde{\lambda}_*)$ corresponding to the phase transition.

By using $l_n^4(w, T/k) = l_n^4(w)$ for $k > T/\bar{\theta}$ and $l_n^4(w, T/k) = 4l_n^3(w)T/k$ for $k < T/\bar{\theta}$, with $\bar{\theta}$ between θ_1 and θ_2 , our procedure simplifies even further. It may be summarized as “run up in four dimensions, run down in three dimensions”, with a matching of the k -dependent couplings at the scale $T/\bar{\theta}$, $\bar{\theta} \approx 0.25$. In practice we take the “threshold correction” from the different running for $T/\theta_2 < k < T/\theta_1$ into account numerically. In the case that $\rho_0(k, T)$ becomes zero at some non-zero k_s we continue with the equations for the symmetric regime with boundary conditions $m^2(k_s, T) = 0$ and $\lambda(k_s, T)$ given by its value at the end of the running in the spontaneously broken regime.

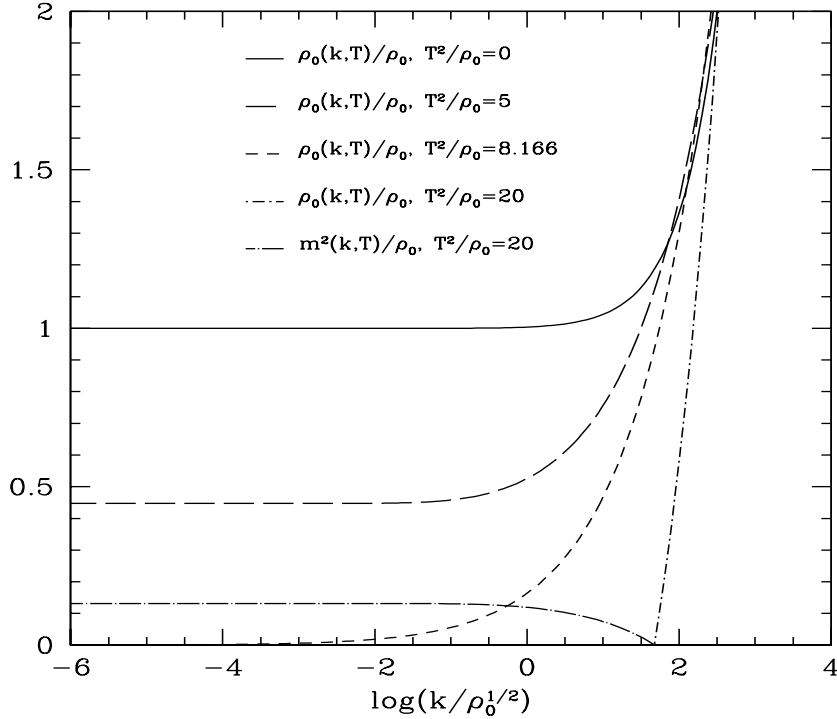


Figure 33: *The evolution of the minimum of the potential $\rho_0(k, T)$ at various temperatures. For $T > T_{cr}$ the evolution of the mass term $m^2(k, T)$ in the symmetric regime is also displayed. $N = 1$ and $\lambda_R = 0.1$.*

The results of the numerical integration of the flow equations for $N = 1$ are presented in figs. 33, 34 for a zero-temperature theory with renormalized quartic coupling $\lambda_R = 0.1$. The solid line in fig. 33 displays the “quadratic renormalization” of the minimum of the zero-temperature average potential. At non-zero temperature (dashed lines) we notice the deviation from the zero temperature behaviour. For low temperatures, in the limit $k \rightarrow 0$, $\rho_0(k, T)$ reaches an asymptotic value $\rho_0(0, T) < \rho_0(0) \equiv \rho_0$. This value corresponds to the vacuum expectation value of the non-zero temperature theory and we denote it by $\rho_0(T) = \rho_0(0, T)$. At a specific temperature T_{cr} , $\rho_0(T)$ becomes zero and this signals the restoration of symmetry for $T \geq T_{cr}$. The running of $\lambda(k)$, $\lambda(k, T)$ is shown in fig. 34. We observe the logarithmic running of $\lambda(k)$ (solid line) which is stopped by the mass term. For non-zero temperatures $\lambda(k, T)$ deviates from the zero temperature running and reaches a non-zero value in the limit $k \rightarrow 0$. We observe that $\lambda(k, T)$ runs to zero for $T \rightarrow T_{cr}$ [200, 42]. For $T > T_{cr}$ the running

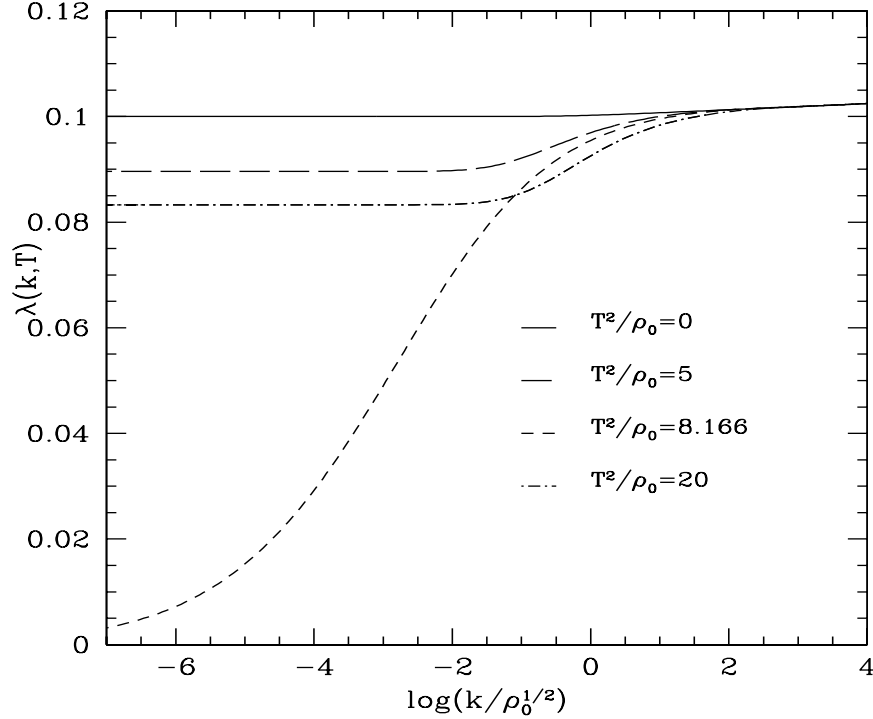


Figure 34: *Scale dependence of the quartic coupling $\lambda(k, T)$ at various temperatures. The strong drop near the critical temperature is characteristic for the critical behavior.*

in the spontaneously broken regime ends at a non-zero k_s , at which $\rho_0(k_s, T)$ equals zero. From this point on we continue the evolution in the symmetric regime. The running of the mass term at the origin $m^2(k, T)$ is depicted in fig. 33, while the evolution of $\lambda(k, T)$ proceeds continuously in the new regime as shown in fig. 34.

The procedure of “running up in four dimensions” and “running down in three dimensions” provides the connection between the renormalized quantities at zero and non-zero temperature. We define the zero temperature theory in terms of the location of the minimum ρ_0 and the renormalized quartic coupling $\lambda_R = \lambda(0)$. Through the solution of the evolution equations we obtain $\rho_0(T)$ and $\lambda_R(T) = \lambda(0, T)$ for non-zero temperatures $T < T_{cr}$. For $T \geq T_{cr}$ the symmetry is restored ($\rho_0(T) = 0$) and the non-zero temperature theory is described in terms of $m_R^2(T) = m^2(0, T)$ and $\lambda_R(T)$. In fig. 35 we plot $\rho_0(T)/\rho_0$, $\lambda_R(T)$ and $m_R^2(T)/T^2$ as a function of temperature for $N = 1$ and $\lambda_R = 0.1$. As the temperature increases towards T_{cr} we observe a continuous transition from the spontaneously broken to the symmetric phase. This clearly indicates a second order phase transition. The renormalized quartic coupling $\lambda_R(T)$ remains close to its zero temperature value λ_R for a large range of temperatures and drops quickly to zero at $T = T_{cr}$. Recalling our parametrization of the average potential in terms of its successive ρ derivatives at the minimum, we conclude that, at T_{cr} , the first non-zero term in the expression for the effective potential is the ϕ^6 term (which we have neglected in our truncated solution). For $T \gg T_{cr}$ the coupling $\lambda_R(T)$ quickly grows to approximately its zero temperature value λ_R , while $m_R^2(T)$ asymptotically becomes proportional to T^2 as $T \rightarrow \infty$. In the temperature range where $\lambda_R(T) \lesssim 0.5\lambda_R(0)$ the fluctuations are important and the

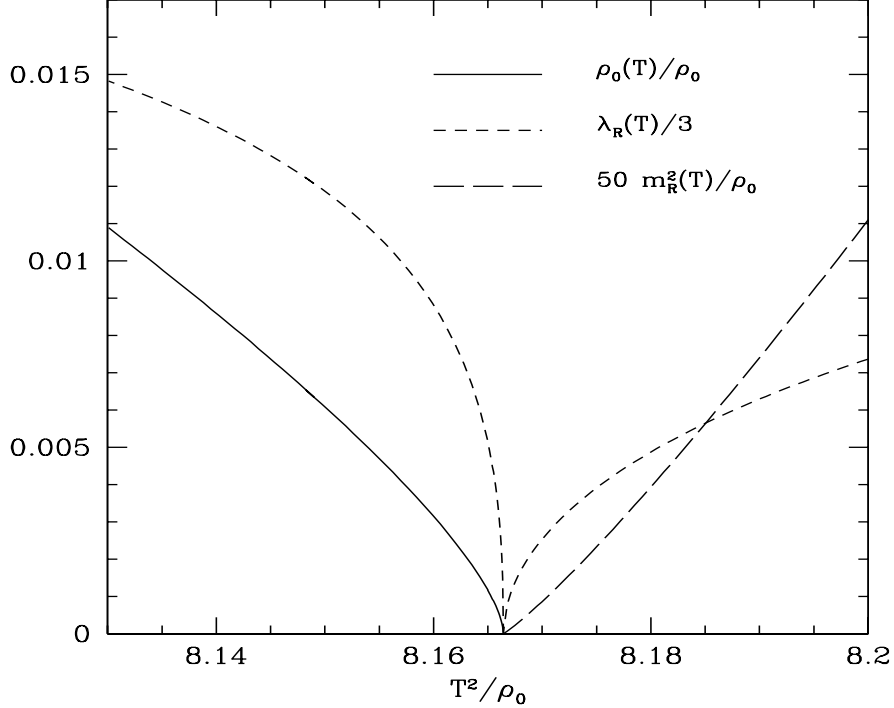


Figure 35: *High temperature symmetry restoration: We show the temperature dependence of the order parameter $\rho_0(T)$, the renormalized mass $m_R^2(T)$ and the quartic coupling $\lambda_R(T)$ near T_{cr} . The critical behavior of a second order phase transition is apparent.*

universal critical behavior becomes dominant (cf. sect. 1.2).

The value of the critical temperature T_{cr} in terms of the zero temperature quantities has been calculated in the context of “naive” perturbation theory [197, 198, 199]. It was found that it is given by $T_{cr}^2 = 24\rho_0/(N+2)$, independently of the quartic coupling in lowest order. This prediction was confirmed in ref. [42] for various values of N . Another parameter which can be compared with the perturbative predictions is $m_R^2(T)$ in the limit $T \rightarrow \infty$. In ref. [42] it was shown that the quantity $\left[\frac{m_R^2(T)}{\lambda_R(T)(N+2)T^2}\right]^{-1}$ becomes equal to 24 for $T^2/\rho_0 \rightarrow \infty$ and small λ_R , again in agreement with the perturbative result.

The most important aspect of our approach is related to the infrared behaviour of the theory for $T \rightarrow T_{cr}$. The temperature dependence of $\rho_0(T)$, $\lambda_R(T)$, $m_R^2(T)$ near T_{cr} is presented in fig. 35 ($\lambda_R = 0.1$). We have already mentioned that all the above quantities become zero at $T = T_{cr}$. What becomes apparent in this figure is a critical behaviour which can be characterized by critical exponents. Following the notation of statistical mechanics, we parametrize the critical behaviour of $\rho_0(T)$ and $m_R^2(T)$ as

$$\begin{aligned} \rho_0(T) &\propto (T_{cr}^2 - T^2)^{2\beta} \\ m_R^2(T) &\propto (T^2 - T_{cr}^2)^{2\nu}. \end{aligned} \quad (7.32)$$

We also define a critical exponent ζ for $\lambda_R(T)$ in the symmetric regime:

$$\lambda_R(T) \propto (T^2 - T_{cr}^2)^\zeta. \quad (7.33)$$

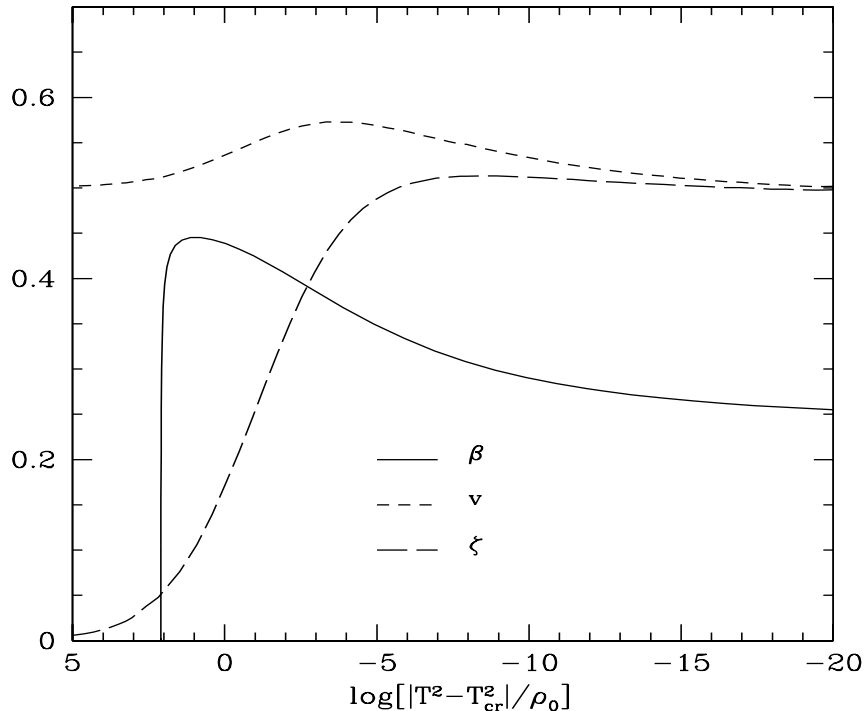


Figure 36: *Temperature dependent effective critical exponents β, ν and ζ . As the critical temperature is approached ($T \rightarrow T_{cr}$) they become equal to the critical exponents of the zero-temperature three-dimensional theory.*

These exponents are plotted as function of the logarithm of $|T^2 - T_{cr}^2|$ in fig. 36. We notice that in the limit $T \rightarrow T_{cr}$ the critical exponents approach asymptotic values. These are independent of λ_R and therefore fall into universality classes determined only by N . They are equal to the critical exponents of the zero temperature three-dimensional theory. This fact can be understood by recalling that the evolution in the high-temperature region is determined by an effective three-dimensional theory whose phase diagram has a fixed point corresponding to the phase transition. For $T \rightarrow T_{cr}$ the evolution of $\rho_0(k, T), \lambda(k, T)$ in the high temperature region is given by a line in the phase diagram very close to the critical line. In this case $\rho_0(k, T), \lambda(k, T)$ spend an arbitrarily long “time” t close to the fixed point and, as a result, lose memory of their “initial values” $\rho_0(T/\theta_2, T), \lambda(T/\theta_2, T)$. The critical behaviour is determined solely by the fixed point. Our crude truncation for the potential results in the values $\beta = 0.25$, $\nu = \zeta = 0.5$, which can be compared with the more accurate ones presented in section 4 (cf. tables 2 and 5). Notice that these values satisfy the correct scaling law $\nu = 2\beta$ in the limit of zero wave-function renormalization.

The critical behaviour of $\lambda_R(T)$ is related to the resolution of the problem of the infrared divergences which cause the breakdown of the “naive” perturbative expansion in the limit $T \rightarrow T_{cr}$ [197, 199]. The infrared problem is manifest in the presence of higher order contributions to the effective potential which contain increasing powers of $\lambda_R(T)T/k$, where k is the effective infrared cutoff of the theory. If the evolution of $\lambda(k, T)$ is omitted and $\lambda_R(T)$ is approximated by its zero-temperature value λ_R , these contributions diverge and the

perturbative expansion breaks down. A similar situation appears for the zero-temperature three-dimensional theory in the critical region [200]. In this case the problem results from an effective expansion in terms of the quantity $u/[M^2 - M_{cr}^2]^{1/2}$, where u is the bare three-dimensional quartic coupling and $[M^2 - M_{cr}^2]^{1/2}$ is a measure of the distance from the point where the phase transition occurs as it is approached from the symmetric phase. The two situations can be seen to be of identical nature by simply remembering that the high-temperature four-dimensional coupling λ corresponds to an effective three-dimensional coupling λT and that the effective infrared cutoff in the symmetric phase is equal to $m_R(T)$. In the three-dimensional case the problem has been resolved [200] by a reformulation of the calculation in terms of an effective parameter λ_3/m , where λ_3 is the renormalized 1-PI four point function in three dimensions (the renormalized quartic coupling) and m the renormalized mass (equal to the inverse correlation length). It has been found [200, 123] that the above quantity has an infrared stable fixed point in the critical region $m \rightarrow 0$. No infrared divergences arise within this approach. Their only residual effect is detected in the strong renormalization of λ_3 . In our scheme the problem is formulated in terms of the effective dimensionless parameters $\tilde{\kappa}(k, T) = \rho_0(k, T)/kT$, $\tilde{\lambda}(k, T) = \lambda(k, T)T/k$ (see equations (7.29)), for which a fixed point corresponding to the phase transition is found. The critical behaviour is determined by this fixed point in the limit $k \rightarrow 0$. Everything remains finite in the vicinity of the critical temperature, and the only memory of the infrared divergences is reflected in the strong renormalization of $\lambda_R(T)$ near T_{cr} . We conclude that the infrared problem disappears if formulated in terms of the appropriate renormalized quantities. When expressed in the correct language, it becomes simply a manifestation of the strong renormalization effects in the critical region. In ref. [42] the quantity $\lambda_R(T)T/m_R(T)$ was calculated in the limit $T \rightarrow T_{cr}$. It reaches a universal asymptotic value depending only on N . For $N = 1$ we find $\lambda_R(T)T/m_R(T) = 6.8$ within our crude truncation, to be compared with the more accurate result $\lambda_R(T)T/m_R(T) \approx 8$ shown in table 6. Moreover, the existence of this asymptotic value explains the equality of the critical exponents ν and ζ .

Finally, we point out that the “non-universal quantities” as the critical temperature or the non-universal amplitudes are completely determined by the renormalized zero-temperature couplings λ_R , ρ_0 . No additional free parameters (amplitudes) appear in fig. 7.1. The microphysics at the scale Λ may not be known precisely, similarly to the situation often encountered in statistical mechanics. Nevertheless, most of the memory of the microphysics is already lost at the scale $k \approx T$, except from the relevant parameter ρ_0 and the marginal coupling λ_R . This predictive power for the amplitudes is an example of quantum universality.

8 Fermionic models

8.1 Introduction

Shortly after the discovery of asymptotic freedom [209] it was realized [210] that at sufficiently high temperature or density the theory of strongly interacting elementary particles, quantum chromodynamics (QCD), differs in important aspects from the corresponding zero temperature

or vacuum properties. A phase transition at some critical temperature T_c or a relatively sharp crossover may separate the high and low temperature physics [211]. At nonzero baryon density QCD is expected to have a rich phase structure with different possible phase transitions as the density varies [15, 16, 17, 30].

We will concentrate in the following on properties of the chiral phase transition in QCD and consider an application of the average action method to an effective fermionic model. The vacuum of QCD contains a condensate of quark–antiquark pairs, $\langle \bar{\psi}\psi \rangle \neq 0$, which spontaneously breaks the (approximate) chiral symmetry of QCD and has profound implications for the hadron spectrum. At high temperature this condensate is expected to melt, i.e. $\langle \bar{\psi}\psi \rangle \simeq 0$, which signals the chiral phase transition. We will investigate the chiral phase transition within the linear quark meson model [167] for two quark flavors. Truncated nonperturbative flow equations are derived at nonzero temperature [28] and chemical potential [212]. Whereas the renormalization group flow leads to spontaneous chiral symmetry breaking in vacuum, the symmetry gets restored in a second order phase transition at high temperature for vanishing quark mass. The description [28] covers both the low temperature chiral perturbation theory domain of validity as well as the high temperature domain of critical phenomena. In particular, we obtain a precise estimate of the universal equation of state in the vicinity of critical points. We explicitly connect the physics at zero temperature and realistic quark mass with the universal behavior near the critical temperature T_c and the chiral limit. An important property will be the observation that certain low energy properties are effectively independent of the details of the model even away from the phase transition. This behavior is caused by a strong attraction of the renormalization group flow to approximate partial infrared fixed points [167, 28]. Within this approach at high density we find [212] a chiral symmetry restoring first order transition. The results imply the presence of a critical endpoint in the phase diagram in the universality class of the three dimensional Ising model [29, 30]. The universal properties of this endpoint have been discussed in section 4.4. For details of the QCD aspects of this approach see the reviews [213] and [17] for a discussion of the phase diagram. Similar nonperturbative renormalization group studies of QCD motivated models can be found in [214, 215, 216]. Field theories with scalars and fermions have been investigated using similar techniques in [217, 218, 219, 220].

8.2 Linear quark meson model

We consider a Nambu–Jona-Lasinio type model for QCD in which quarks interact via effective fermionic interactions, with $a, b, c, d = 1, 2$ flavors and $i, j = 1, 2, 3$ colors. The model is defined at some “high” momentum scale $k_\Phi \approx 600 - 700$ MeV

$$\Gamma_{k_\Phi}[\bar{\psi}, \psi] = \int d^4x \{ \bar{\psi}_a^i(x) Z_{\psi, k_\Phi} [i\gamma^\mu \partial_\mu + m(x)\gamma_5] \psi_i^a(x) \} + \Gamma_{k_\Phi}^{(\text{int})}[\bar{\psi}, \psi] \quad (8.1)$$

with given fermion wave function renormalization constant Z_{ψ, k_Φ} . The curled brackets around the fermion bilinears in (8.1) indicate contractions over the Dirac spinor indices which are suppressed. For later purposes we allow for a non-constant mass term $m(x)\gamma_5$ and we

concentrate at the end on equal constant current quark masses $m = \frac{1}{2}(m_u + m_d)$.⁵⁷ The fermions interact via a four-fermion interaction which in momentum space is given by

$$\begin{aligned} \Gamma_{k_\Phi}^{(\text{int})}[\bar{\psi}, \psi] &= -\frac{1}{8} \int \left(\prod_{l=1}^4 \frac{d^4 p_l}{(2\pi)^4} \right) (2\pi)^4 \delta(p_1 + p_2 - p_3 - p_4) \bar{h}_{k_\Phi}^2 G(p_l) \\ &\quad \left[\{ \bar{\psi}_a^i(-p_1) i(\tau^z)_b^a \psi_i^b(p_2) \} \{ \bar{\psi}_c^j(p_4) i(\tau_z)_d^c \psi_j^d(-p_3) \} \right. \\ &\quad \left. + \{ \bar{\psi}_a^i(-p_1) \gamma^5 \psi_i^a(p_2) \} \{ \bar{\psi}_b^j(p_4) \gamma^5 \psi_j^b(-p_3) \} \right]. \end{aligned} \quad (8.2)$$

We consider a momentum dependent four-fermion interaction

$$G^{-1} = \bar{m}_{k_\Phi}^2 + Z_{\Phi, k_\Phi} (p_1 + p_2)^2 \quad (8.3)$$

The action is invariant under the chiral flavor group $SU(2)_L \times SU(2)_R$ except for the mass term.

Let us define composite fields

$$\begin{aligned} O^z[\bar{\psi}, \psi; q] &= -\frac{1}{2} \int \frac{d^4 p}{(2\pi)^4} \bar{h} \bar{\psi}_a^i(p) i(\tau^z)_b^a \psi_i^b(q+p), \\ O_{(5)}[\bar{\psi}, \psi; q] &= -\frac{1}{2} \int \frac{d^4 p}{(2\pi)^4} \bar{h} \bar{\psi}_a^i(p) \gamma^5 \psi_i^a(q+p) \end{aligned} \quad (8.4)$$

and rewrite

$$\begin{aligned} \Gamma_{k_\Phi}[\bar{\psi}, \psi] &= -\int \frac{d^4 q}{(2\pi)^4} \left\{ Z_{\psi, k_\Phi} \bar{\psi}_a^i(q) \gamma^\mu q_\mu \psi_i^a(q) + 2\bar{h}^{-1} Z_{\psi, k_\Phi} m(q) O_{(5)}[\bar{\psi}, \psi; -q] \right. \\ &\quad \left. + \frac{1}{2} G(q^2) \left(O^z[\bar{\psi}, \psi; -q] O_z[\bar{\psi}, \psi; q] + O_{(5)}[\bar{\psi}, \psi; -q] O_{(5)}[\bar{\psi}, \psi; q] \right) \right\}. \end{aligned} \quad (8.5)$$

It is advantageous to consider an equivalent formulation which introduces bosonic collective fields with the quantum numbers of the fermion bilinears appearing in (8.5). This amounts to replace the effective action (8.1) by

$$\begin{aligned} \hat{\Gamma}_{k_\Phi}[\bar{\psi}, \psi; s, \pi] &\equiv \Gamma_{k_\Phi}[\bar{\psi}, \psi] + \int \frac{d^4 q}{(2\pi)^4} \left(s(-q) - 2Z_{\psi, k_\Phi} \bar{h}^{-1} m(-q) - O_{(5)}(-q) G(q^2) \right) \\ &\quad \left(s(q) - 2Z_{\psi, k_\Phi} \bar{h}^{-1} m(q) - O_{(5)}(q) G(q^2) \right) \frac{1}{2G(q^2)} \\ &\quad + \int \frac{d^4 q}{(2\pi)^4} \left(\pi^z(-q) - O^z(-q) G(q^2) \right) \left(\pi_z(q) - O_z(q) G(q^2) \right) \frac{1}{2G(q^2)}. \end{aligned} \quad (8.6)$$

The scalar fields π^z and s have the quantum numbers of the pions and the σ -field. The terms added to $\Gamma_{k_\Phi}[\bar{\psi}, \psi]$ are quadratic in the fermion bilinears. They cancel the original four-fermion interaction (8.2) and introduce a Yukawa interaction between fermions and collective

⁵⁷We use chiral conventions in which the (real) mass term is multiplied by γ_5 . The more common version of the fermion mass term can be obtained by a chiral rotation.

fields, as well as a propagator term for the collective fields:

$$\begin{aligned}
\hat{\Gamma}_{k_\Phi}[\bar{\psi}, \psi; s, \pi] &= \int \frac{d^4 q}{(2\pi)^4} \left\{ -Z_{\psi, k_\Phi} \bar{\psi}_a^i(q) \gamma^\mu q_\mu \psi_i^a(q) \right. \\
&+ \frac{1}{2} [Z_{\Phi, k_\Phi} q^2 + \bar{m}_{k_\Phi}^2] \left(s(-q)s(q) + \pi^z(-q)\pi_z(q) \right) - j(-q)s(q) \\
&\left. + \int \frac{d^4 p}{(2\pi)^4} \bar{\psi}_a^i(p) \frac{\bar{h}\gamma_5}{2} \left(s(q)\delta_b^a + i\pi^z(q)(\tau_z)_b^a \gamma^5 \right) \psi_i^b(p-q) \right\}
\end{aligned} \tag{8.7}$$

where we dropped field independent terms in (8.6). The above replacement of $\Gamma_{k_\Phi}[\bar{\psi}, \psi]$ by $\hat{\Gamma}_{k_\Phi}[\bar{\psi}, \psi; s, \pi]$ corresponds to a Hubbard-Stratonovich transformation in the defining functional integral for the effective action, in which the collective fields are introduced by inserting identities into the functional integral. The introduction of collective fields in the context of flow equations is discussed in refs. [78, 28]. The equivalence of $\hat{\Gamma}_{k_\Phi}[\bar{\psi}, \psi; s, \pi]$ with the original formulation in terms of fundamental fields only is readily established by solving the field equations for s and π

$$\begin{aligned}
\frac{\delta \hat{\Gamma}_{k_\Phi}[\bar{\psi}, \psi; s, \pi]}{\delta s} &= 0 \quad , \quad s_0 = GO_{(5)}[\bar{\psi}, \psi] + 2Z_{\psi, k_\Phi} \bar{h}^{-1} m \\
\frac{\delta \hat{\Gamma}_{k_\Phi}[\bar{\psi}, \psi; s, \pi]}{\delta \pi^z} &= 0 \quad , \quad \pi_0^z = GO^z[\bar{\psi}, \psi]
\end{aligned} \tag{8.8}$$

and inserting the solution in the effective action $\hat{\Gamma}_{k_\Phi}[\bar{\psi}, \psi; s_0, \pi_0] = \Gamma_{k_\Phi}[\bar{\psi}, \psi]$. The $SU(2)_L \times SU(2)_R$ symmetry is most manifest in a 2×2 matrix notation

$$\Phi \equiv \frac{1}{2} (s + i\pi^z \tau_z) \tag{8.9}$$

The quark mass term in the original fermionic description appears now as a source term which is proportional to m

$$j(q) \equiv 2\bar{h}^{-1} Z_{\psi, k_\Phi} m(q) (\bar{m}_{k_\Phi}^2 + Z_{\Phi, k_\Phi} q^2) . \tag{8.10}$$

We will be mainly interested in momentum independent sources $j(q \equiv 0)$ or constant fermion masses. Since the chiral symmetry breaking is linear in Φ we can define a chirally symmetric effective action

$$\Gamma_k[\psi, \Phi] = \hat{\Gamma}_k[\bar{\psi}, \psi; s, \pi] + \int d^4 x j \text{tr} \Phi \tag{8.11}$$

The flow of Γ_k will conserve the chiral symmetries. The explicit chiral symmetry is now reflected by the field equation

$$\frac{\delta \Gamma_k}{\delta s} = j \tag{8.12}$$

Knowledge of Γ_0 for an arbitrary constant field $\Phi = \text{diag}(\bar{\sigma}_0, \bar{\sigma}_0)$ contains the information on the model for arbitrary quark masses. Spontaneous chiral symmetry breaking manifests itself by $\bar{\sigma}_0 \neq 0$ for $j \rightarrow 0$. Our approach allows therefore for a simple unified treatment of spontaneous and explicit chiral symmetry breaking.

The effective action at the scale k_Φ specifies the “initial condition” for the renormalization flow of the average action Γ_k . For scales $k < k_\Phi$ we allow for a more general form and consider a truncation ($\rho = (s^2 + \pi^z \pi_z)/2 = \text{tr} \Phi^\dagger \Phi$)

$$\Gamma_k[\psi, \Phi] = \int d^4x \left\{ i Z_{\psi,k} \bar{\psi}_a^i \gamma^\mu \partial_\mu \psi_i^a + \bar{h}_k \bar{\psi}_a^i \left[\frac{1 + \gamma^5}{2} \Phi^a{}_b - \frac{1 - \gamma^5}{2} (\Phi^\dagger)^a{}_b \right] \psi_i^b + Z_{\Phi,k} \partial_\mu (\Phi^\dagger)_{ab} \partial^\mu \Phi^{ba} + U_k(\rho) \right\}. \quad (8.13)$$

which takes into account the most general field dependence of the $O(4)$ -symmetric average potential U_k . Here $Z_{\Phi,k}$ and $Z_{\psi,k}$ denote scale dependent wave function renormalizations for the bosonic fields and the fermionic fields, respectively. We note that in our conventions the scale dependent Yukawa coupling \bar{h}_k is real.

In terms of the renormalized expectation value

$$\sigma_0 = Z_\Phi^{1/2} \bar{\sigma}_0 \quad (8.14)$$

we obtain the following expressions for quantities as the pion decay constant f_π , chiral condensate $\langle \bar{\psi} \psi \rangle$, constituent quark mass M_q and pion and sigma mass, m_π and m_σ , respectively ($d = 4$) [28]

$$\begin{aligned} f_{\pi,k} &= 2\sigma_{0,k}, \\ \langle \bar{\psi} \psi \rangle_k &= -2\bar{m}_{k_\Phi}^2 \left[Z_{\Phi,k}^{-1/2} \sigma_{0,k} - m \right], \\ M_{q,k} &= h_k \sigma_{0,k}, \\ m_{\pi,k}^2 &= Z_{\Phi,k}^{-1/2} \frac{\bar{m}_{k_\Phi}^2 m}{\sigma_{0,k}} = Z_{\Phi,k}^{-1/2} \frac{J}{2\sigma_{0,k}}, \\ m_{\sigma,k}^2 &= Z_{\Phi,k}^{-1/2} \frac{\bar{m}_{k_\Phi}^2 m}{\sigma_{0,k}} + 4\lambda_k \sigma_{0,k}^2. \end{aligned} \quad (8.15)$$

Here we have defined the dimensionless, renormalized couplings

$$\begin{aligned} \lambda_k &= Z_{\Phi,k}^{-2} \frac{\partial^2 U_k}{\partial \rho^2} (\rho = 2\bar{\sigma}_{0,k}^2), \\ h_k &= Z_{\Phi,k}^{-1/2} Z_{\psi,k}^{-1} \bar{h}_k. \end{aligned} \quad (8.16)$$

We are interested in the “physical values” of the quantities (8.15) in the limit $k \rightarrow 0$ where the infrared cutoff is removed, i.e. $f_\pi = f_{\pi,k=0}$, $m_\pi^2 = m_{\pi,k=0}^2$, etc.

8.3 Flow equations and infrared stability

The dependence of the effective action Γ_k on the infrared cutoff scale k is given by the exact flow equation (7.15) or (2.19) for fermionic fields ψ (quarks) and bosonic fields Φ (mesons) [9, 81], ($t = \ln(k/k_\Phi)$)

$$\frac{\partial}{\partial t} \Gamma_k[\psi, \Phi] = \frac{1}{2} \text{Tr} \left\{ \frac{\partial R_{kB}}{\partial t} \left(\Gamma_k^{(2)}[\psi, \Phi] + R_k \right)^{-1} \right\} - \text{Tr} \left\{ \frac{\partial R_{kF}}{\partial t} \left(\Gamma_k^{(2)}[\psi, \Phi] + R_k \right)^{-1} \right\}. \quad (8.17)$$

Here $\Gamma_k^{(2)}$ is the matrix of second functional derivatives of Γ_k with respect to both fermionic and bosonic field components. The first trace in the rhs of (8.17) effectively runs only over the bosonic degrees of freedom. It implies a momentum integration and a summation over flavor indices. The second trace runs over the fermionic degrees of freedom and contains in addition a summation over Dirac and color indices. The infrared cutoff function R_k has a block substructure with entries R_{kB} and R_{kF} for the bosonic and the fermionic fields, respectively (cf. section 7.2). We compute the flow equation for the effective potential U_k from equation (8.17) using the ansatz (8.13) for Γ_k . The bosonic contribution to the running effective potential corresponds exactly to eq. (2.36) for the scalar $O(4)$ model in lowest order of the derivative expansion. The fermionic contribution to the evolution equation for the effective potential can be computed without much additional effort from (8.13) since the fermionic fields appear only quadratically. The respective flow equation is obtained by taking the second functional derivative evaluated at $\psi = \bar{\psi} = 0$.

For the study of phase transitions it is convenient to work with rescaled, dimensionless and renormalized variables. We introduce (with a generalization to arbitrary dimension d)

$$u(t, \tilde{\rho}) \equiv k^{-d} U_k(\rho), \quad \tilde{\rho} \equiv Z_{\Phi, k} k^{2-d} \rho, \quad h_k = Z_{\Phi, k}^{-1/2} Z_{\psi, k}^{-1} k^{d-4} \bar{h}_k. \quad (8.18)$$

Combining the bosonic and the fermionic contributions one obtains the flow equation [28]

$$\begin{aligned} \frac{\partial}{\partial t} u &= -du + (d - 2 + \eta_{\Phi}) \tilde{\rho} u' \\ &+ 2v_d \left\{ 3l_0^d(u'; \eta_{\Phi}) + l_0^d(u' + 2\tilde{\rho}u''; \eta_{\Phi}) - 2^{\frac{d}{2}+1} 3l_0^{(F)d} \left(\frac{1}{2} \tilde{\rho} h^2; \eta_{\psi} \right) \right\}. \end{aligned} \quad (8.19)$$

Here $v_d^{-1} \equiv 2^{d+1} \pi^{d/2} \Gamma(d/2)$ and primes denote derivatives with respect to $\tilde{\rho}$. The bosonic, l_0^d , and the fermionic, $l_0^{(F)d}$, threshold functions are defined in section 3.2 and appendix A. The first two terms of the second line in (8.19) denote the contributions from the pions and the σ field, and the last term corresponds to the fermionic contribution from the u, d quarks.

Eq. (8.19) is a partial differential equation for the effective potential $u(t, \tilde{\rho})$ which has to be supplemented by the flow equation for the Yukawa coupling h_k and expressions for the anomalous dimensions, where

$$\eta_{\Phi} = \frac{d}{dt} (\ln Z_{\Phi, k}) \quad , \quad \eta_{\psi} = \frac{d}{dt} (\ln Z_{\psi, k}) . \quad (8.20)$$

Here the wave function renormalizations are evaluated for a k -dependent background field $\rho_{0, k}$ or $\kappa \equiv k^{2-d} Z_{\Phi, k} \rho_{0, k}^2$ determined by the condition

$$u'(t, \kappa) = \frac{j_0}{\sqrt{2\kappa}} k^{-\frac{d+2}{2}} Z_{\Phi, k}^{-1/2} \equiv \epsilon_g , \quad (8.21)$$

with j_0 some fixed source. For a study of realistic quark masses the optimal choice is given by (8.10), whereas an investigation of the universal critical behavior for $m_q \rightarrow 0$ should employ $j_0 = 0$. Equation (8.21) allows us to follow the flow of κ according to

$$\frac{d}{dt} \kappa = \frac{\kappa}{\epsilon_g + 2\kappa\lambda} \left\{ [\eta_{\Phi} - d - 2] \epsilon_g - 2 \frac{\partial}{\partial t} u'(t, \kappa) \right\} \quad (8.22)$$

with $\lambda \equiv u''(t, \kappa)$. We also define the Yukawa coupling at $\tilde{\rho} = \kappa$ and its flow equation reads [167, 221]

$$\begin{aligned}
\frac{d}{dt}h^2 &= (d - 4 + 2\eta_\psi + \eta_\phi) h^2 \\
&- 2v_d h^4 \left\{ 3l_{1,1}^{(FB)d} \left(\frac{1}{2}h^2\kappa, \epsilon_g; \eta_\psi, \eta_\Phi \right) - l_{1,1}^{(FB)d} \left(\frac{1}{2}h^2\kappa, \epsilon_g + 2\lambda\kappa; \eta_\psi, \eta_\Phi \right) \right\} \\
&+ 4v_d h^4 \kappa \left\{ 3\lambda l_{1,2}^{(FB)d} \left(\frac{1}{2}h^2\kappa, \epsilon_g; \eta_\psi, \eta_\Phi \right) \right. \\
&- \left. (3\lambda + 2\kappa u'''(\kappa)) l_{1,2}^{(FB)d} \left(\frac{1}{2}h^2\kappa, \epsilon_g + 2\lambda\kappa; \eta_\psi, \eta_\Phi \right) \right\} \\
&+ 2v_d h^6 \kappa \left\{ 3l_{2,1}^{(FB)d} \left(\frac{1}{2}h^2\kappa, \epsilon_g; \eta_\psi, \eta_\Phi \right) - l_{2,1}^{(FB)d} \left(\frac{1}{2}h^2\kappa, \epsilon_g + 2\lambda\kappa; \eta_\psi, \eta_\Phi \right) \right\}. \quad (8.23)
\end{aligned}$$

Similarly, the scalar anomalous dimension is inferred from

$$\begin{aligned}
\eta_\Phi &\equiv -\frac{d}{dt} \ln Z_{\Phi,k} = 4\frac{v_d}{d} \left\{ 4\kappa\lambda^2 m_{2,2}^d(\epsilon_g, \epsilon_g + 2\lambda\kappa; \eta_\Phi) \right. \\
&+ \left. 2^{\frac{d}{2}} N_c h^2 m_4^{(F)d} \left(\frac{1}{2}h^2\kappa; \eta_\psi \right) + 2^{\frac{d}{2}-1} N_c h^4 \kappa m_2^{(F)d} \left(\frac{1}{2}h^2\kappa; \eta_\psi \right) \right\} \quad (8.24)
\end{aligned}$$

and the quark anomalous dimension reads

$$\begin{aligned}
\eta_\psi &\equiv -\frac{d}{dt} \ln Z_{\psi,k} = 2\frac{v_d}{d} h^2 \left\{ 3m_{1,2}^{(FB)d} \left(\frac{1}{2}h^2\kappa, \epsilon_g; \eta_\psi, \eta_\Phi \right) \right. \\
&+ \left. m_{1,2}^{(FB)d} \left(\frac{1}{2}h^2\kappa, \epsilon_g + 2\lambda\kappa; \eta_\psi, \eta_\Phi \right) \right\}, \quad (8.25)
\end{aligned}$$

which constitutes a linear set of equations for the anomalous dimensions. The threshold functions $l_{n_1, n_2}^{(FB)d}$, m_{n_1, n_2}^d , $m_2^{(F)d}$, $m_4^{(F)d}$ and $m_{n_1, n_2}^{(FB)d}$ are specified in appendix A.

Most importantly for practical applications to QCD, the system of flow equations for the effective potential $U_k(\rho)$, the Yukawa coupling h_k and the wave function renormalizations $Z_{\Phi,k}$, $Z_{\psi,k}$ exhibits an approximate partial fixed point [167, 28]. For a small initial value of the scalar wave function renormalization, $Z_{\Phi, k_\Phi} \ll 1$ at the scale k_Φ , one observes a large renormalized meson mass term $Z_{\Phi, k_\Phi}^{-2} U'_{k_\Phi}$ and a large renormalized Yukawa coupling $h_{k_\Phi} = Z_{\Phi, k_\Phi}^{-1/2} \bar{h}_{k_\Phi}$ (for $Z_{\psi, k_\Phi} = 1$). In this case, for the initial running one can neglect in the flow equations all scalar contributions with threshold functions involving the large meson masses. This yields the simplified equations [28, 167] for the rescaled quantities ($d = 4, v_4^{-1} = 32\pi^2$)

$$\begin{aligned}
\frac{\partial}{\partial t} u &= -4u + (2 + \eta_\Phi) \tilde{\rho} u' - \frac{N_c}{2\pi^2} l_0^{(F)4} \left(\frac{1}{2} \tilde{\rho} h^2 \right), \\
\frac{d}{dt} h^2 &= \eta_\Phi h^2, \\
\eta_\Phi &= \frac{N_c}{8\pi^2} h^2, \\
\eta_\psi &= 0.
\end{aligned} \quad (8.26)$$

Of course, this approximation is only valid for the initial range of running below k_Φ before the (dimensionless) renormalized scalar mass squared $u'(t, \tilde{\rho} = 0)$ approaches zero near the chiral symmetry breaking scale. The system (8.26) is exactly soluble and we find [28]

$$\begin{aligned} h^2(t) &= Z_\Phi^{-1}(t) = \frac{h_I^2}{1 - \frac{N_c}{8\pi^2} h_I^2 t}, \\ u(t, \tilde{\rho}) &= e^{-4t} u_I(e^{2t} \tilde{\rho} \frac{h^2(t)}{h_I^2}) - \frac{N_c}{2\pi^2} \int_0^t dr e^{-4r} l_0^{(F)4} \left(\frac{1}{2} h^2(t) \tilde{\rho} e^{2r} \right). \end{aligned} \quad (8.27)$$

Here $u_I(\tilde{\rho}) \equiv u(0, \tilde{\rho})$ denotes the effective average potential at the scale k_Φ and h_I^2 is the initial value of h^2 at k_Φ , i.e. for $t = 0$. To make the behavior more transparent we consider an expansion of the initial value effective potential $u_I(\tilde{\rho})$ in powers of $\tilde{\rho}$ around $\tilde{\rho} = 0$

$$u_I(\tilde{\rho}) = \sum_{n=0}^{\infty} \frac{u_I^{(n)}(0)}{n!} \tilde{\rho}^n. \quad (8.28)$$

Expanding also $l_0^{(F)4}$ in eq. (8.27) in powers of its argument one finds for $n > 2$

$$\frac{u^{(n)}(t, 0)}{h^{2n}(t)} = e^{2(n-2)t} \frac{u_I^{(n)}(0)}{h_I^{2n}} + \frac{N_c}{\pi^2} \frac{(-1)^n (n-1)!}{2^{n+2} (n-2)} l_n^{(F)4}(0) [1 - e^{2(n-2)t}]. \quad (8.29)$$

For decreasing $t \rightarrow -\infty$ the initial values $u_I^{(n)}$ become rapidly unimportant and $u^{(n)}/h^{2n}$ approaches a fixed point. For $n = 2$, i.e., for the quartic coupling, one finds

$$\frac{u^{(2)}(t, 0)}{h^2(t)} = 1 - \frac{1 - \frac{u_I^{(2)}(0)}{h_I^2}}{1 - \frac{N_c}{8\pi^2} h_I^2 t} \quad (8.30)$$

leading to a fixed point value $(u^{(2)}/h^2)_* = 1$. As a consequence of this fixed point behavior the system loses all its ‘‘memory’’ on the initial values $u_I^{(n \geq 2)}$ at the compositeness scale k_Φ ! Furthermore, the attraction to partial infrared fixed points continues also for the range of k where the scalar fluctuations cannot be neglected anymore.

On the other hand, the initial value for the bare dimensionless mass parameter

$$\frac{u_I'(0)}{h_I^2} = \frac{\overline{m}_{k_\Phi}^2}{k_\Phi^2} \quad (8.31)$$

is never negligible. In other words, for $h_I \rightarrow \infty$ the infrared behavior of the linear quark meson model will depend (in addition to the value of the compositeness scale k_Φ and the quark mass m) only on one parameter, $\overline{m}_{k_\Phi}^2$. One can therefore add higher scalar self-interactions to Γ_{k_Φ} in eq. (8.7) without changing the result much. We have numerically verified this feature by starting with different values for the quartic scalar self-interaction $u_I^{(2)}(0)$. Indeed, the differences in the physical observables were found to be small. For definiteness, the numerical analysis of the full system of flow equations [28] is performed with the idealized initial value $u_I(\tilde{\rho}) = u_I'(0)\tilde{\rho}$ in the limit $h_I^2 \rightarrow \infty$. Deviations from this idealization lead only to small numerical deviations in the infrared behavior of the linear quark meson model as long as say $h_I \gtrsim 15$.

8.4 High temperature chiral phase transition

Strong interactions in thermal equilibrium at high temperature T differ in important aspects from the well tested vacuum or zero temperature properties. A phase transition at some critical temperature T_c or a relatively sharp crossover may separate the high and low temperature physics [211]. It was realized early that the transition should be closely related to a qualitative change in the chiral condensate according to the general observation that spontaneous symmetry breaking tends to be absent in a high temperature situation. A series of stimulating contributions [24, 26, 27] pointed out that for sufficiently small up and down quark masses, m_u and m_d , and for a sufficiently large mass of the strange quark, m_s , the chiral transition is expected to belong to the universality class of the $O(4)$ Heisenberg model. It was suggested [26, 27] that a large correlation length may be responsible for important fluctuations or lead to a disoriented chiral condensate. One main question we are going to answer using non-perturbative flow equations for the linear quark meson model is: How small m_u and m_d would have to be in order to see a large correlation length near T_c and if this scenario could be realized for realistic values of the current quark masses.

In order to solve our model we need to specify the “initial condition” Γ_{k_Φ} for the renormalization flow of Γ_k . We will choose in the following a normalization of ψ, Φ such that $Z_{\psi, k_\Phi} = \bar{h}_{k_\Phi} = 1$. We therefore need as initial values at the scale k_Φ the scalar wave function renormalization Z_{Φ, k_Φ} and the shape of the potential U_{k_Φ} . We will make here the important assumption that $Z_{\Phi, k}$ is small at the compositeness scale k_Φ (similarly to what is usually assumed in Nambu–Jona-Lasinio–like models)

$$Z_{\Phi, k_\Phi} \ll 1. \quad (8.32)$$

This results in a large value of the renormalized Yukawa coupling $h_k = Z_{\Phi, k}^{-1/2} Z_{\psi, k}^{-1} \bar{h}_k$. A large value of h_{k_Φ} is phenomenologically suggested by the comparably large value of the constituent quark mass M_q . The latter is related to the value of the Yukawa coupling for $k \rightarrow 0$ and the pion decay constant $f_\pi = 92.4\text{MeV}$ by $M_q = hf_\pi/2$ (with $h = h_{k=0}$), and $M_q \simeq 300\text{MeV}$ implies $h^2/4\pi \simeq 3.4$. For increasing k the value of the Yukawa coupling grows rapidly for $k \gtrsim M_q$. Our assumption of a large initial value for h_{k_Φ} is therefore equivalent to the assumption that the truncation (8.13) can be used up to the vicinity of the Landau pole of h_k . The existence of a strong Yukawa coupling enhances the predictive power of our approach considerably. It implies a fast approach of the running couplings to partial infrared fixed points as shown in section 8.3 [167, 28]. In consequence, the detailed form of U_{k_Φ} becomes unimportant, except for the value of one relevant parameter corresponding to the scalar mass term $\bar{m}_{k_\Phi}^2$. In this work we fix $\bar{m}_{k_\Phi}^2$ such that $f_\pi = 92.4\text{MeV}$ for $m_\pi = 135\text{MeV}$. The value $f_\pi = 92.4\text{MeV}$ (for $m_\pi = 135\text{MeV}$) sets our unit of mass for two flavor QCD which is, of course, not directly accessible by observation. Besides $\bar{m}_{k_\Phi}^2$ (or f_π) the other input parameter used in this work is the constituent quark mass M_q which determines the scale k_Φ at which h_{k_Φ} becomes very large. We consider a range $300\text{MeV} \lesssim M_q \lesssim 350\text{MeV}$ and find a rather weak dependence of our results on the precise value of M_q . The results presented in the following are for $M_q = 303\text{MeV}$.

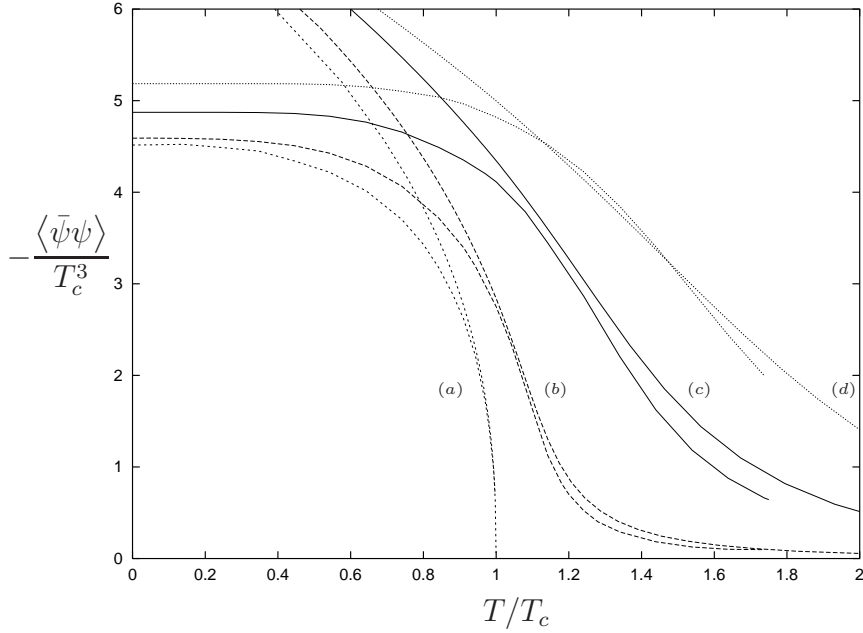


Figure 37: *Chiral equation of state for a phase transition or crossover in two-flavor QCD. The plot shows the chiral condensate $\langle\bar{\psi}\psi\rangle$ as a function of temperature T . Lines (a), (b), (c), (d) correspond at zero temperature to $m_\pi = 0, 45\text{MeV}, 135\text{MeV}, 230\text{MeV}$, respectively. For each pair of curves the lower one represents the full T -dependence of $\langle\bar{\psi}\psi\rangle$ whereas the upper one shows for comparison the universal scaling form of the equation of state for the $O(4)$ Heisenberg model (cf. fig. 6). The critical temperature for zero quark mass is $T_c = 100.7\text{MeV}$. The chiral condensate is normalized at a scale $k_\Phi \simeq 620\text{MeV}$.*

We first consider the model at nonzero temperature T . The case for nonvanishing baryon number density will be presented in section 8.5. Figure 37 shows our results [28] for the chiral condensate $\langle\bar{\psi}\psi\rangle$ as a function of the temperature T for various values of the average quark mass $m = (m_u + m_d)/2$. Curve (a) gives the temperature dependence of $\langle\bar{\psi}\psi\rangle$ in the chiral limit $m = 0$. We first consider only the lower curve which corresponds to the full result. One observes that the order parameter $\langle\bar{\psi}\psi\rangle$ goes continuously (but non-analytically) to zero as T approaches the critical temperature in the massless limit $T_c = 100.7\text{MeV}$. The transition from the phase with spontaneous chiral symmetry breaking to the symmetric phase is second order. The curves (b), (c) and (d) are for non-vanishing values of the average current quark mass m . The transition turns into a smooth crossover. Curve (c) corresponds to m_{phys} or, equivalently, $m_\pi(T = 0) = 135\text{MeV}$. The transition turns out to be much less dramatic than for $m = 0$. We have also plotted in curve (b) the results for comparably small quark masses $\simeq 1\text{MeV}$, i.e. $m = m_{\text{phys}}/10$, for which the $T = 0$ value of m_π equals 45MeV . The crossover is considerably sharper but a substantial deviation from the chiral limit remains even for such small values of m .

For comparison, the upper curves in figure 37 use the universal scaling form of the equation of state of the *three dimensional* $O(4)$ -symmetric Heisenberg model which has been computed explicitly in section 4.3. The scaling equation of state in terms of the chiral condensate for

m_π/MeV	0	45	135	230
T_{pc}/MeV	100.7	$\simeq 110$	$\simeq 130$	$\simeq 150$

Table 10: *Critical and “pseudocritical” temperature for various values of the zero temperature pion mass. Here T_{pc} is defined as the inflection point of $\langle\bar{\psi}\psi\rangle(T)$.*

the general case of a temperature and quark mass dependence is

$$\langle\bar{\psi}\psi\rangle = -\bar{m}_{k_\Phi}^2 T_c \left(\frac{j/T_c^3}{f(x)}\right)^{1/\delta} + j \quad (8.33)$$

as a function of $T/T_c = 1 + x(j/T_c^3 f(x))^{1/\beta\delta}$. The curves shown in figure 37 correspond to quark masses $m = 0$, $m = m_{\text{phys}}/10$, $m = m_{\text{phys}}$ and $m = 3.5m_{\text{phys}}$ or, equivalently, to zero temperature pion masses $m_\pi = 0$, $m_\pi = 45\text{MeV}$, $m_\pi = 135\text{MeV}$ and $m_\pi = 230\text{MeV}$, respectively. We see perfect agreement of both curves in the chiral limit for T sufficiently close to T_c which is a manifestation of universality and the phenomenon of dimensional reduction. In particular, we reproduce the critical exponents of the $O(4)$ -model given in table 3 of section 4.3. Away from the chiral limit we find for a realistic pion mass that the $O(4)$ universal equation of state provides a reasonable approximation for $\langle\bar{\psi}\psi\rangle$ in the crossover region $T = (1.2 - 1.5)T_c$.

In order to facilitate comparison with lattice simulations which are typically performed for larger values of m_π we also present results for $m_\pi(T = 0) = 230\text{MeV}$ in curve (d). One may define a “pseudocritical temperature” T_{pc} associated to the smooth crossover as the inflection point of $\langle\bar{\psi}\psi\rangle(T)$. Our results for T_{pc} are presented in table 10 for the four different values of m or, equivalently, $m_\pi(T = 0)$. The value for the pseudocritical temperature for $m_\pi = 230\text{MeV}$ compares well with the lattice results for two flavor QCD. This may be taken as an indication that the linear quark meson model gives a reasonable picture of the chiral properties in two-flavor QCD. An extension of the truncation for the linear quark meson model may lead to corrections in the value of T_c , but we do not expect qualitative changes of the overall picture. One should mention, though, that a determination of T_{pc} according to this definition is subject to sizeable numerical uncertainties for large pion masses as the curve in figure 37 is almost linear around the inflection point for quite a large temperature range. A problematic point in lattice simulations is the extrapolation to realistic values of m_π or even to the chiral limit. Our results may serve here as an analytic guide. The overall picture shows the approximate validity of the $O(4)$ scaling behavior over a large temperature interval in the vicinity of and above T_c once the (non-universal) amplitudes are properly computed. We point out that the link between the universal behavior near T_c and zero current quark mass on the one hand and the known physical properties at $T = 0$ for realistic quark masses on the other hand is crucial to obtain all non-universal information near T_c .

A second important result is the temperature dependence of the space-like pion correlation length $m_\pi^{-1}(T)$. (We will often call $m_\pi(T)$ the temperature dependent pion mass since it coincides with the physical pion mass for $T = 0$.) Figure 38 shows $m_\pi(T)$ and one again observes the second order phase transition in the chiral limit $m = 0$. For $T < T_c$

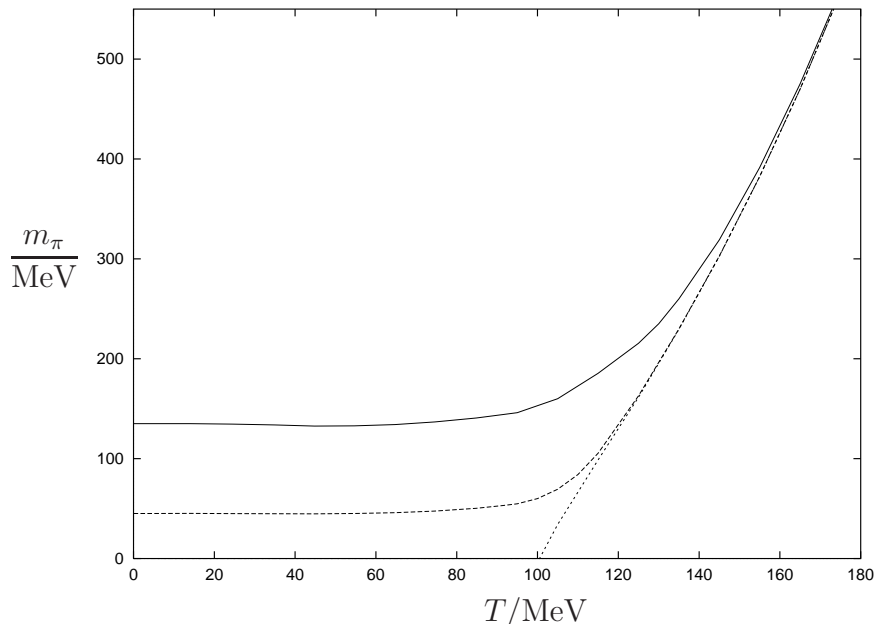


Figure 38: *Temperature dependence of the pion mass: The plot shows m_π as a function of temperature T for three different values of the average light current quark mass m . The solid line corresponds to the realistic value $m = m_{\text{phys}}$ whereas the dotted line represents the situation without explicit chiral symmetry breaking, i.e., $m = 0$. The intermediate, dashed line assumes $m = m_{\text{phys}}/10$.*

the pions are massless Goldstone bosons whereas for $T > T_c$ they form with the sigma a degenerate vector of $O(4)$ with mass increasing as a function of temperature. For $m = 0$ the behavior for small positive $T - T_c$ is characterized by the critical exponent ν , i.e. $m_\pi(T) = (\xi^+)^{-1} T_c ((T - T_c)/T_c)^\nu$ and we obtain $\nu = 0.787$, $\xi^+ = 0.270$. For $m > 0$ we find that $m_\pi(T)$ remains almost constant for $T \lesssim T_c$ with only a very slight dip for T near $T_c/2$. For $T > T_c$ the correlation length decreases rapidly and for $T \gg T_c$ the precise value of m becomes irrelevant. We see that the universal critical behavior near T_c is quite smoothly connected to $T = 0$. The full functional dependence of $m_\pi(T, m)$ allows us to compute the overall size of the pion correlation length near the critical temperature and we find $m_\pi(T_{pc}) \simeq 1.7m_\pi(0)$ for the realistic value m_{phys} . This correlation length is even smaller than the vacuum ($T = 0$) one and gives no indication for strong fluctuations of pions with long wavelength.⁵⁸ We will discuss the possibility of a tricritical point with a massless excitation in the two-flavor case at non-zero baryon number density in section 8.6. We also point out that the present investigation for the two flavor case does not take into account a possible “effective restoration” of the axial $U_A(1)$ symmetry at high temperature [24, 222].

⁵⁸For a QCD phase transition far from equilibrium long wavelength modes of the pion field can be amplified [26, 27].

8.5 Renormalization flow at nonzero chemical potential

At nonzero temperature and chemical potential μ associated to the conserved quark number we consider the following ansatz for Γ_k

$$\Gamma_k = \int_0^{1/T} dx^0 \int d^3x \left\{ i\bar{\psi}_i^a (\gamma^\mu \partial_\mu + \mu\gamma^0) \psi_a^i + \bar{h}_k \bar{\psi}_i^a \left[\frac{1+\gamma^5}{2} \Phi_a^b - \frac{1-\gamma^5}{2} (\Phi^\dagger)_a^b \right] \psi_b^i + Z_{\Phi,k} \partial_\mu \Phi_{ab}^* \partial^\mu \Phi^{ab} + U_k(\rho; \mu, T) \right\}. \quad (8.34)$$

A nonzero μ to lowest order results in the term $\sim i\mu\bar{\psi}^a\gamma^0\psi_a$ appearing in the rhs of (8.34). We neglect here the running of the fermionic wave function renormalization constant and the dependence of $Z_{\Phi,k}$ and \bar{h}_k on μ and T . The temperature dependence of $Z_{\Phi,k}$ and \bar{h}_k , which has been taken into account for the results presented in section 8.4, is indeed small [28]. We also neglect a possible difference in normalization of the quark kinetic term and the baryon number current.

There is a substantial caveat concerning the approximation (8.34) at nonzero density. At sufficiently high density diquark condensates form, opening up a gap at the quark Fermi surfaces [223, 224]. In order to describe this phenomenon in the present framework, the above ansatz for Γ_k has to be extended to include diquark degrees of freedom. However, a nonzero diquark condensate only marginally affects the equation of state for the chiral condensate [29]. In particular, in the two flavor case the inclusion of diquark degrees of freedom hardly changes the behavior of the chiral condensate at nonzero density and the order of the transition to the chirally symmetric phase. For NJL-type models diquark condensation is suppressed at low density by the presence of the chiral condensate [29, 225]. We therefore expect the ansatz (8.34) to give a good description of the restoration of chiral symmetry within the present model. It is straightforward to generalize our method to include diquark degrees of freedom. For simplicity we concentrate here on the chiral properties and neglect the superconducting properties at high densities.

We employ the same exponential infrared cutoff function for the bosonic fields R_{kB} (2.17) as in the previous section at nonzero temperature. At nonzero density a mass-like fermionic infrared cutoff simplifies the computations considerably compared to an exponential cutoff like (7.22) because of the trivial momentum dependence. In presence of a chemical potential μ we use

$$R_{kF} = -(\gamma^\mu q_\mu - i\mu\gamma^0)r_{kF}. \quad (8.35)$$

The effective squared inverse fermionic propagator is then of the form

$$\begin{aligned} P_{kF} &= [(q_0 - i\mu)^2 + \bar{q}^2](1 + r_{kF})^2 \\ &= (q_0 - i\mu)^2 + \bar{q}^2 + k^2\Theta(k_\Phi^2 - (q_0 - i\mu)^2 - \bar{q}^2), \end{aligned} \quad (8.36)$$

where the second line defines r_{kF} and one observes that the fermionic infrared cutoff acts as an additional mass-like term $\sim k^2$.

We compute the flow equation for the effective potential U_k from equation (8.17) using the ansatz (8.34) for Γ_k . The only explicit dependence on the chemical potential μ appears in

the fermionic contribution to the flow equation for U_k , whereas the derivation of the bosonic part strictly follows section 8.3. It is instructive to consider the fermionic part of the flow equation in more detail and to perform the summation of the Matsubara modes explicitly for the fermionic part. Since the flow equations only involve one momentum integration, standard techniques for one loop expressions apply [203] and we find

$$\begin{aligned} \frac{\partial}{\partial k} U_{kF}(\rho; T, \mu) = & -8N_c \int_{-\infty}^{\infty} \frac{d^4 q}{(2\pi)^4} \frac{k \Theta(k_\Phi^2 - q^2)}{q^2 + k^2 + h_k^2 \rho/2} + 4N_c \int_{-\infty}^{\infty} \frac{d^3 \vec{q}}{(2\pi)^3} \frac{k}{\sqrt{\vec{q}^2 + k^2 + h_k^2 \rho/2}} \\ & \times \left\{ \frac{1}{\exp \left[(\sqrt{\vec{q}^2 + k^2 + h_k^2 \rho/2} - \mu)/T \right] + 1} + \frac{1}{\exp \left[(\sqrt{\vec{q}^2 + k^2 + h_k^2 \rho/2} + \mu)/T \right] + 1} \right\} \end{aligned} \quad (8.37)$$

For simplicity, we sent here $k_\Phi \rightarrow \infty$ in the μ, T dependent second integral. This is justified by the fact that in the μ, T dependent part the high momentum modes are exponentially suppressed.

For comparison, we note that within the present approach one obtains standard mean field theory results for the free energy if the meson fluctuations are neglected, $\partial U_{kB}/\partial k \equiv 0$, and the Yukawa coupling is kept constant, $h_k = h$ in (8.37). The remaining flow equation for the fermionic contribution could then easily be integrated with the (mean field) initial condition $U_{k_\Phi}(\rho) = \overline{m}_{k_\Phi}^2 \rho$. In the following we will concentrate on the case of vanishing temperature. We find (see below) that a mean field treatment yields relatively good estimates only for the μ -dependent part of the free energy $U(\rho; \mu) - U(\rho; 0)$. On the other hand, mean field theory does not give a very reliable description of the vacuum properties encoded in $U(\rho; 0)$. The latter are important for a determination of the order of the phase transition at $\mu \neq 0$.

In the limit of vanishing temperature one expects and observes a non-analytic behavior of the μ -dependent integrand of the fermionic contribution (8.37) to the flow equation for U_k because of the formation of Fermi surfaces. Indeed, the explicit μ -dependence of the flow equation reduces to a step function

$$\begin{aligned} \frac{\partial}{\partial k} U_{kF}(\rho; \mu) = & - 8N_c \int_{-\infty}^{\infty} \frac{d^4 q}{(2\pi)^4} \frac{k \Theta(k_\Phi^2 - q^2)}{q^2 + k^2 + h_k^2 \rho/2} \\ & + 4N_c \int_{-\infty}^{\infty} \frac{d^3 \vec{q}}{(2\pi)^3} \frac{k}{\sqrt{\vec{q}^2 + k^2 + h_k^2 \rho/2}} \Theta \left(\mu - \sqrt{\vec{q}^2 + k^2 + h_k^2 \rho/2} \right) \end{aligned} \quad (8.38)$$

The quark chemical potential μ enters the bosonic part of the flow equation only implicitly through the meson mass terms $U'_k(\rho; \mu)$ and $U'_k(\rho; \mu) + 2\rho U''_k(\rho; \mu)$ for the pions and the σ -meson, respectively. For scales $k > \mu$ the Θ -function in (8.38) vanishes identically and there is no distinction between the vacuum evolution and the $\mu \neq 0$ evolution. This is due to the fact that our infrared cutoff adds to the effective quark mass $(k^2 + h_k^2 \rho/2)^{1/2}$. For a chemical potential smaller than this effective mass the “density” $-\partial U_k/\partial \mu$ vanishes whereas for larger μ one can view $\mu = [\vec{q}_F^2(\mu, k, \rho) + k^2 + h_k^2 \rho/2]^{1/2}$ as an effective Fermi energy for given k and

ρ . A small infrared cutoff k removes the fluctuations with momenta in a shell close to the physical Fermi surface⁵⁹ $\mu^2 - h_k^2 \rho/2 - k^2 < q^2 < \mu^2 - h_{k=0}^2 \rho/2$. Our flow equation realizes the general idea [226] that for $\mu \neq 0$ the lowering of the infrared cutoff $k \rightarrow 0$ should correspond to an approach to the physical Fermi surface. For a computation of the meson effective potential the approach to the Fermi surface in (8.38) proceeds from below and for large k the effects of the Fermi surface are absent. By lowering k one “fills the Fermi sea”.

As discussed in section 8.3 the observed fixed point behavior in the symmetric regime allows us to fix the model by only two phenomenological input parameters and we use $f_\pi = 92.4\text{MeV}$ and $300\text{MeV} \lesssim M_q \lesssim 350\text{MeV}$. The results for the evolution in vacuum [167, 28] show that for scales not much smaller than $k_\Phi \simeq 600\text{MeV}$ chiral symmetry remains unbroken. This holds down to a scale of about $k_{\chi SB} \simeq 400\text{MeV}$ at which the meson potential $U_k(\rho)$ develops a minimum at $\rho_{0,k} > 0$ even for a vanishing source, thus breaking chiral symmetry spontaneously. Below the chiral symmetry breaking scale the running couplings are no longer governed by the partial fixed point. In particular, for $k \lesssim k_{\chi SB}$ the Yukawa coupling h_k and the meson wave function renormalization $Z_{\Phi,k}$ depend only weakly on k and approach their infrared values. At $\mu \neq 0$ we will follow the evolution from $k = k_{\chi SB}$ to $k = 0$ and neglect the k -dependence of h_k and $Z_{\Phi,k}$ in this range. According to the above discussion the initial value $U_{k_{\chi SB}}$ is μ -independent for $\mu < k_{\chi SB}$. We solve the flow equation for U_k numerically as a partial differential equation for the potential depending on the two variables ρ and k for given μ [212]. Nonzero current quark masses result in a pion mass threshold and effectively stop the renormalization group flow of renormalized couplings at a scale around m_π .

In the fermionic part (8.38) of the flow equation the vacuum and the μ -dependent term contribute with opposite signs. This cancellation of quark fluctuations with momenta below the Fermi surface is crucial for the restoration of chiral symmetry at high density⁶⁰. In vacuum, spontaneous chiral symmetry breaking is induced in our model by quark fluctuations which drive the scalar mass term $U'_k(\rho = 0)$ from positive to negative values at the scale $k = k_{\chi SB}$. (Meson fluctuations have the tendency to restore chiral symmetry because of the opposite relative sign, cf. (8.17).) As the chemical potential becomes larger than the effective mass $(k^2 + h_k^2 \rho/2)^{1/2}$ quark fluctuations with momenta smaller than $\vec{q}_F^2(\mu, k, \rho) = \mu^2 - k^2 - h_k^2 \rho/2$ are suppressed. Since \vec{q}_F^2 is monotonically decreasing with ρ for given μ and k the origin of the effective potential is particularly affected. We will see in the next section that for large enough μ this leads to a second minimum of $U_{k=0}(\rho; \mu)$ at $\rho = 0$ and a chiral symmetry restoring first order transition.

⁵⁹If one neglects the mesonic fluctuations one can perform the k -integration of the flow equation (8.38) in the limit of a k -independent Yukawa coupling. One recovers (for $k_\Phi^2 \gg k^2 + h^2 \rho/2, \mu^2$) mean field theory results except for a shift in the mass, $h^2 \rho/2 \rightarrow h^2 \rho/2 + k^2$, and the fact that modes within a shell of three-momenta $\mu^2 - h^2 \rho/2 - k^2 \leq \vec{q}^2 \leq \mu^2 - h^2 \rho/2$ are not yet included. Because of the mass shift the cutoff k also suppresses the modes with $q^2 < k^2$. For $k > 0$ no infrared singularities appear in the computation of U_k and its ρ -derivatives.

⁶⁰The renormalization group investigation of a linear sigma model in $4 - \epsilon$ dimensions misses this property [227].

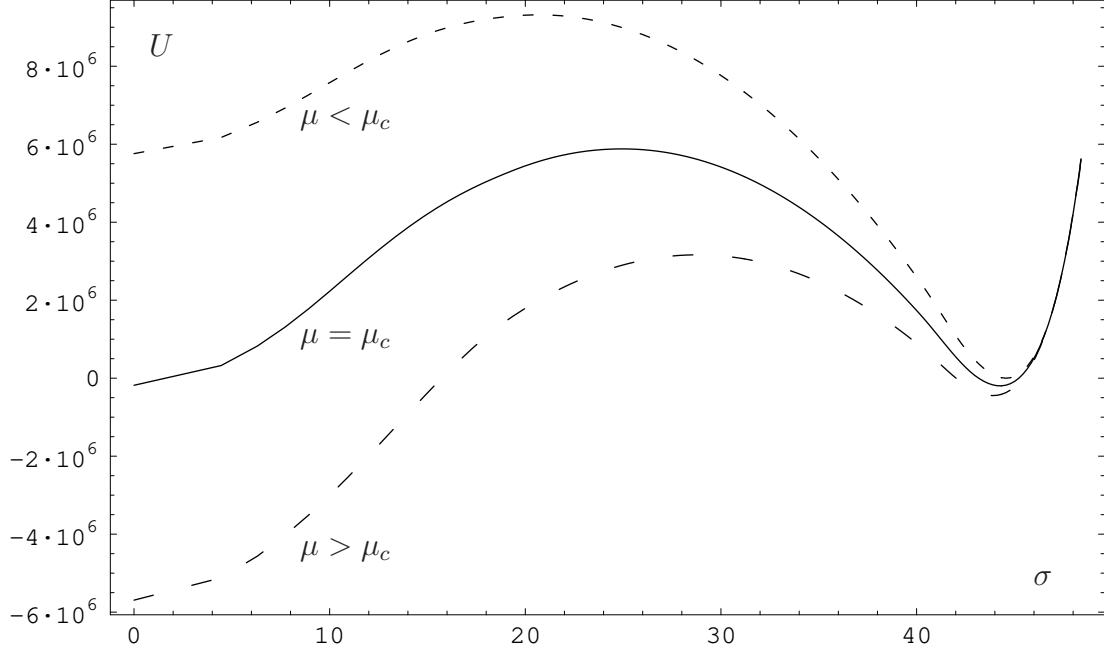


Figure 39: *High density chiral phase transition in the NJL model. The zero temperature effective potential U (in MeV^4) as a function of $\sigma = (Z_{\Phi,k=0} \rho/2)^{1/2}$ (in MeV) is shown for different chemical potentials. One observes two degenerate minima for a critical chemical potential $\mu_c/M_q = 1.025$ corresponding to a first order phase transition at which two phases have equal pressure and can coexist ($M_q = 316.2\text{MeV}$).*

8.6 High density chiral phase transition

In vacuum or at zero density the effective potential U as a function of $\sigma = \sqrt{Z_{\Phi,k=0} \rho/2}$ has its minimum at a nonvanishing value $f_\pi/2$ corresponding to spontaneously broken chiral symmetry. As the quark chemical potential μ increases, U can develop different local minima. The lowest minimum corresponds to the state of lowest free energy and is favored. In Figure 39 we plot the free energy as a function of σ for different values of the chemical potential $\mu = 322.6, 324.0, 325.2 \text{ MeV}$. Here the effective constituent quark mass is $M_q = 316.2\text{MeV}$. We observe that for $\mu < M_q$ the potential at its minimum does not change with μ . Since

$$n_q = -\frac{\partial U}{\partial \mu} \Big|_{\min} \quad (8.39)$$

we conclude that the corresponding phase has zero density. In contrast, for a chemical potential larger than M_q we find a low density phase where chiral symmetry is still broken. The quark number density as a function of μ is shown in Figure 40. One clearly observes the non-analytic behavior at $\mu = M_q$ which denotes the “onset” value for nonzero density. From Figure 39 one also notices the appearance of an additional local minimum at the origin of U . As the pressure $p = -U$ increases in the low density phase with increasing μ , a critical value μ_c is reached at which there are two degenerate potential minima. Before μ can increase any further the system undergoes a first order phase transition at which two phases have equal pressure and can coexist. In the high density phase chiral symmetry is restored as can be seen from the

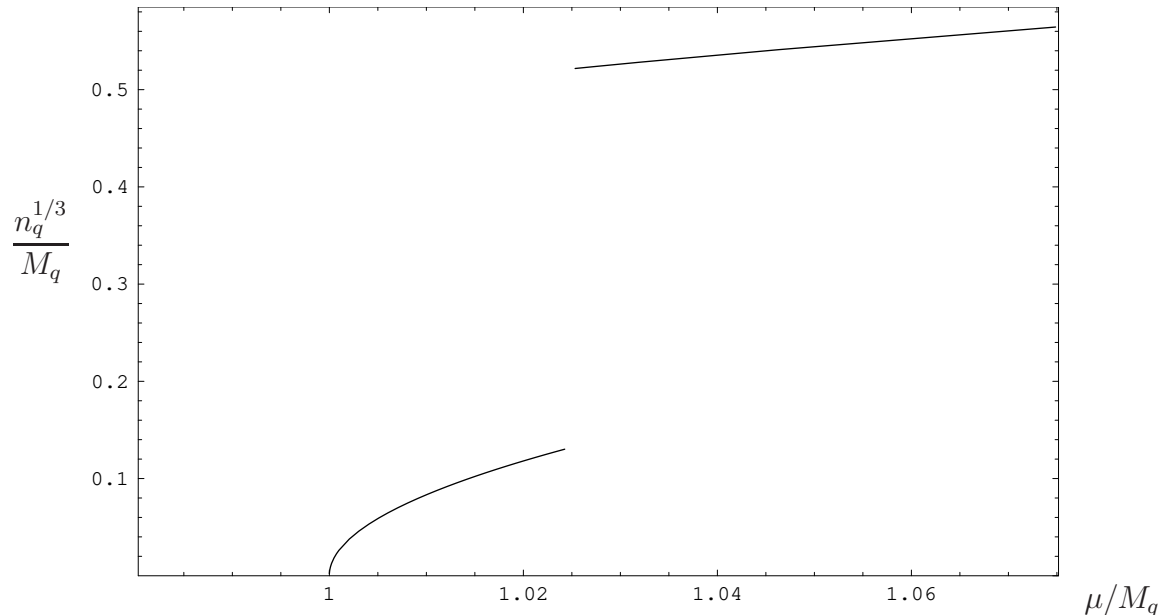


Figure 40: *Density discontinuity in the NJL model at $T = 0$. The plot shows $n_q^{1/3}$, where n_q denotes the quark number density as a function of μ in units of the effective constituent quark mass ($M_q = 316.2\text{MeV}$).*

vanishing order parameter for $\mu > \mu_c$. We note that the relevant scale for the first order transition is M_q . For this reason we have scaled our results for dimensionful quantities in units of M_q .

For the class of quark meson models considered here (with M_q/f_π in a realistic range around 3 – 4) the first order nature of the high density transition has been clearly established. In particular, these models comprise the corresponding Nambu–Jona-Lasinio models where the effective fermion interaction has been eliminated by the introduction of auxiliary bosonic fields. In summary, we find that the linear quark meson model exhibits in the chiral limit a high temperature second order chiral transition at zero chemical potential (cf. section 8.4) and a first order high density chiral transition at zero temperature. By continuity these transitions meet at a tricritical point in the (μ, T) -plane. Away from the chiral limit, the second order chiral transition turns into a smooth crossover. The first order line of transitions at low temperatures now terminates in a critical endpoint in the Ising universality class with long-range correlations [29, 30].

It is an interesting question to what extent the phase diagram for the NJL-type models reflects features of two-flavor QCD. The prominent property of QCD which is missing in the NJL-models is confinement which binds the quarks to color-neutral baryons. As a consequence one should use for QCD baryons instead of quarks as the relevant fermionic degrees of freedom for low momenta or low k . For the high temperature behavior at zero density the effects of confinement are presumably not too important. The reason is the effective decoupling of the quarks for $k \lesssim 300$ MeV due to their constituent mass. This decoupling would only

be enhanced by the binding to nucleons and we do not expect qualitative changes⁶¹. The situation is different for the high density behavior at zero temperature [98]. The mass of the fermions has an important influence on their Fermi surface. The high density transition in the NJL-type models describes in the chiral limit a transition from a “constituent quark liquid” at low density to a “massless quark liquid” at high density. Especially the low density constituent quark liquid has no direct correspondence in QCD where one rather encounters a gas of nucleons and a liquid of nuclear matter.

Acknowledgements: The work of J.B. is supported in part by funds provided by the U.S. Department of Energy (D.O.E.) under cooperative research agreement # DE-FC02-94ER40818. The work of N.T. is supported by the E.C. under contract Nos. ERBFMRXCT960090 and ERBFMBICT983132. The work of C.W. is supported in part by the Deutsche Forschungsgemeinschaft and by the E.C. contract ERBFMRX-CT97-0122.

Appendix A Threshold functions

In this appendix we list the various definitions of threshold functions appearing in the flow equations and the expressions for the anomalous dimensions. They involve the inverse scalar average propagator for the IR cutoff (2.17)

$$P(q) = q^2 + Z_{\Phi,k}^{-1} R_k(q) = \frac{q^2}{1 - \exp\left\{-\frac{q^2}{k^2}\right\}} \quad (\text{A.1})$$

and the corresponding fermionic function P_F which can be chosen as (cf. section 7.2)

$$P_F(q) = P(q) \equiv q^2 (1 + r_F(q))^2 . \quad (\text{A.2})$$

We abbreviate

$$x = q^2 , \quad P(x) \equiv P(q) , \quad \dot{P}(x) \equiv \frac{\partial}{\partial x} P(x) , \quad \tilde{\partial}_t \dot{P} \equiv \frac{\partial}{\partial x} \tilde{\partial}_t P , \quad (\text{A.3})$$

etc., and define

$$\tilde{\partial}_t \equiv \frac{1}{Z_{\Phi,k}} \frac{\partial R_k}{\partial t} \frac{\partial}{\partial P} + \frac{2}{Z_{\psi,k}} \frac{P_F}{1 + r_F} \frac{\partial [Z_{\psi,k} r_F]}{\partial t} \frac{\partial}{\partial P_F} . \quad (\text{A.4})$$

The bosonic threshold functions read

$$\begin{aligned} l_n^d(w; \eta_\Phi) &= l_n^d(w) - \eta_\Phi \hat{l}_n^d(w) \\ &= \frac{n + \delta_{n,0}}{2} k^{2n-d} \int_0^\infty dx x^{\frac{d}{2}-1} \left(\frac{1}{Z_{\Phi,k}} \frac{\partial R_k}{\partial t} \right) (P + wk^2)^{-(n+1)} \\ l_{n_1, n_2}^d(w_1, w_2; \eta_\Phi) &= l_{n_1, n_2}^d(w_1, w_2) - \eta_\Phi \hat{l}_{n_1, n_2}^d(w_1, w_2) \\ &= -\frac{1}{2} k^{2(n_1+n_2)-d} \int_0^\infty dx x^{\frac{d}{2}-1} \tilde{\partial}_t \left\{ (P + w_1 k^2)^{-n_1} (P + w_2 k^2)^{-n_2} \right\} \end{aligned} \quad (\text{A.5})$$

⁶¹There may be some quantitative influence of this effect on the value of T_c , however.

where $n, n_1, n_2 \geq 0$ is assumed. For $n \neq 0$ the functions l_n^d may also be written as

$$l_n^d(w; \eta_\Phi) = -\frac{1}{2} k^{2n-d} \int_0^\infty dx x^{\frac{d}{2}-1} \tilde{\partial}_t (P + wk^2)^{-n} . \quad (\text{A.6})$$

The fermionic integrals $l_n^{(F)d}(w; \eta_\psi) = l_n^{(F)d}(w) - \eta_\psi \check{l}_n^{(F)d}(w)$ are defined analogously as

$$l_n^{(F)d}(w; \eta_\psi) = (n + \delta_{n,0}) k^{2n-d} \int_0^\infty dx x^{\frac{d}{2}-1} \frac{1}{Z_{\psi,k}} \frac{P_F}{1+r_F} \frac{\partial [Z_{\psi,k} r_F]}{\partial t} (P + wk^2)^{-(n+1)} . \quad (\text{A.7})$$

Furthermore one has

$$\begin{aligned} l_{n_1, n_2}^{(FB)d}(w_1, w_2; \eta_\psi, \eta_\Phi) &= l_{n_1, n_2}^{(FB)d}(w_1, w_2) - \eta_\psi \check{l}_{n_1, n_2}^{(FB)d}(w_1, w_2) - \eta_\Phi \hat{l}_{n_1, n_2}^{(FB)d}(w_1, w_2) \\ &= -\frac{1}{2} k^{2(n_1+n_2)-d} \int_0^\infty dx x^{\frac{d}{2}-1} \tilde{\partial}_t \left\{ \frac{1}{[P_F(x) + k^2 w_1]^{n_1} [P(x) + k^2 w_2]^{n_2}} \right\} \\ m_{n_1, n_2}^d(w_1, w_2; \eta_\Phi) &\equiv m_{n_1, n_2}^d(w_1, w_2) - \eta_\Phi m_{n_1, n_2}^d(w_1, w_2) \\ &= -\frac{1}{2} k^{2(n_1+n_2-1)-d} \int_0^\infty dx x^{\frac{d}{2}} \tilde{\partial}_t \left\{ \frac{\dot{P}(x)}{[P(x) + k^2 w_1]^{n_1}} \frac{\dot{P}(x)}{[P(x) + k^2 w_2]^{n_2}} \right\} \\ m_2^{(F)d}(w; \eta_\psi) &= m_2^{(F)d}(w) - \eta_\psi \check{m}_2^{(F)d}(w) \\ &= -\frac{1}{2} k^{6-d} \int_0^\infty dx x^{\frac{d}{2}} \tilde{\partial}_t \left(\frac{\dot{P}_F(x)}{[P_F(x) + k^2 w]^2} \right)^2 \\ m_4^{(F)d}(w; \eta_\psi) &= m_4^{(F)d}(w) - \eta_\psi \check{m}_4^{(F)d}(w) \\ &= -\frac{1}{2} k^{4-d} \int_0^\infty dx x^{\frac{d}{2}+1} \tilde{\partial}_t \left(\frac{\partial}{\partial x} \frac{1+r_F(x)}{P_F(x) + k^2 w} \right)^2 \\ m_{n_1, n_2}^{(FB)d}(w_1, w_2; \eta_\psi, \eta_\Phi) &= m_{n_1, n_2}^{(FB)d}(w_1, w_2) - \eta_\psi \check{m}_{n_1, n_2}^{(FB)d}(w_1, w_2) - \eta_\Phi m_{n_1, n_2}^{(FB)d}(w_1, w_2) \\ &= -\frac{1}{2} k^{2(n_1+n_2-1)-d} \int_0^\infty dx x^{\frac{d}{2}} \tilde{\partial}_t \left\{ \frac{1+r_F(x)}{[P_F(x) + k^2 w_1]^{n_1}} \frac{\dot{P}(x)}{[P(x) + k^2 w_2]^{n_2}} \right\} . \end{aligned} \quad (\text{A.8})$$

The dependence of the threshold functions on the anomalous dimensions arises from the t -derivative acting on $Z_{\Phi,k}$ and $Z_{\psi,k}$ within R_k and $Z_{\psi,k} r_F$, respectively. We furthermore use the abbreviations

$$\begin{aligned} l_n^d(\eta_\Phi) &\equiv l_n^d(0; \eta_\Phi) \quad , \quad l_n^{(F)d}(\eta_\psi) \equiv l_n^{(F)d}(0; \eta_\psi) \\ l_n^d(w) &\equiv l_n^d(w; 0) \quad , \quad l_n^d \equiv l_n^d(0; 0) \end{aligned} \quad (\text{A.9})$$

etc. and note that in four dimensions the integrals

$$l_2^4(0, 0) = l_2^{(F)4}(0, 0) = l_{1,1}^{(FB)4}(0, 0) = m_4^{(F)4}(0) = m_{1,2}^{(FB)4}(0, 0) = 1 \quad (\text{A.10})$$

are independent of the particular choice of the infrared cutoff.

Appendix B Anomalous dimension in the sharp cutoff limit

It is instructive to evaluate ξ_k as defined by eq. (3.73) in the sharp cutoff limit. In this limit one has

$$M_0^{-1}(\rho, q^2) = (Z_k(\rho, q^2)q^2 + U'_k(\rho))^{-1}\Theta(q^2 - k^2) \quad (\text{B.1})$$

and

$$\frac{\partial_t R_k(p)}{M_0^2(\rho, p^2)} = \frac{2}{Z_k}(z(\rho) + u'(\rho))^{-1}\delta(p^2 - k^2) \quad (\text{B.2})$$

with similar expressions for M_1^{-1} and $\partial_t R_k/M_1^2$. The momentum integration in $\partial_t G^{-1}$ (3.72) therefore reduces to an angular integration for the angle between p and q , $(pq) = |p||q|\cos\theta$. For an evaluation of $\partial_t G^{-1}(\rho, k^2)$ one has $q^2 = p^2 = k^2$ and

$$M_0^{-1}(\rho, (p+q)^2) = [2k^2 Z_k(\rho, 2k^2(1+\cos\theta)) (1+\cos\theta) + U'_k]^{-1}\Theta(1+2\cos\theta) \quad (\text{B.3})$$

Let us define for $p^2 = q^2 = k^2$, $(pq) = k^2 \cos\theta$

$$\begin{aligned} \tilde{\lambda}_k^{(1)}(\rho, s) &= Z_k^{-2}k^{d-4}\lambda_k^{(1)}(\rho; p, q), \quad \tilde{\lambda}_k^{(2)}(\rho, s) = Z_k^{-2}k^{d-4}\lambda_k^{(2)}(\rho; q, -q, p), \\ \tilde{\lambda}_k^{(3)}(\rho, s) &= Z_k^{-2}k^{d-4}\lambda_k^{(2)}(\rho; q, p, -q), \quad \tilde{\gamma}_k^{(2)}(\rho, s) = Z_k^{-3}k^{2d-6}\gamma_k^{(2)}(\rho; p, -p, q) \end{aligned} \quad (\text{B.4})$$

where we have introduced the variable

$$s = 2(1 + \cos\theta) \quad (\text{B.5})$$

With

$$\lambda^{(1)}(\rho; -q - p, q) = Z_k^2 k^{4-d} \tilde{\lambda}^{(1)}(\rho, 2 - \sqrt{s}) \quad (\text{B.6})$$

one finds⁶² for $d = 3$

$$\begin{aligned} \partial_t G^{-1}(\rho, k^2) &= \frac{1}{2}v_d k^2 Z_k \left[4\tilde{\rho} \int_1^4 ds \right. \\ &\quad \{ (\tilde{\lambda}^{(1)}(\tilde{\rho}, s))^2 (z + \tilde{\rho}\tilde{y} + u' + 2\tilde{\rho}u'')^{-1} [s(z + \Delta z(\tilde{\rho}, s)) + u']^{-1} \\ &\quad + (\tilde{\lambda}^{(1)}(\tilde{\rho}, 2 - \sqrt{s}))^2 (z + u')^{-1} [s(z + \tilde{\rho}\tilde{y} + \Delta z(\tilde{\rho}, s) + \tilde{\rho}\Delta\tilde{y}(\tilde{\rho}, s)) + u' + 2\tilde{\rho}u'']^{-1} \} \\ &\quad - \int_0^4 ds \{ (z + u')^{-1} ((N-1)\tilde{\lambda}^{(2)}(\tilde{\rho}, s) + 2\tilde{\lambda}^{(3)}(\tilde{\rho}, s)) \\ &\quad \left. + (z + \tilde{\rho}\tilde{y} + u' + 2\tilde{\rho}u'')^{-1} (\tilde{\lambda}^{(2)}(\tilde{\rho}, s) + 2\tilde{\rho}\tilde{\gamma}^{(2)}(\tilde{\rho}, s)) \} \right] \quad (\text{B.7}) \end{aligned}$$

Next one uses the relations (3.66)

$$\begin{aligned} \tilde{\lambda}^{(1)}(\tilde{\rho}, s) &= u''(\tilde{\rho}) + \frac{s}{2}(z'(\tilde{\rho}) + \Delta z'(\tilde{\rho}, \frac{s}{2})) + \frac{1}{2}\tilde{y}(\tilde{\rho}) + \Delta\tilde{\lambda}^{(1)}(\tilde{\rho}, s) \\ \tilde{\lambda}^{(2)}(\tilde{\rho}, s) &= u''(\tilde{\rho}) + 2z'(\tilde{\rho}) + \Delta\tilde{\lambda}^{(2)}(\tilde{\rho}, s) \\ \tilde{\lambda}^{(3)}(\tilde{\rho}, s) &= u''(\tilde{\rho}) + (2-s)(z'(\tilde{\rho}) + \Delta z'(\tilde{\rho}, 2-s)) + \frac{1}{2}s(\tilde{y}(\tilde{\rho}) + \Delta\tilde{y}(\tilde{\rho}, s)) + \Delta\tilde{\lambda}^{(3)}(\tilde{\rho}, s) \\ \tilde{\gamma}^{(2)}(\tilde{\rho}, s) &= u'''(\tilde{\rho}) + z''(\tilde{\rho}) + \frac{1}{2}\tilde{y}'(\tilde{\rho}) + \Delta\tilde{\gamma}^{(2)}(\tilde{\rho}, s) \end{aligned} \quad (\text{B.8})$$

⁶²For $d \neq 3$ the integration measure contains an additional Jacobian $J^{(d)}(s)$.

where

$$\begin{aligned}\Delta\tilde{\lambda}^{(1)}(\tilde{\rho}, 0) &= 0, \quad \Delta\tilde{\lambda}^{(2,3)}(\tilde{\rho}) = \frac{1}{4} \int_0^4 ds \Delta\tilde{\lambda}^{(2,3)}(\tilde{\rho}, s), \\ \Delta\tilde{\gamma}^{(2)}(\tilde{\rho}) &= \frac{1}{4} \int_0^4 ds \Delta\tilde{\gamma}^{(2)}(\tilde{\rho}, s)\end{aligned}\tag{B.9}$$

and finally finds the exact expression

$$\begin{aligned}\xi_k(\tilde{\rho}, 1) &= -2v_d\tilde{\rho} \int_1^4 ds \left\{ (u'' + \frac{s}{2}(z' + \Delta z'(\frac{s}{2}))) + \frac{1}{2}\tilde{y} + \Delta\tilde{\lambda}^{(1)}(s) \right\}^2 \\ & [s(z + \Delta z(s)) + u']^{-1} [z + \tilde{\rho}\tilde{y} + u' + 2\tilde{\rho}u'']^{-1} \\ & + (u'' + (1 - \frac{\sqrt{s}}{2})(z' + \Delta z'(2 - \sqrt{s}))) + \frac{1}{2}\tilde{y} + \Delta\tilde{\lambda}^{(1)}(2 - \sqrt{s}) \right\}^2 \\ & [s(z + \tilde{\rho}\tilde{y} + \Delta z(s) + \tilde{\rho}\Delta\tilde{y}(s)) + u' + 2\tilde{\rho}u'']^{-1} [z + u']^{-1} + 2v_d \{ (z + u')^{-1} \\ & [2u'' + (N + 3 - 2s)z' + 2(2 - s)\Delta z'(2 - s) + s\tilde{y} + s\Delta\tilde{y}(s) + (N - 1)\Delta\tilde{\lambda}^{(2)} + 2\Delta\tilde{\lambda}^{(3)}] \\ & - (z + \tilde{\rho}\tilde{y} + u' + 2\tilde{\rho}u'')^{-1} [2u'' - z' - 2\tilde{\rho}z'' + \tilde{y} - \Delta\tilde{\lambda}^{(2)} - 2\tilde{\rho}\Delta\tilde{\gamma}^{(2)}] \}\end{aligned}\tag{B.10}$$

The first order in the hybrid derivative expansion neglects the momentum-dependent corrections $\Delta\tilde{\lambda}^{(i)}$, $\Delta\tilde{\gamma}^{(2)}$, Δz and $\Delta\tilde{y}$. This yields the evolution equation for $z(\tilde{\rho})$

$$\begin{aligned}\partial_t z &= \eta z + (d - 2 + \eta)\tilde{\rho}z' + 2v_d\tilde{\rho} (u'' + \sigma_z z' + \frac{1}{2}\tilde{y})^2 \\ & \left\{ \frac{1}{z} \ln \left(\frac{4z + u'}{z + u'} \right) (z + \tilde{\rho}\tilde{y} + u' + 2\tilde{\rho}u'')^{-1} \right. \\ & \left. + \frac{1}{z + \tilde{\rho}\tilde{y}} \ln \left(\frac{4(z + \tilde{\rho}\tilde{y}) + u' + 2\tilde{\rho}u''}{z + \tilde{\rho}\tilde{y} + u' + 2\tilde{\rho}u''} \right) (z + u')^{-1} \right\} \\ & - 2v_d \{ (z + u')^{-1} [2u'' + (N + 2)z' + \frac{1}{2}\tilde{y}] \\ & - (z + \tilde{\rho}\tilde{y} + u' + 2\tilde{\rho}u'')^{-1} [2u'' - z' - 2\tilde{\rho}z'' + \tilde{y}] \}\end{aligned}\tag{B.11}$$

where we have replaced for simplicity in the third term the correct s -integration of the terms $\sim z'(z')^2$ by an approximate expression with $\sigma_z \approx 0.5 - 1$. The anomalous dimension reads for $\kappa > 0$

$$\begin{aligned}\eta &= (1 + \kappa z'_0)^{-1} \left\{ [(2 - d)\kappa - \partial_t \kappa] z'_0 \right. \\ & - 2v_d \kappa (\lambda + \sigma_z z'_0 + \frac{1}{2}\tilde{y}_0)^2 \left((1 + \kappa\tilde{y}_0 + 2\lambda\kappa)^{-1} \ln 4 \right. \\ & \left. \left. + (1 + \kappa\tilde{y}_0)^{-1} \ln \left(\frac{4(1 + \kappa\tilde{y}_0) + 2\lambda\kappa}{1 + \kappa\tilde{y}_0 + 2\lambda\kappa} \right) \right) \right. \\ & \left. + 2v_d \left[\frac{2\lambda(2\lambda\kappa + \kappa\tilde{y}_0)}{1 + 2\lambda\kappa + \kappa\tilde{y}_0} + (N + 2)z'_0 + \frac{1}{2}\tilde{y}_0 \right. \right. \\ & \left. \left. + (1 + 2\lambda\kappa + \kappa\tilde{y}_0)^{-1} (z'_0 + 2\kappa z''_0 - \tilde{y}_0) \right] \right\}\end{aligned}\tag{B.12}$$

where we have defined

$$\lambda = u''(\kappa) , z'_0 = z'(\kappa) , z''_0 = z''(\kappa) , \tilde{y}_0 = \tilde{y}(\kappa) \quad (\text{B.13})$$

We observe that eq. (B.11) is well defined as long as $z, z + u', z + \tilde{\rho}\tilde{y}$ and $z + \tilde{\rho}\tilde{y} + u' + 2\tilde{\rho}u''$ remain all positive. These are the same conditions as those required for a consistent flow of the potential. The problems that a sharp cutoff engenders for a definition of the anomalous dimension at $q^2 = 0$ are avoided by the use of the hybrid derivative expansion with the definition (3.74).

For large N the characteristic scaling $\tilde{\rho} \sim N, u' \sim 1, u'' \sim 1/N$ implies for the solution of eq. (B.11) $z' \sim 1/N^2, z'' \sim a/N^3$. On the other hand the evolution equation for the inverse radial propagator $\tilde{G}^{-1}(\rho, q^2) = M_1(\rho, q^2) - R_k(q)$ leads to $\tilde{y} \sim 1/N$ and \tilde{y} contributes in order $\eta \sim 1/N$. Taking nevertheless $\tilde{y} = 0$ for a first discussion, one finds the anomalous dimension

$$\eta = 2v_d \lambda^2 \kappa \left(\frac{4}{1+2\lambda\kappa} - \frac{\ln 4}{1+2\lambda\kappa} - \ln \left(\frac{4+2\lambda\kappa}{1+2\lambda\kappa} \right) \right) + 2v_d N z'_0 - \kappa z'_0 \quad (\text{B.14})$$

For $d = 3$ one may insert for the scaling solution the leading expression $\lambda\kappa = 1$ (cf. (3.59)) so that

$$\eta = \frac{1}{N} \left\{ \frac{4}{3} - \frac{1}{3} \ln 4 - \ln 2 \right\} = \frac{0.178}{N} \quad (\text{B.15})$$

For a computation of the exact expression for η in order $1/N$ one needs to include effects from $\tilde{y}_0 \neq 0$. Also the contribution $-2(\partial\Delta z(\kappa, y)/\partial y)(y = 1)$ has to be added in order $1/N$. In the same approximation as above the scaling solution for $z(\tilde{\rho})$ obeys the differential equation

$$\begin{aligned} & \tilde{\rho} z' + 2v_d \tilde{\rho} (u'')^2 \left\{ (1 + u' + 2\tilde{\rho}u'')^{-1} \ln \left(\frac{4 + u'}{1 + u'} \right) \right. \\ & \left. + (1 + u')^{-1} \ln \left(\frac{4 + u' + 2\tilde{\rho}u''}{1 + u' + 2\tilde{\rho}u''} \right) \right\} \\ & - 2v_d \left\{ \frac{2u'' + Nz'}{1 + u'} - \frac{2u''}{1 + u' + 2\tilde{\rho}u''} \right\} = -\eta z \end{aligned} \quad (\text{B.16})$$

By differentiation with respect to $\tilde{\rho}$ eq. (B.16) implies for the scaling regime

$$\begin{aligned} & z'_0(1 + 2v_d N \lambda) + z''_0(\kappa - 2v_d N) = \\ & -2v_d \left\{ \frac{\lambda}{(1 + 2\lambda\kappa)^2} (\lambda + 2\gamma\kappa - \lambda\kappa(\lambda - 2\gamma\kappa)) \ln 4 \right. \\ & \left. + \lambda(\lambda + 2\gamma\kappa - \lambda^2\kappa) \ln \left(\frac{4 + 2\lambda\kappa}{1 + 2\lambda\kappa} \right) \right. \\ & \left. - \lambda^2\kappa \left[\frac{1}{1 + 2\lambda\kappa} \left(\frac{15}{4}\lambda + 2\gamma\kappa \right) - \frac{3\lambda + 2\gamma\kappa}{4 + 2\lambda\kappa} \right] \right. \\ & \left. + 2\lambda^2 - 2\gamma + \frac{2\gamma}{1 + 2\lambda\kappa} - \frac{2\lambda(3\lambda + 2\gamma\kappa)}{(1 + 2\lambda\kappa)^2} \right\} \end{aligned} \quad (\text{B.17})$$

For $d = 3, 2v_d N = \kappa, \lambda\kappa = 1, \gamma\kappa = 2\lambda/3$, this yields

$$N\kappa z'_0 = \frac{89}{216} - \frac{4}{27} \ln 4 - \frac{2}{3} \ln 2 \quad (\text{B.18})$$

and we see indeed $z'_0 \sim 1/N^2$.

References

- [1] L.P. Kadanoff, *Physica* **2** (1966) 263.
- [2] K. G. Wilson, *Phys. Rev.* **B4** (1971) 3174; 3184 K. G. Wilson and I. G. Kogut, *Phys. Rep.* **12** (1974) 75.
- [3] F. Wegner and A. Houghton, *Phys. Rev.* **A8** (1973) 401; F.J. Wegner in *Phase Transitions and Critical Phenomena*, vol. 6, eds. C. Domb and M.S. Greene, Academic Press (1976).
- [4] J.F. Nicoll and T.S. Chang, *Phys. Lett.* **A62** (1977) 287; T. S. Chang, D. D. Vvedensky and J. F. Nicoll, *Phys. Rep.* **217** (1992) 280.
- [5] S. Weinberg, *Critical phenomena for field theorists*, in *Understanding the Fundamental Constituents of Matter*, p. 1, Ed. by A. Zichichi (Plenum Press, N.Y. and London, 1978).
- [6] J. Polchinski, *Nucl. Phys.* **B231** (1984) 269;
- [7] A. Hasenfratz and P. Hasenfratz, *Nucl. Phys.* **B270** (1986) 685; P. Hasenfratz and J. Nager, *Z. Phys.* **C37** (1988) 477.
- [8] C. Wetterich, *Nucl. Phys.* **B352** (1991) 529; *Z. Phys.* **C57** (1993) 451; **C60** (1993) 461.
- [9] C. Wetterich, *Phys. Lett.* **B301** (1993) 90.
- [10] E.C.G. Stueckelberg and A. Peterman, *Helv. Phys. Acta* **26** (1953) 499; M. Gell-Mann and F.E. Low, *Phys. Rev.* **95** (1954) 1300; C.G. Callan, *Phys. Rev.* **D2** (1970) 1541; K. Symanzik, *Comm. Math. Phys.* **18** (1970) 227.
- [11] M. Reuter and C. Wetterich, *Nucl. Phys.* **B408** (1993) 91.
- [12] C. Wetterich, in “Electroweak Physics and the Early Universe”, eds. J. Romao and F. Freire, Plenum Press (1994) 229 (hep-th/9408054).
- [13] O. Philipsen, M. Teper and H. Wittig, *Nucl. Phys.* **B528** (1998) 379.
- [14] R. Stock, *Nucl. Phys.* **A661** (1999) 282; Berndt Müller, *Nucl. Phys.* **A661** (1999) 272.
- [15] For a review see K. Rajagopal, *Nucl. Phys.* **A661** (1999) 150.
- [16] F. Wilczek, Lectures at 9th CRM Summer School: Theoretical Physics at the End of the 20th Century, Banff, Alberta, Canada, 27 Jun - 10 Jul 1999, hep-ph/0003183.
- [17] J. Berges, Lectures at the 11th Summer School and Symposium on Nuclear Physics (NuSS 98): Effective Theories of Matter (1), Seoul, Korea, 23-27 Jun 1998, hep-ph/9902419.
- [18] K. Osterwalder, R. Schrader, *Commun. Math. Phys.* **31** (1973) 83.

- [19] K. Kajantie, M. Laine, K. Rummukainen and M. Shaposhnikov, Phys. Rev. Lett. **77** (1996) 2887.
- [20] F. Karsch, T. Neuhaus, A. Patkos and J. Rank, Nucl. Phys. **B474** (1996) 217; M. Gürtler, E. Ilgenfritz and A. Schiller, Phys. Rev. **D56** (1997) 3888.
- [21] W. Buchmüller and O. Philipsen, Nucl. Phys. **B443** (1995) 47.
- [22] B. Bergerhoff and C. Wetterich, in “Current Topics in Astrofundamental Physics”, eds. N. Sanchez and A. Zichichi, World Scientific (1997) 132 (hep-ph/9611462).
- [23] K. Rummukainen, M. Tsypin, K. Kajantie, M. Laine, M. Shaposhnikov, Nucl. Phys. **B532** (1998) 283.
- [24] R.D. Pisarski and F. Wilczek, Phys. Rev. **D29** (1984) 338;
- [25] F. Wilczek, Int. J. Mod. Phys. **A7** (1992) 3911.
- [26] K. Rajagopal and F. Wilczek, Nucl. Phys. **B399** (1993) 395; Nucl. Phys. **B399** (1993) 577.
- [27] K. Rajagopal, Quark-Gluon Plasma 2 (1995) 484 (hep-ph/9504310).
- [28] J. Berges, D.–U. Jungnickel and C. Wetterich, Phys. Rev. **D59** (1999) 034010.
- [29] J. Berges, K. Rajagopal, Nucl. Phys. **B538** (1999) 215.
- [30] M.A. Halasz, A.D. Jackson, R.E. Shrock, M.A. Stephanov, J.J.M. Verbaarschot, Phys. Rev. **D58** (1998) 096007.
- [31] K. E. Newman and E. K. Riedel, Phys. Rev. **B30** (1984) 6615; E. K. Riedel, G. R. Golner and K. E. Newman, Ann. Phys. (N.Y.) **161** (1985) 178; see also G. R. Golner and E. K. Riedel, Phys. Rev. Lett. **34** (1975) 856; Phys. Lett. **A58** (1976) 11.
- [32] F. J. Wegner, Phys. Rev. **B5** (1972) 4529.
- [33] J. F. Nicoll, T. S. Chang and H. E. Stanley, Phys. Rev. Lett. **33** (1974) 540; Phys. Rev. **A13** (1976) 1251.
- [34] A. Parola and L. Reatto, Phys. Rev. Lett. **53** (1984) 2417; Phys. Rev. **A31** (1985) 3309.
- [35] J. F. Nicoll and T. S. Chang, Phys. Rev. **A17**, 2083 (1978).
- [36] J. Berges, N. Tetradis and C. Wetterich, Phys. Rev. Lett. **77** (1996) 873.
- [37] J. Berges and C. Wetterich, Nucl. Phys. **B487** (1997) 675.
- [38] S. Seide and C. Wetterich, Nucl. Phys. **B562** (1999) 524.
- [39] A. Strumia and N. Tetradis, Nucl. Phys. **B542** (1999) 719.

- [40] A. Strumia, N. Tetradis and C. Wetterich, Phys. Lett. **B467** (1999) 279.
- [41] T. Morris, Phys. Lett. **B345** (1995) 139.
- [42] N. Tetradis and C. Wetterich, Nucl. Phys. **B398** (1993) 659; Int. J. Mod. Phys. **A9** (1994) 4029.
- [43] B. Bergerhoff, F. Freire, D. Litim, S. Lola, C. Wetterich, Phys. Rev. **B53** (1996) 5734; B. Bergerhoff, D. Litim, S. Lola and C. Wetterich, Int. J. Mod. Phys. **A11** (1996) 4273.
- [44] N. Tetradis, Nucl. Phys. **B488** (1997) 92.
- [45] C. Bagnuls and C. Bervillier, this volume, hep-th/0002034.
- [46] M. E. Fisher, Rev. Mod. Phys. **70**, 653 (1998).
- [47] M. Reuter and C. Wetterich, Nucl. Phys. **B391** (1993) 147; **B417** (1994) 181; **B427** (1994) 291; Phys. Rev. **D56** (1997) 7893.
- [48] C. Becchi, Lecture given at the Parma Theoretical Physics Seminar, Sep 1991, preprint GEF-TH-96-11 (hep-th/9607188).
- [49] M. Bonini, M. D'Attanasio, and G. Marchesini, Nucl. Phys. **B418** (1994) 81; **B421** (1994) 429; **B437** (1995) 163; **B444** (1995) 602; Phys. Lett. **B346** (1995) 87; M. Bonini, G. Marchesini and M. Simionato, Nucl. Phys. **B483** (1997) 475.
- [50] U. Ellwanger, Phys. Lett. **B335** (1994) 364; U. Ellwanger, M. Hirsch and A. Weber, Z. Phys. **C69** (1996) 687; Eur. Phys. J. **C1** (1998) 563.
- [51] C. Wetterich, hep-th/9501119; Z. Phys. **C72** (1996) 139.
- [52] T. R. Morris, Phys. Lett. **B357** (1995) 225.
- [53] B. Bergerhoff and C. Wetterich, Nucl. Phys. **B440** (1995) 171.
- [54] F. Freire and C. Wetterich, Phys. Lett. **B380** (1996) 337.
- [55] M. Reuter, Phys. Rev. **D53** (1996) 4430.
- [56] M. Reuter, Phys. Rev. **D53** (1996) 4430.
- [57] M. D'Attanasio and T. R. Morris, Phys. Lett. **B378** (1996) 213.
- [58] M. Reuter, Mod. Phys. Lett. **A12** (1997) 2777.
- [59] J. Pawłowski, Phys. Rev. **D58** (1998) 045011.
- [60] N. Tetradis, Phys. Lett. **B409** (1997) 355.
- [61] S.-B. Liao, Phys. Rev. **D56** (1997) 5008.

- [62] D. F. Litim, N. Tetradis and C. Wetterich, *Mod. Phys. Lett.* **A12** (1997) 2287.
- [63] K.-I. Aoki, K. Morikawa, J.-I. Sumi, H. Terao and M. Tomoyose, *Progr. Theor. Phys.* **97** (1997) 479.
- [64] M. Reuter and C. Wetterich, *Nucl. Phys.* **B506** (1997) 483.
- [65] B. Bergerhoff and C. Wetterich, *Phys. Rev.* **D57** (1998) 1591.
- [66] U. Ellwanger, *Nucl. Phys.* **B531** (1998) 593.
- [67] U. Ellwanger, *Eur. Phys. J.* **C7** (1999) 673.
- [68] D.F. Litim and J.M. Pawłowski, *Phys. Lett.* **B435** (1998) 181; *Nucl. Phys.* **B74** [FS] (1999) 325; 329; hep-ph/9901063.
- [69] T.R. Morris, Lectures at the Workshop on the Exact Renormalization Group, Faro, Portugal, Sept. 10-12, 1998 (hep-th/9810104); hep-th/9910058.
- [70] M. Simionato, hep-th/9809004; hep-th/9810117.
- [71] M. Bonini, M. D'Attanasio and G. Marchesini, *Phys. Lett.* **B329** (1994) 249; M. Bonini and F. Vian, *Nucl. Phys.* **B511** (1998) 479.
- [72] M. Bonini and F. Vian, *Nucl. Phys.* **B532**, 473 (1998).
- [73] M. Pernici, M. Raciti and F. Riva, *Nucl. Phys.* **B520** (1998) 469.
- [74] S. Hirano, hep-th/9910256.
- [75] S. Arnone and A. Panza, *Int. J. Mod. Phys.* **A14** (1999) 3935.
- [76] F. Freire and D. Litim, hep-ph/0002153.
- [77] A. Bonanno and D. Zappalà, *Phys. Rev.* **D55** (1997) 6135; M. Reuter, *Phys. Rev.* **D57** (1998) 971; W. Souma, *Prog. Theor. Phys.* **102** (1999) 181.
- [78] U. Ellwanger and C. Wetterich, *Nucl. Phys.* **B423** (1994) 137.
- [79] A. Ringwald, C. Wetterich, *Nucl. Phys.* **B334** (1990), 506.
- [80] N. Tetradis, C. Wetterich, *Nucl. Phys.* **B383** (1992), 197.
- [81] C. Wetterich, *Z. Phys.* **C48** (1990) 693; S. Bornholdt and C. Wetterich, *Phys. Lett.* **B282** (1992) 399; *Z. Phys.* **C58** (1993) 585.
- [82] J. Comellas, Y. Kubyshev and E. Moreno, *Nucl. Phys.* **B490** (1997) 653.
- [83] M. Alford, *Phys. Lett.* **B336** (1994) 237.

- [84] T. R. Morris, Nucl. Phys. **B458** [FS] (1996) 477.
- [85] A. Bonanno and D. Zappalà, Phys. Rev. **D57** (1998) 7383.
- [86] A. Bonanno, V. Branchina, H. Mohrbach and D. Zappalà, Phys. Rev. **D60** (1999) 065009.
- [87] R.D. Ball, P.E. Haagensen, J. Latorre and E. Moreno, Phys. Lett. **B347** (1995) 80.
- [88] D.F. Litim, Phys. Lett. **B393** (1997) 103.
- [89] S.-B. Liao, J. Polonyi and M. Strickland, Nucl. Phys. **B567** (2000) 493.
- [90] J.-I. Sumi, W. Souma, K.-I. Aoki, H. Terao, and K. Morikawa, hep-th/0002231.
- [91] G. Keller, C. Kopper and M. Salmhofer, Helv. Phys. Acta **65** (1992) 32; G. Keller and G. Kopper, Phys. Lett. **B273** (1991) 323.
- [92] M. Bonini, M. D' Attanasio and G. Marchesini, Nucl. Phys. **B409** (1993) 441.
- [93] T. R. Morris, Int. J. Mod. Phys. **A9** (1994) 2411.
- [94] U. Ellwanger, Z. Phys. **C62** (1994) 503.
- [95] R. D. Ball and R. S. Thorne, Ann. Phys. (N.Y.) **236** (1994) 117.
- [96] U. Ellwanger, Z. Phys. **C58** (1993) 619.
- [97] C. Wetterich, Int. J. Mod. Phys. **A9** (1994) 3571.
- [98] J. Berges, D.U. Jungnickel, C. Wetterich, hep-ph/9811387.
- [99] Yu. M. Ivanchenko, A. A. Lisyansky and A. E. Filippov, Phys. Lett. **A150** (1990) 100.
- [100] R. J. Myerson, Phys. Rev. **B12** (1975) 2789.
- [101] G. R. Golner, Phys. Rev. **B33** (1986) 7863.
- [102] T. R. Morris and J. F. Tighe, JHEP **9908** (1999) 007.
- [103] K.-I. Aoki, K. Morikawa, W. Souma, J.-I. Sumi and H. Terao, Prog. Theor. Phys. **99** (1998) 451.
- [104] K. I. Aoki, K. Morikawa, W. Souma, J.-I. Sumi and H. Terao, Prog. Theor. Phys. **95** (1996) 409.
- [105] A. Margaritis, G. Ódor and A. Patkós, Z. Phys. **C39** (1988) 109.
- [106] P. E. Haagensen, Y. Kubyshev, J. I. Latorre and E. Moreno, Phys. Lett. **B323** (1994) 330.

- [107] T. Morris, Phys. Lett. **B334** (1994) 355.
- [108] F.J. Dyson, Phys. Rev. **75** (1949) 1736; J. Schwinger, Proc. Nat. Acad. Sc. **37** (1951) 452.
- [109] J. Adams, J. Berges, S. Bornholdt, F. Freire, N. Tetradis and C. Wetterich, Mod. Phys. Lett. **A10** (1995) 2367.
- [110] J. Comellas and A. Travesset, Nucl. Phys. **B498** (1997) 539.
- [111] J.M. Kosterlitz and D.J. Thouless, J. Phys. **C6** (1973) 1181; J.M. Kosterlitz, J. Phys. **C7** (1974) 1046.
- [112] N.D. Mermin and H. Wagner, Phys. Rev. Lett. **17** (1966) 1133.
- [113] N. Tetradis and C. Wetterich, Nucl. Phys. **B422** [FS] (1994) 541.
- [114] R. Neves, Y. Kubyshin and R. Potting, Proceedings of Workshop on the Exact Renormalization Group, Faro, Portugal, 10-12 Sep 1998 (hep-th/9811151).
- [115] A.M. Polyakov, Phys. Lett. **B59** (1975) 79; A. d’Adda, M. Lüscher and P. di Vecchia, Nucl. Phys. **B146** (1978) 63; E. Witten, Nucl. Phys. **B149** (1979) 285; S. Hikami and E. Brezin, J. Phys. **A11** (1978) 1141; W. Bernreuther and F. Wegner, Phys. Rev. Lett. **57** (1986) 1383.
- [116] M. Gräter and C. Wetterich, Phys. Rev. Lett. **75** (1995) 378.
- [117] S. Coleman, Comm. Math. Phys. **31** (1973) 259.
- [118] G. Felder, Com. Math. Phys. **111** (1987) 101.
- [119] A. E. Filippov and S. A. Breus, Phys. Lett. **A158** (1991) 300; S. A. Breus and A. E. Filippov, Physica **A192** (1993) 486; A. E. Filippov, Theor. Math. Phys. **91** (1992) 551.
- [120] T. Morris, Phys. Lett. **B329** (1994) 241.
- [121] N. Tetradis and D. F. Litim, Nucl. Phys. **B464** [FS] (1996) 492.
- [122] M. D’Attanasio and T. R. Morris, Phys. Lett. **B409** (1997) 363.
- [123] J. Zinn–Justin, *Quantum Field Theory and Critical Phenomena* (3rd ed., Oxford University Press, 1996).
- [124] C. Wetterich, Mod. Phys. Lett. **A11** (1996) 2573.
- [125] M. Alford, J. Berges and C. Wetterich, to be published.
- [126] K. Symanzik, Comm. Math. Phys. **16** (1970) 48; I. Iliopoulos, C. Itzykson and A. Martin, Rev. Mod. Phys. **47** (1975) 165; L. O’Raifeartaigh, A. Wipf and Y. Yoneyama, Nucl. Phys. **B271** (1986) 653.

- [127] J. Alexandre, V. Branchina, J. Polonyi, Phys. Lett. **B445** (1999) 351; I. Nandori, J. Polonyi, K. Sailer, hep-th/9910167; J. Alexandre, J. Polonyi, hep-th/9906017.
- [128] B. Widom, J. Chem. Phys. **43** (1965) 3898.
- [129] K.G. Wilson and M.E. Fisher, Phys. Rev. Lett. **28** (1972) 240.
- [130] G. v. Gersdorff and C. Wetterich, to be published.
- [131] R. Guida and J. Zinn-Justin, J. Phys. **A31** (1998) 8103; J. Zinn-Justin, hep-th/0002136.
- [132] I. Kondor and T. Temesvari, J. Phys. Lett. (Paris) **39** (1978) L99.
- [133] P. Butera and M. Comi, Phys. Rev. **B56** (1997) 8212.
- [134] T. Reisz, Phys. Lett. **B360** (1995) 77.
- [135] S.Y. Zinn, S.N. Lai, M.E. Fisher, Phys. Rev. **E54** (1996) 1176.
- [136] B. Li, N. Madras, A.D. Sokal, J. Statist. Phys. **80** (1995) 661.
- [137] H.G. Ballesteros, L.A. Fernandez, V. Martin-Mayor, A. Munoz Sudupe, Phys. Lett. **B387** (1996) 125 (values for $N = 1$ quoted from [131]).
- [138] T.R. Morris and M.D. Turner, Nucl. Phys. **B509** (1998) 637; T. R. Morris, Nucl. Phys. **B495** (1997) 477; T. R. Morris, Int. J. Mod. Phys. **B12** (1998) 1343.
- [139] D. Toussaint, Phys. Rev. **D55** (1997) 362.
- [140] E. Brezin, D.J. Wallace and K.G. Wilson, Phys. Rev. **B7** (1973) 232.
- [141] K. Rummukainen, M. Tsypin, K. Kajantie, M. Laine, M. Shaposhnikov, hep-lat/9805013.
- [142] M.M. Tsypin, Phys. Rev. Lett. **73** (1994), 2015.
- [143] M.M. Tsypin, Phys. Rev. **B55** (1997), 8991.
- [144] M. Caselle, M. Hasenbusch, J. Phys. **A30** (1997) 4963; M. Hasenbusch, J. Phys. **A32** (1999) 4851.
- [145] R. Guida, J. Zinn-Justin, Nucl. Phys. **B489** [FS] (1997) 626
- [146] M. Campostrini, A. Pelissetto, P. Rossi and E. Vicari, Phys. Rev. **E60** (1999) 3526.
- [147] V. Privman, P.C. Hohenberg, A. Aharony, *Universal Critical Point Amplitude Relation*, in: Phase Transitions and Critical Phenomena vol. 14 (Academic Press 1991).
- [148] J.K. Kim, L.D. Landau, Nucl. Phys. Proc. Suppl. **53** (1997) 706.

- [149] P. Butera, M. Comi, Phys. Rev. **E55** (1997) 6391.
- [150] P. De Gennes, Introduction to polymer dynamics, Cambridge University Press, 1990.
- [151] J. Berges, M. Gräter and C. Wetterich, unpublished.
- [152] J.P. Cotton, J. Physique Lett. (Paris) **41** (1980) L231.
- [153] T. R. Morris, Phys. Lett. **B345** (1995) 139.
- [154] Y. Kubyshin, R. Neves and R. Potting, Proceedings of Workshop on the Exact Renormalization Group, Faro, Portugal, 10-12 Sep 1998 (hep-th/9811151).
- [155] M. Lüscher, P. Weisz, U. Wolff, Nucl.Phys. **B359** (1991) 221.
- [156] T. Papenbrock and C. Wetterich, Z. Phys. **C65** (1995) 519.
- [157] F.J. Wegner, Z. Phys. **206** (1967) 465; W. Bernreuther, F.J. Wegner, Phys. Rev. Lett. **57** (1986) 1383; E. Brézin, J. Zinn-Justin, Phys. Rev. Lett. **36** (1976) 691; E. Brézin, J. Zinn-Justin, Phys. Rev. **B14** (1976) 3110.
- [158] F. Wegner, Z. Phys. **B35** (1979) 207; **B38** (1980) 113; Phys. Rep. **67** (1980) 15; K.B. Efetov, A.I. Larkin and D.E. Kheml'nitskiĭ, Soc. Phys. JETP **52** (1980) 568.
- [159] See e.g. P.G. de Gennes and J. Prost, *The physics of liquid crystals*, 2. ed. (Oxford, Clarendon Press, 1995).
- [160] For a review see P. Di Francesco, P. Ginsparg and J. Zinn-Justin, Phys. Rep. **254** (1995) 1.
- [161] H. Meyer-Ortmanns, H.-J. Pirner and A. Patkos, Phys. Lett. **B295** (1992) 255; Int. J. Mod. Phys. **C3** (1992) 993; D. Metzger, H. Meyer-Ortmanns and H.-J. Pirner, Phys. Lett. **B321** (1994) 66; Phys. Lett. **B328** (1994) 547; H. Meyer-Ortmanns and B.-J. Schäfer, Phys. Rev. **D53** (1996) 6586.
- [162] R.D. Pisarski, hep-ph/9503330.
- [163] B. Delamotte, D. Mouhanna and P. Lecheminant, Phys. Rev. **B59** (1999) 6006; M. Tissier, D. Mouhanna and B. Delamotte, cond-mat/9908352.
- [164] M. Tissier, B. Delamotte and D. Mouhanna, cond-mat/0001350.
- [165] D.-U. Jungnickel and C. Wetterich, Eur. Phys. J. **C1** (1998) 669.
- [166] D.-U. Jungnickel and C. Wetterich, Eur. Phys. J. **C2** (1998) 557.
- [167] D. U. Jungnickel and C. Wetterich, Phys. Rev. **D53** (1996) 5142.

- [168] S. Bornholdt, N. Tetradis and C. Wetterich, Phys. Lett. **B348** (1995) 89; Phys. Rev. **D53** (1996) 4552; S. Bornholdt, P. Büttner, N. Tetradis and C. Wetterich, Int. J. Mod. Phys. **A14** (1999) 899; N. Tetradis, Phys. Lett. **B431** (1998) 380.
- [169] M. Alford and J. March-Russell, Nucl. Phys. **B417** (1994) 527.
- [170] S. Coleman and E. Weinberg, Phys. Rev. **D7** (1973) 1888.
- [171] A. J. Paterson, Nucl. Phys. **B190** [FS3] (1981) 188;
R. D. Pisarski and D. L. Stein, Phys. Rev. **B23** (1981) (3549); J. Phys. **A14** (1981) 3341; R. D. Pisarski and F. Wilczek, Phys. Rev. **D29** (1984) 338.
- [172] P. Dreher, Phys. Lett. **B281** (1992) 127;
Y. Shen, Nucl. Phys. **B** (Proc. Suppl.) **34** (1994) 712.
- [173] S. Y. Khlebnikov and R. G. Schnathorst, Phys. Lett. **B358** (1995) 81.
- [174] D.U. Jungnickel and C. Wetterich, Phys. Lett. **B389** (1996) 600.
- [175] J.D. Gunton, M. San Miguel and P.S. Sahni, in *Phase Transitions and Critical Phenomena*, Vol. 8, eds. C. Domb and J.L. Lebowitz (Academic Press, London, 1983).
- [176] P.A. Rikvold and B.M. Gorman, Ann. Rev. Comput. Phys. I, ed. D. Stauffer, p. 149 (World Scientific, Singapore, 1994).
- [177] J. Langer, Ann. Phys. **41** (1967) 108; **54** (1969) 258; Physica **73** (1974) 61.
- [178] S. Coleman, Phys. Rev. **D15** (1977) 2929.
- [179] C.G. Callan and S. Coleman, Phys. Rev. **D16** (1977) 1762.
- [180] I. Affleck, Phys. Rev. Lett. **46** (1981) 388.
- [181] A.D. Linde, Nucl. Phys. **B216** (1983) 421.
- [182] J. Berges, N. Tetradis, C. Wetterich, Phys. Lett. **B393** (1997) 387.
- [183] E. Weinberg and A. Wu, Phys. Rev. **D36** (1987) 2474.
- [184] E. Weinberg, Phys. Rev. **D47** (1993) 4614.
- [185] W.N. Cottingham, D. Kalafatis and R. Vinh Mau, Phys. Rev. **B48** (1993) 6788.
- [186] J. Baacke and V.G. Kiselev, Phys. Rev. **D48** (1993) 5648; J. Baacke, Phys. Rev. **D52** 6760 (1995).
- [187] J. Kripfganz, A. Laser and M.G. Schmidt, Nucl. Phys. **B433** (1995) 467.
- [188] M. Gleiser, G.C. Marques and R.O. Ramos, Phys. Rev. **D48** (1993) 1571; G.H. Flores, R.O. Ramos and N.F. Svaiter, Int. J. Mod. Phys. **A14** (1999) 3715.

- [189] A. Strumia and N. Tetradis, Nucl. Phys. **B554** (1999) 697.
- [190] A. Strumia and N. Tetradis, Nucl. Phys. **B560** (1999) 482.
- [191] A. Strumia and N. Tetradis, JHEP **9911** (1999) 023.
- [192] G. Münster, A. Strumia and N. Tetradis, cond-mat/0002278.
- [193] S. Coleman, in *The Whys of Subnuclear Physics*, Proceedings of the International School, Erice, Italy, 1977, ed. by A. Zichichi, Subnuclear Series Vol. 15 (Plenum, New York, 1979).
- [194] M. Gleiser, E.W. Kolb and R. Watkins, Nucl. Phys. **B364** (1991) 411; M. Gleiser and E.W. Kolb, Phys. Rev. Lett. **69** (1992) 1304; Phys. Rev. **D48** (1993) 1560; N. Tetradis, Z. Phys. **C57** (1993) 331; G. Gelmini and M. Gleiser, Nucl. Phys. **B419** (1994) 129; M. Gleiser, Phys. Rev. Lett. **73** (1994) 3495; Phys. Rev. **D49** (1994) 2978; E.J. Copeland, M. Gleiser and H.-R. Müller, Phys. Rev. **D52** (1995) 1920; M. Gleiser, A. Heckler and E.W. Kolb, Phys. Lett. **B405** (1997) 121; J. Borrill and M. Gleiser, Nucl. Phys. **B483** (1997) 416.
- [195] D. Boyanovsky, H.J. de Vega, R. Holman, D.S. Lee and A. Singh, Phys. Rev. **D51** (1995) 4419; D. Boyanovsky, M. D’Attanasio, H.J. de Vega, R. Holman and D.S. Lee, Phys. Rev. **D52** (1995) 6805; F. Cooper, S. Habib, Y. Kluger and E. Mottola, Phys. Rev. **D55** (1997) 6471; D. Boyanovsky, H.J. de Vega, R. Holman, S. Prem Kumar and R.D. Pisarski, Phys. Rev. **D57** (1998) 3653; D. Boyanovsky, H.J. de Vega, R. Holman and J. Salgado, preprint LPTHE-98-45 and hep-ph/9811273.
- [196] M. Alford and M. Gleiser, Phys. Rev. **D48** (1993) 2838.
- [197] D.A. Kirzhnits and A.D. Linde, Phys. Lett. **B42** (1972) 471; Ann. Phys. **101** (1976) 195.
- [198] L. Dolan and R. Jackiw, Phys. Rev. **D9** (1974) 3320.
- [199] S. Weinberg, Phys. Rev. **D9** (1974) 3357.
- [200] G. Parisi, J. Stat. Phys. **23** (1980) 49; Statistical field theory, Addison-Wesley (1988).
- [201] D. O’Connor, C.R. Stephens, Int. J. Mod. Phys. **A9** (1994) 2805; Erratum **A9** (1994) 5851; Nucl. Phys. **B360** (1991) 297; J. Phys. **A25** (1992) 101; F. Freire, C.R. Stephens, Z. Phys. **C60** (1993) 127; M.A. van Eijck, D. O’Connor, C.R. Stephens, Int. J. Mod. Phys. **A10** (1995) 3343.
- [202] S. Weinberg, Phys. Lett. **B91** (1980) 51; T. Appelquist and R. Pisarski, Phys. Rev. **D23** (1981) 2305; S. Nadkarni, Phys. Rev. **D27** (1983) 917.
- [203] J. Kapusta, *Finite Temperature Field Theory* (Cambridge University Press, 1989).

- [204] M. Reuter, N. Tetradis and C. Wetterich, Nucl. Phys. **B401** (1993) 567.
- [205] S.-B. Liao and M. Strickland, Phys. Rev. **D52** (1995) 3653; hep-th/9604192; Nucl. Phys. **B497** (1997) 611; Nucl. Phys. **B532** (1998) 753.
- [206] J. Alexandre, V. Branchina and J. Polonyi, in Eger 1997, Strong electroweak matter '97, 140-159 (hep-th/9709060).
- [207] T. Umekawa, K. Naito and M. Oka, hep-ph/9905502.
- [208] B. Bergerhoff and J. Reingruber, Phys. Rev. **D60** (1999) 105036.
- [209] D.J. Gross and F.A. Wilczek, Phys. Rev. Lett. **30** (1973) 1343; H.D. Politzer, Phys. Rev. Lett. **30** (1973) 1346.
- [210] J.C. Collins and M.J. Perry, Phys. Rev. Lett. **34** (1975) 1353.
- [211] For a review see H. Meyer–Ortmanns, Rev. Mod. Phys. **68** (1996) 473.
- [212] J. Berges, D.-U. Jungnickel, C. Wetterich, Eur. Phys. J. **C13** (2000) 323.
- [213] D.-U. Jungnickel and C. Wetterich, Lectures at Workshop on the Exact Renormalization Group, Faro, Portugal, 10-12 Sep 1998, hep-ph/9902316.
- [214] G. Papp, B.J. Schaefer, H.J. Pirner and J. Wambach, Phys. Rev. **D61** (2000) 096002; J. Meyer, G. Papp, H.J. Pirner and T. Kunihiro, Phys. Rev. **C61** (2000) 035202; B.J. Schaefer and H.J. Pirner, Nucl. Phys. **A660** (1999) 439; Nucl. Phys. **A627** (1997) 481.
- [215] B. Bergerhoff and J. Reingruber, hep-ph/9912474.
- [216] K.-I. Aoki, K. Morikawa, J.-I. Sumi, H. Terao, M. Tomoyose, Phys. Rev. **D61** (2000) 045008; Prog. Theor. Phys. **102** (1999) 1151; K. I. Kubota and H. Terao, Prog. Theor. Phys. **102** (1999) 1163.
- [217] M. Maggiore, Z. Phys. **C41** (1989) 687.
- [218] T. E. Clark, B. Haeri and S. T. Love, Nucl. Phys. **B402** (1993) 628.
- [219] S.-B. Liao and J. Polonyi, Nucl. Phys. **A570** (1994) 203c; S.-B. Liao, J. Polonyi and D. Xu, Phys. Rev. **D51** (1995) 748.
- [220] H. Kodama and J.-I. Sumi, hep-th/9912215.
- [221] H. Lamecker and C. Wetterich, to be published.
- [222] E. Shuryak, Comm. Nucl. Part. Phys. **21** (1994) 235.
- [223] B. Barrois, Nucl. Phys. **B129** (1977) 390; S. Frautschi, Proceedings of workshop on hadronic matter at extreme density, Erice 1978, CALT-68-701; D. Bailin and A. Love, Phys. Rept. **107** (1984) 325.

- [224] M. Alford, K. Rajagopal and F. Wilczek, Phys. Lett. **B422** (1998) 247; R. Rapp, T. Schäfer, E. V. Shuryak and M. Velkovsky, Phys. Rev. Lett. **81** (1998) 53.
- [225] G. Carter and D. Diakonov, Phys. Rev. **D60** (1999) 016004.
- [226] J. Polchinski, Lectures presented at *TASI 92*, Boulder, CO, June 3–28, 1992, hep-th/9210046
- [227] S. Hsu, M. Schwetz, Phys. Lett. **B432** (1998) 203.